Université de Toulouse

THÈSE

En vue de l'obtention du

DOCTORAT DE L'UNIVERSITÉ DE TOULOUSE

Délivré par :
Université Toulouse III Paul Sabatier (UT3 Paul Sabatier)

Discipline ou spécialité :

Biologie Structurale

Présentée et soutenue par :
Parthasarathi RATH

le : 14th Décembre, 2012

Titre :

Structural and functional characterization of PorA and PorH;
the two major porins from Corynebacterium glutamicum

Ecole doctorale :
Biologie, Santé, Biotechnologies (BSB)

Unité de recherche :
RMN et interactions Protein - Membrane, IPBS/CNRS

Directeur(s) de Thèse :

Alain Milon

Rapporteurs :

James STURGIS, Professeur de l'université Méditerranée, AIX - MARSEILLE
Arnaud BONDON, Directeur de recherche CNRS, RENNES

Membre(s) du jury :

Laurent MAVEYRAUD, Professeur de l'université Paul Sabatier, TOULOUSE, Président
James STURGIS, Professeur de l'université Méditerranée, AIX - MARSEILLE, Rapporteur
Arnaud BONDON, Directeur de recherche CNRS, RENNES, Rapporteur
Alain MILON, Professeur de l'université Paul Sabatier, TOULOUSE, Directeur de Thèse

Acknowledgements

The thesis work presented here would not have been possible without the support and guidance of many people associated with the research project. Besides a fantastic scientific environment, a friendly culture and healthy environment were always a plus to produce decent results during the thesis period. Before going to write my thesis I would like to give my sincere gratitude to them with the following few words.

First of all, I would like to thank my supervisor Alain Milon for giving me this opportunity to work on the thesis project funded by the Marie Curie initial training network for structural biology of membrane proteins (SBMP). I truly enjoyed his support, motivation and time to time suggestions throughout the thesis period. Besides the scientific endeavors, the adventurous skiing trips to the Pyrenees with him and the group members at IPBS will always be in my memory in the future.

A special word of thanks is well deserved by the wonderful biochemist, Pascal Demange with whom I spent a lot of time on wet lab, for improving my knowledge in the field of membrane protein biochemistry. His diverse experimental ideas are always a plus to get maximum results with limited period of time but it might be risky if you lose control over them. Also his personal suggestions make me more mature now in the research career when working among greatly scientific collaborations. So thank you again.

A significant part of this thesis work has been done in the group at IPBS which is well known for the study of *Mycobacterial* cell envelope. I would like to thank Mamadou Daffe' and Marielle Tropis for giving this opportunity to work in the team and have some good experience with them. Besides them I would also like to thank Emily Huc and Francoise Laval and other group members for their support, motivation and wonderful discussions on lipid chemistry.

I am very grateful to thank Olivier Saurel for his help either in liquid or solid state NMR experiments for the thesis work and also for his effort to teach me NMR. Besides research, it's nice to have some sports activities together with him. Hopefully we will play tennis again…

Also I would sincerely like to thank Jerzy Czaplicki for his help for the molecular dynamics simulations work in the later part of the thesis. It is such a great experience for me to share the same office with such a senior member in our team and also for the discussions about computer programs and science in general.

Beside his engineer and quality management duties, he spared some time for explaining me the NMR basics and helping me in solving all those technical problems in the lab. Therefore a special word of thanks goes to Pascal Ramos.

Without the help of Corinne Hazan and subsequently Muriel Tauzin- the European project managers for SBMP network, I don't think I could carry out all the administrative works during my stay. So thank you to both of you.

I would also like to thank other team members of this NMR group in Toulouse for their continuous support, motivation and thoughtful discussions throughout the thesis period. These are: Virginie Gervais, Valerie Réat, Isabelle Muller, Isabelle Saves, Marie Renault, Nathalie Doncescu, Deborah Gater, Louic Vermeer, Jade Durand, Mansi Trivedi, Helene Eury, Guillaume Nars and Gregory Menchon.

For the significant part of this thesis work, I wish to express my sincere gratitude to Frank Bernhard and the team members in Frankfurt for educating me cell-free expression system and further developing the system in Toulouse. Honestly your support has been great for producing such important results of the thesis work. In this regard I would also like to thank Volker Dotsch and Frank Lohr for their support and guidance during my stay in Frankfurt.

An important part of the thesis was “channel recordings” which was done in the lab of Alexandre Ghazi at regular time intervals during the thesis period. Therefore a word of thanks is also appropriate for you for your valuable suggestions for the project and also for your effort to teach me such great experiment for ion channel conductance measurements.

Later on at the end of this thesis I am quite happy to produce some results and gain some nice experience on Electron Microscopy experiments. For this achievement I would like thank Stephanie Balor and Celia Plisson from the Biotoul platform (IBCG/CNRS-Toulouse) for their help and support. I would also like to thank the Master Students Marie-Ange Angladon and Pauline Oriol for their help respectively for the extraction and purification of lipids and cell-free expression experiments.

I want to thank the members of the jury, James Sturgis and Arnaud Bondon for their careful reading of this thesis and for coming all the way to Toulouse for the defense. I appreciated their questions and the discussions we had after my presentation.

Sebastien Campagne, Olivier Cala, Iordan Iordanov and Bertrand Fabre: being scientific or non-scientific discussions, I truly enjoyed your companion throughout my stay in Toulouse. And to Christian Roos, Susane Stefer, Stefan Haberstock, Lei Kai, Davide Proverbio and Umesh Ghoshdastider for your motivation and support during my stay in Frankfurt. Thank you guys…

Moreover, I have an immense pleasure to work in the institutes working on various aspects of structural biology and biophysics, specifically the Crystallography team and the Proteomics and Mass Spectrometry team. I really enjoyed your support for the biophysical and mass spectrometry experiments. So thank you to all members. In addition the Iconographic service managed by Francoise Viala, the Informatics service and the Laverie service in the IPBS are always prepared to help during all sorts of scientific necessities. Thank you all. Furthermore, I truly enjoyed all sorts of extracurricular activities provided by the University which are really an advantage to be always fit and active physically and mentally to carry out scientific research. Merci a tous….

For providing bulk of finances and support, I am really grateful to the Marie Curie Fellow Associations of SBMP network for providing enough financial support to complete my thesis work. I feel really proud to be a part of this network and also enjoyed the annual meetings and workshops and thereby a wonderful discussions among the eminent scientists in the field of membrane proteins. Besides many other scientists, I would specifically like to thank Jean-Louic Popot, Donald Engelman and Andreas Engel for their valuable suggestions for the improvement of the thesis work.

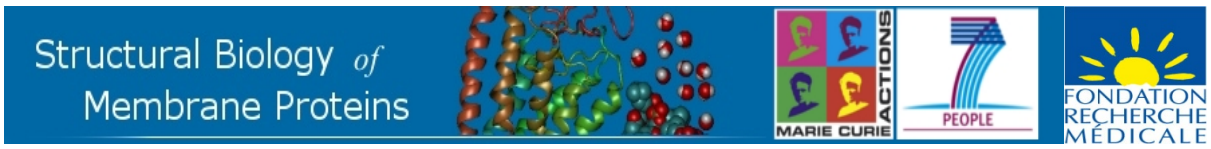

These studies and the IPBS NMR equipment were financed by the French Research Ministry, CNRS, Université Paul Sabatier, the Région Midi-Pyrénées and European structural funds. The research leading to these results has received funding from the European Community's Seventh Framework Program FP7/2007-2013 under grant agreement n° 211800 and the “Fondation pour la Recherche Médicale” (FRM) – Paris.

Besides the NMR family in Toulouse and cell-free family in Frankfurt, an honorable mention goes to my family members and friends back in the motherland, India. Thank you for your constant moral support and faith in me for completing this thesis work. I would also like to mention the small Indian community here in the name of “Indian in Toulouse” for all the memorable events and cultural occasions which never make me feel nostalgic though studying miles away from home. Finally I dedicate this thesis to all my teachers throughout the academic life from my school, college up to university.

So Merci and Thanks again to all of you.

CONTENTS **Page No.**

Page No.

Page No.

Annexes

I: Molecular biology

II- Expression and purification in *C. glutamicum*

III-Expression and purification in Cell - Free expression system

IV- Biochemical methods

Page No.

Summary

PorA (5 kDa) and PorH (7 kDa) are two major membrane proteins from the outer membrane of *Corynebacterium glutamicum* which belongs to the suprageneric group of Gram-positive bacteria containing number of human pathogens such as *Mycobacterium tuberculosis*, *M. leprae* and *C. diphtheriae*. Both PorA and PorH have been shown to form heteromeric ion channels and to be post-translationally modified by mycolic acids (α-alkyl, β-hydroxy fatty acids).

Both proteins were produced in their natural host with mycolic acid modification, as well as in *E. coli* based continuous exchange cell-free expression system and thus devoid of mycolic acid modification. The presence or absence of mycolic acid modification on *in vivo* and *in vitro* expressed proteins was confirmed by MALDI-TOF mass spectrometry. CD and NMR spectra of $^{15}N/^{13}C$ uniformly labeled PorA and PorH solubilized in LDAO micelles indicated mono-dispersed and partially folded proteins, compatible with structure determination by NMR. However, functional assays (via black lipid membrane ion-channel conductance measurements) confirmed that a complex associating both proteins is required for function and that the mycolic acid modification on PorA (but not PorH), is an absolute requirement for the formation of a voltage dependent ion-channel.

To understand further the importance of covalent or non-covalent interaction of their natural lipid environment on the complex formation, the major *C. glutamicum* outer membrane lipids [Trehalose dimycolate (TDM), Trehalose monomycolate (TMM) and Cardiolipin (CL)] were purified using adsorption and ion exchange chromatography, both in protonated and perdeuterated form. Prior to proteoliposome reconstitution, the membrane forming properties of TDM alone or in mixture with CL were studied by ^{2}H-NMR, Dynamic Light Scattering and Electron Microscopy. Furthermore, after *in vitro* reconstitution of PorA and PorH in TDM vesicles (and not in LDAO micelles or DMPC vesicles), evidence for the formation of the hetero oligomeric complex was observed. The 3D structure determination, by liquid and/or solid state NMR, of a functional PorA-PorH complex in its natural lipid environment is now feasible.

Résumé

PorA (5 kDa) et PorH (7kDa) sont les deux protéines membranaires majeures de la membrane externe de *Corynebacterium glutamicum* qui appartient au groupe supragénérique des bactéries Gram-positives contenant plusieurs agents pathogènes i.e. *Mycobacterium tuberculosis*, *M. leprae* et *C. diphtheriae*. Les deux protéines forment des canaux ioniques hétéromériques et présentent la particularité d'avoir une modification post-traductionnelle : estérification par l'acide mycolique.

Les deux protéines ont été produites dans deux systèmes d'expression : chez *C. glutamicum* et dans un système acellulaire utilisant des extraits de *E. coli*. La présence ou l'absence de modification post-traductionnelle, sur les protéines produites *in vivo* et *in vitro* a été caractérisée par spectrométrie de masse MALDI-TOF. Les spectres de dichroïsme cellulaire et de RMN de PorA et PorH uniformément marquées et solubilisées en micelles de LDAO sont caractéristiques de protéines mono-disperses, partiellement structurées, et de qualité compatible avec une détermination de structure par RMN. Le test fonctionnel des protéines, par mesure de conductivité ionique après reconstitution dans une membrane lipidique (technique dite de BLM pour « black lipid membrane ») a montré que a) la modification post-traductionnelle de PorA par un acide mycolique est essentielle (contrairement à celle de PorH) b) la présence simultanée de PorA et de PorH est requise pour la formation d'un canal ionique voltage dépendant typique d'une porine.

Afin de mieux comprendre l'importance de l'acide mycolique pour l'activité canal ionique, le complexe protéique PorA-PorH a été reconstitué dans son environnement naturel. Les principaux lipides de la membrane externe du *C. glutamicum* [Tréhalose dimycolate (TDM), tréhalose monomycolate (TMM) et cardiolipide (CL)] ont été extraits et purifiés par chromatographie d'adsorption et échange d'ions, sous forme protonée et sous forme perdeutériée. Après formation de protéoliposomes les propriétés membranaires de TDM seul ou en mélange avec CL ont été étudiées RMN du deutérium, diffusion dynamique de la lumière et microscopie électronique. L'insertion de PorA et PorH dans des vésicules de TDM a permis de mettre en évidence la reconstitution de l'hétéro-oligomère (contrairement aux micelles de LDAO). Ceci ouvre la voie à la détermination de structure 3D du complexe PorA-PorH fonctionnel par RMN solide et/ou liquide.

Chapter I

Porins of *Corynebacterineae*

I.1. INTRODUCTION

Corynebacteria-Mycobacteria-Nocardia (CMN) group of bacteria belongs to the suprageneric group of Gram-positive microorganisms in the suborder *Corynebacterineae*. This group of bacteria has a unique characteristics, in contrast to other Gram-negative bacteria, possessing an additional lipid bilayer predominantly composed of long chain fatty acids, named mycolic acids covalently linked to the intermediate polysaccharide layer (1). Based on the 16S rRNA phylogenetic trees, a new classification system was proposed (2, 3). Accordingly, in the class *Actinobacteria*, the mycolic acid containing bacteria are grouped in the suborder *Corynebacterineae* which is composed of the respective bacterial families such as *Corynebacteriaceae*, *Nocardiaceae* and *Mycobacteriaceae*. Interestingly these bacteria use a huge part of their genome in making enzymes responsible for fatty acid biosynthesis compared to Gram-negative bacteria, even though both group of bacteria have similar genome sizes (4, 5). Moreover, such extra bilayer makes these bacteria highly impermeable to hydrophilic solutes, other nutrients and hence making them highly resistant to antibiotics and therapeutic agents. Hence a major question arises, how the bacterial permeability is maintained? To address this question, the role of mycolic acids and channel forming porins in this group of bacteria recently gave rise to numerous publications. Furthermore, the elucidation of several atomic resolution protein structures (MspA from *M. smegmatis* (6), OmpATb from *M. tuberculosis* (7, 8) and PorB from *C. glutamicum* (9)) opens the possibility of approaching this diffusion processes across the cell envelope with molecular details.

The general scientific interest relies in the paramount medical importance of this CMN group of bacteria, since this group contains a number of human pathogens. For instance, *Mycobacterium tuberculosis* alone kills nearly three million people each year causing different types of tuberculosis, while *M. leprae* causing chronic leprosis affects nearly ten million people worldwide (10). Other species of *Corynebacteria* such as *Corynebacterium diphtheriae*, infecting the upper respiratory tract, causes diphtheria; *C. minutissimum* causes erythrasma, a skin disease; C. *jeikeium* causes opportunistic infections commonly observed in bone marrow transplant patients. Pathogens of *Nocardia* such as *N. asteroides* and *N. brasiliensis* cause nocardiosis by infecting the lung and other organs. Besides the huge medical importance of this group of bacteria, they also possess great industrial applications. For example, *C. glutamicum* is currently used for the production amino acids such as L-glutamate (10^6 tons per year) and L-lysine (10^5 tons per year) (11, 12). The diseases causes by these bacteria as well as the efficiency of amino acid excretion strongly depend on the growth of the bacteria in the host

organism or in the culture medium. In fact, the expression of the channel forming proteins seems to have a direct influence on the physiology of these various microorganisms.

Enormous developments happened recently in understanding the complex cell envelope of this group of bacteria in connection with their pathogenicity; many channel forming proteins have been functionally characterized and published recently. It is thus time to write a comprehensive review about the channel forming proteins and their functional activities. This chapter will summarize briefly the overall architecture of the cell envelope, and a strong focus will be given to the functional characterization of channel forming proteins, their voltage gating, multiple conducting states and kinetic properties.

I.2. THE CELL ENVELOPE

The original model of the cell envelope of CMN group of bacteria, based on a bilayer structure, was first proposed by Minnikin (1). This model was not accepted initially (13, 14) but the existence of this bilayer was confirmed later on by X-ray diffraction and cryo-electron microscopic techniques (15-17). Accordingly, the cell envelope consists of a typical inner plasma membrane (PM), an intermediate cell wall core and an outer layer. The PM is surrounded by a periplasmic space which differs in thickness among species. The thick cell wall core is composed of peptidoglycan-arabinogalactan layer covalently linked to mycolic acids by ester bonds. Beyond this cell wall core, the outer layer mostly consists of glycolipids, mostly trehalose derivatives of mycolic acids. It has been proposed that these lipids make a bilayer which functions like an outer permeability barrier to this CMN group and also play a role similar to the outer membrane of Gram-negative bacteria (18-21).

Although the composition and the biosynthetic pathways of the cell envelope components have been widely studied qualitatively, and reviewed (20), the quantitative composition of the cell envelope (*C. glutamicum*) has only been examined recently by *Bansal-Mutalik et al* (22) and *Marchand et al* (23). Both groups have shown that the outer layer is predominantly composed of glycolipids such as Trehalose dimycolate (TDM) and Trehalose monomycolate (TMM), whereas the inner PM is composed of phospholipids. The most common phospholipids are phosphatidylglycerol, diphosphatidylglycerol (cardiolipin), phosphatidylethanolamine, phosphatidylinositol and its mannosides. Other lipids such as glycol-peptido-lipids, phtiocerol dimycocerosate and sulpholipids are only present in specific species (1, 24-31). Additionally *Bansal-Mutalik et al* found a large quantity of non-extractable cardiolipin in the inner cell wall core in complex association with the peptidoglycan-

arabinogalactan layer. In addition, the presence of surface exposed capsule layer and its pathogenic property has been investigated (21, 32)

Besides the existence of different kind of lipids, the large quantity of free mycolic acids and their role in pathogenicity cannot be ignored. Generally, mycolic acids are high molecular weight, α-alkyl, β-hydroxy fatty acids of various chain lengths either present freely or esterified to the arabinogalactan layer. In *Corynebacteria* and *Nocardia*, mycolic acids contain about 22 to 60 carbon atoms, whereas in *Mycobacteria* they are relatively longer from 70 to 90 carbon atoms (33). The pathogenic properties of mycolic acids and their derivative lipids have been studied extensively in the articles as cited (34, 35). Again to restrict the discussion of this chapter to porin based outer membrane permeability of this CMN group, the details about the cell wall architecture and biosynthetic pathways will not be described further here and can be found in the cited articles and reviews (36).

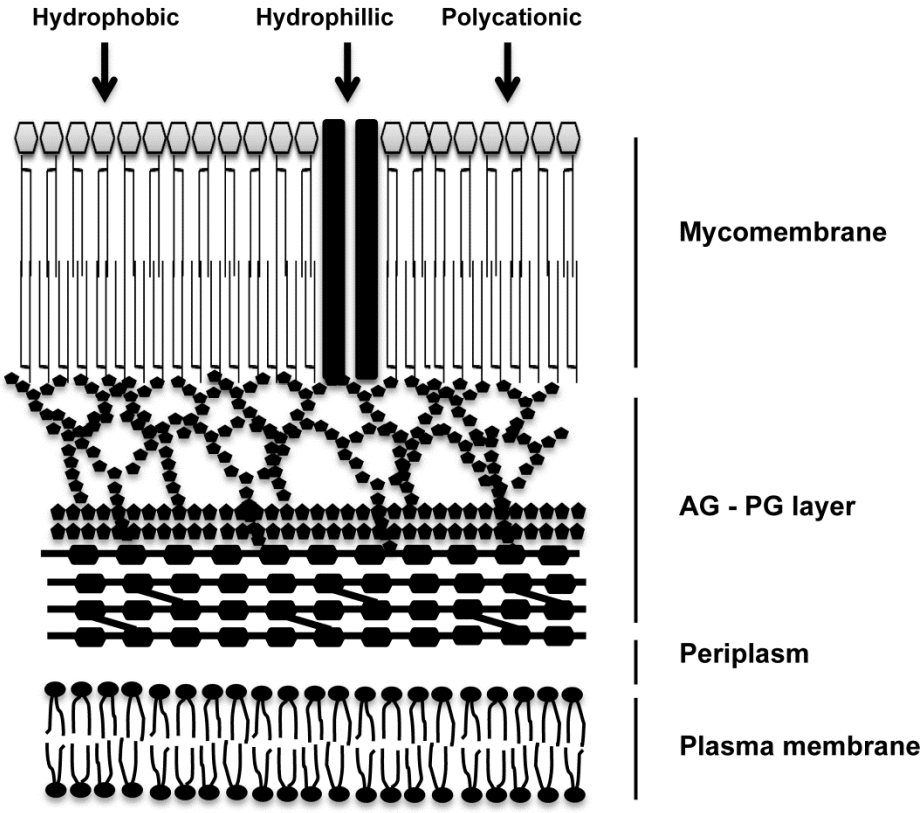

Fig. I-1: Schematic representation of the cell envelope of CMN group of bacteria. The arrangement of the lipids as a bilayer was first proposed by Minnikin (1982)(1). The inner leaf let of the outer membrane is composed of long chain mycolic acids which are covalently attached to the underlying arabinogalactan (AG) – peptidoglycan (PG) layer. The outer leaflet consists of a variety of extractable lipids such as trehalose-dimycolate (TDM), trehalose-monomycolate (TMM), glycol-peptido-lipids, sulpholipids, glycerol-phospholipids, phenolic glycolipids and lipopolysacharides (29). The inner membrane is mostly composed of phospholipids such as phosphatidylglycerol, diphosphatidylglycerol (cardiolipin), phosphatidylethanolamine, phosphatidylinositol and its mannosides. The thickness of each layer varies among the various groups of bacteria. It has been estimated by electron microscopy and is reported in (15, 16). The general transport through the bacterial outer membrane occurs through two common pathways; the small and hydrophilic solutes diffuse through non-specific water filled porins, whereas hydrophobic compounds traverse by diffusing directly through the lipid bilayer. The polycationic compounds are supposed to be entering the outer membrane by distabilizing the bilayer (36-39).

I.3. CLASSICAL PORINS AND THEIR BIOLOGICAL RELEVANCE

Being strict to its definition, porins are defined as the class of channel proteins which allow the non-specific influx of hydrophilic solutes or nutrients and efflux of excreted products through the bacterial cell wall. After the first discovery of a porin channel in 1976 (40), porins were found to be widely distributed in various groups of Gram-positive and Gram-negative bacteria (36, 37). In fact, these non-specific channel proteins have been shown to be the major hydrophilic pathway across the cell wall of these organisms. During the same period, mitochondrial porins (VDAC: Voltage Dependent Anion Channels) were also discovered (41, 42). Such VDACs were shown to form β-barrel structures similar to bacterial porins with relatively large diameters (43, 44). However porins can be classified according to their selectivity towards various cations or anions and hence named cation or anion selective channels. Further, the slow or fast diffusion rate of specific molecules and their unique transmembrane β-barrel structure distinguishes them from the rest of ion channels with some exceptions. Excellent reviews about the families of classical porins from various groups of Gram-negative bacteria were written by by H. Nikaido (36, 38). Herein, we will focus further on the different classes of known porins from CMN group of bacteria.

An extremely important question, over the last decades, has been to determine whether these non-specific ion channels on the bacterial cell envelope play a crucial biological role, in particular concerning the pathogenic and phylogenetic properties?

Porins as a major pathway for nutrients across the cell envelope

With the first experimental evidence comparing the permeability of cephalosporins, glycerol and glucose in the cell wall of *M. chelonae* and Gram-negative bacteria such as *E. coli* and *Pseudomonas aeruginosa*, the group of Nikaido proposed the existence of three major transport pathways for hydrophilic and hydrophobic molecules across the bacterial cell envelope, the mechanisms were described as cited (18, 20, 37, 38, 45, 46). (1) Small and hydrophilic compounds traverse the cell wall through non-specific porin channels, while few *E. coli* porins shows specificity towards maltodextrins (47) and nucleosides (48). (2) Hydrophobic compounds prefer the lipid bilayer pathway to traverse the cell wall. The lipid composition, in particular, the length of mycolic acids and the number of cis/trans double bonds and cyclopropane groups (in case of some *Mycobacteria*) play a major role on the membrane fluidity and phase transition temperatures and thus affect solubilities in the lipid phase (20, 49, 50). (3) Many polycationic compounds create their own pathway, called “self-

mediated uptake", by inducing disorder in the outer membrane (51, 52). As these CMN group of bacteria has a distinct inner membrane and outer envelope (Fig. I-1), the general transport pathways across the outer envelope occurs through the porins, whereas nutrient molecules cross the inner membrane through specific transporters. The existence and characterization of inner membrane transporters for carbohydrates, lipids, phosphorous, sulfur and nitrogen containing solutes, inorganic cations and amino acids have been widely investigated and is reviewed in (36). Finally, many aspects of the transport pathways in the periplasmic space still remain to be fully understood.

Porins as a major factor of intracellular persistence and growth rate

Many members of this CMN group are opportunistic and non-pathogenic while some of them are highly pathogenic and cause severe human diseases. One of the reasons for the pathogenicity of *M. tuberculosis* is linked to its intracellular persistence inside the macrophages. The mechanism of such persistence and concomitantly their slow growth inside the macrophage is highly debated in the literature (53-55). This put forward two basic questions such as, (i) why the pathogenic species are slow-growers whereas, non-pathogenic belongs to fast-growers? And (2) is this slow growth is a proof of principle of their virulence? To answer these questions mutational studies has been carried out to investigate these physiological functions. But creation of the multiple porin mutant strains is rather a difficult task in case of bacteria (*M. smegmatis*, *C. glutamicum* etc) containing number of porins and against some unknown proteins bearing porin like functions.

The general members of *M. tuberculosis* are known to have intra cellular persistence inside macrophages (56) and protozoa (57), while *M. smegmatis* has been shown to be killed by human monocytes and by *Amoeba castellanii* (54, 55). MspA and MspA-MspC deletion mutants of *M. smegmatis* were shown to be impaired in nutrient uptake, diffusion of antibiotics and concomitantly had enhanced survival rates in the cysts of *A. castellanii* under extremely unfavorable conditions (58, 59). Moreover, the introduction of MspA into *M. bovis* BCG and *M. tuberculosis* increased the cell wall permeability to glucose with simultaneous increase in multiplication rate in macrophages and pneumocytes (60-62). Furthermore, it was shown that the deletion of MspA reduced the outer membrane permeability towards glucose (63), phosphate (64), amino acids (65) and also to irons (66). *Raynaud et al. 2002* described that OmpATb deletion mutant of *M. tuberculosis* has a diminished growth at lower pH and also in macrophages. This deletion mutant was unable to grow in normal mice whereas growth was

less affected in mice lacking T cells (67). In a recent article, the effect of OmpATb operon expression on ammonia secretion was studied and further explained its role in adaptation of the bacteria to acidic environments (68). In addition, its potential to be used as a novel antigen for diagnosis of bovine tuberculosis with improved specificity and sensitivity has been investigated (69).

As PorA is the major porin identified in *C. glutamicum* outer envelope, its effect on the growth of the bacteria was studied (70, 71). It was observed that the PorA deletion mutant, although not lethal, had a slower growth than the wild type strain. The PorA deletion has no substantial effect in the transport of different carbon sources (glucose, maltose, sucrose, ribose, pyruvate and lactate), except for citrate, where the growth was significantly delayed when used as a carbon source on this mutant. Furthermore, the PorA mutant was not affected in its glutamate production (70, 72). However, a mutant strain with the deletion of multiple Porins from *C. glutamicum* has not yet been studied in the growth and survival of this group of bacteria. Interestingly, it was shown that mutation of the gene NCgl1221 which is homologous to mechanosensitive channels from *C. glutamicum* plays a significant role in L-glutamate secretion (73). The deletion mutant of two strains with mechanosensitive channels, MscL and MscS from *C. glutamicum* increase the efficiency of efflux of solutes during hypoosmotic stress which is supposed to be carried out by an unknown mechanosensitive channel. In contrast, the deletion of MscL and MscS was lethal to *E. coli* under the same condition (74). The mechanosensitive channels are located in the inner membrane and help to adapt the bacterium to hypoosmotic stress. However, the transport of solutes across the outer membrane through porins cannot be ignored during the adaptation of *C. glutamicum* to hyperosmotic stress (75-77).

Porins as a pathway for antibiotics

Although, it was first predicted by *Nikaido et al* that hydrophobic antibiotics can directly diffuse through lipid membrane while hydrophilic antibiotics utilize the porin pathway, it was only recently verified with experimental evidence that hydrophilic fluoroquilonones and chloramphenicol diffuse through porins in mycobacteria. Specifically the hydrophilic norfloxacin uses the Msp porins, whereas the hydrophobic moxifloxacin directly diffuse through the outer membrane of *M. smegmatis* (78). The uptake of antibiotics: b-lactams, tetracyclines, fluoroquinolones, chloramphenicol, and cycloserine was shown to take the porin pathway in Gram-negative bacteria (36). It is well known now that *M. tuberculosis* is

intrinsically resistant to many antibiotics and drugs and also OmpATb, the only channel protein so far characterized in its outer membrane. In contrast, the OmpATb mutant does not show increased drug resistance (67) and there is no clear evidence of the role of OmpA in antibiotic uptake. Again *M. tuberculosis* lacks Msp-like porins (39) but it is susceptible to both nofloxacin and moxifloxacin. Hence it is possible that the presence of other porin like proteins enables the diffusion through its outer membrane. In the case of *C. glutamicum*, the deletion of PorA results in a substantial increase in antibiotic resistance towards kanamycin and streptomycin, however no inhibition of growth was observed for ampicillin and tetracycline (71). This indicates that PorA has a certain role in the transport of antibiotic across the outer membrane of *C. glutamicum*.

Porins role in host-pathogen interaction

Interestingly, MspA and OmpATb do not show any sequence homology rather has similar effect on deletion mutants on different classes of *Mycobacteria* towards uptake of nutrients, for the adaptation to low pH and their survival in macrophages and mice. These evidences will take forward the role of porins towards host-pathogen interactions. The extra cellular loops of these proteins have a definite role in binding to the surface antigens. In fact the role of porins in host pathogen interactions are well analyzed in Gram-negative bacteria. i.e. binding sites for components of the complement cascade, to promote adhesion to macrophase, invasion of endothelial cells, to influence maturation of dendritic cells and phagosomes, to affect cytokine release and to modulate apoptosis (79-82).

A major determinant for deciding cell wall impermeability

MspA forms a tetrameric complex with a single central pore of 10 nm length whereas, Gram-negative bacteria forms trimeric porins with one 4 nm long pore per monomer (6, 83). In other words, MspA contain one channel per porin molecule whereas *E.coli* porins contains three channels per porin molecules. Further, the two component porin system in *Corynebacteria* and *Nocardia* species indicate a different class of porins with completely different structures (84, 85). *M. smegmatis* possesses 1000 MspA like pores / μm^2 cell wall (nearly 70 % of all pores) (86). Hence the density of porin present in the cell wall should allow a proper balance between the nutrient supply and antimicrobial activities. The 45 fold lower number of porins and exceptional length in compare to Gram-negative bacteria are the two major factors for the low permeability of the outer membrane (86, 87).

I.4. KNOWN PORINS FROM CMN GROUP AND THEIR BIOCHEMICAL PROPERTIES

I.4-i: Porins from *Mycobacteriaceae*

Porins were first discovered in the outer membrane of mycobacteria by *Trias et al.* in 1992 (46). By planar bilayer experiment, they found that the detergent solubilized *M. chelonae* cell wall fraction contained a 59 kDa protein which formed water-filled channel of 2.2 nm diameter and had an average single channel conductance of 2.7 nS in 1 M KCl. The low abundance of the protein and low specific channel activity could be related to the low permeability of the cell wall compared to Gram-negative bacteria such as *E. coli* and *P. aeruginosa* (18). The channel was shown to be cation selective bearing 2.5 point negative charges at both sides of the channel. Furthermore the channel was characterized by slow and fast closing between open and closed states with asymmetric voltage dependence (88). In a similar approach, *Niederweis et al,* in 1999 showed the existence of a similar porin, MspA in the cell wall of *M. smegmatis*. The oligomeric 100 kDa cation selective channel showed multiple conductance from 2 to 5 nS in 1 M KCl. Interestingly, when the oligomeric form was disrupted by boiling in 80 % DMSO, the monomeric forms did not show any channel activity (89). Mutational studies showed decreased outer membrane permeability towards hydrophilic nutrients and established MspA as the major porin in *M. smegmatis* (63). Negatively stained electron microscopy of the purified protein showed the channel has a diameter of 2.5 nm which is in agreement with the estimation with conductance measurements and further in the crystal structure (6, 86, 88, 89). 33 homologous MspA like porins have been identified in the fast growing *Mycobacteria* as well as in some of their pathogenic forms, *M. avium* and *M. ulcerans* (39).

Moreover, two channels were identified in the organic solvent and detergent extracts of *M. bovis* BCG cells. One is a cation selective channel producing 4 nS in 1 M KCl with similar characteristic to *M. chelonae* and *M. smegmatis* channels. Whereas, the other channel is anion selective producing small conductance of 0.7 nS (90). Furthermore, a porin homologous to MspA was identified from *M. phlei* which migrates to 135 kDa in SDS PAGE and dissociated into 22 kDa subunits when boiled in 80 % DMSO (91)

Another channel protein, OmpATb was identified in *M. tuberculosis* H37Rv which was claimed to be homologous to Gram-negative OmpA family of outer membrane proteins (92). The protein migrates to 38 kDa in SDS PAGE and shows lower conductance of 0.7 nS in

planar bilayer measurement. In fact, this protein is active under acidic condition at pH 5.5 and the deletion of the gene has impaired growth of the bacteria in macrophages and mice (67). The central domain ($OmpATb_{73-220}$) was shown to be sufficient for channel activity, with low cation selectivity and an asymmetric voltage dependence in a 4 to 8 pH range (93). Rv1698 of *M. tuberculosis* was identified as another channel forming protein showing unspecific transport across the membrane. When expressed in *M. smegmatis* mutant lacking the major porin MspA, restored its sensitivity towards ampicillin and chloramphenicol whereas, inability to take glucose was partially complemented. This new class of protein shows average single channel conductance of 4.5 nS in 1M KCl (94). The authors claim a probable role of this channel protein in nutrient uptake and host-pathogen interaction as shown in case of Gram-negative *Neisserial* porins (80, 95).

I.4-ii: Porins from *Corynebacteriaceae*

The major porin in *C. glutamicum*, PorA was first discovered in the organic solvent cell wall extracts producing high single-channel conductance of 5.5 nS in 1 M KCl (96). The channel was shown to be highly cation selective with the presence of negative charges at the channel entrance. Based on the conductance the channel diameter was estimated to be 2.2 nm. Surprisingly this channel consists of a very low molecular mass polypeptide of only 45 amino acids lacking any N-terminal extension which was confirmed by amino acid sequencing (71, 97). The deletion of PorA reduced drastically the channel activity, but did not affect much to the growth of *C. glutamicum*. This lead to the discovery of another channel, PorB which was shown to form fairly small anion selective channels with an average single channel-conductance of 0.7 nS in 1 M KCl and an estimated channel diameter of 1.4 nm (70). PorB contains 126 amino acids and has an N-terminal extension of 27 amino acids. Another protein, PorC with 30 % identity to PorB was identified downstream of PorB in the genome and is annotated in the same gene cluster. Both PorB and PorC are thought to be cotranscribed and to form other transport pathway across the outer membrane of *C. glutamicum*. Few years later, PorH, a 57 residue small peptide was further characterized to be a cation selective channel across the outer membrane of *C. glutamicum* and *C. callunae* (98, 99).

More recently, it was observed that PorA and PorH are present in an operon in the genome of different species of *Corynebacteria*. With the delta PorA-PorH construct, and using recombinantly expressed and purified PorA and PorH, it was shown that the actual porin channel needs the obligatory presence of both proteins. Such two component PorA-PorH

heterooligomeric channels were also observed in other species in the genus *Corynebacteria* such as *C. efficiens*, *C. diphtheriae* and *C. callunae* (84). Interestingly, it was further found that both PorA and PorH class of proteins are post-translationally modified with O-mycoloylation and that this modification is essential for the channel activity (100). Furthermore, using *E. coli* based cell-free expression to produce unmodified polypeptides, it was whown that the mycoloylation of PorA (but not PorH) is an absolute requirement for the channel formation (101).

I.4-iii: Porins from *Nocardiaceae*

Porins have also been reported in the cell wall of *Nocardia* species. The first oligomeric channel of 87 kDa protein was found in *N. farcinica* which was stable in normal SDS PAGE but dissociated into nearly 20 kDa subunits upon boiling for a longer time. The channel produces average single channel-conductance of 3.0 nS in 1 M KCl and was found to be cation selective with asymmetric voltage dependence. The channel diameter was estimated to be 1.4 to 1.6 nm (102). Recently a hetero-oligomeric channel consisting of NfpA and NfpB with molecular mass of nearly each 30 kDa was reported in the cell wall of *N. farcinica* (85). It was shown that individual proteins do not make any channel rather the 1:1 mixture shows cation selective channel with similar properties to the oligomeric channel previously identified (102). Furthermore, these proteins have similar characteristics to MspA of *M. smegmatis* and also shares 11 % sequence identity with conserved Alanines and Glycines suggesting a similar octameric β-strand structure in the outer envelope of the bacteria. Porin channels were also identified in *N. asteroides* and the non-pathogenic *N. corynebacteroides* cell wall with similar functional properties (103, 104). From the same suborder *Corynebacterineae*, porins have been found in the cell wall of *Rhodococcus erythropolis* (105), *R. equi* (106) and Tsukamurella inchonensis (107).

Cell wall porins	Λ/nS	Monomeric [oligomer] MW (kDa)	Channel diameter (nm)	Ion selectivity in 1M KCl	Reference
Corynebacteria					
C. glutamicum					
PorA / PorH	2.5 / 5.5	4.7 / 6.2	2.2	cation	Barth et al., 2010
PorB*	0.7	10.6	1.4	anion	Costa-riu et al., 2003
C. diphthereae					
PorA / PorH	2.3	4.6 / 6.8	2.2	anion	Barth et al., 2010
C. callunae					
PorA / PorH	2.3	4.8 / 6.0	ND	cation	Barth et al., 2010
C. efficiens					
PorA / PorH	2.0 / 4.0	4.6 / 5.9	ND	cation	Barth et al., 2010
Mycobacteria					
M. chelonae	2.7	59	2.2	cation	Trias and Benz, 1993
M. phlei	4.5	22 [135]	2.0	cation	Ries et al., 2001
M. smegmatis					
MspA*	4.6	20 [100]	1.8	cation	Niederweis et al., 1999
M. tuberculosis					
OmpATb*	0.7	38	1.8	ND	Senaratne et al., 1998
M. bovis					
$PorA_{Mbo}$	4.0	ND	ND	cation	Lichtinger et al., 1999
$PorB_{Mbo}$	0.78	ND	ND	anion	
Norcadia					
N. farcinica					
NfpA* / NfpB*	3.0	19.1 / 19.7 [87]	1.6	cation	Klackta et al., 2011
N. corynebacteroides	5.5	23 [134]	1.0	cation	Reis and Benz, 2000
N. asteroides	3.0	84	1.4	cation	Ries et al., 1999
Rhodococcus					
R. erythropolis	6.0	8.4 [67]	2.0	cation	Lichtinger et al., 2000
R. equi					
$PorA_{Req}$	4.0	67	2.0	cation	Ries et al., 2003
$PorB_{Req}$	0.3	11	1.4	anion	
Tsukamurellae					
T. inchonensis	4.5	33	2.0	cation	Dorner et al., 2004

Table 1: Presentation of the list of porins characterized functionally in the CMN group of bacteria. Porins from *Rhodococcus* and *Tsukamurellae* belong to the same suborder *Corynebacterineae* are also listed. Porins with star mark have an extension at their N-terminus which helps for recognition and transport to the outer membrane.

I.5: Transport of expressed porins to the outer mycomembrane and their folding pathways

Mycobacteria use the general secretion (Sec) and twin-arginine translocation (Tat) pathways to export bulk of their membrane proteins (108, 109). These two pathways are usually conserved in wide range of bacteria, from Gram-negatives to Gram-positives. They also have specialized pathways for specific group of proteins. For example, the accessory SecA2 system and the ESX export systems are important for virulence and the vital physiological processes. This evolving mechanism has been described in various research or review articles (110-116).

Recent studies by two different groups provide strong evidence for the localization of these porins in the outer mycomembrane of the cell envelope (22, 23). However, the exact transport pathways of these proteins which range from a very small monomeric molecular weight (*Corynebacterial* porins) to very large molecular weight (*Mycobacterial* porins) are not yet clearly understood. Moreover, most of the proteins (MspA from *M. smegmatis*; OmpATb from *M. tuberculosis*; NfpA/NfpB from *N. farcinica*; PorB/PorC from *C. glutamicum* etc) have a signal sequence at their N-terminus (marked with star in Table 1) which help for their transport, while some of them (PorA/PorH from various species from *Corynebacteria*) do not possess a signal sequence. In fact, the proteins which do not have signal sequence are located as bicistronic porin transcript, downstream of a gene coding for shock-regulated GroEL chaperon (84, 117). Hence the translated polypeptides which have the signal sequences are supposed to be transported through the plasma membrane by the Sec apparatus, whereas those which lack the signal sequences might be using the chaperons for their transport. Translated proteins are usually exported in an unfolding state and fold to their natural conformation in the mycolic acid containing outer membrane in the absence or presence of periplasmic chaperones. Moreover, some proteins (PorA and PorH from *C. glutamicum*) are post-translationally modified by mycolic acids (100, 101), hence the role of this covalent modification on the folding of such channels cannot be ignored. These proteins are thought to be esterified by the periplasmic mycoloyltransferases, the enzyme responsible for the synthesis of mycolic acid containing glycolipids (Trehalose dimycolate and Trehalose monomycolate) in the outer membrane (118, 119).

I.6: Characterization of porins in planar bilayer measurements

With the first discovery and characterization of porin channel in *Mycobacteria* and subsequently other porins in the same group of mycolic acid containing *Actinomycetes*, three common characteristics have been observed in most of these channel forming proteins by planar bilayer measurements. First, these channels exhibit stepwise stair like appearance with multiple insertions and producing different conducting states. Second, they display slow and fast flickering behavior with systematic opening and closing of one single channel at different time scales but with unique conductance. And third, these channels are voltage-gated, either in a symmetrical or asymmetrical manner (Fig. I-2). These three characteristics are considered as 'fingerprints' of porins in bilayer measurements, and may be used as a filter before naming "porin" any newly found outer membrane protein.

The first observed characteristic of the porins from CMN group of bacteria in planar bilayer measurement is the high resolution step wise increase in conductance at a constant low applied membrane potential (10 to 20 mV) and at sufficient low concentration of the purified protein in the measurement chamber (< 10 ng/ml, even if at pg/ml concentration) (Fig I-2A). Each step corresponds to the incorporation of one channel forming unit into the membrane or to the formation of a functional channel after membrane insertion of independent subunits in the case of two component hetero-oligomeric channel such as observed in *Corynebacteria* and *Nocardia* species (84, 85). In fact these channels have a longer life time at small transmembrane potential. This indicates the presence of stable oligomeric structures in the artificial membrane during channel recordings. Another important observation is that we can see a range of conductance from 2 to 6 nS in various porins of this group in which they show either one or two conducting states producing maximum conductance. In addition, there is a continuous transition between these multiple conducting states. The reason could be that channels are formed with multiple oligomers of different number of monomers in the artificial membrane. These results are conssistent with the fact that though the channels produced by *C. glutamicum*, *M. chelonae* and *N. farcinica* shows substantial similarities, their monomeric molecular mass differs significantly (Table 1) (46, 84, 85, 89).

In their biophysical characterization, it was observed that there is preferential selectivity of transport of ions by individual porins. While a majority of porins in the CMN group shows cation selectivity (PorA/PorH, MspA, NfpA/NfpB etc), several display anion selectivity (PorB, PorC). Moreover, these porins form wide water-filled channels without any

selectivity filters i.e. no binding sites for specific ions. By studying the channel conductance with various cations or anions, the channel diameter were estimated (120, 121). The values thus obtained for MspA were in good agreement with the first resolved crystallographic structure (6, 86).

In another observation, we can found that the single-channel conductance of *Corynebacterial* (*C. glutamicum*) porins shows higher conductance compared to porins from *Mycobacteria* (*M. chelonae* and *M. smegmatis*) or *Nocardia* (*N. farcinica*) species. But their estimated channel diameters are similar (Table 1). This result seems contradictory but we should not ignore that the thickness of their outer mycomembranes differs (33, 122): the mycolic acids of *Corynebacterial* cell wall are shorter (22-40 carbons) while the mycolic acids of *Norcardia* (40-60 carbons) and *Mycobacteria* (60-90 carbons) are relatively longer. This indicates that the porin channels of *Corynebacteria* are presumably narrower compared to *Nocardia* or *Mycobacterial* channels.

The second observed characteristic of these porins in planar bilayer measurement is that at low applied membrane potential, they show a flickering slow and fast opening and closing of the channels, with unique low conductance. The opening and closing of the channels occurs with two kinetics, one with a millisecond time scale and the other with a ~ second time scale (Fig I-2B). Interestingly, during this flickering behavior, the channels do not close permanently. Instead, there is a transition between both step like channels and the flickering channels. This indicates that there is possible reconstitution of two different configurations of the same channel or the channels once reconstituted alters between multiple configurations, rather than the occurrence of two separate channels in the artificial membrane. These observations were specifically shown in the channel recording of *M. chelonae* and *C. glutamicum* (PorA/PorH) channels (88, 89, 101).

The most important functional characteristic of these porins is their voltage-gating properties, which provide an important evidence of their physiological importance in the cell membrane. The channels need to close under environmental stimuli such as extreme pH, voltage or with specific interaction with ligand molecules. Since under low applied voltage, all the multiple step wise insertions observed are in upward direction, every channel are in a continuous open state in the membrane. When higher potential (from ± 40 up to ± 120 mV) is applied across the membrane, the current decreases exponentially as function of time both for negative and positive potentials (Fig. I-2C). When the channels close only for negative

potentials, as shown in case of MspA of *M. chelonae* (88), channels of *N. farcinica* (85, 102) and *N. asteroides* (104), it suggests there is an asymmetric insertion of the channels into the membrane. However, in certain channels (*C. glutamicum* PorA/PorH) observed current decreases at both positive and negative side of applied potential leading to symmetric voltage dependence (101).

In another important observation, it was shown that the cell wall channels of most of this CMN group of bacteria such as *M. chelonae, M. smgmatis, M. bovis, M. phlei, N. asteroid* and *N. farcinica* shows voltage dependent closure only at negative side of the potential. More than 50 % of channels close at very low potential, starting from -20 to -30 mV, and complete closure at higher potentials whereas, the current was not influenced at higher positive potentials even up to 120 mV. The authors postulated two probable reconstitutions of the cell wall channel into the planar membrane. First, this indicates 100 % orientation of the channel reconstituted in the planar bilayer. Second, it is also possible that the hydrophilic part of the channel is exposed to the aqueous phase of the bilayer whereas the hydrophobic part is embedded as transmembrane channel. If the *in vitro* situation exists in the natural membrane of these mycolic acid containing bacteria, then the hydrophobic part of the channel is obviously present in the mycolic acid bilayer while the hydrophilic part of the channel should be exposed towards the cytoplasmic membrane. In addition, there must be an inner negative membrane potential to control the closure of these channels. However the exact membrane potential of these bacterial cell wall is unknown. Hence it is highly possible that a small voltage across the cell wall may exist which is either due to an intrinsic membrane potential (asymmetry of lipid distribution) or due to a Donnan potential (asymmetry of charge distribution) as more likely the voltage-dependent control of the outer membrane permeability in Gram-negative bacteria (123, 124). Indeed, such asymmetric voltage-dependent closure of channels accounts for the limited cell wall permeability of these mycolic acid containing pathogenic bacteria in the suborder *Corynebacterineae*.

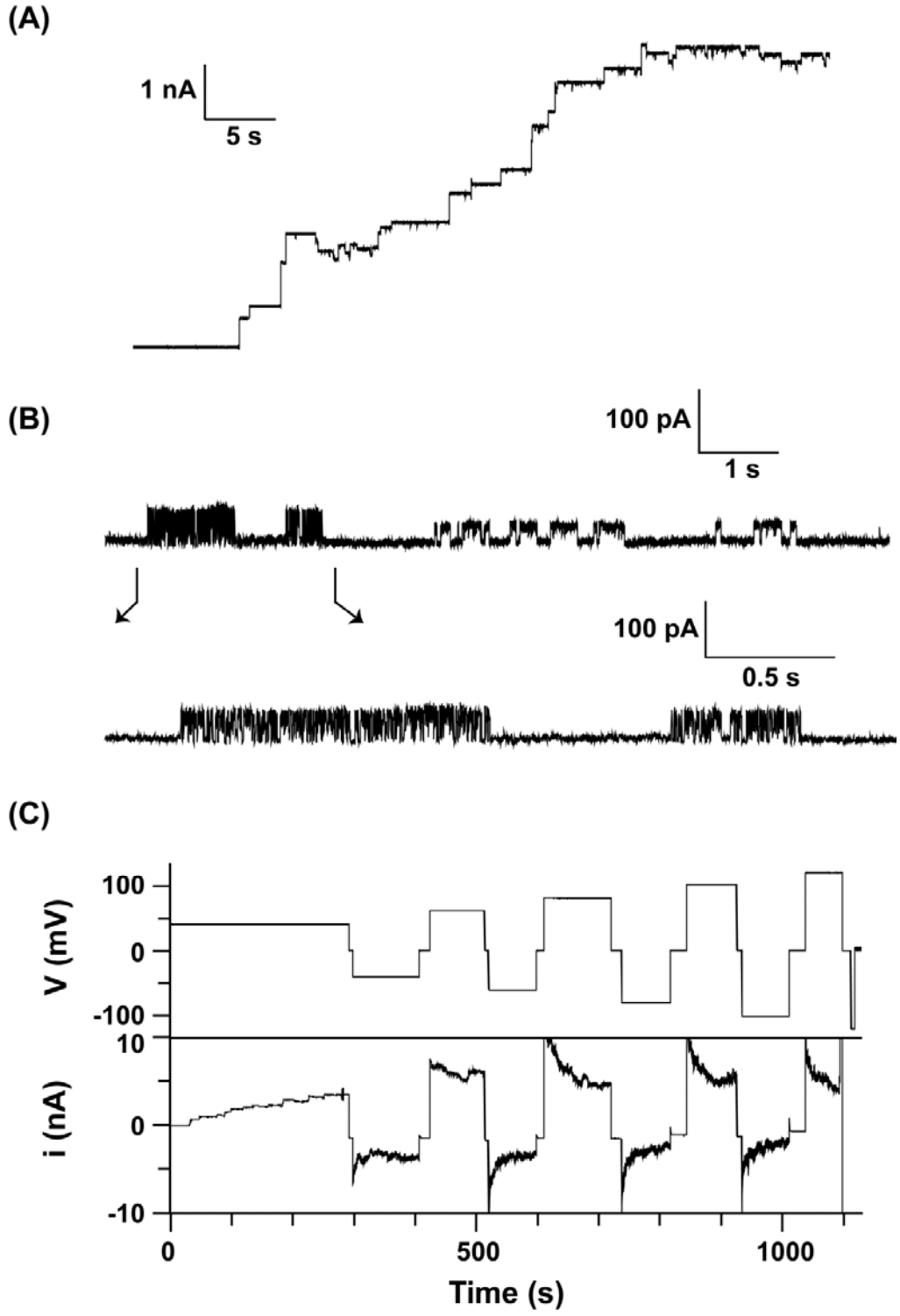

Fig. I-2: Three common characteristics have been observed in most of these channel forming proteins by planar bilayer measurements. (A) First, these channels exhibit stepwise appearance with multiple insertions and producing different conducting states, (B) Second, they display slow and fast flickering behavior with systematic opening and closing of one single channel at different time scales but with unique conductance and (C) Third, these channels are voltage-gated, either symmetrical or asymmetrical manner. The channel forming properties of PorA and PorH from *C. glutamicum* are shown in this figure.

I.7: AVAILABLE HIGH RESOLUTION STRUCTURES

I.7-i: MspA structure from *M. smegamatis*

The first atomic resolution structure of a porin, MspA from the Gram-positive *M. smegmatis*, was solved by Faller et al, 2004 (6). The 2.5 Å resolution crystal structure revealed a tightly interconnected homooctamer with eight fold rotation symmetry that resembles a goblet-like conformation with a single central channel (Fig I-3). The height of the goblet is 9.6 nm with the largest outer diameter of 8.8 nm. These data corresponds to values derived from negatively stained electron microscopic images of the purified protein (86). Interestingly, the structure is different from typical trimeric porins from Gram-negative bacteria which have one pore per monomer with approximate length of 5 nm (125). The structure also showed that the central zone consists of 16 Asp residues which explain the cation selectivity of MspA as observed before by planar bilayer measurement (89). Moreover, the structure contains two consecutive β-barrels of 3.7 nm length and a hydrophilic globular rim domain. This length contradicts to the typical length of mycobacterial outer membrane which is nearly 5 to 10 nm. Hence it was assumed that this hydrophobic mismatch may be due to partial or complete entry of the hydrophilic rim domain into the outer membrane. This hypothesis was later confirmed by cysteine scanning mutagenesis and Cys accessibility to a membrane impermeable biotinylation reagent (126).

I.7-ii: PorB structure from *C. glutamicum*

The second X-ray structure in the group of porin family from these mycolic acid containing bacteria was a major surprise since PorB appeared to be mostly α-helical (9) (Fig. I-3). The 1.8 Å resolution structure has a 70 residue globular core, based on a four α-helices hold together via a hydrophobic interior like in soluble proteins and stabilized by a disulphide bridge. A pentameric model was proposed in order to explain the ion channel activity (70). The protein has been expressed and purified in fusion with glutathione S-transferase (GST, cleaved with factor Xa on the GST affinity column) in the absence of any detergent, in a water buffer at pH 8, and the fold is stabilized by a disulfide bridge presumably formed during the purification steps. Although the crystallization conditions required the presence of a detergent, one may wonder if the observed conformation does not result from purification conditions, imposing a soluble fold, and if it is really present *in vivo*. In comparison, the β-barrel oligomeric form of MspA had been obtained prior to crystallization by adding detergent and incubating overnight: in these conditions the monomeric MspA converted to oligomers with a high yield. Further

structural studies, for instance using cellular solid state NMR (127) will be required to fully address the question of the *in vivo* PorB fold.

I.7-iii: OmpATb structure from *M. tuberculosis*

The 326 residue OmpATb consists of three domains, the N-terminal domain (1-72 aa), a central B domain (73-200 aa) and a C-terminal domain (201 – 326 aa). The N-terminal domain is responsible for membrane translocation. The B and C domains are separated by a proline rich flexible linker. It has been shown that the B domain alone is capable of forming ion channels, while the C domain is structurally homologous to OmpA-C-like superfamily of periplasmic peptidoglycan-binding sequences. The B and C domain structures have been solved independently by two groups by solution state NMR spectroscopy (7, 8) (Fig. I-3). These NMR solution structures exhibited a mixed α + β fold. The C terminal domain fold is similar to the X-ray structure of OmpA-like domain of the RmpM protein from *N. meningitides* (128). In order to account for ion channel activities of the B domain the authors proposed a pentameric model of OmpATb. However here again, the protein being expressed in a soluble for from *E. coli*, it remains to be demonstrated that the observed structure in solution is identical to the structure in the outer membrane.

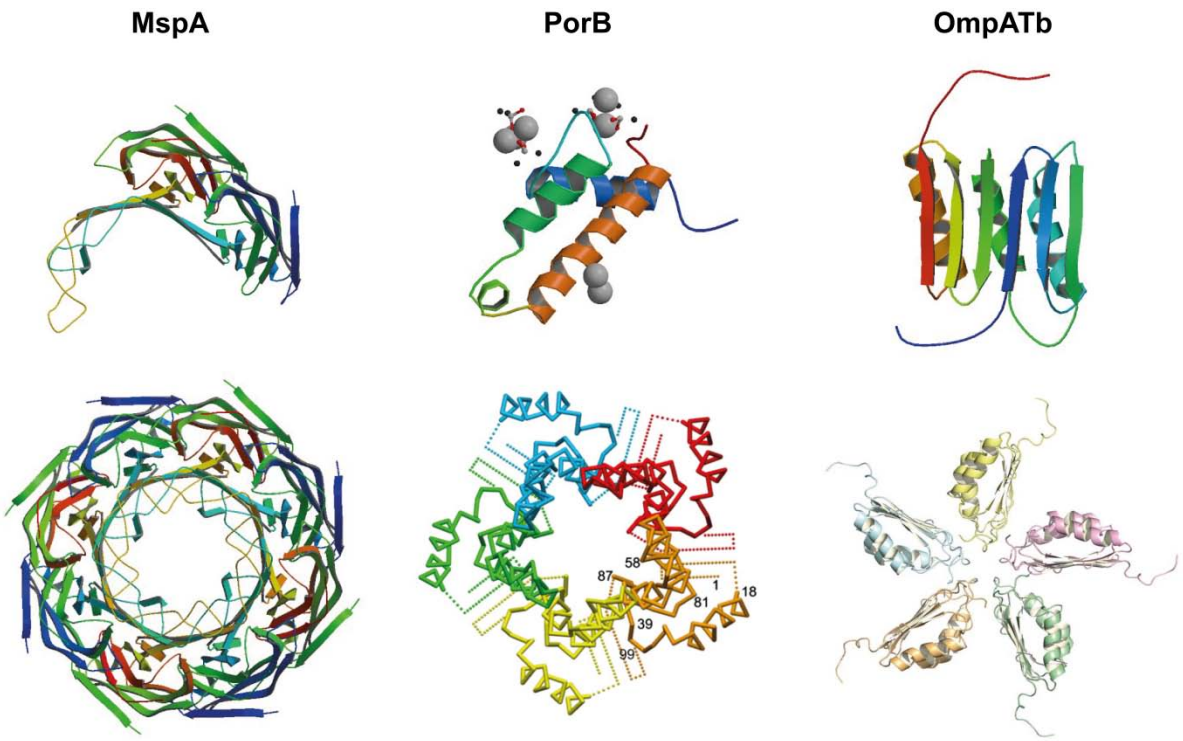

Fig. I-3: High resolution structures of MspA [PDB : 1UUN] (*M. smegmatis*) (6), PorB [PDB : 2VQG] (*C. glutamicum*) (9) and OmpATb central B domain [PDB : 2KSM and 2KGS] (*M. tuberculosis*) (7, 8) are presented. The upper pictures represent their monomeric form whereas, bottom pictures shows their oligomeric structure. While the oligomeric structure of MspA was derived directly from X-ray data, the oligomeric structures of PorB and OmpATb were modeled in order to account for the ion channel activities of these proteins in a bilayer.

I.8: How to move forward for high resolution structural studies?

It is thus essential to characterize the porins functionally before proceeding towards their structure determination and to determine how the extraction procedures have an impact on the channel activities? So far for the functional characterization of the porins from *Mycobacteria*, *Corynebacteria* or *Nocardia*, the cell wall channels were either extracted by organic solvents or by detergents from wild type strains or strains containing over-expressing plasmid constructs. It was observed that the channel forming properties differed whether the channels were extracted with organic solvents or by various detergents. However, in some cases (*M. tuberculosis* channels) the detergent extracted and purified channels show better reconstitution and characteristic properties (as explained above) in planar bilayer measurements. For example, MspA from *M. smegmatis* showed different properties when extracted in Genapol, SDS, and LDAO or in organic solvents (89, 129).

Expression in the native bacterial host versus *E. coli* overexpression

To obtain high resolution structures, a sufficient quantity of stable and functional proteins is required. Therefore, channel proteins have to be produced using various recombinant expression systems. The first porin structure of MspA was solved with over expression of the protein in *E. coli*. MspA lacking the signal peptide was cloned into T7 promoter based vector, pET24+ (Novagen). Over expression in *E. coli* BL21(DE3) cells resulted soluble monomeric form of the polypeptide which is an inactive form of MspA. However, by addition of detergent (0.6 % octyltetraoxethylene, C_8E_4) and overnight incubation of the ammonium sulphate precipitated fraction, functional oligomers was obtained (130). The oligomeric fraction formed suitable crystals and hence an attractive structure of the first discovered porin from *Mycobacteria* was solved (6).

Likewise, PorB from *C. glutamicum* structure was solved after over expressing the protein with GST fusion tag in *E. coli* BL21 (DE3) cells. The protein was purified in a soluble monomeric form, and crystals could be obtained in the presence of detergent at lower pH. (9). However, functional studies of other channel proteins (PorA and PorH) from *Corynebacteria* genus were carried out in the mutant *C. glutamicum* ΔPorA ΔPorH strain. The proteins of interest were cloned into an *E. coli* based shuttle vector pXMJ19 before their over expression (84). But, expression of these proteins from *Corynebacteria* leads to toxicity upon expression in *E. coli* (unpublished result). The other channel proteins from *N. farcinica*, NfpA and NfpB were also expressed similarly in *E. coli* and functionally characterized (85).

In an alternative approach, Cell-Free (CF) expression provides a new and remarkably successful strategy for the production of membrane proteins for which toxicity, membrane targeting and degradation are key issues (131-133). In addition, reaction conditions can easily be modified in order to modulate the quality of synthesized protein samples. With the more efficient continuous exchange CF (CECF) configuration, ion channels can either be synthesized as precipitate form which can be further resolubilized in various detergents or can be directly produced as proteomicelles in presence of non-toxic detergents as was described in case of aquaporins (101, 134, 135). Furthermore, the translated MPs can directly be reconstituted into preformed nanodiscs for structural or functional purpose (136, 137). By doing so, we were able to produce large quantity of PorA and PorH from *C. glutamicum* devoid of their natural mycolic acid modification as re-solubilized precipitates and directly as

proteo-micelles. The CF expressed proteins, devoid of mycoloylations, helped characterizing their role on the channel forming ability (101).

I.9: OUTLOOK AND PERSPECTIVES

We have seen that the CMN group from the class of *Actinobacteria* evolved with a high diversity giving a large number of pathogens and saprophytes. First of all, there is a difference in their genome size compared to their growth properties. The genome size of the pathogenic, slow growing *M. tuberculosis* and *M. leprae* are 4.4 Mb and 3.27 Mb respectively; whereas, the non-pathogenic fast growing *M. smegmatis* has 7 Mb (4). This indicates that the slow growing bacteria are the most recently evolved microorganisms. Moreover, their survival inside protozoa has developed their ability to survive with the deadly conditions inside the macrophages in which a normal saprophyte can't (59, 138, 139). These pathogens are the most ingenious microorganisms which develop some amazing defense mechanism by creating a highly impermeable outer membrane to persist in difficult environments.

To understand the function of such class of membrane proteins, channel activity of the purified proteins is necessary but is certainly not a sufficient requirement to classify them as porins. Indeed, many outer membrane proteins display channel like behavior but have no physiological functions of classical porins. Porins functions to form transient open channels for the passage of solutes across the outer membrane (36, 39, 51). Although their conductance properties shows similarities, there is a huge difference in their amino acid sequence, molecular weights, oligomeric forms, even in their three dimensional folds (Table 1) (6-9). This indicates the presence of a different classes of porin channels functioning in the outer membrane with completely different 3D structures. However, only three porins structures are so far being solved at atomic resolution, though numbers of porins from this group are functionally characterized. Hence, a thorough functional, biochemical and structural analysis of this class of membrane proteins is a prerequisite to fully understand the transport processes across the outer membrane of CMN group of bacteria. This will allow for structure and function based drug discovery against the pathogenic forms.

REFERENCES

1. Minnikin, D. (1982) *The Biology of Mycobacteria*, Academic, London.
2. Stackebrandt, E., Rainey, F. A.&WardRainey, N. L. (1997) Proposal for a new hierarchic classification system, Actinobacteria classis nov *International Journal of Systematic Bacteriology* **47**: 479-491.
3. Fu, L. M.&Fu-Liu, C. S. (2002) Is Mycobacterium tuberculosis a closer relative to Gram-positive or Gram-negative bacterial pathogens? *Tuberculosis* **82**: 85-90.
4. Brosch, R., Pym, A. S., Gordon, S. V.&Cole, S. T. (2001) The evolution of mycobacterial pathogenicity: clues from comparative genomics *Trends Microbiol* **9**: 452-8.
5. Cole, S. T., *et al.* (1998) Deciphering the biology of Mycobacterium tuberculosis from the complete genome sequence (vol 393, pg 537, 1998) *Nature* **396**: 190-198.
6. Faller, M., Niederweis, M.&Schulz, G. E. (2004) The structure of a mycobacterial outer-membrane channel *Science* **303**: 1189-92.
7. Teriete, P., *et al.* (2010) Mycobacterium tuberculosis Rv0899 Adopts a Mixed alpha/beta-Structure and Does Not Form a Transmembrane beta-Barrel *Biochemistry* **49**: 2768-2777.
8. Yang, Y. S., *et al.* (2011) Structure of the Mycobacterium tuberculosis OmpATb protein: A model of an oligomeric channel in the mycobacterial cell wall *Proteins-Structure Function and Bioinformatics* **79**: 645-661.
9. Ziegler, K., Benz, R.&Schulz, G. E. (2008) A putative alpha-helical porin from Corynebacterium glutamicum *J Mol Biol* **379**: 482-91.
10. Bleed, D., Watt, C., Dye, C. (2001), WHO Report, Geneva, 2001).
11. Eggeling, L.&Sahm, H. (1999) L-Glutamate and L-lysine: traditional products wiU1 impetuous developments *Applied Microbiology and Biotechnology* **52**: 146-153.
12. Eggeling, L.&Sahm, H. (2001) The cell wall barrier of Corynebacterium glutamicum and amino acid efflux *Journal of Bioscience and Bioengineering* **92**: 201-213.
13. Wheeler, P. R.&Ratledge, C. (1988) Metabolism in Mycobacterium-Leprae, M-Tuberculosis and Other Pathogenic Mycobacteria *British Medical Bulletin* **44**: 547-561.
14. McNeil, M. R.&Brennan, P. J. (1991) Structure, function and biogenesis of the cell envelope of mycobacteria in relation to bacterial physiology, pathogenesis and drug resistance; some thoughts and possibilities arising from recent structural information *Res Microbiol* **142**: 451-63.
15. Nikaido, H., Kim, S. H.&Rosenberg, E. Y. (1993) Physical organization of lipids in the cell wall of Mycobacterium chelonae *Mol Microbiol* **8**: 1025-30.
16. Zuber, B., *et al.* (2008) Direct visualization of the outer membrane of mycobacteria and corynebacteria in their native state *J Bacteriol* **190**: 5672-80.
17. Puech, V., *et al.* (2001) Structure of the cell envelope of corynebacteria: importance of the non-covalently bound lipids in the formation of the cell wall permeability barrier and fracture plane *Microbiology* **147**: 1365-82.
18. Jarlier, V.&Nikaido, H. (1990) Permeability barrier to hydrophilic solutes in Mycobacterium chelonei *J Bacteriol* **172**: 1418-23.
19. Liu, J., Barry, C. E., 3rd, Besra, G. S.&Nikaido, H. (1996) Mycolic acid structure determines the fluidity of the mycobacterial cell wall *J Biol Chem* **271**: 29545-51.

20. Brennan, P. J.&Nikaido, H. (1995) The envelope of mycobacteria *Annu Rev Biochem* **64**: 29-63.
21. Daffe, M.&Draper, P. (1998) The envelope layers of mycobacteria with reference to their pathogenicity *Advances in Microbial Physiology, Vol 39* **39**: 131-203.
22. Bansal-Mutalik, R.&Nikaido, H. (2011) Quantitative lipid composition of cell envelopes of Corynebacterium glutamicum elucidated through reverse micelle extraction *Proc Natl Acad Sci U S A* **108**: 15360-5.
23. Marchand, C. H., *et al.* (2012) Biochemical disclosure of the mycolate outer membrane of Corynebacterium glutamicum *J Bacteriol* **194**: 587-97.
24. Daffe, M. (2005) in *Handbook of Corynebacterium glutamicum*, ed. Bott, L. E. a. M. (CRC Press, Inc., Boca Raton, FL., pp. 121-148.
25. Minnikin, D. E., Patel, P. V., Alshamaony, L.&Goodfellow, M. (1977) Polar Lipid-Composition in Classification of Nocardia and Related Bacteria *International Journal of Systematic Bacteriology* **27**: 104-117.
26. Minnikin, D. E. (1991) Chemical principles in the organization of lipid components in the mycobacterial cell envelope *Res Microbiol* **142**: 423-7.
27. Minnikin, D. E., Kremer, L., Dover, L. G.&Besra, G. S. (2002) The methyl-branched fortifications of Mycobacterium tuberculosis *Chem Biol* **9**: 545-53.
28. Rastogi, N. (1991) Recent observations concerning structure and function relationships in the mycobacterial cell envelope: elaboration of a model in terms of mycobacterial pathogenicity, virulence and drug-resistance *Res Microbiol* **142**: 464-76.
29. Ortalo-Magne, A., *et al.* (1996) Identification of the surface-exposed lipids on the cell envelopes of Mycobacterium tuberculosis and other mycobacterial species *J Bacteriol* **178**: 456-61.
30. Ortalo-Magne, A., Andersen, A. B.&Daffe, M. (1996) The outermost capsular arabinomannans and other mannoconjugates of virulent and avirulent tubercle bacilli *Microbiology* **142 (Pt 4)**: 927-35.
31. Brennan, P. J. (1988) *In Microbial Lipids, ed* (London: Academic.
32. Lemassu, A.&Daffe, M. (1994) Structural features of the exocellular polysaccharides of Mycobacterium tuberculosis *Biochem J* **297 (Pt 2)**: 351-7.
33. Minnikin, D. E., Patel, P.&Goodfellow, M. (1974) Mycolic acids of representative strains of Nocardia and the 'rhodochrous' complex *FEBS Lett* **39**: 322-4.
34. Barry, C. E., *et al.* (1998) Mycolic acids: Structure, biosynthesis and physiological functions *Progress in Lipid Research* **37**: 143-179.
35. Barry, C. E. (2001) Interpreting cell wall 'virulence factors' of Mycobacterium tuberculosis *Trends in Microbiology* **9**: 237-241.
36. Nikaido, H. (2003) Molecular basis of bacterial outer membrane permeability revisited *Microbiology and Molecular Biology Reviews* **67**: 593-+.
37. Nikaido, H. (1992) Porins and Specific Channels of Bacterial Outer Membranes *Molecular Microbiology* **6**: 435-442.
38. Nikaido, H.&Vaara, M. (1985) Molecular-Basis of Bacterial Outer-Membrane Permeability *Microbiological Reviews* **49**: 1-32.
39. Niederweis, M. (2003) Mycobacterial porins--new channel proteins in unique outer membranes *Mol Microbiol* **49**: 1167-77.

40. Nakae, T. (1976) Outer membrane of Salmonella. Isolation of protein complex that produces transmembrane channels *J Biol Chem* **251**: 2176-8.
41. Schein, S. J., Colombini, M.&Finkelstein, A. (1976) Reconstitution in planar lipid bilayers of a voltage-dependent anion-selective channel obtained from paramecium mitochondria *J Membr Biol* **30**: 99-120.
42. Zalman, L. S., Nikaido, H.&Kagawa, Y. (1980) Mitochondrial outer membrane contains a protein producing nonspecific diffusion channels *J Biol Chem* **255**: 1771-4.
43. Mannella, C. A., Forte, M.&Colombini, M. (1992) Toward the molecular structure of the mitochondrial channel, VDAC *J Bioenerg Biomembr* **24**: 7-19.
44. Blachly-Dyson, E.&Forte, M. (2001) VDAC channels *IUBMB Life* **52**: 113-8.
45. Nikaido, H. (1994) Porins and Specific Diffusion Channels in Bacterial Outer Membranes *Journal of Biological Chemistry* **269**: 3905-3908.
46. Trias, J., Jarlier, V.&Benz, R. (1992) Porins in the cell wall of mycobacteria *Science* **258**: 1479-81.
47. Dumas, F., Koebnik, R., Winterhalter, M.&Van Gelder, P. (2000) Sugar transport through maltoporin of Escherichia coli - Role of polar tracks *Journal of Biological Chemistry* **275**: 19747-19751.
48. Maier, C., Bremer, E., Schmid, A.&Benz, R. (1988) Pore-Forming Activity of the Tsx Protein from the Outer-Membrane of Escherichia-Coli - Demonstration of a Nucleoside-Specific Binding-Site *Journal of Biological Chemistry* **263**: 2493-2499.
49. McElhaney, R. N., de Gier, J.&van der Neut-Kok, E. C. (1973) The effect of alterations in fatty acid composition and cholesterol content on the nonelectrolyte permeability of Acholeplasma laidlawii B cells and derived liposomes *Biochim Biophys Acta* **298**: 500-12.
50. Yates, M. D.&Collins, C. H. (1981) Sensitivity of Opportunist Mycobacteria to Rifampicin and Ethambutol *Tubercle* **62**: 117-121.
51. Hancock, R. E. W.&Brinkman, F. S. L. (2002) Function of Pseudomonas porins in uptake and efflux *Annual Review of Microbiology* **56**: 17-38.
52. Hancock, R. E. W., Farmer, S. W., Li, Z. S.&Poole, K. (1991) Interaction of Aminoglycosides with the Outer Membranes and Purified Lipopolysaccharide and Ompf Porin of Escherichia-Coli *Antimicrobial Agents and Chemotherapy* **35**: 1309-1314.
53. Gomez, J. E.&McKinney, J. D. (2004) M-tuberculosis persistence, latency, and drug tolerance *Tuberculosis* **84**: 29-44.
54. Barker, K., *et al.* (1996) Nonadherent cultures of human monocytes kill Mycobacterium smegmatis, but adherent cultures do not *Infect Immun* **64**: 428-33.
55. Cirillo, J. D., Falkow, S., Tompkins, L. S.&Bermudez, L. E. (1997) Interaction of Mycobacterium avium with environmental amoebae enhances virulence *Infect Immun* **65**: 3759-67.
56. Deretic, V.&Fratti, R. A. (1999) Mycobacterium tuberculosis phagosome *Mol Microbiol* **31**: 1603-9.
57. Taylor, S. J., Ahonen, L. J., de Leij, F. A.&Dale, J. W. (2003) Infection of Acanthamoeba castellanii with Mycobacterium bovis and M. bovis BCG and survival of M. bovis within the amoebae *Appl Environ Microbiol* **69**: 4316-9.

58. Miltner, E. C.&Bermudez, L. E. (2000) Mycobacterium avium grown in Acanthamoeba castellanii is protected from the effects of antimicrobials *Antimicrob Agents Chemother* **44**: 1990-4.
59. Steinert, M., Birkness, K., White, E., Fields, B.&Quinn, F. (1998) Mycobacterium avium bacilli grow saprozoically in coculture with Acanthamoeba polyphaga and survive within cyst walls *Appl Environ Microbiol* **64**: 2256-61.
60. Sassetti, C. M., Boyd, D. H.&Rubin, E. J. (2003) Genes required for mycobacterial growth defined by high density mutagenesis *Mol Microbiol* **48**: 77-84.
61. Sassetti, C. M.&Rubin, E. J. (2003) Genetic requirements for mycobacterial survival during infection *Proceedings of the National Academy of Sciences of the United States of America* **100**: 12989-12994.
62. Mailaender, C., *et al.* (2004) The MspA porin promotes growth and increases antibiotic susceptibility of both Mycobacterium bovis BCG and Mycobacterium tuberculosis *Microbiology* **150**: 853-64.
63. Stahl, C., *et al.* (2001) MspA provides the main hydrophilic pathway through the cell wall of Mycobacterium smegmatis *Molecular Microbiology* **40**: 451-464.
64. Wolschendorf, F., Mahfoud, M.&Niederweis, M. (2007) Porins are required for uptake of phosphates by Mycobacterium smegmatis *Journal of Bacteriology* **189**: 2435-2442.
65. Stephan, J., *et al.* (2005) The growth rate of Mycobacterium smegmatis depends on sufficient porin-mediated influx of nutrients *Molecular Microbiology* **58**: 714-730.
66. Jones, C. M.&Niederweis, M. (2010) Role of Porins in Iron Uptake by Mycobacterium smegmatis *Journal of Bacteriology* **192**: 6411-6417.
67. Raynaud, C., *et al.* (2002) The functions of OmpATb, a pore-forming protein of Mycobacterium tuberculosis *Molecular Microbiology* **46**: 191-201.
68. Song, H., *et al.* (2011) Expression of the ompATb operon accelerates ammonia secretion and adaptation of Mycobacterium tuberculosis to acidic environments *Mol Microbiol* **80**: 900-18.
69. Schiller, I., *et al.* (2009) Assessment of Mycobacterium tuberculosis OmpATb as a novel antigen for the diagnosis of bovine tuberculosis *Clin Vaccine Immunol* **16**: 1314-21.
70. Costa-Riu, N., *et al.* (2003) Identification of an anion-specific channel in the cell wall of the Gram-positive bacterium Corynebacterium glutamicum *Mol Microbiol* **50**: 1295-308.
71. Costa-Riu, N., Burkovski, A., Kramer, R.&Benz, R. (2003) PorA represents the major cell wall channel of the Gram-positive bacterium Corynebacterium glutamicum *J Bacteriol* **185**: 4779-86.
72. Lichtinger, T., *et al.* (2001) The low-molecular-mass subunit of the cell wall channel of the Gram-positive Corynebacterium glutamicum. Immunological localization, cloning and sequencing of its gene porA *Eur J Biochem* **268**: 462-9.
73. Nakamura, J., Hirano, S., Ito, H.&Wachi, M. (2007) Mutations of the Corynebacterium glutamicum NCgl1221 gene, encoding a mechanosensitive channel homolog, induce L-glutamic acid production *Appl Environ Microbiol* **73**: 4491-8.
74. Nottebrock, D., Meyer, U., Kramer, R.&Morbach, S. (2003) Molecular and biochemical characterization of mechanosensitive channels in Corynebacterium glutamicum *Fems Microbiology Letters* **218**: 305-309.

75. Ruffert, S., Lambert, C., Peter, H., Wendisch, V. F.&Kramer, R. (1997) Efflux of compatible solutes in Corynebacterium glutamicum mediated by osmoregulated channel activity *European Journal of Biochemistry* **247**: 572-580.
76. Ruffert, S., Berrier, C., Kramer, R.&Ghazi, A. (1999) Identification of mechanosensitive ion channels in the cytoplasmic membrane of Corynebacterium glutamicum *Journal of Bacteriology* **181**: 1673-1676.
77. Morbach, S.&Kramer, R. (2003) Impact of transport processes in the osmotic response of Corynebacterium glutamicum *Journal of Biotechnology* **104**: 69-75.
78. Danilchanka, O., Pavlenok, M.&Niederweis, M. (2008) Role of porins for uptake of antibiotics by Mycobacterium smegmatis *Antimicrobial Agents and Chemotherapy* **52**: 3127-3134.
79. Ellis, T. N.&Kuehn, M. J. (2010) Virulence and immunomodulatory roles of bacterial outer membrane vesicles *Microbiol Mol Biol Rev* **74**: 81-94.
80. Massari, P., Ram, S., Macleod, H.&Wetzler, L. M. (2003) The role of porins in neisserial pathogenesis and immunity *Trends in Microbiology* **11**: 87-93.
81. Kuehn, M. J.&Kesty, N. C. (2005) Bacterial outer membrane vesicles and the host-pathogen interaction *Genes Dev* **19**: 2645-55.
82. Prasadarao, N. V., *et al.* (1996) Outer membrane protein A of Escherichia coli contributes to invasion of brain microvascular endothelial cells *Infect Immun* **64**: 146-53.
83. Cowan, S. W., *et al.* (1992) Crystal-Structures Explain Functional-Properties of 2 Escherichia-Coli Porins *Nature* **358**: 727-733.
84. Barth, E., Barcelo, M. A., Klackta, C.&Benz, R. (2010) Reconstitution experiments and gene deletions reveal the existence of two-component major cell wall channels in the genus Corynebacterium *J Bacteriol* **192**: 786-800.
85. Klackta, C., Knorzer, P., Riess, F.&Benz, R. (2011) Hetero-oligomeric cell wall channels (porins) of Nocardia farcinica *Biochim Biophys Acta* **1808**: 1601-10.
86. Engelhardt, H., Heinz, C.&Niederweis, M. (2002) A tetrameric porin limits the cell wall permeability of Mycobacterium smegmatis *Journal of Biological Chemistry* **277**: 37567-37572.
87. Kessel, M., Brennan, M. J., Trus, B. L., Bisher, M. E.&Steven, A. C. (1988) Naturally Crystalline Porin in the Outer-Membrane of Bordetella-Pertussis *Journal of Molecular Biology* **203**: 275-278.
88. Trias, J.&Benz, R. (1993) Characterization of the channel formed by the mycobacterial porin in lipid bilayer membranes. Demonstration of voltage gating and of negative point charges at the channel mouth *J Biol Chem* **268**: 6234-40.
89. Niederweis, M., *et al.* (1999) Cloning of the mspA gene encoding a porin from Mycobacterium smegmatis *Mol Microbiol* **33**: 933-45.
90. Lichtinger, T., *et al.* (1999) Evidence for a small anion-selective channel in the cell wall of Mycobacterium bovis BCG besides a wide cation-selective pore *Febs Letters* **454**: 349-355.
91. Riess, F. G., Dorner, U., Schiffler, B.&Benz, R. (2001) Study of the properties of a channel-forming protein of the cell wall of the gram-positive bacterium Mycobacterium phlei *J Membr Biol* **182**: 147-57.

92. Senaratne, R. H., *et al.* (1998) Expression of a gene for a porin-like protein of the OmpA family from Mycobacterium tuberculosis H37Rv *Journal of Bacteriology* **180**: 3541-3547.
93. Molle, V., *et al.* (2006) pH-dependent pore-forming activity of OmpATb from Mycobacterium tuberculosis and characterization of the channel by peptidic dissection *Molecular Microbiology* **61**: 826-837.
94. Siroy, A., *et al.* (2008) Rv1698 of Mycobacterium tuberculosis represents a new class of channel-forming outer membrane proteins *Journal of Biological Chemistry* **283**: 17827-17837.
95. Rudel, T., *et al.* (1996) Modulation of Neisseria porin (PorB) by cytosolic ATP/GTP of target cells: Parallels between pathogen accommodation and mitochondrial endosymbiosis *Cell* **85**: 391-402.
96. Niederweis, M., Maier, E., Lichtinger, T., Benz, R.&Kramer, R. (1995) Identification of channel-forming activity in the cell wall of Corynebacterium glutamicum *J Bacteriol* **177**: 5716-8.
97. Lichtinger, T., Burkovski, A., Niederweis, M., Kramer, R.&Benz, R. (1998) Biochemical and biophysical characterization of the cell wall porin of Corynebacterium glutamicum: the channel is formed by a low molecular mass polypeptide *Biochemistry* **37**: 15024-32.
98. Hunten, P., Costa-Riu, N., Palm, D., Lottspeich, F.&Benz, R. (2005) Identification and characterization of PorH, a new cell wall channel of Corynebacterium glutamicum *Biochim Biophys Acta* **1715**: 25-36.
99. Hunten, P., Schiffler, B., Lottspeich, F.&Benz, R. (2005) PorH, a new channel-forming protein present in the cell wall of Corynebacterium efficiens and Corynebacterium callunae *Microbiology* **151**: 2429-38.
100. Huc, E., *et al.* (2010) O-mycoloylated proteins from Corynebacterium: an unprecedented post-translational modification in bacteria *J Biol Chem* **285**: 21908-12.
101. Rath, P., *et al.* (2011) Functional expression of the PorAH channel from Corynebacterium glutamicum in cell-free expression systems: implications for the role of the naturally occurring mycolic acid modification *J Biol Chem* **286**: 32525-32.
102. Riess, F. G., *et al.* (1998) The cell wall porin of Nocardia farcinica: biochemical identification of the channel-forming protein and biophysical characterization of the channel properties *Molecular Microbiology* **29**: 139-150.
103. Riess, F. G.&Benz, R. (2000) Discovery of a novel channel-forming protein in the cell wall of the non-pathogenic Nocardia corynebacteroides *Biochimica Et Biophysica Acta-Biomembranes* **1509**: 485-495.
104. Riess, F. G., Lichtinger, T., Yassin, A. F., Schaal, K. P.&Benz, R. (1999) The cell wall porin of the gram-positive bacterium Nocardia asteroides forms cation-selective channels that exhibit asymmetric voltage dependence *Archives of Microbiology* **171**: 173-182.
105. Lichtinger, T., Reiss, G.&Benz, R. (2000) Biochemical identification and biophysical characterization of a channel-forming protein from Rhodococcus erythropolis *Journal of Bacteriology* **182**: 764-770.
106. Riess, F. G., *et al.* (2003) The cell wall of the pathogenic bacterium Rhodococcus equi contains two channel-forming proteins with different properties *Journal of Bacteriology* **185**: 2952-2960.

107. Dorner, U., Maier, E.&Benz, R. (2004) Identification of a cation-specific channel (tipA) in the cell wall of the Gram-positive mycolata Tsukamurella inchonensis: the gene of the channel-forming protein is identical to mspA of Mycobacterium smegmatis and mppA of Mycobacterium phlei *Biochimica Et Biophysica Acta-Biomembranes* **1667**: 47-55.
108. Hou, J. M., *et al.* (2008) ATPase activity of Mycobacterium tuberculosis SecA1 and SecA2 proteins and its importance for SecA2 function in macrophages *Journal of Bacteriology* **190**: 4880-4887.
109. McDonough, J. A., *et al.* (2008) Identification of functional Tat signal sequences in Mycobacterium tuberculosis proteins *Journal of Bacteriology* **190**: 6428-6438.
110. Braunstein, M., Brown, A. M., Kurtz, S.&Jacobs, W. R. (2001) Two nonredundant SecA homologues function in mycobacteria *Journal of Bacteriology* **183**: 6979-6990.
111. van Wely, K. H. M., Swaving, J., Freudl, R.&Driessen, A. J. M. (2001) Translocation of proteins across the cell envelope of Gram-positive bacteria *Fems Microbiology Reviews* **25**: 437-454.
112. Feltcher, M. E., Sullivan, J. T.&Braunstein, M. (2010) Protein export systems of Mycobacterium tuberculosis: novel targets for drug development? *Future Microbiology* **5**: 1581-1597.
113. Ligon, L. S., Hayden, J. D.&Braunstein, M. (2012) The ins and outs of Mycobacterium tuberculosis protein export *Tuberculosis* **92**: 121-132.
114. Rosch, J.&Caparon, M. (2004) A Microdomain for protein secretion in Gram-positive bacteria *Science* **304**: 1513-1515.
115. Abdallah, A. M., *et al.* (2009) PPE and PE_PGRS proteins of Mycobacterium marinum are transported via the type VII secretion system ESX-5 *Molecular Microbiology* **73**: 329-340.
116. De Buck, E., Lammertyn, E.&Anne, J. (2008) The importance of the twin-arginine translocation pathway for bacterial virulence *Trends in Microbiology* **16**: 442-453.
117. Barreiro, C., Gonzalez-Lavado, E., Patek, M.&Martin, J. F. (2004) Transcriptional analysis of the groES-groEL1, groEL2, and dnaK genes in Corynebacterium glutamicum: Characterization of heat shock-induced promoters *Journal of Bacteriology* **186**: 4813-4817.
118. De Sousa-D'Auria, C., *et al.* (2003) New insights into the biogenesis of the cell envelope of corynebacteria: identification and functional characterization of five new mycoloyltransferase genes in Corynebacterium glutamicum *FEMS Microbiol Lett* **224**: 35-44.
119. Brand, S., Niehaus, K., Puhler, A.&Kalinowski, J. (2003) Identification and functional analysis of six mycolyltransferase genes of Corynebacterium glutamicum ATCC 13032: the genes cop1, cmt1, and cmt2 can replace each other in the synthesis of trehalose dicorynomycolate, a component of the mycolic acid layer of the cell envelope *Arch Microbiol* **180**: 33-44.
120. Nikaido, H.&Rosenberg, E. Y. (1981) Effect on solute size on diffusion rates through the transmembrane pores of the outer membrane of Escherichia coli *J Gen Physiol* **77**: 121-35.
121. Renkin, E. M. (1954) Filtration, diffusion, and molecular sieving through porous cellulose membranes *J Gen Physiol* **38**: 225-43.

122. Collins, M. D., Goodfellow, M.&Minnikin, D. E. (1982) A Survey of the Structures of Mycolic Acids in Corynebacterium and Related Taxa *Journal of General Microbiology* **128**: 129-149.
123. Schindler, H.&Rosenbusch, J. P. (1981) Matrix protein in planar membranes: clusters of channels in a native environment and their functional reassembly *Proc Natl Acad Sci U S A* **78**: 2302-6.
124. Sen, K., Hellman, J.&Nikaido, H. (1988) Porin channels in intact cells of Escherichia coli are not affected by Donnan potentials across the outer membrane *J Biol Chem* **263**: 1182-7.
125. Koebnik, R., Locher, K. P.&Van Gelder, P. (2000) Structure and function of bacterial outer membrane proteins: barrels in a nutshell *Mol Microbiol* **37**: 239-53.
126. Mahfoud, M., Sukumaran, S., Hulsmann, P., Grieger, K.&Niederweis, M. (2006) Topology of the porin MspA in the outer membrane of Mycobacterium smegmatis *J Biol Chem* **281**: 5908-15.
127. Renault, M., *et al.* (2012) Cellular solid-state nuclear magnetic resonance spectroscopy *Proc Natl Acad Sci U S A* **109**: 4863-8.
128. Grizot, S.&Buchanan, S. K. (2004) Structure of the OmpA-like domain of RmpM from Neisseria meningitidis *Mol Microbiol* **51**: 1027-37.
129. Kartmann, B., Stengler, S.&Niederweis, M. (1999) Porins in the cell wall of Mycobacterium tuberculosis *Journal of Bacteriology* **181**: 6543-6546.
130. Heinz, C., Karosi, S.&Niederweis, M. (2003) High-level expression of the mycobacterial porin MspA in Escherichia coli and purification of the recombinant protein *J Chromatogr B Analyt Technol Biomed Life Sci* **790**: 337-48.
131. Savage, D. F., Anderson, C. L., Robles-Colmenares, Y., Newby, Z. E.&Stroud, R. M. (2007) Cell-free complements in vivo expression of the E. coli membrane proteome *Protein Sci* **16**: 966-76.
132. Klammt, C., *et al.* (2006) Cell-free expression as an emerging technique for the large scale production of integral membrane protein *Febs J* **273**: 4141-53.
133. Schwarz, D., Dotsch, V.&Bernhard, F. (2008) Production of membrane proteins using cell-free expression systems *Proteomics* **8**: 3933-46.
134. Schwarz, D., *et al.* (2007) Preparative scale expression of membrane proteins in Escherichia coli-based continuous exchange cell-free systems *Nat Protoc* **2**: 2945-57.
135. Kai, L., *et al.* (2010) Preparative scale production of functional mouse aquaporin 4 using different cell-free expression modes *PLoS One* **5**: e12972.
136. Roos, C., *et al.* (2012) Co-translational association of cell-free expressed membrane proteins with supplied lipid bilayers *Mol Membr Biol*.
137. Lyukmanova, E. N., *et al.* (2012) Lipid-protein nanodiscs for cell-free production of integral membrane proteins in a soluble and folded state: Comparison with detergent micelles, bicelles and liposomes *Biochimica Et Biophysica Acta-Biomembranes* **1818**: 349-358.
138. Brown, M. R.&Barker, J. (1999) Unexplored reservoirs of pathogenic bacteria: protozoa and biofilms *Trends Microbiol* **7**: 46-50.
139. Winiecka-Krusnell, J.&Linder, E. (2001) Bacterial infections of free-living amoebae *Research in Microbiology* **152**: 613-619.

Objectives of the present work

In the light of the comprehensive review of the porins from *Corynebacterineae*, the objectives of this work can be formulated as follows:

1. Expression and Purification of PorA and PorH in *C. glutamicum* and their biophysical characterizations. [Chapter II]

2. Cell – Free expression of PorA and PorH and their biophysical characterization [Chapter III]

3. Biophysical studies of Trehalose 6,6'- dimycolate from *C. glutamicum* [Chapter IV]

4. *In vitro* reconstitution and characterization of PorAH complex in micelles and in trehalose dimycolate vesicles [Chapter V]

Chapter II

Expression and Purification of PorA and PorH in *Corynebacterium glutamicum*

and their biophysical characterizations

Summary

This chapter summarizes the production of PorA and PorH in the host *C. glutamicum* so that the proteins are produced with their natural covalent mycolic acid modification. Various expression conditions in both rich and minimal media were optimized to improve the yield of expression for structural purpose. Samples were purified to homogeneity by both affinity and size exclusion chromatography. The presence of mycolic acid modification on both PorA and PorH were verified by MALDI TOF mass spectrometry analysis. CD and NMR spectra of ^{15}N and ^{13}C uniformly labeled PorA and PorH samples indicated pure and homogeneous sample, compatible with structural analyses. Functional assay of both proteins by black lipid membrane ion channel measurements confirmed that a complex associating both PorA and PorH, with their post translational modification is required to form an ion channel with typical characteristics of bacterial outer membrane porins.

II.1: PorA and PorH DNA constructs

The $PorA_{NHis}$ and $PorH_{CHis}$ constructs used in this work were obtained from Roland Benz's lab (Jacobs University, Bremen, Germany). The constructs were made in *C. glutamicum* / *E. coli* shuttle vector pXMJ19 (annex, page 159). The vector was constructed with a combination of high copy number *E. coli* plasmid (pK18) and the low copy number *C. glutamicum* plasmid (pBL1) as described (1). The resulting pXMJ19 vector has IPTG induced p*tac* promotor, *laq*I repressor and relatively higher chloramphenicol resistance (up to 50 µg/ml). The construction and cloning of $PorA_{NHis}$ and $PorH_{Chis}$ into pXMJ19 were described in the article of Barth et al (2). The original DNA, protein sequences and the physicochemical parameters were noted in the annexes, page 182. As the presence of affinity tags at the N-terminus of PorA affected the activity, we made a PorA construct with histidine tag at the C-terminus of PorA. For expression in *E. coli*, PorA and PorH were sub-cloned into pET28a and pIVEX2.3d vectors respectively as explained in the molecular biology section of annexe.

II.2-i: Optimization of expression in rich medium

The over-expression of PorA and PorH were analyzed in *C. glutamicum* cells harboring pXMJ19 vector containing $PorA_{Nhis}$ and $PorH_{Chis}$ genes and grown in brain heart infusion (BHI) medium. But before the test of over expression we monitored the growth kinetics of *C. glutamicum* cells in BHI medium and we observed that the exponential phase starts at optical density (OD) ~ 2-3, the stationary phase continued from ~ 12 of the growth cycle. Then the growth of the culture without and with induction with 1 mM IPTG was monitored at regular interval by observing the OD at 600 nm. In order to produce the proteins without mycolic acid modification, the over expression of PorA and PorH in *E. coli* (BL21) cells harboring pET28a constructs of respective DNA fragments were analyzed without and with induction with 1mM IPTG by observing their growth in terrific broth (TB) medium. As shown in the figure II-1, the growth of induced *C. glutamicum* cells reduced only slightly compared to non-induced cells, both for PorA and PorH. Instead, the growth of *E. coli* cells over-expressing PorA was almost stationary upon induction leading to death phase of the growth cycle. In the otherhand, though the growth was not much affected in case of PorH, no expression of PorH was observed upon induction (Fig. II-1). This indicates that the over-expression of PorA is toxic to *E. coli*, whereas the over-expression of PorH does not affect the growth of *E. coli* and *C. glutamicum*.

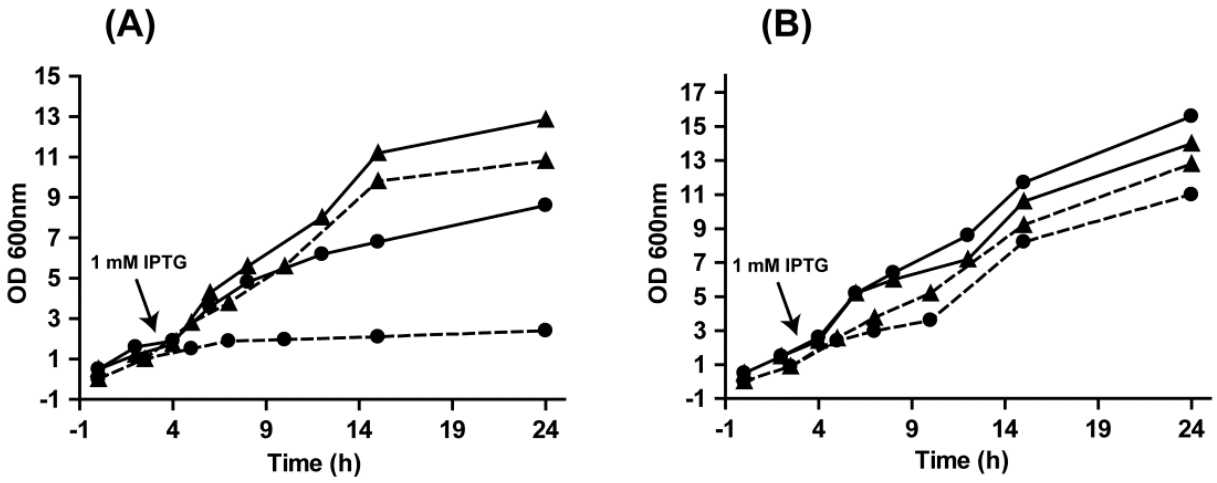

Fig. II-1: Growth curve of *C. glutamicum* (in solid line) and *E. coli* (dotted lines) cells on the expression of (A) PorA and (B) PorH. Curves marked with triangle are without induction, whereas curves marked with circles are cells that are induced with 1mM IPTG in the early exponential phase.

II.2-ii: Optimization of expression in minimal medium

For the industrial production of amino acids such as Lysine and Glutamate *C. glutamicum* is usually grown in a minimal medium (3-6). The minimal medium used in this work is a modification of the composition as cited before (7). The detailed composition of the minimal medium used in this work is given in the experimental procedure (page 165). The media are basically composed of three major groups of components; (i) a source of nitrogen such as NH_4Cl (used in this work) or $(NH_4)_2SO_4$, phosphate buffers of Na and K, a source of Carbon such as glucose (used in this work, other sugars may be preferred) and methanol or ethanol (ii) a mixture of trace or mineral elements and (iii) supplementary components such as biotin and protocatechuic acid, added for enhancing the glucose consumption during the culture.

Similar to rich medium before the test of over expression we monitored the growth kinetics of non-induced *C. glutamicum* cells in minimal medium and we observed that the exponential phase of the cycle starts at OD ~ 5-6, followed by a long stationary phase at the OD from 25 to 35 of the growth cycle (this growth kinetics was observed with a media containing 20 g/L NH_4Cl and 2 % glucose). But the growth curve may change by varying the important components such as the nitrogen and carbon sources in the culture media.

In this work one of the major objectives is to produce sufficient quantities of PorA and PorH for structural studies. Also as both proteins exist in the cell membrane, we tried to maximize the total cell mass after over-expression by varying different quantities of NH_4Cl and glucose in the minimal media. Further, these optimization steps help in increasing the yield of ^{15}N- and ^{13}C- labeled proteins for NMR studies. As shown in the figure II-2, the OD at 600 nm at the stationary phase measure for the various concentrations of glucose significantly affects the growth of *C. glutamicum* cells with substantial quantities of cells obtained beyond 1 % of glucose concentration whereas NH_4Cl has a minimal effect. Hence in this study 2 g/L of NH_4Cl and 2 % glucose in the minimal medium were used for further expression of PorA and PorH. Furthermore, the over expression of PorA and PorH in *E. coli* (BL21) cells were grown in non-inducible and auto-inducible minimal medium. Similar to over-expression in rich medium, PorA expression was more toxic to cells than PorH, in both non-inducible and auto-inducible culture medium (data not shown).

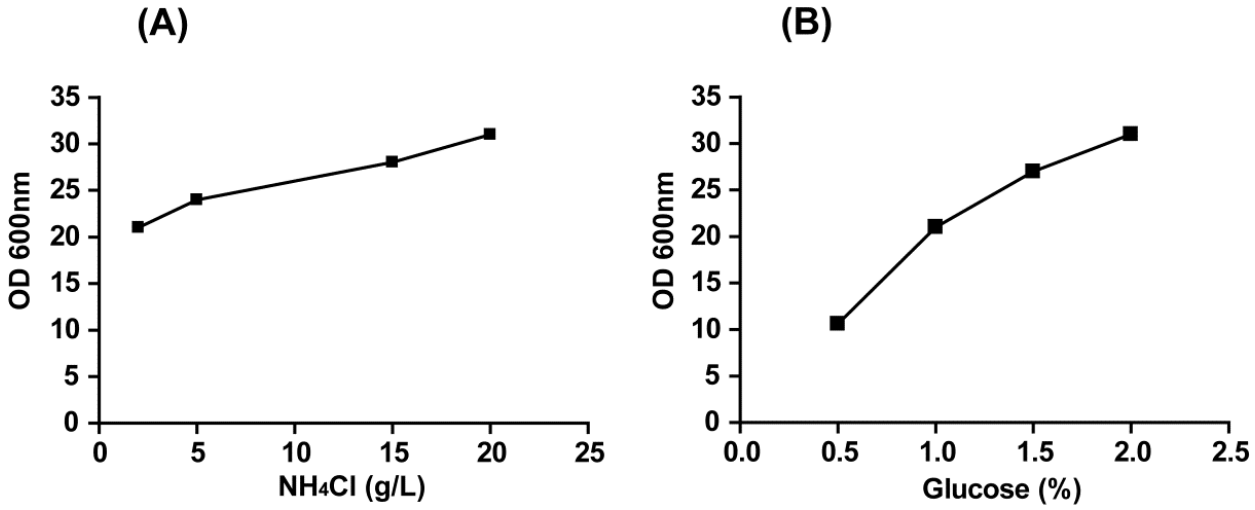

Fig. II-2: Optimization of different (A) NH_4Cl and (B) glucose quantities in the minimal media to increase the total cell mass and thereby the expression of PorA and PorH.

II.3: Extraction and purification of PorA and PorH

Once the over-expression of PorA and PorH were optimized in both rich media and minimal media, the cells were harvested by centrifugation and followed by an extraction step. Generally three different procedures were used to extract the wild type proteins for functional studies from the thick cell wall of *C. glutamicum* (8-10). (i) Breaking the cell by French press followed by isolation of the cell wall proteins by sucrose density and analytical centrifugation, (ii) extraction of cell wall proteins by organic solvent and (iii) extraction of whole cell wall

proteins by detergents. Our attempts to extract PorA and PorH using French press leads to substantial loss of material before purification step. Hence extraction by using organic solvent and various detergents were used in this work to extract and further purify PorA and PorH from the over expressed *C. glutamicum* cells.

II.3-i: Extraction of PorA and PorH using organic solvent

The harvested cells were mixed and agitated over night at room temperature with $CHCl_3$:CH_3OH (1:2) with a proportion of 12 ml of solvent for 1g of total cell mass. The cell extracts were centrifuged and the supernatant were mixed with diethyl ether (2x volume) and kept at -20 ^{0}C for a minimum of 24 hs. During this step most of the cell wall lipids remained soluble in the organic part, while the proteins precipitated. The precipitated proteins were solubilized in 10 mM Tris-Cl, pH 8.0, 100 mM NaCl and 0.4 % LDAO or 1 % Triton X-100 before moving to purification steps.

II.3-ii: Extraction of PorA and PorH using various detergents

As detergents have the properties of mimicking the phospholipids of the cell membrane with its higher hydrophobic content, they have been used to extract the cell wall proteins. In this work various detergents were screened to extract the whole cell wall proteins from the over expressed *C. glutamicum* cells. For this purpose 0.4 g cells expressing $PorA_{His}$ were extracted for 3 hs at room temperature with 2 ml solvent containing 2x CMC (Critical Micelle Concentration) of each $C_{12}E_8$, Brij 35, Triton X-100, OG and LDAO. Each supernatant were purified through Talon affinity column as explained in the experimental procedure (Annex, page 167). Equal amount of the supernatant of whole cell extraction and the eluted protein fractions were analyzed on 16 % Tris-Tricin SDS-PAGE followed by Coomassie blue and silver staining. As shown in the figure II-3A, it is obvious that LDAO, OG and Triton X-100 have higher efficiency of extracting the whole cell wall proteins and also the band intensity indicates higher quantity of PorA in the eluted fractions in LDAO. This was also verified by quantifying the whole cell extraction and eluted proteins by BCA method (described in annexes, page 181). Moreover extractions with higher concentrations (3x, 5x and 10x CMC) of LDAO did not improve the yield of extraction. Hence hereafter all extractions steps of PorA and PorH expressed cells were carried out using 0.4 % LDAO and also kept constant during the purification steps.

II.3-iii: Purification of organic solvent or detergent extracted PorA and PorH

As both proteins have histidine affinity tags either at N-terminus or C-terminus of the construct, after extraction steps (explained above) the proteins were purified by Ni-NTA affinity column. The purification steps were explained in details in the experimental procedures (Annex, page 167). After binding to the affinity column, the contaminant proteins were washed out thoroughly and finally PorA and PorH were eluted by applying higher concentration of imidazole (250 mM) in the washing buffer. After affinity purification step, respective tags were cleaved by specific proteases (Thrombin or Factor Xa) and finally passed through an pre-equilibrated Superdex 200 size exclusion column. The purity and homogeneity of PorA and PorH after each purification steps were analyzed by SDS-PAGE followed by either Coomassie blue or silver staining. Affinity purified proteins were also verified by western blot followed by immunoblotting with anti-his antibodies (Fig. II-3B). Purified proteins were quantified either by BCA method or nanodrop absorbance using the molar extinction co-efficient of PorA (8250 cm^{-1} M^{-1}) and PorH (1280 cm^{-1} M^{-1}) respectively. Purified proteins were further biochemically and biophysically characterized.

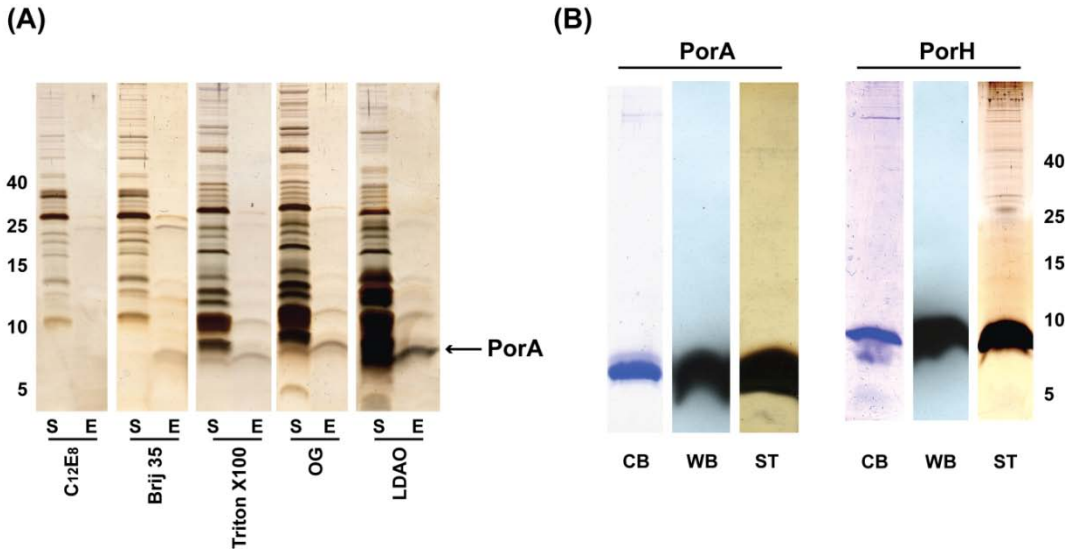

Fig. II-3: Extraction and purification profile of PorA and PorH. (A) Silver stained SDS-PAGE showing extraction of over-expressed $PorA_{Chis}$ from *C. glutamicum* cell wall by 2x - CMC of each detergent mentioned in the figure. S : supernatant after extraction and E : elution after batch purification with Ni-NTA affinity column. (B) Purification of $PorA_{Chis}$ and $PorH_{Chis}$ after Ni-NTA and Superdex S200 size exclusion column, verified with running a SDS-PAGE followed by Coomassie Blue (CB) staining, Western Blotting (WB) with anti-His antibodies and Silver staining (ST).

II.4: Optimization of fermentation condition to maximize yield of expression

When the culture of PorA and PorH were grown in minimal media using batch system, it was observed that during the period of growth the pH of the medium decreases from 7.3 to 4.9 at the end of expression. This is because, *C. glutamicum* during its growth, produces large amount of glutamic acids which acidified the culture medium. Hence to understand whether the change of pH may affect the expression of PorA and PorH or not, a 5 L fermenter (INFORS AG, Bottimgen, Swizerland) was used to maintain the pH (with 3 M NaOH and 20 % H_3PO_4) during the expression. Moreover a great advantage of using a fermenter is that most of the parameters such as oxygenation, pressure, growth temperature and pH are also been monitored and adjusted throughout the expression. Though there is a minor difference in the growth kinetics between batch mode of expression and expression using fermenter, after extraction and purification procedures it was observed that by maintaining the pH the yield of PorA increased by nearly 40 % (Fig. II-4). Hereafter for expression of PorA and PorH in the optimized minimal medium were carried out by using a fermenter making the following parameters constant; stirring = 300 rpm, pO_2 = 25 and pH 7.3.

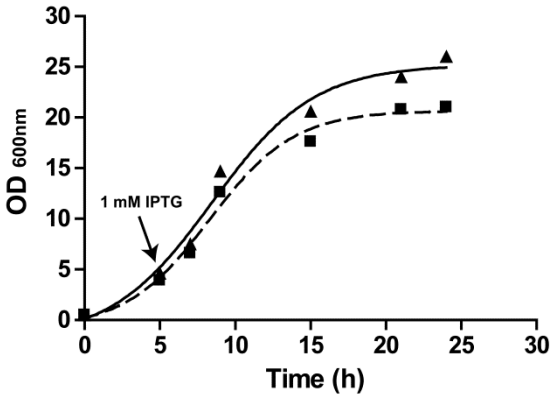

Parameter	Batch	Fermenter
Final pH after expression	4.9	7.3
Yield (mg) / 2 L of culture	3.52	5.76

Fig. II-4: Growth curve of $PorA_{Chis}$ in minimal medium under expression in batch mode (dotted line) and in fermentation mode (solid line). Table shows the increase in quantity of $PorA_{Chis}$ produced when the pH during expression is maintained by using fermenter.

II.5-i: MALDI TOF mass spectrometry

With the recent development in the technique, mass spectrometry (MS) is emerging as an essential tool in the field of proteomics and molecular biology. MS is becoming a method of choice for complex protein analysis such as analysis of protein primary sequence, post-translational modifications (PTMs) and also protein-protein interactions (11-16).

As PorA and PorH are post-translationally modified by mycolic acids, we used MALDI-TOF to analyze the modification of purified proteins. To date nearly 300 PTMs of proteins are discovered physiologically which controls many biological processes and mechanisms of cell regulations including signal transduction. The most common PTMs in proteins are glycosylation, phosphorylation, acetylation, cysteine oxidation, cysteine nitrosylation and ubiquitinilation (17-19). Recently O-linked acetylations are found for the first time in bacteria in the members of *Corynebacterineae* suborder. Proteins of these bacteria including PorA and PorH are esterified by long chain α-alkyl, β-hydroxy fatty acids so called mycolic acids (20).

In the present work, the presence of mycolic acid modification on *C. glutamicum* expressed and purified PorA and PorH were characterized by MALDI-TOF mass spectrometry. The theoretical masses of native PorA and PorH without modification and with initial methionine are, for ($M + H^+$), 4681 Da and 6162 Da (20). In the case of recombinant PorA (with N-terminal His tag) and PorH (with C-terminal His tag) constructs, after cleavage of the affinity tags used for purification of PorA and PorH, the predicted ($M + H^+$) masses without mycoloylation are 4549 Da for PorA, 6617 Da for PorH. To detect the modification, PorA and PorH samples were treated with 0.1 M NaOH for 1 h at room temperature (saponification condition which hydrolyses an ester bond and thus removes the mycolic acid) and spectra were measured. As shown in figure II-5, MALDI-TOF spectra of purified PorA and PorH with and without saponification confirmed the presence of mycolic acid modification with a difference of 478 Da corresponding to C32:0 naturally-occurring corynomycolic residues, as was described earlier.

Sample preparation for MS measurements is an important step to obtain a spectrum with enhanced signal/noise ratio. As purified PorA and PorH contain substantial quantity of LDAO, we used the protocol described by Yeung et. al. using ethyl acetate to eliminate the excess of

detergent (21). Hence the protein samples were washed for a minimum of 5 times with equal volume of ethyl acetate before mixing with sinapinnic acid (3,5-dimethoxy-4-hydroxycinnamic acid) as matrix (Annex, page 183).

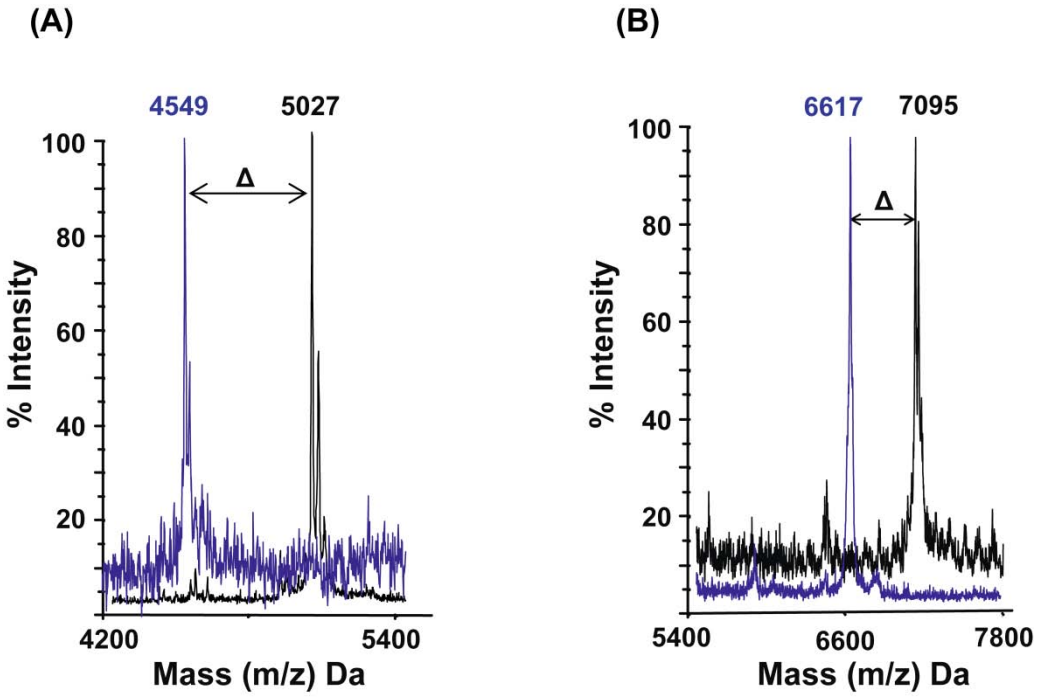

Fig. II-5: MALDI TOF mass spectra of (A) PorA and (B) PorH with (in black) and without (in blue) mycolic acid (Δ = 478 Da) modification. The protein samples were saponified with 0.1 M NaOH to break the ester bond between the mycolic acid and protein.

II.5-ii: Circular Dichroism of PorA and PorH

Circular Dichroism (CD) is an excellent tool for estimation of secondary structure, folding properties and interactions of proteins obtained using recombinant technique or directly purified from natural sources. Besides folding properties, it provides a rapid way for evaluating the conformational stability of the protein or interacting proteins in various buffers or solutions *in vitro* (22-24).

When a protein molecule is kept in the optically polarized light, each structural content shows its characteristic CD spectra. α- helical proteins have negative bands at 222 and 208 nm. Proteins with antiparallel β-sheets have negative bands at 218 nm and positive bands at 195 nm, whereas disordered proteins have low ellipticity above 210 nm and negative band nearly at 195 nm (25-27). Although CD does not provide secondary structural determinants of specific residues unlike X-ray crystallography or NMR spectroscopy, it has the great advantage of obtaining the overall structural contents, rapidly, at moderate concentrations (in µg quantity) of proteins, in solution under physiological condition.

To obtain the secondary structural contents of expressed and purified PorA and PorH with mycolic acid modification, CD spectra were recorded in a Jobin Ivon spectrometer and the data were processed in the online software Dichroweb (28, 29). The same samples used for NMR HSQC measurements were used for CD measurement in order to compare the secondary structural contents using both methods. Protein samples in 10 mM Na_2HPO_4, pH 6.8 containing LDAO were centrifuged at higher speed (20,000 *g* for 10 mins) and taken in a 0.001 cm cuvette for measurement. As accurate protein concentration is important for calculation, we measured the protein concentration using three different methods; (i) nanodrop: according to the molar extinction co-efficient of each proteins, (ii) BCA method and (iii) Lowry method as described in the annex (page 181). In fact, all three methods showed comparable data for the protein concentration of PorA, whereas for PorH the value from nanodrop differs from the other two methods. This is because PorH has less aromatic residues like Tryptophan or Tyrosines. Hence we used the protein concentration obtained by the BCA method for the calculation of % of secondary structural contents in PorA and PorH.

Dichroweb (CONTIN, Provencher and Glockner method, reference database 7) was used to calculate the secondary structural contents in PorA and PorH (28, 29). As shown in the figure II-6, PorA has nearly 42 % helical content, whereas PorH has lesser, 22 % helical content

rather contains higher un-ordered fractions as random coil. Moreover, this value does not change when PorA and PorH samples were taken in different detergent (DHPC), different pH from 4 to 9 and at various temperatures from 4 to 40 ^{0}C. Surprisingly these values are in contrast to typical β-barrel behavior of bacterial porins.

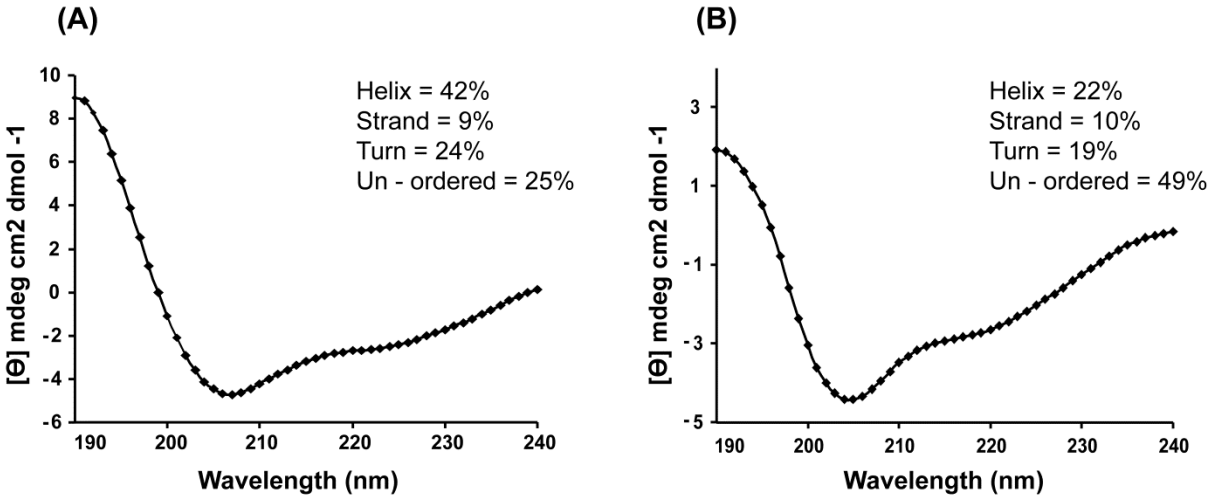

Fig. II-6: CD spectra of (A) PorA and (B) PorH expressed and purified from *C. glutamicum* with mycolic acid modification. CD spectra were recorded in Jobin Ivon CD-spectrometer and the secondary structural contents were calculated using Dichroweb.

II.6: Ion channel activity of PorA and PorH

The functionality of PorA and PorH has been studied with protein extract from the cell wall of *C. glutamicum* and results indicate that the formation of a functional complex out of both proteins (2). In addition the requirement of mycolic acid modifications (on position Ser-15 in the case of PorA) for pore-forming activity was also analyzed (20).

In the present work, the ion channel activity was investigated using expressed and purified protein samples from *C. glutamicum*. These measurements were performed using the black lipid membrane approach, in collaboration with Dr A. Ghazi (University of Orsay, Paris-sud). In this case, we used purified proteins, without any chemical treatment and after mass spectrometry and CD characterizations. The assembly of the BLM apparatus and experimental procedures were explained in the annexe (page 188). When PorA and PorH at very high concentrations (0.5 to 1 µg/ml) were added to the chambers separately, noisy perturbations of the membrane were detected indicating that some proteins might be inserted in the bilayer (Fig. II-7).

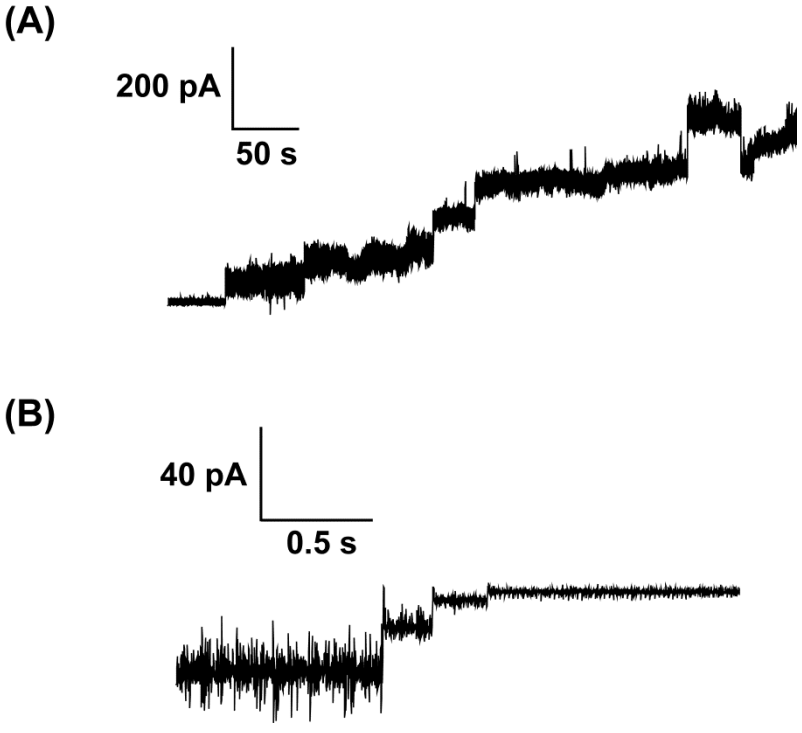

Fig. II-7: Channel activity measurements of (A) PorA and (B) PorH. The proteins were added separately at a protein concentration of 0.5 to 1 µg/ml in the chamber. Noisy perturbation of the bilayer could only be observed without any characteristic behavior of ion channels.

In the other hand, when a mixture of PorA and PorH were added to the chamber, porin like channel activity were observed for a concentration as low as 1 ng/ml. Fig. II-8A shows the profile characteristic of multiple channel insertion in the bilayer with time. Fig. II-8B shows that opening and closing of the channels occurred with two distinct kinetics; one with faster kinetics in a millisecond time scale, the other with a slower kinetics in second time scale. Moreover multiple conducting states are clearly observed. The channels which were opened at around zero mV, closed upon application of a membrane potential, at both positive and negative side (Fig. II-8C). The rate of closing of channels is faster at higher potential from 100 to 120 mV. This results confirmed that the requirement of both PorA and PorH to form a proper ion channel (2). They show in addition that the PorA-PorH channel shares the characteristic finger-prints of channels such as bacterial porins (30) and also mitochondrial porin (31): closure at positive and negative potential with fast and slow kinetics, asymmetric voltage dependence and multiple conductance states. Similar porin channels can be found in related families of bacteria, *C. diphtheria*, *C. efficiens*, *N. farcinia* (2, 32, 33).

The presence of extra residues (used for His-tag affinity purification) at both N- and C-terminus of PorA and PorH was further investigated. When the mixture of $PorA_{His}$ and $PorH_{His}$ were applied in the chamber, some insertions were observed, but these insertions were relatively noisy and did not show the channel characteristics in compare to the proteins used without any additional residues (as explained above). As shown in the figure II-9, better channels were observed when PorA was used without any additional tags compared to PorH. It should be noted that the addition of tag at the N-terminus of the protein has a drastic effect on the channel forming properties of the protein mixtures. Hence for further *in vitro* characterization of the complex, either both proteins or at least PorA should be free from extra residues after purification steps.

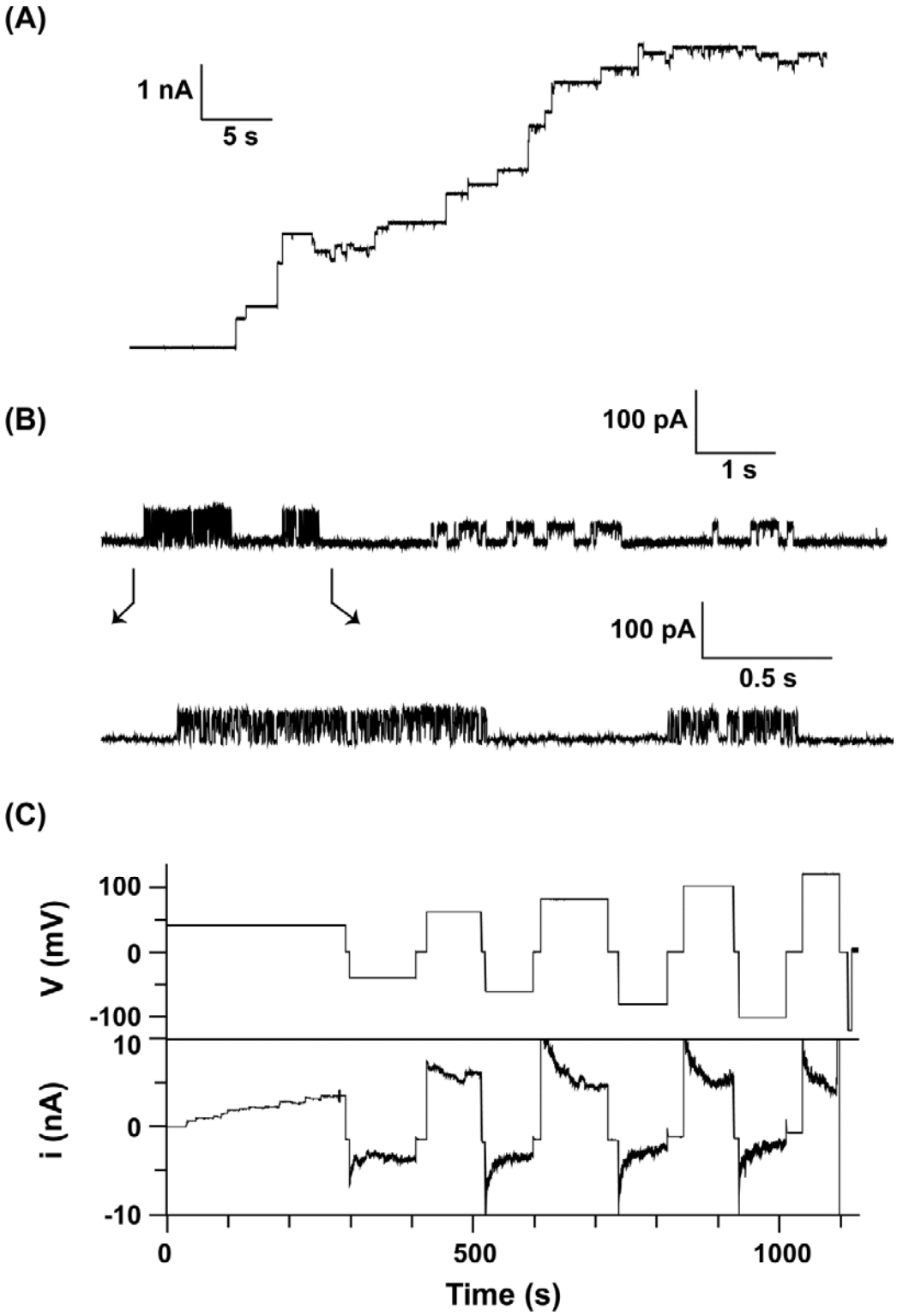

Fig. II-8: Porin channel activity of a mixture of PorA and PorH. (A) Shows multiple insertions in the membrane upon addition of the protein mixture in the chamber. (B) Shows slow and fast kinetics of opening and closing of the channels at 40 mV at second and millisecond time scales respectively. (C) Shows voltage dependence at both positive and negative side of the potential ranging from ± 40 mV to ± 120 mV.

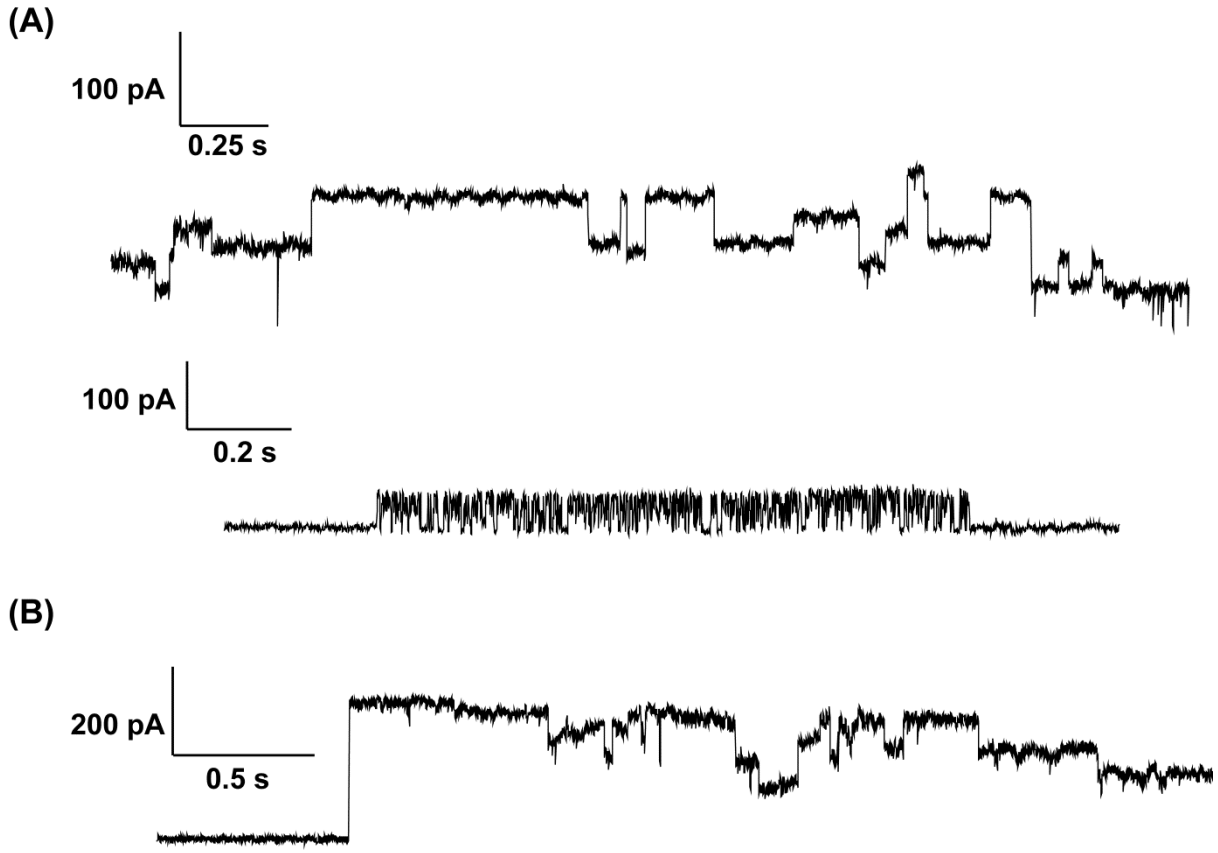

Fig. II-9: Influence of affinity tags on porin channel activity. Channel recording with a mixture containing (A) PorA and $PorH_{Chis}$, (B) $PorA_{Chis}$ and PorH. Better channels showing porin like characteristics were observed when the affinity tag is removed from PorA compare to PorH.

II.7: NMR spectroscopy of PorA and PorH

Solution NMR spectroscopy has been widely established as an excellent tool not only to study structure of proteins and protein complexes but also to study their dynamics (34-38). In specific applications this methods provides a way to determine membrane protein structures which numbers are lagging far behind the soluble proteins in the protein database (39). Membrane proteins in their natural lipid environments are not agreeable to solution NMR techniques because of their slow rotations, highly anisotropic behavior with unfavorable relaxations and having very broad resonance line widths. They may be studied in favorable cases after solubilisation in detergent micelles (47,48). However, in recent years solid state NMR techniques are rapidly developing to allow the direct observation of membrane proteins in lipid bilayers or even in their native membrane environment. (40-42). Further the invent of Dynamic Nuclear Polarization (DNP) NMR ease the way for membrane protein structure determination which can be achieved at µmolar protein concentration (43, 44).

II.7-i: Transverse relaxation-optimized spectroscopy (TROSY)

TROSY was developed by Pervushin et al. in 1997 and since then it has been used extensively in various multidimensional NMR measurements of large macromolecules (45, 46). Whether large proteins or membrane proteins in detergents, the overall size is relatively large for their structure determination by NMR. As the overall size is larger, the decay of NMR signal is faster because of small transverse relaxation time (T_2) and hence leading to weaker signal with broad line widths. At higher magnetic field Chemical Shift Anisotropy (CSA) and Dipole-Dipole (DD) interactions of ^{1}H, ^{15}N and ^{13}C nuclei builds a significant source of relaxation with higher rate of transverse relaxation at higher polarizing magnetic field, B_o (annex, page 189). TROSY reduces T_2 relaxation further by using the interference between CSA and DD coupling. In a ^{15}N labeled protein the cross-correlated relaxation caused by DD and CSA leads to different relaxation rates of the individual multiplet components in a two coupled spin ½ systems such as ^{15}N - ^{1}H part of a peptide bond. Hence TROSY has been used successively for sequential assignment and structure determination of several membrane proteins in solution as follows: the β-barrel outer membrane proteins OmpA (47, 48) and OmpX (49), the KcsA potassium channel (50), diacylglycerol kinase – consisting four bundles of α-helical proteins (51), Mistic (52), pentameric phospholambgan (53) and the PhoPQ – activated gene product P (PagP) (54).

II.7-ii: Finding good conditions (detergent, pH, temperature) for obtaining high quality HSQC NMR spectra

^{15}N-PorH and ^{15}N-PorA samples in 10 mM Na_2HPO_4 and ~10 % LDAO were used to record 2D HSQC in a BRUKER 600 MHz spectrometer. The TROSY / HSQC spectra were recorded at various pH (4.8, 6.8 and 7.3) and temperatures (10, 25 and 40 ^{0}C). The best condition, with the highest resolution and maximum number of peaks with better signal/noise, was observed at pH 6.8 and 25 ^{0}C (Fig. II-10). To see the effect of detergent on spectral quality, protein samples were exchanged on column to DHPC (~ 300 mM). On superposition of both spectra in LDAO and DHPC, it was observed that both spectra were nearly similar with identical line widths (data not shown). For more details about selection of detergents for membrane protein studies by NMR following articles can be referred (48, 55, 56).

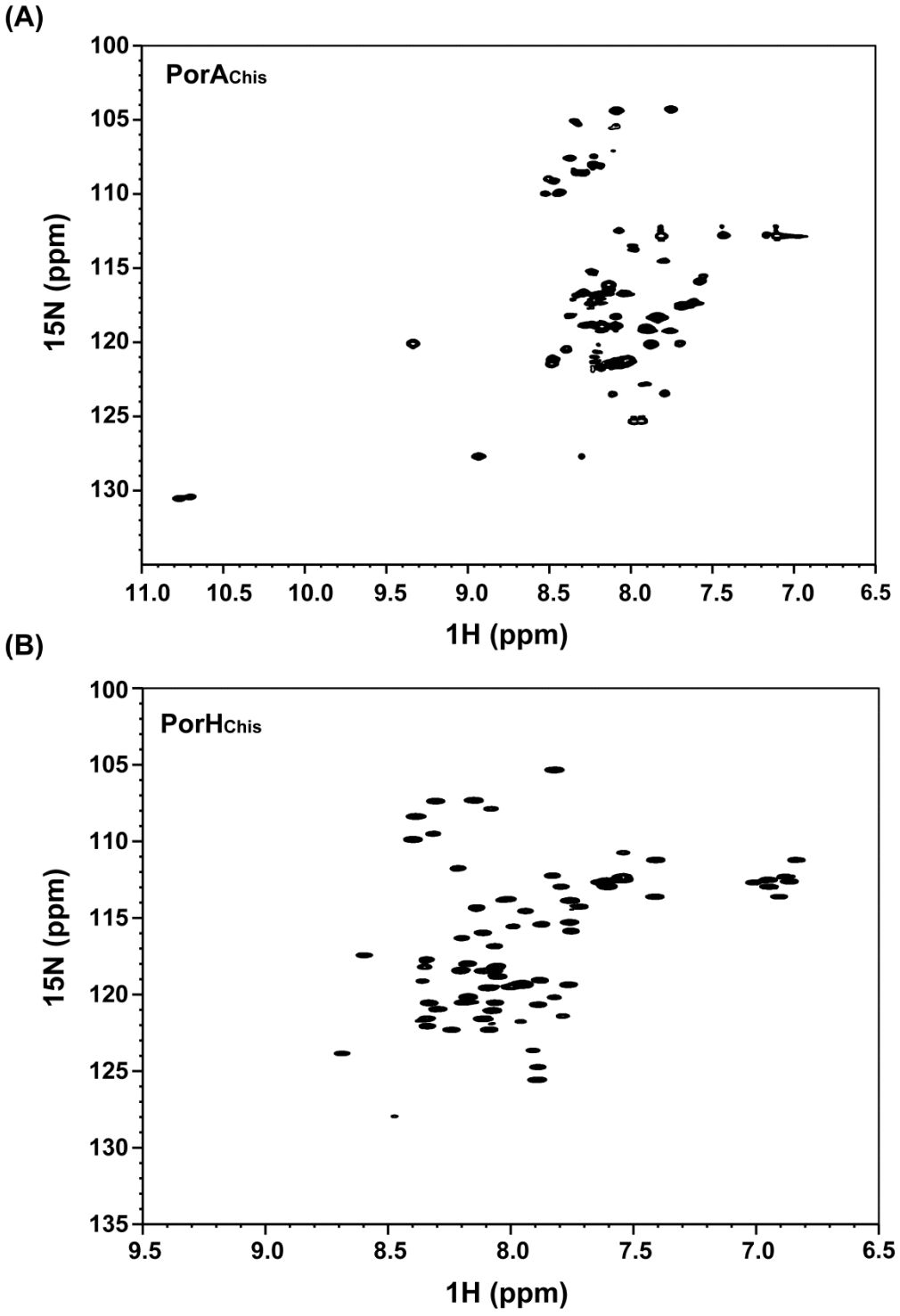

Fig. II-10: ^{15}N / ^{1}H TROSY spectra of uniformly labeled (A) ^{15}N-PorA and (B) ^{15}N-PorH in 10 mM Na_2HPO_4, pH 6.8 containing ~10 % LDAO at 25 ^{0}C.

II.7-iii: TROSY for rotational correlation times (TRACT)

The correlation time, τ_c is an important parameter for NMR spectroscopy of macromolecules in solution. In other words, it modulates the anisotropic spin-spin interaction in macromolecules because of Brownian motion of the molecules in solution. Moreover, the knowledge of τ_c enables to estimate the NMR spin relaxation rates and also indicates about sample quality (possible aggregation or not). Actually, with the high LDAO concentration, we were not able to obtain the oligomeric state of both PorA and PorH by Native gel electrophoresis. Hence we decided to use TRACT experiment to see the overall size of PorA and PorH after reconstituting in LDAO micelles. The theory of TRACT and NMR pulse scheme were explained in the article by Lee et al. in 2005 (57). Briefly, [^{15}N, ^{1}H] TRACT based on the principle of TROSY in which it suppresses the DD relaxation by distant protons in ^{15}N - ^{1}H part of the peptide backbone. Only one – dimensional spectra are to be recorded and can be rapidly analyzed. For proteins with molecular weight < 30 kDa, τ_c is estimated from the ratio of longitudinal and transverse relaxation rates. But, the value of τ_c for larger proteins can't be reliable because of intramolecular motion on the longitudinal relaxation.

To estimate the overall size of PorA and PorH in LDAO, τ_c of each sample were calculated using TRACT principle. Series of 1D spectrum were recorded at 700 MHz Bruker spectrometer with variable relaxation periods (milliseconds). The decay of the relative intensity of the ^{1}H signal, I_{rel} were determined from integration of the1D NMR spectrum over the range of 6.5 -11 ppm in case of PorA and 6.5 – 9.0 ppm in case of PorH. The slow relaxing α-spin state and the fast relaxing β-spin state of ^{15}N are clearly observed in the figure II-11. Exponential fits, calculated using GOSA software (58) are indicated in the figure II-11. Using the R_α and R_β values from the curve τ_c for PorA / LDAO and PorH / LDAO was calculated to be 14.55 ns and 6.36 ns respectively. These values correspond to the size of 36 kDa for PorA and 14 kDa for PorH in LDAO micelles. Practically TRACT has also been used to estimate the size of other membrane proteins in detergent micelles such as OmpA/DHPC (48), OmpX/DHPC (63) as well as for soluble proteins (59, 60).

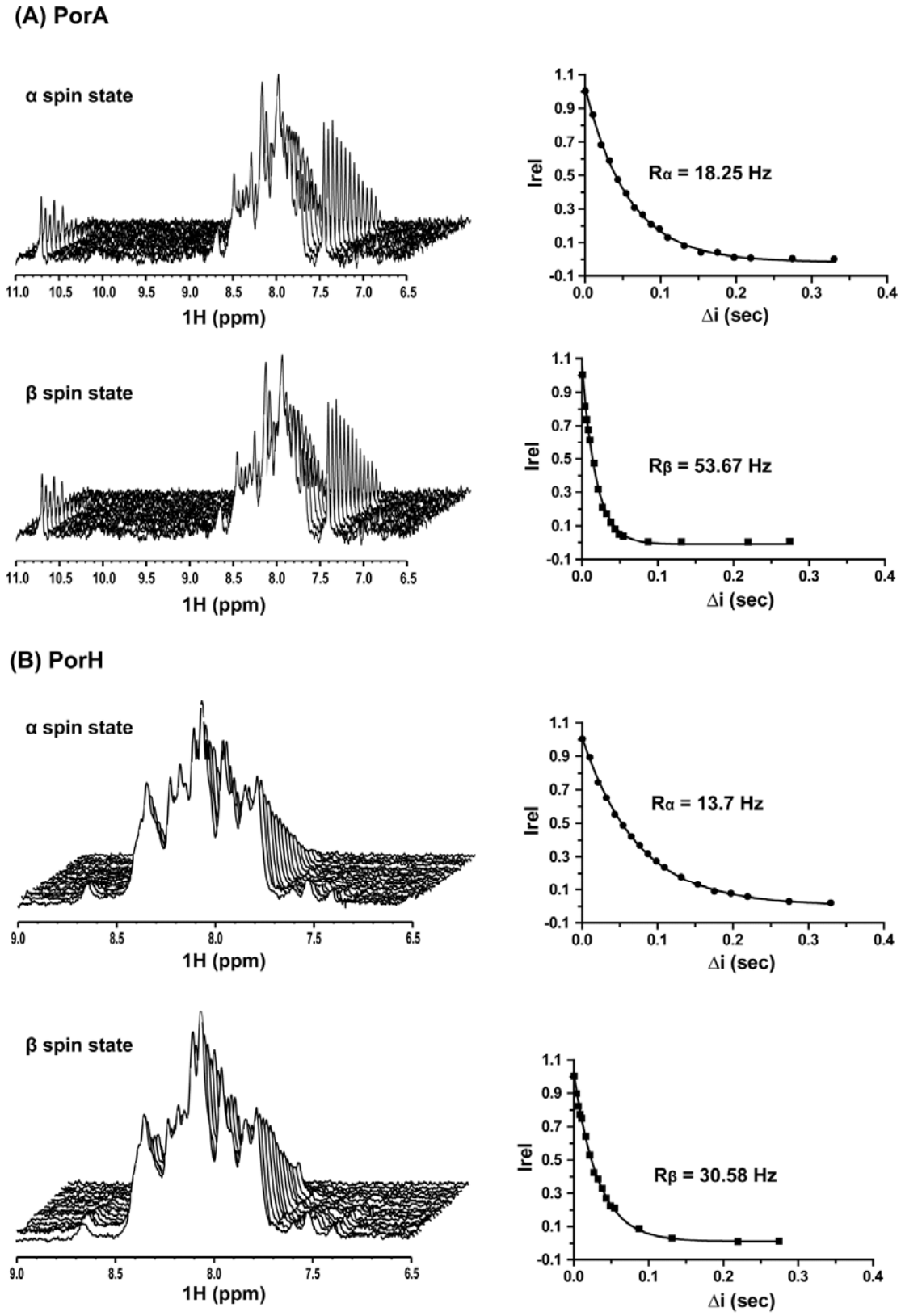

Fig. II-11: Stacked 1D $^{15}N/^{1}H$ spectra of (A) PorA /LDAO and (B) PorH/LDAO with variable relaxation periods and corresponding plots show the decay of the relative intensity of the ^{1}H NMR signal with slow (α-spin state) and fast (β-spin state) relaxation rates.

II.7-IV: Localization of mycolic acid modification on PorH by NMR

Although mutational experiments and tandem mass spectrometry approaches succeeded to localize the position of mycolic acid modification on PorA (at Ser15) but failed in case of PorH (20). Therefore, we thought to apply NMR based sequential assignment and NOE measurements to localize the position of modification. As previously shown in case of ghrelin, a shift of ~ 0.6 – 0.8 ppm on amide NH protons has been observed between modified and unmodified protein (65, 66). Hence an uniformly labeled $^{15}N/^{13}C$-PorH sample (193 µM) was produced *in vivo* and 3D NMR experiments like HNCA, HN(CO)CA, HNCACB and HN(CO)CB were measured in Bruker 600 and 900 MHz spectrometers. So far as shown in fig. II-12A, the backbone of PorH could only be assigned partially due to low signal to noise ratio, line broadening, molecular and chemical heterogeneity in LDAO micelles (~200 mM). The hydroxyl groups of Serines and Threonines are the major targets for modifications. But, 3 Ser and one Thr out of the 7 Ser and 6 Thr could not be assigned (Fig. II-12B). Furthermore separate peaks showing identical chemical shifts indicate the presence of multiple oligomeric states (molecular heterogeneity) (Fig. II-12C). Hence 3D NMR measurements in organic solvents like DMSO have been recorded and the assignment is under progress.

(A)

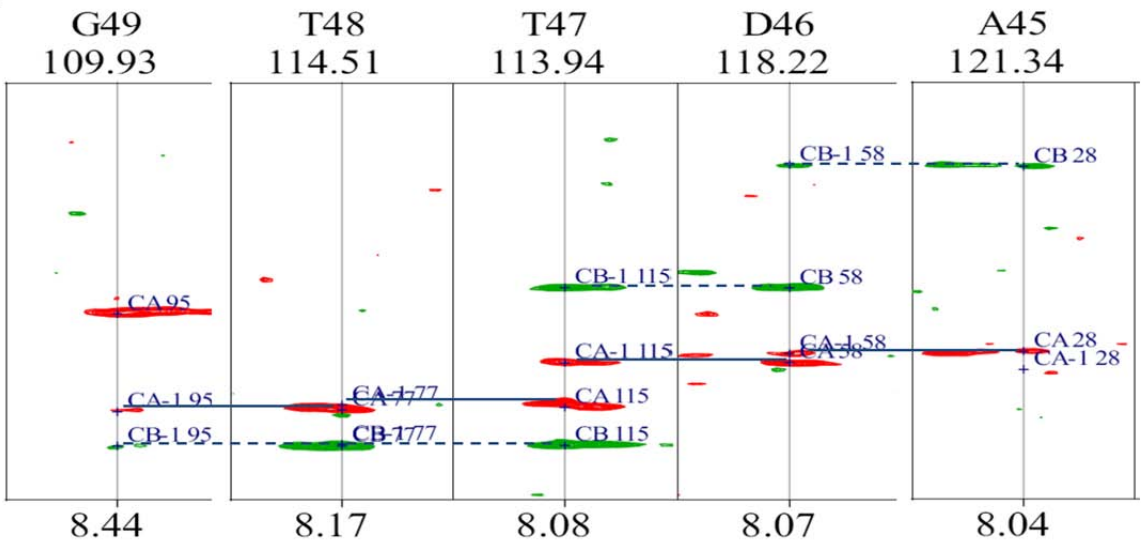

(B)

M 1 D 2 L 3 S 4 L 5 L 6 K 7 E 8 T L 10 G 11 N 12 Y 13 E 14 T 15 F 16 G 17 G 18 N 19 I 20 G 21 T 22
A 23 L 24 Q 25 S 26 I 27 P 28 T 29 L 30 L 31 D 32 S 33 I 34 L 35 N 36 F 37 F 38 D 39 N 40 F 41 G 42
D 43 L 44 A 45 D 46 T 47 T 48 G 49 E 50 N 51 L 52 D 53 N 54 F 55 S 56 S 57 I 58 E 59 G 60 R 61 A 62
S 63 R 64 G 65 S 66 H 67 H 68 H 69 H 70 H 71 H 72 H 73 H 74

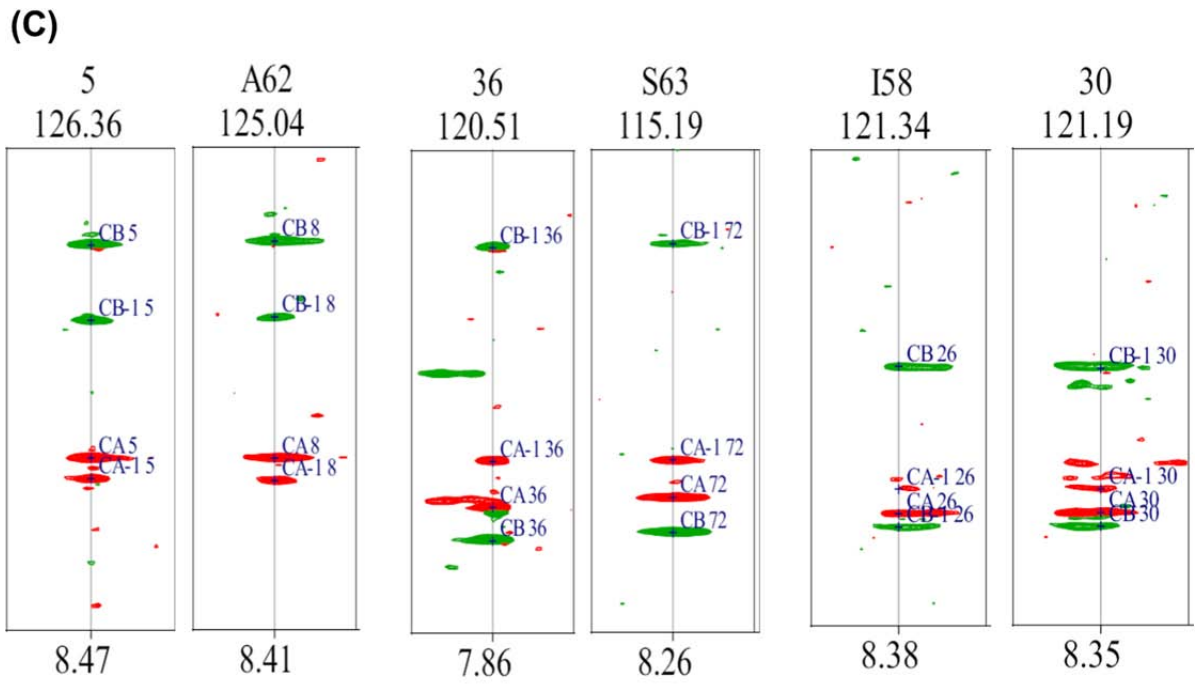

Fig. II-12: Partial sequential assignment of $^{15}N/^{13}C$-PorH (193 µM in 10 mM Na_2HPO_4, pH 6.7 and ~200 mM LDAO) with mycolic acid modification. (A) HNCACB fragment showing the correlation between C_α and C_β of neighboring residues. (B) 38 residues (in green) out of 66 residues (besides 8 x His tag at the c-terminus) have been assigned. But, 4 Serines (in red) and 1 Threonine (in red) as the major targets of mycolic acid modification could not be assigned due to lack of signals in the 3D NMR measurements like HNCACB and CBCA(CO)NH. (C) Shows HNCACB strips with identical chemical shifts of two different HSQC peaks indicating the presence of molecular and chemical heterogeneity of PorH sample in LDAO.

REFERENCES

1. Jakoby, M., Ngouoto-Nkili, C. E.&Burkovski, A. (1999) Construction and application of new Corynebacterium glutamicum vectors *Biotechnology Techniques* **13**: 437-441.
2. Barth, E., Barcelo, M. A., Klackta, C.&Benz, R. (2010) Reconstitution experiments and gene deletions reveal the existence of two-component major cell wall channels in the genus Corynebacterium *J Bacteriol* **192**: 786-800.
3. Tateno, T., *et al.* (2009) Direct production of cadaverine from soluble starch using Corynebacterium glutamicum coexpressing alpha-amylase and lysine decarboxylase *Applied Microbiology and Biotechnology* **82**: 115-121.
4. Vrljic, M., Sahm, H.&Eggeling, L. (1996) A new type of transporter with a new type of cellular function: L-lysine export from Corynebacterium glutamicum *Molecular Microbiology* **22**: 815-826.
5. Sahm, H., Eggeling, L., Eikmanns, B.&Kramer, R. (1996) Construction of L-lysine-, L-threonine-, or L-isoleucine-overproducing strains of Corynebacterium glutamicum *Recombinant DNA Biotechnology Iii: The Integration of Biological and Engineering Sciences* **782**: 25-39.
6. Morbach, S., Sahm, H.&Eggeling, L. (1996) L-Isoleucine production with Corynebacterium glutamicum: Further flux increase and limitation of export *Applied and Environmental Microbiology* **62**: 4345-4351.
7. Keilhauer, C., Eggeling, L.&Sahm, H. (1993) Isoleucine Synthesis in Corynebacterium-Glutamicum - Molecular Analysis of the Ilvb-Ilvn-Ilvc Operon *Journal of Bacteriology* **175**: 5595-5603.
8. Lichtinger, T., Burkovski, A., Niederweis, M., Kramer, R.&Benz, R. (1998) Biochemical and biophysical characterization of the cell wall porin of Corynebacterium glutamicum: the channel is formed by a low molecular mass polypeptide *Biochemistry* **37**: 15024-32.
9. Costa-Riu, N., *et al.* (2003) Identification of an anion-specific channel in the cell wall of the Gram-positive bacterium Corynebacterium glutamicum *Mol Microbiol* **50**: 1295-308.
10. Costa-Riu, N., Burkovski, A., Kramer, R.&Benz, R. (2003) PorA represents the major cell wall channel of the Gram-positive bacterium Corynebacterium glutamicum *J Bacteriol* **185**: 4779-86.
11. Aebersold, R.&Mann, M. (2003) Mass spectrometry-based proteomics *Nature* **422**: 198-207.
12. Aebersold, R.&Goodlett, D. R. (2001) Mass spectrometry in proteomics *Chemical Reviews* **101**: 269-295.
13. Mann, M., Hendrickson, R. C.&Pandey, A. (2001) Analysis of proteins and proteomes by mass spectrometry *Annual Review of Biochemistry* **70**: 437-473.
14. Pandey, A.&Mann, M. (2000) Proteomics to study genes and genomes *Nature* **405**: 837-846.
15. Witze, E. S., Old, W. M., Resing, K. A.&Ahn, N. G. (2007) Mapping protein post-translational modifications with mass spectrometry *Nature Methods* **4**: 798-806.
16. Link, A. J., *et al.* (1999) Direct analysis of protein complexes using mass spectrometry *Nature Biotechnology* **17**: 676-682.

17. Karas, M.&Hillenkamp, F. (1988) Laser Desorption Ionization of Proteins with Molecular Masses Exceeding 10000 Daltons *Analytical Chemistry* **60**: 2299-2301.
18. Fenn, J. B., Mann, M., Meng, C. K., Wong, S. F.&Whitehouse, C. M. (1990) Electrospray Ionization-Principles and Practice *Mass Spectrometry Reviews* **9**: 37-70.
19. Fenn, J. B., Mann, M., Meng, C. K., Wong, S. F.&Whitehouse, C. M. (1989) Electrospray Ionization for Mass-Spectrometry of Large Biomolecules *Science* **246**: 64-71.
20. Huc, E., *et al.* (2010) O-mycoloylated proteins from Corynebacterium: an unprecedented post-translational modification in bacteria *J Biol Chem* **285**: 21908-12.
21. Yeung, Y. G., Nieves, E., Angeletti, R. H.&Stanley, E. R. (2008) Removal of detergents from protein digests for mass spectrometry analysis *Anal Biochem* **382**: 135-7.
22. Beychok, S. (1966) Circular dichroism of biological macromolecules *Science* **154**: 1288-99.
23. Chen, Y. H., Yang, J. T.&Chau, K. H. (1974) Determination of the helix and beta form of proteins in aqueous solution by circular dichroism *Biochemistry* **13**: 3350-9.
24. Greenfield, N. J. (2006) Using circular dichroism spectra to estimate protein secondary structure *Nature Protocols* **1**: 2876-2890.
25. Holzwarth, G.&Doty, P. (1965) The Ultraviolet Circular Dichroism of Polypeptides *J Am Chem Soc* **87**: 218-28.
26. Greenfield, N.&Fasman, G. D. (1969) Computed circular dichroism spectra for the evaluation of protein conformation *Biochemistry* **8**: 4108-16.
27. Venyaminov, S., Baikalov, I. A., Shen, Z. M., Wu, C. S.&Yang, J. T. (1993) Circular dichroic analysis of denatured proteins: inclusion of denatured proteins in the reference set *Anal Biochem* **214**: 17-24.
28. Sreerama, N.&Woody, R. W. (2000) Estimation of protein secondary structure from circular dichroism spectra: comparison of CONTIN, SELCON, and CDSSTR methods with an expanded reference set *Anal Biochem* **287**: 252-60.
29. Whitmore, L.&Wallace, B. A. (2004) DICHROWEB, an online server for protein secondary structure analyses from circular dichroism spectroscopic data *Nucleic Acids Res* **32**: W668-73.
30. Benz, R., Janko, K.&Lauger, P. (1979) Ionic selectivity of pores formed by the matrix protein (porin) of Escherichia coli *Biochim Biophys Acta* **551**: 238-47.
31. Berrier, C., *et al.* (2004) Cell-free synthesis of a functional ion channel in the absence of a membrane and in the presence of detergent *Biochemistry* **43**: 12585-91.
32. Schiffler, B., Barth, E., Daffe, M.&Benz, R. (2007) Corynebacterium diphtheriae: identification and characterization of a channel-forming protein in the cell wall *J Bacteriol* **189**: 7709-19.
33. Klackta, C., Knorzer, P., Riess, F.&Benz, R. (2011) Hetero-oligomeric cell wall channels (porins) of Nocardia farcinica *Biochim Biophys Acta* **1808**: 1601-10.
34. Wuthrich, K. (1986) *NMR of Proteins and Nucleic Acids* (Wiley, New York.
35. Opella, S. J.&Marassi, F. M. (2004) Structure determination of membrane proteins by NMR spectroscopy *Chem Rev* **104**: 3587-606.
36. Hiller, S.&Wagner, G. (2009) The role of solution NMR in the structure determinations of VDAC-1 and other membrane proteins *Current Opinion in Structural Biology* **19**: 396-401.
37. Tamm, L. K.&Liang, B. Y. (2006) NMR of membrane proteins in solution *Progress in Nuclear Magnetic Resonance Spectroscopy* **48**: 201-210.

38. Madl, T., Gabel, F.&Sattler, M. (2011) NMR and small-angle scattering-based structural analysis of protein complexes in solution *Journal of Structural Biology* **173**: 472-482.
39. White, S. H. (2004) The progress of membrane protein structure determination *Protein Sci* **13**: 1948-9.
40. Baldus, M. (2006) Solid-state NMR spectroscopy: molecular structure and organization at the atomic level *Angew Chem Int Ed Engl* **45**: 1186-8.
41. Baldus, M. (2006) Molecular interactions investigated by multi-dimensional solid-state NMR *Curr Opin Struct Biol* **16**: 618-23.
42. Renault, M., *et al.* (2012) Cellular solid-state nuclear magnetic resonance spectroscopy *Proc Natl Acad Sci U S A* **109**: 4863-8.
43. Jacso, T., *et al.* (2012) Characterization of membrane proteins in isolated native cellular membranes by dynamic nuclear polarization solid-state NMR spectroscopy without purification and reconstitution *Angew Chem Int Ed Engl* **51**: 432-5.
44. Renault, M., *et al.* (2012) Solid-state NMR spectroscopy on cellular preparations enhanced by dynamic nuclear polarization *Angew Chem Int Ed Engl* **51**: 2998-3001.
45. Pervushin, K., Riek, R., Wider, G.&Wuthrich, K. (1997) Attenuated T-2 relaxation by mutual cancellation of dipole-dipole coupling and chemical shift anisotropy indicates an avenue to NMR structures of very large biological macromolecules in solution *Proceedings of the National Academy of Sciences of the United States of America* **94**: 12366-12371.
46. Fernandez, C.&Wider, G. (2003) TROSY in NMR studies of the structure and function of large biological macromolecules *Current Opinion in Structural Biology* **13**: 570-580.
47. Arora, A., Abildgaard, F., Bushweller, J. H.&Tamm, L. K. (2001) Structure of outer membrane protein A transmembrane domain by NMR spectroscopy *Nature Structural Biology* **8**: 334-338.
48. Renault, M., *et al.* (2009) Solution state NMR structure and dynamics of KpOmpA, a 210 residue transmembrane domain possessing a high potential for immunological applications *J Mol Biol* **385**: 117-30.
49. Fernandez, C., Adeishvili, K.&Wuthrich, K. (2001) Transverse relaxation-optimized NMR spectroscopy with the outer membrane protein OmpX in dihexanoyl phosphatidylcholine micelles *Proceedings of the National Academy of Sciences of the United States of America* **98**: 2358-2363.
50. Chill, J. H., Louis, J. M., Miller, C.&Bax, A. (2006) NMR study of the tetrameric KcsA potassium channel in detergent micelles *Protein Science* **15**: 684-698.
51. Oxenoid, K., Kirn, H. J., Jacob, J., Sonnichsen, F. D.&Sanders, C. R. (2004) NMR assignments for a helical 40 kDa membrane protein *Journal of the American Chemical Society* **126**: 5048-5049.
52. Roosild, T. P., *et al.* (2005) NMR structure of Mistic, a membrane-integrating protein for membrane protein expression *Science* **307**: 1317-1321.
53. Oxenoid, K.&Chou, J. J. (2005) The structure of phospholamban pentamer reveals a channel-like architecture in membranes *Proceedings of the National Academy of Sciences of the United States of America* **102**: 10870-10875.
54. Hwang, P. M., *et al.* (2002) Solution structure and dynamics of the outer membrane enzyme PagP by NMR *Proceedings of the National Academy of Sciences of the United States of America* **99**: 13560-13565.

55. Columbus, L., *et al.* (2009) Mixing and Matching Detergents for Membrane Protein NMR Structure Determination *Journal of the American Chemical Society* **131**: 7320-7326.
56. Zhang, Q., *et al.* (2008) Microscale NMR screening of new detergents for membrane protein structural biology *J Am Chem Soc* **130**: 7357-63.
57. Lee, D., Hilty, C., Wider, G.&Wuthrich, K. (2006) Effective rotational correlation times of proteins from NMR relaxation interference *Journal of Magnetic Resonance* **178**: 72-76.
58. Czaplicki, J., Cornelissen, G.&Halberg, F. (2006) GOSA, a simulated annealing-based program for global optimization of nonlinear problems, also reveals transyears *J Appl Biomed* **4**: 87-94.
59. Lee, D., *et al.* (2002) NMR structure of the unliganded Bombyx mori pheromone-binding protein at physiological pH *Febs Letters* **531**: 314-318.
60. Salzmann, M., Pervushin, K., Wider, G., Senn, H.&Wuthrich, K. (2000) NMR assignment and secondary structure determination of an octameric 110 kDa protein using TROSY in triple resonance experiments *Journal of the American Chemical Society* **122**: 7543-7548.
61. Salzmann, M., Wider, G., Pervushin, K., Senn, H.&Wuthrich, K. (1999) TROSY-type triple-resonance experiments for sequential NMR assignments of large proteins *Journal of the American Chemical Society* **121**: 844-848.
62. Yang, D. W., Venters, R. A., Mueller, G. A., Choy, W. Y.&Kay, L. E. (1999) TROSY-based HNCO pulse sequences for the measurement of (HN)-H-1-N-15, N-15-(CO)-C-13, (HN)-H-1-(CO)-C-13, (CO)-C-13-C-13(alpha) and (HN)-H-1-C-13(alpha) dipolar couplings in N-15, C-13, H-2-labeled proteins *Journal of Biomolecular Nmr* **14**: 333-343.
63. Yang, D. W.&Kay, L. E. (1999) TROSY triple-resonance four-dimensional NMR spectroscopy of a 46 ns tumbling protein *Journal of the American Chemical Society* **121**: 2571-2575.
64. Wider, G. (1998) Technical aspects of NMR spectroscopy with biological macromolecules and studies of hydration in solution *Progress in Nuclear Magnetic Resonance Spectroscopy* **32**: 193-275.
65. Elipe, M. V. S., Bednarek, M. A.&Gao, Y. D. (2001) H-1 NMR structural analysis of human ghrelin and its six truncated analogs *Biopolymers* **59**: 489-501.
66. Grossauer, J., Kosol, S., Schrank, E.&Zangger, K. (2010) The peptide hormone ghrelin binds to membrane-mimetics via its octanoyl chain and an adjacent phenylalanine *Bioorganic & Medicinal Chemistry* **18**: 5483-5488.

Chapter III

Cell – Free Expression and Purification of PorA and PorH

and their biophysical characterizations

Summary

This chapter introduces the Cell-Free expression system based on *E. coli* cell extract and T7 RNA polymerase to produce PorA and PorH without mycolic acid modification. It describes the different systems, methods of expression and protocols to optimize the cell-free production of membrane proteins. The toxicity of PorA and PorH in standard *E. coli* expression was overcome by the use of cell-free expression system. Both proteins were produced successfully in high quantity, as precipitates in the absence of detergent, and in soluble form in the presence of detergents. The absence of mycolic acid modification was confirmed by MALDI TOF mass spectrometry. The quality of expressed and purified samples was verified by CD and NMR spectroscopy. Functional studies on BLM measurements have revealed that the mycoloylation of PorA is required for the channel forming ability of the PorA - PorH complex, while the modification on PorH is not an absolute requirement.

Abbreviations:

Brij-35 : polyethylene-(23)-lauryl-ether

Brij-58 : polyoxyethylene-(20)-cetyl-ether

Brij-72 : polyoxyethelene-(2)-stearyl-ether

Brij-98 : polyoxyethylene-(20)-oleyl-ether

CF : Cell-Free

CECF : Continuous exchange CF

D-CF : production of MPs as soluble form in presence of detergent micelles

FM : Feeding mixture

MPs : Membrane Proteins

DDM : n-dodecyl-β-D-maltoside

DHPC : 1,2-dihexanoyl-sn-glycero-3-phosphocholine

DPC : dodecyl-phosphocholine

LDAO : Lauryldimethylamine-oxide

LMPG : 1-myristoyl-2-hydroxy-sn-glycero-3-[phosphor-rac-(1-glycerol)]

LMPC : 1-myristoyl-2-hydroxy-sn-glycero-3-phosphocholine

LPPG : 1-palmitoyl-2-hydroxy-sn-glycero-3-[phosphor-rac-(1-glycerol)]

β-OG : n-octyl-β-D-glucopyranoside

P-CF : production of MPs as a precipitate

RM : Reaction mixture

SDS : sodium dodecylsulphate

T7RNAP : T7 RNA polymerase

III.1: Introduction

Cell-free (CF) expression system emerged as an efficient technique in the field of proteomics and molecular biology. This approach not only provides a rapid way to produce globular soluble proteins but also paved the way for expressing sufficient quantity of functional membrane proteins (MPs) (1-6). CF expression has many advantages which overcomes all sorts of difficulties in production of MPs for structural and functional purpose, such as (i) toxicity effects due to insertion of MPs into the host cellular membrane, (ii) improper translocation or inefficient transport of over-expressed MPs to the outer membrane destination, (iii) proteolytic cleavage by cytoplasmic protein degradation machinery and (iv) lack of stability during *in vivo* MP extraction from the cell membrane. In parallel, some disadvantages of CF expression system like failure to translate proteins with complex mRNA secondary structures and chance of MPs mis-folding or unfolding are under investigations (7, 8).

III.2: CF expression and Structural biology (NMR and crystallography application)

Membrane proteins account for nearly 25 % of all open reading frames in the available genome sequence databases. However, MP structures lag behind significantly in comparison to soluble protein structures imposing a challenge in the field of structural biology (9). One reason is the difficulty in expressing and purifying MPs for high resolution structural methods such as, Electron Microscopy (EM), X-ray diffraction and NMR spectroscopy. Usually, *in vivo* expression systems produce only small quantities of MPs which may be sufficient for functional studies but not for structural analysis. In an alternative and faster way, CF expression provides mg quantities of purified functional MPs per ml of reaction mixture which facilitates MP structure determinations. Moreover, CF expression system is an ‘open system’ which means that the reaction products are easily accessible and also beneficial compounds can be added during the course of protein synthesis. Several CF expressed MP structures have been solved over the last years (10, 11) and CF expression technique steadily spread in most structural biology laboratories around the world for structural study of novel integral MPs like G-protein-coupled receptors (GPCR), ion-channels and drug transporters (12-20).

III.3: Why CF expression of PorA and PorH ?

As described in the previous chapter, the unique feature in both PorA and PorH is that both peptides are post-translationally modified by corynomycolic acids. Also the bilayer measurements showed that this modification plays a crucial role in their functional properties. Actually, in the *C. glutamicum* genome both PorA and PorH are present in the same operon and also both genes lack signal sequences in the N-terminus (21). The transport pathway of these proteins to the outer membrane after their synthesis and the location, where this modification occurs in the cell (in cytoplasm or in the outer envelope?) is not yet fully understood. Hence to understand the importance of the covalent modification on the structural and functional stability of both proteins requires the production both proteins without modification. Furthermore, as shown in the previous chapter, our initial attempts to produce these proteins in *E. coli* were unsuccessful due to their toxicity effects. Therefore we used the advantage of *E. coli* based CF expression (*in vitro* expression) system to produce both proteins lacking the mycolic acid modification.

III.4: CF expression machinery

Before going in details about the CF expression machinery, the basic concept of the CF system is described in the figure III-1. The CF expression system is also called an *in vitro* expression system in which every components starting from transcription of the genetic material in mRNAs up to translation of these mRNAs in polypeptides are kept in one reaction chamber. This also includes the major components such as: T7 RNA polymerase, the ribosomes, tRNAs, the transcription and translation factors, the energy regenerating systems besides the minor components such as, the amino acids, the NTPs and buffers containing source of Mg^{2+} and K^{+}. The important reactions such as transcription and translation can be coupled together for better yield of the reaction as the chance of mRNA degradation can be avoided (6, 22-25).

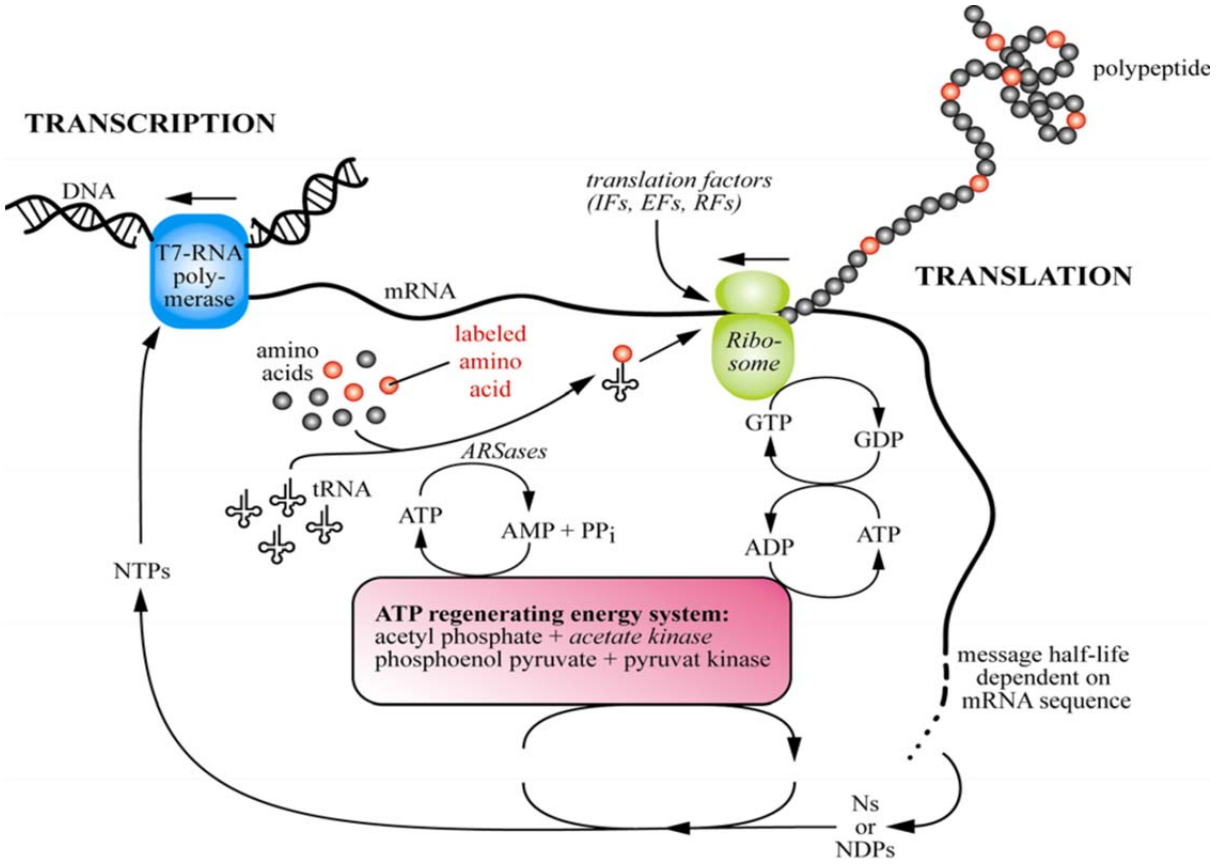

Fig. III-1: Schematic view of *E. coli* based coupled transcription-translation system consisting of all protein synthesizing machinery. It represents all essential components from transcription system (T7RNAP, plasmid DNA, NTPs etc) to the components of protein synthesizing translation machinery, such as; the ribosomes, the translation factors, tRNAs, the transcribed mRNA, and of course an efficient energy regenerating system. In fact, the *E. coli* S30 cell extract provides most of the components of the translation system.

III.4: Preparation of basic reaction components

III.4-i: Preparation of cell extract

Up to date only few extract sources are considered for cell-free expression systems. Out of all, the most commonly used extracts are from *E. coli* and from wheat germ embryos. A variety of *E. coli* strains such as A19, D10 and BL21 are suitable for extract preparation. The *E. coli* S30 (sedimentation at 30,000 *g*) extract is prepared by centrifugation of the lysed cells at 30,000 *g* which contains the essential components of the protein translation system such as ribosomes, aminoacyl- tRNAs, translation cofactors necessary for initiation, elongation and termination processes during protein synthesis. Nevertheless, some additional *E. coli* lipids and acetate kinase are present in the cell extract which may play significant role in membrane protein expression. In general, *E. coli* S30 extract is used in coupled transcription / translation process where double stranded DNA and/or circular and linear plasmid DNA or PCR reaction products can be used as template. Importantly, endogenous mRNA and low molecular weight amino acid has to be eliminated during extract preparation to increase specific target protein expression and reduce the background expression. *E. coli* S30 extract can be prepared according to the standard protocol as described in the experimental procedures (page 172) (26, 27) or can be commercially available from companies like Invitrogen, Roche Applied Science or Qiagen.

Alternatively, assuring eukaryotic protein folding systems, wheat germ extracts could be an option to produce large eukaryotic proteins which are problematic to produce in *E. coli* cell-free expression system (28-30). Compared to *E. coli* cell extracts, wheat germ extracts are difficult to prepare because of the thick endosperm surrounding the embryo containing large number of proteins, nucleic acids degrading enzymes and translational inhibitors. Also, wheat germ system is uniquely a translational system because of the difference in Mg^{2+} optima compared to transcription and therefore only supplied mRNA can be used as template in the reaction mixture. Besides wheat germ extract, rabbit reticulocyte lysates or insect cell extract may be used for the production of eukaryotic membrane proteins (25, 31). In addition, the PURE (protein synthesis using recombinant elements) system consisting of separately produced and purified components of translational process (aminoacyl-tRNA synthetase, translation factors and also the ribosomes) can be used directly in the *in vitro* expression system (32, 33). In this system, better defined conditions can be applied which is certainly an advantage over other expression systems in studying protein folding pathways or translation kinetics. However such PURE expression system is only limited to analytical scale and also to lower yield of expression.

***E. coli* versus Eukaryotic cell extracts for cell-free expression: (Advantages / Disadvantages)**

E. coli cell extract

Advantages:

1. Maximum yield with high translation rate
2. Simple and universal genetic constructs (vectors) are used
3. Compatible with coupled transcription / translation process
4. Mutant strains with reduced nucleases, protease, phosphatases activity can be used

Dis-advantages:

1. High rate of degradation of DNA template, proteins and energy sources
2. Relatively shorter life time
3. Higher chance of expressed protein degradation
4. Potential problems with high molecular weight mammalian proteins

Eukaryotic cell extract

Advantages:

1. Higher stability and longer life time
2. Removal of degrading enzymes of ribosomes, template mRNA and other components of translation machinery
3. Compatible with protein expression with post-translational modifications

Dis-advantages:

1. Lower expression rate
2. Insufficient knowledge and complexity of building effective genetic constructs

III.4-ii: Preparation of T7 RNA polymerase

In *E. coli* coupled transcription / translation system, the transcription process is controlled by the *E. coli* T7 RNA polymerase (T7RNAP). This enzyme is highly specific on T7 promoter and also highly active on both supercoiled plasmid DNA and as well as on linear DNA templates. Moreover, it neither recognizes the endogenous *E. coli* promoters present in the plasmid templates nor in the remaining chromosomal DNA fragments. Therefore the background expression resulting from the residual *E. coli* polymerase present from S30 extract preparation is strictly suppressed. The activity of T7RNAP is limited upon oxidation during reaction incubation and hence addition of extra T7RNAP might be supplemented after certain reaction periods. Furthermore, dithiothreitol (DTT) is required to maintain reducing environments in the reaction mixture and to stabilize T7RNAP, although it may prevent the formation of di-sulfide bridge formation in the expressed target protein. As substrates for T7RNAP and transcription process, nucleoside triphosphates (ATP/GTP/CTP/UTP) have to be added in the reaction mixture. To protect the transcribed mRNA from degradation, RNAse inhibitors have to be supplemented in the reaction. A wide range of protease inhibitors may be used to stabilize the synthesized protein target. Commercial T7RNAP is highly expensive and also not sufficiently concentrated to be supplied in higher quantity in the reaction mixture. But, it can easily be produced as a recombinant protein in *E. coli* and purified by standard protocols as described in the experimental procedures (page 174) (27, 34).

III.4-iii: Preparation of DNA template (N-terminal tag variation)

As *E. coli* CF expression system is a coupled transcription / translation system, and also is based upon the strong activity of *E. coli* T7RNA polymerase, standard T7 promoter based vectors such as pET (Novagen) or pIVEX (Roche Biosciences) can be used to clone the target gene without any modification. Moreover, an efficient T7 terminator has to be included to suppress nonproductive consumption of precursors. The productivity of CF expression system strongly depends on the rate of initiation of translation, and thus complex secondary structures at the 5’-untranslated regions of mRNA could prevent the accessibility of ribosome binding site to the ribosome. To overcome this problem two possible ways can be chosen. First, the extra unfavorable sequences of the mRNA are removed after scanning of the mRNA sequence using commercial program ProteoExpert. Second, the N-terminus of the target gene can be modified with addition of extra expression tags such as; T7-tag, poly $(His)_6$-tag, longer or shorter AT sequences; small fusion proteins (thioredoxin) can be considered specifically for eukaryotic MP

expression (35-40). Some of the tags can also help in immunodetection of the expressed protein and for optimizing the expression conditions. Furthermore, affinity tags like poly $(His)_8$ or Streptavidin tags can be used at the C-terminus for fast and efficient purification. However, for structural studies like NMR or X-ray crystallography it may be necessary to remove the additional residues. Hence specific protease recognition site should be considered to remove the extra amino acids after protein expression.

Linear PCR templates can be good considerations to be used directly in the reaction mixture without time-consuming cloning steps. To obtain such template multiple PCR approaches with primers consisting of T7 promoter and terminator sequences have to be used to amplify the target gene. But such linear templates have a greater chance of degradation due to exonucleases in the cell extract preparations. Therefore to prevent such degradation mostly at the 3'-end of the mRNA, several stabilizing T7 terminator sequences or poly-G stem-loop structures are sometimes included (41-44).

Most importantly high quality DNA templates are necessary to have a good rate of expression. Therefore plasmid DNA should be prepared using commercial kits (Qiagen) which allow complete removal of RNA and other contaminants. The concentration of template DNA in water should be > 0.15 µg/ml for a good protein expression.

Accordingly, the DNA constructs of PorA and PorH were prepared in T7 promoter based vector pET28a and pIVEX2.3d. 6x-Histidine affinity tags at N- or C-terminus with Factor Xa or Thrombine cleavage sites were introduced. Sequences of different N-terminal expression tags used in the PCR reaction, figure showing the concept of tag variation and all cloning steps were described in details in the molecular biology sections of the experimental procedure (Annex, page 162).

III.4-iv: Preparation of basic reaction components

All 20 basic amino acid mixtures at a final concentration between 0.5 to 1 mM are enough for a normal CF reaction set up. However, depending upon the amino acid composition on specific MP target the individual amino acid concentration might be considered for better level of expression. Furthermore, highly degradable amino acids like Arg, Cys, Trp, Met, Glu and Asp may be added up to 5 mM concentrations to enhance the rate of translation and prolong the life time of cell-free systems. Folinic acid has to be added to ensure for the formation of formyl-methionine during initiation of translation. The endogenous amino acids of S30 extract

are eliminated during the dialysis step. Hence the amino acid concentration in the CF reaction is completely controlled by the operator himself. For structural applications such as NMR spectroscopy or X-ray crystallography, specific labeling can be made by respective incorporation of ^{15}N and/or ^{13}C labeled amino acids or modified amino acids such as seleno-methionine in the reaction mixture (45 – 47). Moreover, such incorporation of labeled amino acids can further suppress the problem of isotope scrambling occurs during recombinant *E. coli* expression (48).

An efficient energy regenerating system is an absolute requirement to provide ATP and GTP in the CF expression reactions. The most general energy sources for bacterial cell-free expression system are either phosphoenol pyruvate (with exogenous pyruvate kinase), or acetyl phosphate (with acetate kinase present endogenously in the S30 extract), or creatine phosphate (with exogenous creatine kinase). Instead of supplying these compounds exogenously, *in situ* generation of high energy phosphate bond is preferred. Excessive phosphate ions generated during the break down of ATP or GTP may act as inhibitors of translations process particularly during batch configuration of CF expression system. Therefore for batch systems, modified energy regenerating systems using substrates of glycolytic pathways (glucose, glucose-6-phosphate, and pyruvate) is suited for the requirement of ATP in addition with concomitant intake of reaction by-products. Pyruvate oxidase when added in the reaction mixture with thiamine pyrophosphate and flavin adenine dinucleotide, catalyzed the generation of acetyl phosphate from pyruvate and inorganic phosphate in the presence of oxygen. Subsequently, pyruvate/CoA/NAD/oxalate system was developed in which the RM was supplemented with each of the above components (6, 49-51).

To induce macromolecular crowding effect by mimicking the cytoplasm of *E. coli*, polymers like polyethylene glycol (PEG) or Ficols are used in the reaction mixture. These polymers stabilize the mRNA produced from transcription process. Besides these polymers, natural polyamines such as putrescine or spermidine can be used which stabilize DNA, RNAs during translation process as well as stimulating the activity of T7RNAP.

CF reactions are buffered at pH 7.0 mimicking the general intra cellular conditions. Also, essential cations such as Mg^{2+} and K^{+} are necessary for the activity of various biological reactions and hence their concentrations must be optimized for each new S30 extract preparation as well as for new target MP to improve the yield of expression. In general, for *E. coli* CF system, the Mg^{2+} concentration varies over a large range of 8-22 mM, while it varies between 2 to 4 mM concentrations for eukaryotic CF expression system. Potassium and ammonium acetates

or glutamates are included in the CF reactions at a higher concentration between 200-300 mM. It has to be taken care that inorganic phosphates, resulting from energy regenerating system, have a high tendency to form complexes with Mg^{2+} and accumulates in the reaction mixture resulting in lower yield in batch CF expression systems.

III.5: Configuration and devices of CF expression system

Generally CF system can be configured into (A) Batch CF system and (B) Continuous action CF systems (Fig. III-2).

(A) Batch CF system: In this mode of CF expression, all the reaction components are kept inside one chamber or can be carried out a in test tube. Depending upon the reaction conditions, the reaction time is limited to few hours as there is rapid degradation of precursor elements, as well as accumulation of inhibitory by-products in the reaction tube. Therefore the yield of expression is quite low (< mg per ml of reaction mixture) which might be sufficient for functional studies but is inadequate for structural applications. However such expression system is ideal for high throughput screening of the conditions of expression even with small scale (µl) reaction volumes. The set-up can be even adapted to by using micro plate formats as reaction chambers implemented with automated pipetting robots.

(B) Continuous action CF systems: A simple strategy to overcome the problem of batch system was developed based on the principle of a living cell i.e. the CF reaction is performed on the basis of continuous supply of substrates and release of products across a permeable membrane (24, 52, 53). In principle the higher molecular weight components (the ribosomes, aminoacyl-tRNA synthatases, mRNA, tRNA, translation factors and other enzymes) (so called the reaction mixture, RM) are retained by the semi-permeable membrane, whereas low molecular components such as amino acids and NTPs (so called the feeding mixture, FM) are either in an active flow (continuous flow CF system, CFCF) or in a passive diffusional exchange (continuous exchange CF system, CECF) across a dialysis membrane. Both CFCF and CECF are highly efficient in preparative scale production of both soluble and membrane proteins (> 2 mg per ml of RM). CFCF system has multiple advantages over CECF system such as (i) the synthesized protein coming out in the flow can be directly purified on affinity column (ii) it has a longer life time and hence a higher productivity and (iii) the CF reaction is under the control of the operator himself, i.e. protein synthesis and folding can be monitored, composition of RM can be modified during the reaction and the whole process can easily be automated and computerized. But, CFCF

system is more complicated, expensive and is mostly restricted to soluble protein synthesis. Therefore CECF system has been widely used in the production of both soluble as well as membrane proteins in the recent era of *in vitro* protein synthesis.

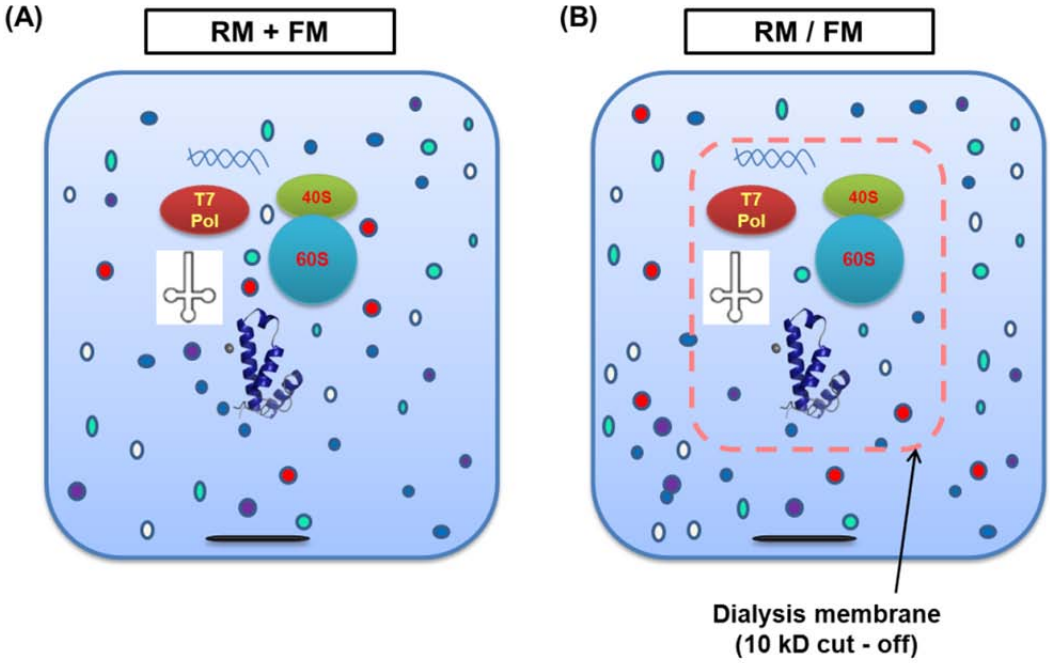

Fig. III-2: Production of MPs in (A) batch system in which RM and FM were mixed in one reaction chamber, and in (B) continuous exchange system in which the RM is separated from the FM by a semi-permeable membrane to avoid toxic effect of some metabolites.

Continuous Exchange CF system (CECF):

As previously mentioned, with a simple strategy, one compartment (RM) containing all higher molecular weight components is separated from the other compartment (FM) containing low molecular components by a semi-permeable membrane. The molecular weight cut-off of the membrane can be in the range of 10 – 50 kD assuring no leakage of essential components from the RM and also depends on the size of expressed membrane protein target. The efficiency of exchange across the membrane is assured by vigorous shaking during reaction incubation. There is continuous flow of precursors from the FM to the RM while in the reverse direction there is simultaneous release of inhibitory by-products from RM to FM. This continuous process significantly prolongs the lifetime of CF reaction and thereby increases the yield of expression up to several mg of proteins per ml of reaction mixture. The ratio of RM/FM in volume varies between 1:10 to 1:50 however depending on the cost of precursor elements; the ratio of 1:12 for analytical scale and 1:15 for preparative scale results in maximum yield of recombinant protein expression (22, 27, 53).

Reaction devices: A number of commercially available containers with different molecular cut-offs can be used as CECF reaction devices, such as - MicroDispoDialysers (spectrum, Rancho Dominguez). The dialyzers have to be washed thoroughly in distilled water before use. The RM of ~70 µl is kept at the inner compartment and the dialyzer is placed in a plastic container containing the FM. Both compartments are fixed together with parafilm and incubated in a temperature controlled shaker. Dialyzers can be reused if stored in S30 buffer containing 0.1 % NaN_3. Alternatively, Plexiglas containers can be used in place of MicroDispoDialysers. The bottom part of 1.5 cm long tube with diameter of ~5 mm is covered by a dialysis membrane of definite size cut offs and fixed well with the tube by a Teflon ring. This tube can be filled with 70 to100 µl of RM and kept inside the cavity of a 24 well microplate containing the FM. Then the complete set up is incubated at 30 ^{0}C in a shaker incubator. For preparative scale reactions commercially available Slide-A-lyzer dialysis cassettes (Pierce) from 1 to 3 ml capacity can be used as RM containers. The FM can be homemade Plexiglas chambers of 50 to 70 ml volume. The complete reaction device is incubated at 30 ^{0}C in a shaker incubator with vigorous shaking for efficient exchange between the reaction compartments.

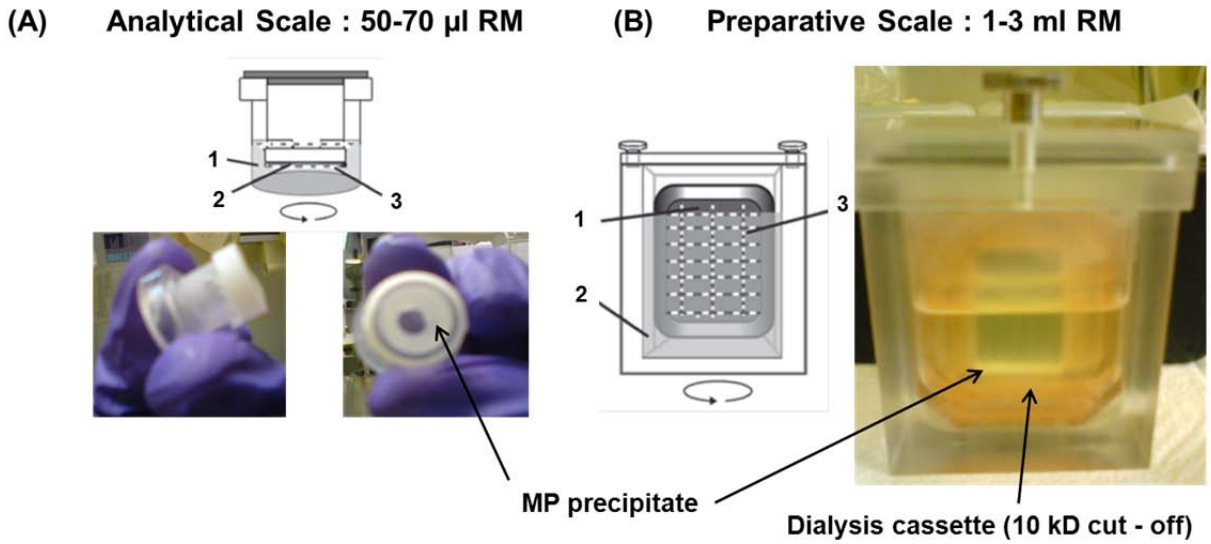

Fig. III-3: CECF production of MPs in (A) lesser analytical scale and in (B) larger preparative scale. 1 RM, 2 FM and 3 dialysis membrane.

III.6: Optimization strategies for CF expression of PorA and PorH:

CECF reaction protocols described above were used as basis to optimize the expression of PorA and PorH. At first the expression of PorA and PorH was evaluated in analytical scale P-CF reactions with the constructs pET28-PorA, pIVEX2.3-PorA, pET28-PorH and pIVEX2.3-PorH as templates (see annex page 162 for their description). Good expression levels of PorA from both constructs were observed. The location of the poly(His)$_6$-tag at either N- or C-terminus had no detectable effect on expression of PorA. However, no expression of PorH was observed from both templates after analysis by either Coomassie blue stained SDS-PAGE or by western blot analysis with anti-His antibodies [Fig. III-4].

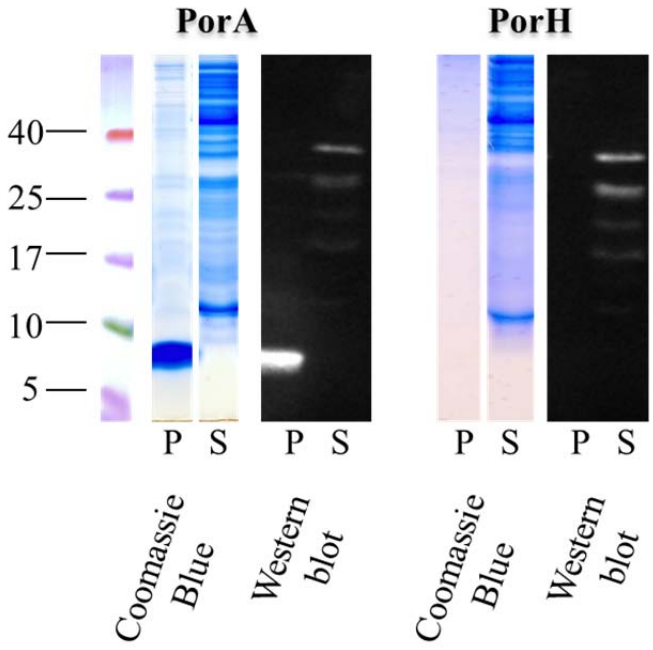

Fig. III-4: Analytical scale expression of PorA and PorH in P-CF mode. As shown in the figure, high level expression of PorA and absolute no expression of PorH was observed which was verified upon loading 5 µl precipitate (P) and 3 µl supernatant (S) of the reaction mixture on 16 % SDS-PAGE and further analysed by both Coomassie blue staining and western blotting.

Considering the reduced complexity of protein production in CF systems, complex mRNA secondary structures preventing efficient translation initiation at the translational start codon are primary reasons of insufficient expression yields. The 5'-end of the PorH coding region was therefore modified by various expression tags or sequences encoding for 4 to 18 additional amino acids (details in experimental procedures, page 163). The addition of the AT rich expression tags (their descriptions are given below) improved production of PorH to high levels [Fig. III-5].

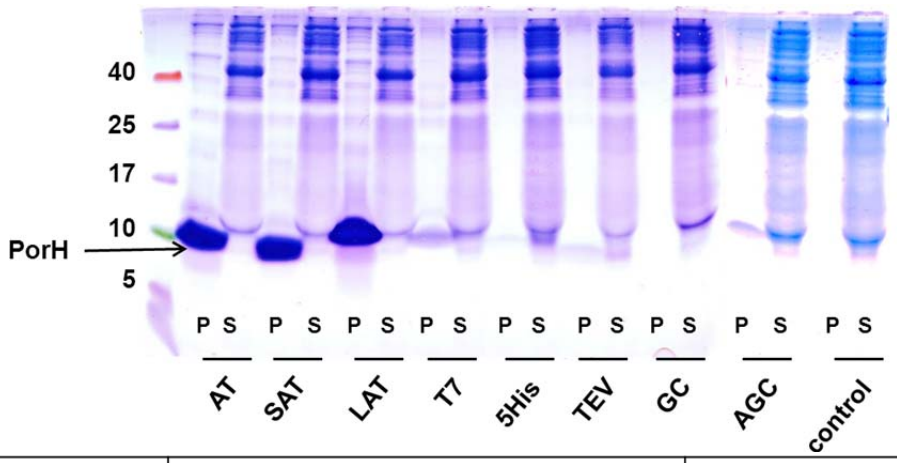

Nucleic acid sequence	Protein sequence	Expression
X	PorH	
GC	MRRRRRR-PSc-PorH	
AGC	MKRRRRR-PSc-PorH	
5His	MKSSSSS-Psc-PorH	
T7	MTHLLSTRHASH-PSc-PorH	
AT	MKYYKYY-PSc-PorH	
sAT	MKYY-PSc-PorH	
lAT	MKYYKYYKYY-PSc-PorH	

PSc : PreScission protease site (LEVLFQGP)

Fig. III-5: Analytical scale production of PorH using the various PCR constructs of modified PorH at the N-terminus with different expression tags. As shown by the arrow and in the table, high level expression of PorH was observed by addition of AT rich sequences compare to other expression tags. In the control, without the N-terminal tag variation of PorH, absolutely no precipitate could be detected either by Coomassie blue staining or by western blotting.

SAT - PorH: MKYY**LEVLFQGP** – PorH

AT - PorH: MKYYKYY**LEVLFQGP –** PorH

LAT – PorH: MKYYKYYKYYK**LEVLFQGP –** PorH (named as T - PorH)

S – PorH: MKYY – PorH

(PreScission protease site is shown in bold letters)

As the expression level could be affected by the concentration of K^+ and Mg^{2+} ions, the expression yields of PorA and S-PorH or T-PorH were further maximized by optimizing Mg^{2+} concentrations in the CF reaction. After Mg^{2+} screening in the range of 8-22 mM, a broad optimum in between 10-18 mM was identified for PorA, while S-PorH or T-PorH showed a rather narrow optimum in between of 14-16 mM [Fig. III-6]. These identified conditions were used for subsequent preparative scale productions in the P-CF and D-CF mode reactions. Fig. III-7 shows a general flowchart which is followed in the production of PorA and PorH using different steps of CF expression system and can be applied to the synthesis of other MP targets.

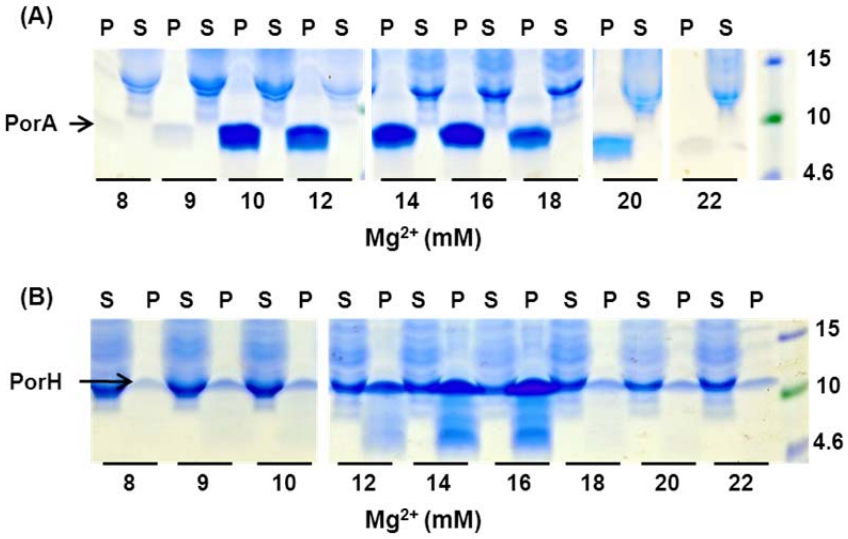

Fig. III-6: Mg^{2+} screening in analytical scale P-CF reactions of (A) PorA and (B) T-PorH. 6 µl of resuspended precipitate and 3 µl of supernatant was loaded in each well of 16 % Tris-tricin SDS-PAGE followed by Coomassie blue staining. PorA has a broad optimum from 10 to 18 mM whereas T-PorH has a narrow optimum from 14 to 16 mM. P = precipitate, S = supernatant. Molecular weight markers (kDa) are shown on the right lane.

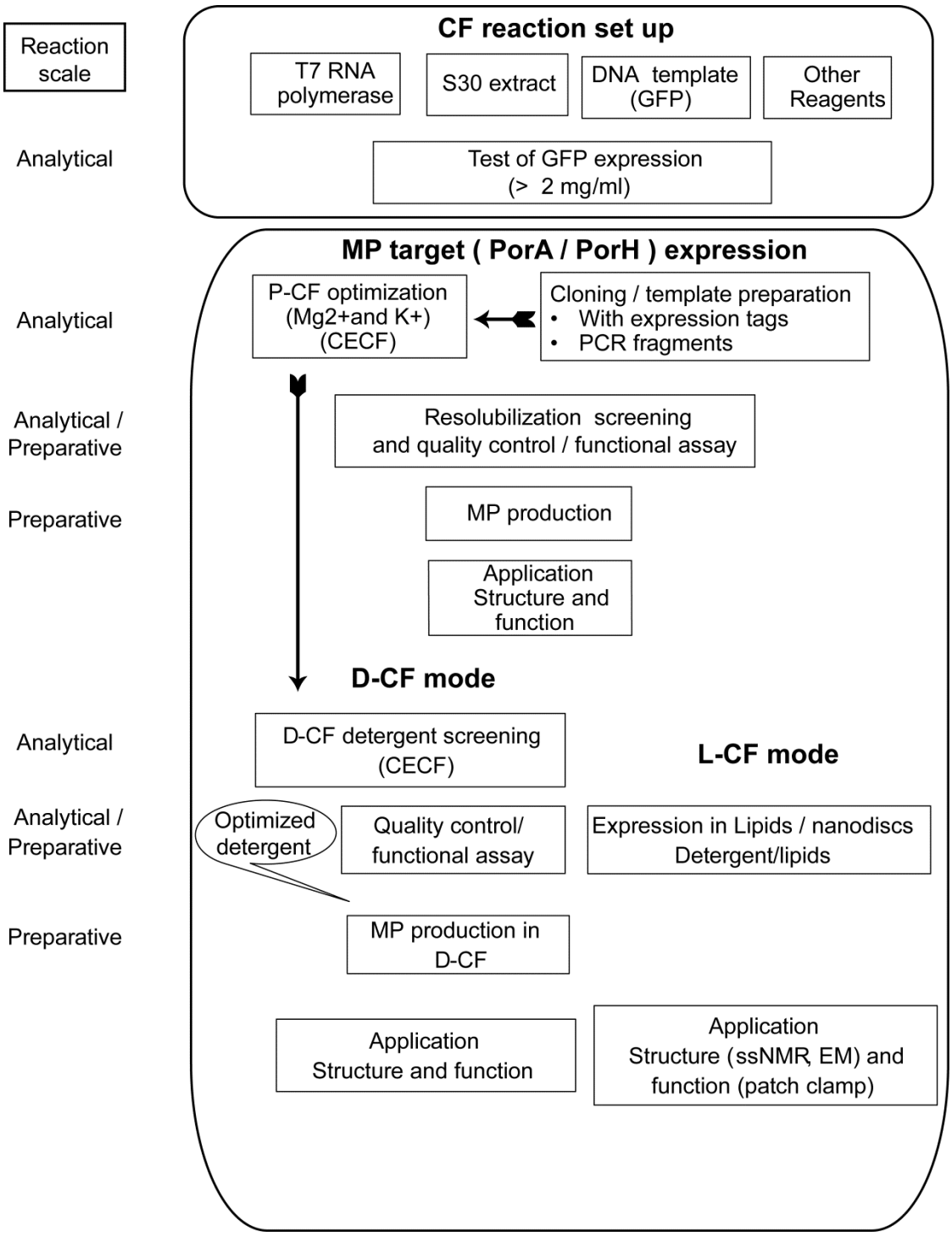

Fig. III-7: A general flowchart of MP synthesis in CF expression system. From preparation steps with various reaction components up to expression steps using different modes and further functional or structural studies can be achieved using the step by step protocols.

III.7: Expression of PorA and PorH in different CF reaction modes

Besides the existence of different expression systems (*E. coli* or wheat germ) and different configurations (batch or CECF), the choice of different reaction modes has to be considered as a major issue specifically in the synthesis of MPs. In general a CF expression system happened in the absence of hydrophobic environments such as membranes or lipids. The presence of such membrane is absolutely negligible as the lysed cells are centrifuged during S30 extract preparation. However certain amount of lipids < 100 µg/ml in the reaction mixture can be detected from the extract preparation. Also it is unclear whether those residual lipids form membranes or vesicles or not, and/or they may be associated with other proteins. CF reaction system can be divided into three different modes such as

(i) production of MPs as precipitate (P-CF)

(ii) production of MPs as soluble form in presence of detergent micelles (D-CF) and

(iii) production of MPs in presence of membranes and liposomes (L-CF)

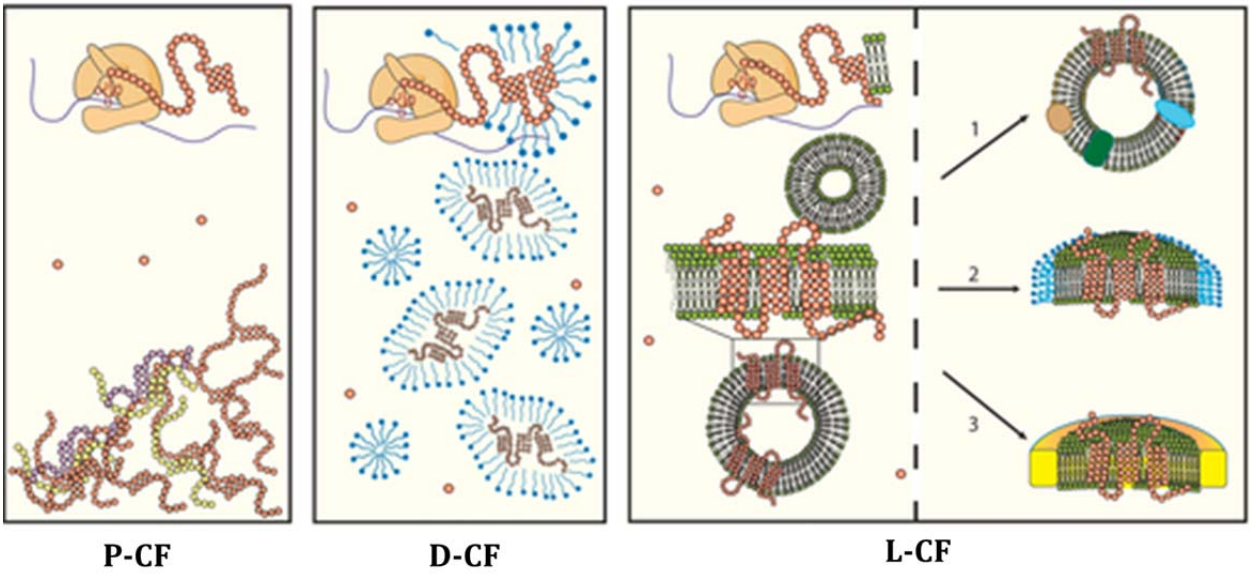

Fig. III-8: Production of MPs in various expression modes: as precipitates in absence of any hydrophobic environments (P-CF), as proteo-micelles in presence of detergents (D-CF) and in presence of artificial membranes such as liposomes, bicelles or nanodiscs (L-CF). The figure is adapted from Swartz et al, Nat Protocol (2008)

III.7-i: Production of MPs as precipitate (P-CF): In the absence of any hydrophobic environment the CF expressed MPs instantly precipitate and this mode of CF expression is called the P-CF mode. The MP precipitate has to be re-solubilized and diverse detergents may be tried, from anionic, cationic or zwitterionic forms. It should be noted that this expressed MP precipitates are different from inclusion bodies produced in normal *E. coli* over expression as (i) P-CF generated MP precipitates are efficiently solubilized only in presence of detergents with gentle shaking for few hours, but MPs as inclusion bodies need to be solubilized first with strong denaturants like urea or Gn-HCl at higher concentration and then refolded back in presence of detergents by buffer exchanges or excessive dialysis. (ii) Occurrence of MP as precipitate is a standard event in PCF mode expression, whereas inclusion body formation is rather rare unless specific strain of *E. coli* is used. (iii) Re-solubilization of MP precipitates often resulted in functional MP however refolding of alpha-helical MP from inclusion body is exceptional (23). The quality of re-solubilized MP has to be verified by functional measurements. This PCF mode expression offers to screen a wide variety of detergents for re-solubilization process and activity measurements. Also the amino acid specific labeled precipitate obtained in the PCF expression can be used directly to study the folding and dynamics of MPs by solid state NMR spectroscopy (46, 54, 55).

PCF mode expression of PorA and T-PorH

In P-CF reactions, PorA and T-PorH precipitated after translation in the RM. However, as explained above that many P-CF produced MPs can efficiently be resolubilized in a variety of detergents according to their solubilization efficiency (13, 54). A resolubilization screen was performed. The precipitates were centrifuged at 15,000 *g* for 15 min and washed with 20 mM Tris-Cl, pH 7.7, 100 mM NaCl (Buffer A) followed by immediate resolubilization in various detergents. For resolubilization screening, the following detergents were evaluated: LMPG (1 %), LMPC (1 %), LPPG (1 %), DHPC (1 %), DPC (1 %), DDM (1 %), LDAO (1 %), SDS (1 %) and β-OG (2 %). After incubation for 2 h at 30 ^{0}C with gentle shaking, the supernatant and residual precipitates were again separated by centrifugation and analyzed by SDS-PAGE (56). In comparison with controls, PorA precipitates were completely solubilized in LPPG, LMPG, LMPC, DPC and SDS and to a minor extent but still up to 50 % in DHPC, LDAO, DDM and β-OG. Solubilization of P-CF produced T-PorH was complete only in LPPG, LMPG and SDS and up to 50 % in DPC, LDAO and LMPC. Only minor fractions of PorH were solubilized in DHPC, DDM, Triton X-100 and β-OG [Fig. III-9].

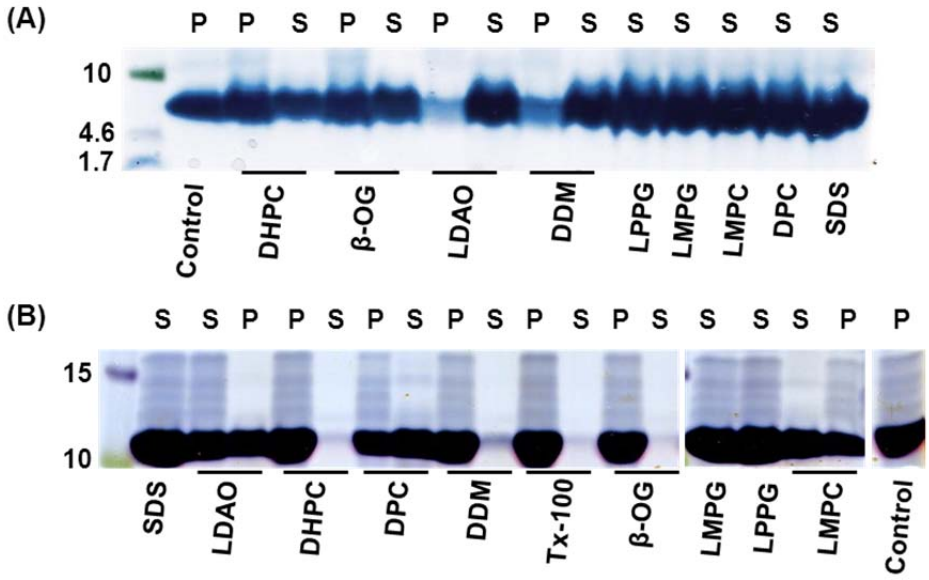

Fig. III-9: Resolubilization screening of P-CF expressed (A) PorA and (B) T-PorH. Precipitates of P-CF reactions were resuspended in equal volumes (60 µl) of buffer (20 mM Tris-Cl, pH 7.7, 150 mM NaCl) containing 1 % of one of the detergents LDAO, LPPG, LMPG, LMPC, DHPC, DPC, DDM, Tx-100, SDS or 2 % β-OG for 2 h at 30 ^{0}C. Non-solubilized proteins were precipitated by centrifugation and 5 µl of each, supernatant and remaining precipitate suspended in the initial volume of buffer, were analyzed by 16 % Tris-Tricin SDS-PAGE, and followed by Coomassie blue staining. Control is the corresponding initial P-CF precipitate. P = precipitate, S = supernatant. Molecular weight marker (kDa) is shown on the left lane.

III.7-ii: Production of MPs as soluble form in the presence of detergent micelles (D-CF): When an artificial hydrophobic environment is supplied in the RM, the translated MPs are surrounded by detergent micelles to form proteo-micelles rather than going to the precipitated form. The formation of proteo-micelles occurs with nonspecific hydrophobic interactions and also does not require any translocation machineries for MP insertion into the membrane. Hence this mode of MP expression eliminates the transport and translocation process which is often problematic in conventional expression in living cells. It also avoids the extraction process with harsh detergents from the membrane compartments (13, 22, 54).

Not every detergent is suitable to keep the target MP in soluble form. Therefore a variety of detergents have to be screened. Normally detergents with high CMC (β-OG, CHAPS etc) inhibit CF expression system. So that better expression levels are observed with long chain polyoxyethylene-ether derivatives (Brij 35, Brij 58, Brij 72 and Brij 98). Brij derivatives are

extremely mild detergents, efficient in keeping MPs in soluble form, without interfering with protein synthesis. They do not solubilize native membranes and hence are not used for extraction of membrane proteins from native membranes. Other detergents like Digitonin, Triton-X and DDM are also efficient for D-CF mode expression of MPs. During the CF reaction partial precipitation of expressed MP may be observed which is eliminated by using higher concentration of suitable detergent. This mode of CF expression can tolerate > 100 times CMC of specific detergent. Therefore the type and final concentration of detergent in the reaction mixture can strongly play a role on D-CF mode expression of target MPs.

Alternatively, mixed micelle approach with different detergent mixtures can be considered for soluble CF expression. Also lipids are important structural elements for the folding and stabilization of MPs and hence the use of detergent / lipid mixture in D-CF mode expression is an interesting approach. Furthermore, the use of amphipols with their strong hydrophobic nature can also be effective for soluble expression of MPs. It has been shown before that the extremely mild amphipols do not interfere with the protein-protein or protein-lipid interaction and thereby maintain the proper fold of MPs during their soluble expression (57-59).

D-CF mode expression of PorA and T-PorH

Alternatively to the resolubilization of P-CF precipitates, PorA and T-PorH were produced directly in soluble form in the presence of detergents by using the D-CF expression mode. Suitable detergents that do not inhibit the CF expression system were screened in analytical scale reactions. Detergents selected at initial final concentrations were Brij-35 (0.5 %), Brij-58 (1 %), Brij-72 (1 %), Brij-98 (1 %), digitonin (0.4 %) and TritonX-100 (0.1 %). All Brij derivatives could completely solubilize PorA in the D-CF mode and no residual PorA precipitate was detectable. The presence of different detergents also modulated the expression efficiency to some extent, and the highest yields were obtained with Brij-72 [Fig. III-10A]. In contrast, the D-CF solubilization of T-PorH was generally much less effective and the protein was not fully solubilized in any of the analyzed detergents [Fig. III-10B]. The highest solubilization efficiency was obtained with Brij-72 and complete solubilization was obtained after further increase of the final detergent concentration to 1.2 %.

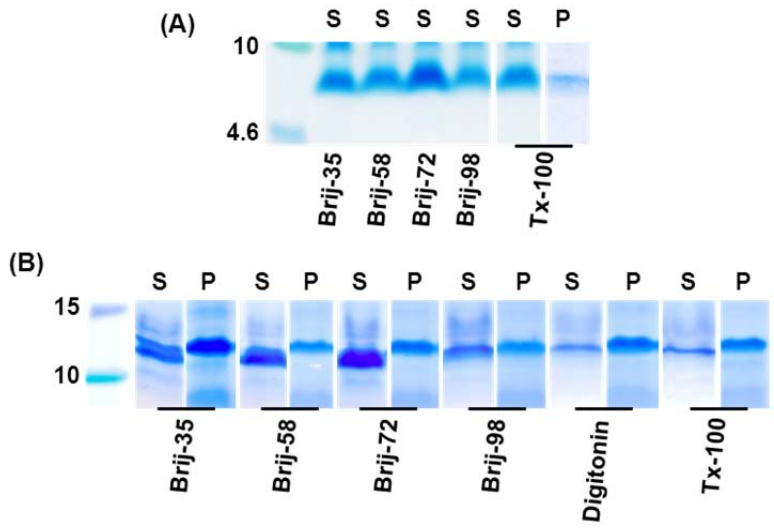

Fig. III-10: Detergent screening in analytical scale D-CF mode expression of (A) PorA and (B) T-PorH. Detergents at final concentrations of Brij-35 (0.5 %), Brij-58 (1 %), Brij-72 (1 %), Brij-98 (1 %), Tx-100 (0.1 %) and Digitonin (0.4 %) were used. 2 µl each of supernatant and suspended precipitate was analyzed by 16 % Tris-tricin SDS-PAGE and followed by Coomassie blue staining. P = precipitate, S = supernatant. Protein markers (kDa) are indicated in the left lanes.

III.7-iii: Production of MPs in the presence of membranes, liposomes and nanodiscs (L-CF):

The direct expression of MPs to form proteo-liposomes in the presence of liposomes in the reaction mixture is called L-CF mode of CF expression. Microsomal fractions from lysed cells can also be used in the reaction mixture. In a screening process so far only short chain lipids (DMPC, DOPC) have been partially successful in L-CF mode expression, for example 50 % production occurred in case of bacteriorhodopsin. In contrary higher chain length phospholipids (distearoyl-phosphatidylcholine) reduced the expression of bacteriorhopsin (15). In general, protocols for reconstitution process, purified and solubilized MPs are used in the presence of artificial liposomes. P-CF or D-CF expressed MPs can also be used for reconstitution process in pre-formed liposomes and considered for functional characterization (14, 60). However such L-CF based MP expression is limited so far to analytical scale and preparative scale production is still an emerging process to follow in the coming decades of CF expression. The major problem in such mode of expression is that the efficiency of insertion is not as much because of the unclear translocation mechanism of translated MPs into the liposomes. In addition, the thickness

of lipid bilayer might be crucial for insertion of particular MP target. Hence higher amount of MPs remains as aggregated or precipitated form in the reaction mixture and also it is difficult to separate them from the partially reconstituted proteo-liposomes. Nanodisc or bilayer disc approaches were developed in CF expression recently and also successful in the production of membrane proteins for functional and structural studies (58, 59, 61, 62). Expression of PorA and PorH in L-CF mode was not attempted considering their high expression in P-CF and D-CF mode. However this approach can be applied to express the proteins in more native like environments in future (details in perspective section).

III.8: Purification of P-CF and D-CF expressed PorA and PorH

As the *C. glutamicum* expressed protein samples were analyzed in LDAO (0.4 %), we kept the same detergent for sample preparation of CF expressed PorA and S-PorH or T-PorH. The direct resolubilization of P-CF expressed PorA and S-PorH or T-PorH in LDAO resulted in relatively pure protein and hence those samples were directly used for further characterizations. As a second option, the two proteins were expressed in the D-CF mode in presence of Brij-72 and the detergent was then exchanged to LDAO upon immobilization of the proteins at Ni-NTA affinity columns. The immobilized proteins were washed with 20 mM imidazole and finally eluted in LDAO micelles with 500 mM imidazole. The purity and homogeneity of CF expressed proteins were analyzed by SDS-PAGE followed by Coomassie blue staining [Fig. III-11]. After cleavage of the C-terminal poly$(His)_6$ tags and N-terminal expression tags (in the case of PorH) the samples were further characterized by mass spectrometry and with respect to their pore forming activities. A final expression yield of 200 µmoles / ml of RM were obtained upon quantification.

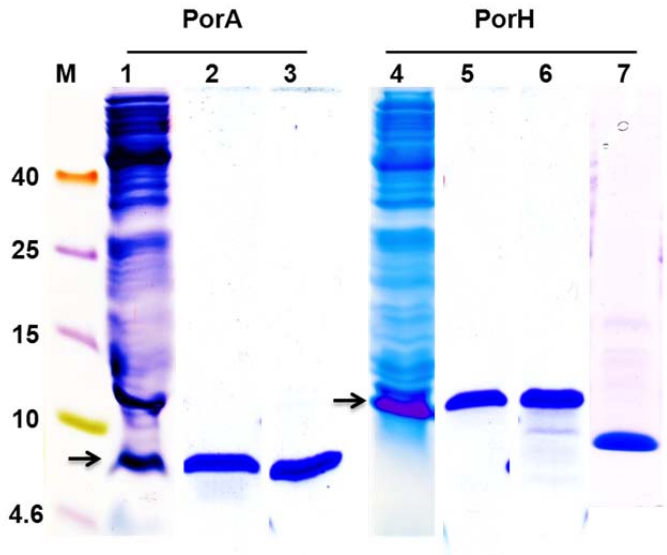

Fig. III-11: Purification of PorA and PorH (S-PorH and T-PorH for CF). Samples were analyzed by 16 % Tris-Tricin SDS-PAGE and Coomassie Blue staining. Lane 1 and 4: CF reaction mixture after D-CF expression; lane 2 and 5: Ni-NTA purified sample from D-CF expression; lane 3 and 6: P-CF expressed and resolubilized samples; lane 7: P-CF expressed and resolubilized S-PorH. The difference between PorH with long AT (lane 6) and short AT (lane 7) modifications can be visualized. M, protein marker in kDa.

III.9: Biophysical characterizations:

III.9-i: Mass Spectrometry

The absence of mycolic acid modification on CF expressed and purified PorA and PorH were characterized by MALDI-TOF mass spectrometry. The theoretical masses of native PorA and PorH without modification and with initial methionine are, for ($M + H^+$), 4681 Da and 6162 Da respectively (63). In the case of the recombinant PorA and PorH with C-terminal His-tag, after cleavage of the His-tag, the predicted ($M + H^+$) masses without mycoloylation are 5149 Da and 6618 Da for PorH respectively. As the N-terminus of PorH was modified with short AT (named as S-PorH), short AT with Thrombine cleavage site (named as ST-PorH) and long AT with PreScission protease site (named as T-PorH); the corresponding theoretical masses after cleavage of the respective expression tags were 7205 Da, 6761 Da and 9124 Da respectively (The masses of each protein with and without modification are shown in a table in the annex part, page 182).

As shown in the figure III-12, MALDI-TOF spectra of purified PorA expressed in *C. glutamicum* and Cell-Free synthesis confirmed the absence of mycolic acid modification in the CF expressed PorA with a difference of 506 Da corresponding to C34:0 naturally-occurring corynomycolic residues, as was described (63). Similarly, we observed the absence of mycolic acid modification on Cell-Free expressed S-PorH, ST-PorH and T-PorH samples according to their theoretical MW. The increase in molecular mass of CF expressed T-PorH resulted from the N-terminal modification with the AT rich expression tags [Fig. III-13].

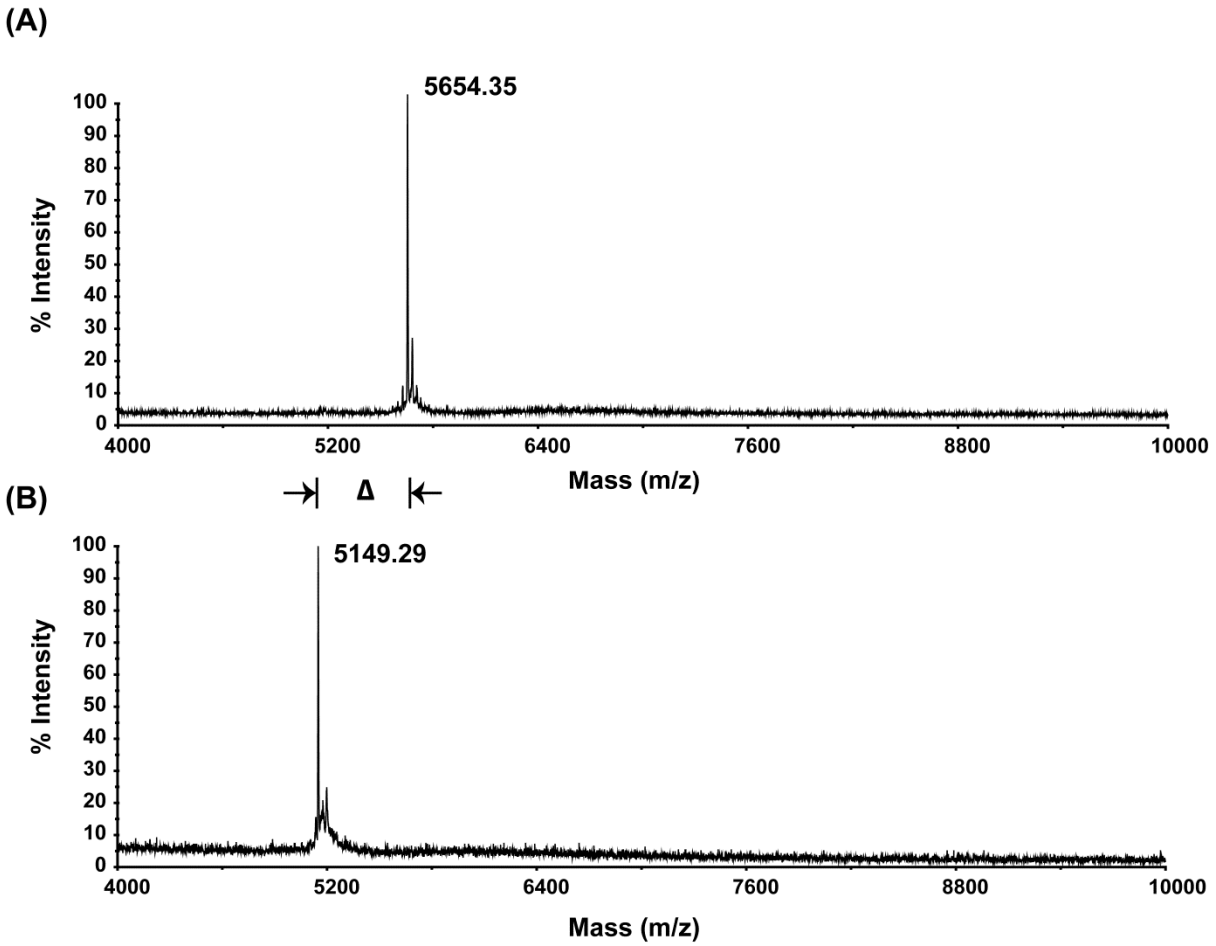

Fig. III-12: MALDI-TOF mass spectra of (A) *C. glutamicum* expressed and (B) CF expressed PorA displaying the absence of mycolic acid Δ (C34:0) modification.

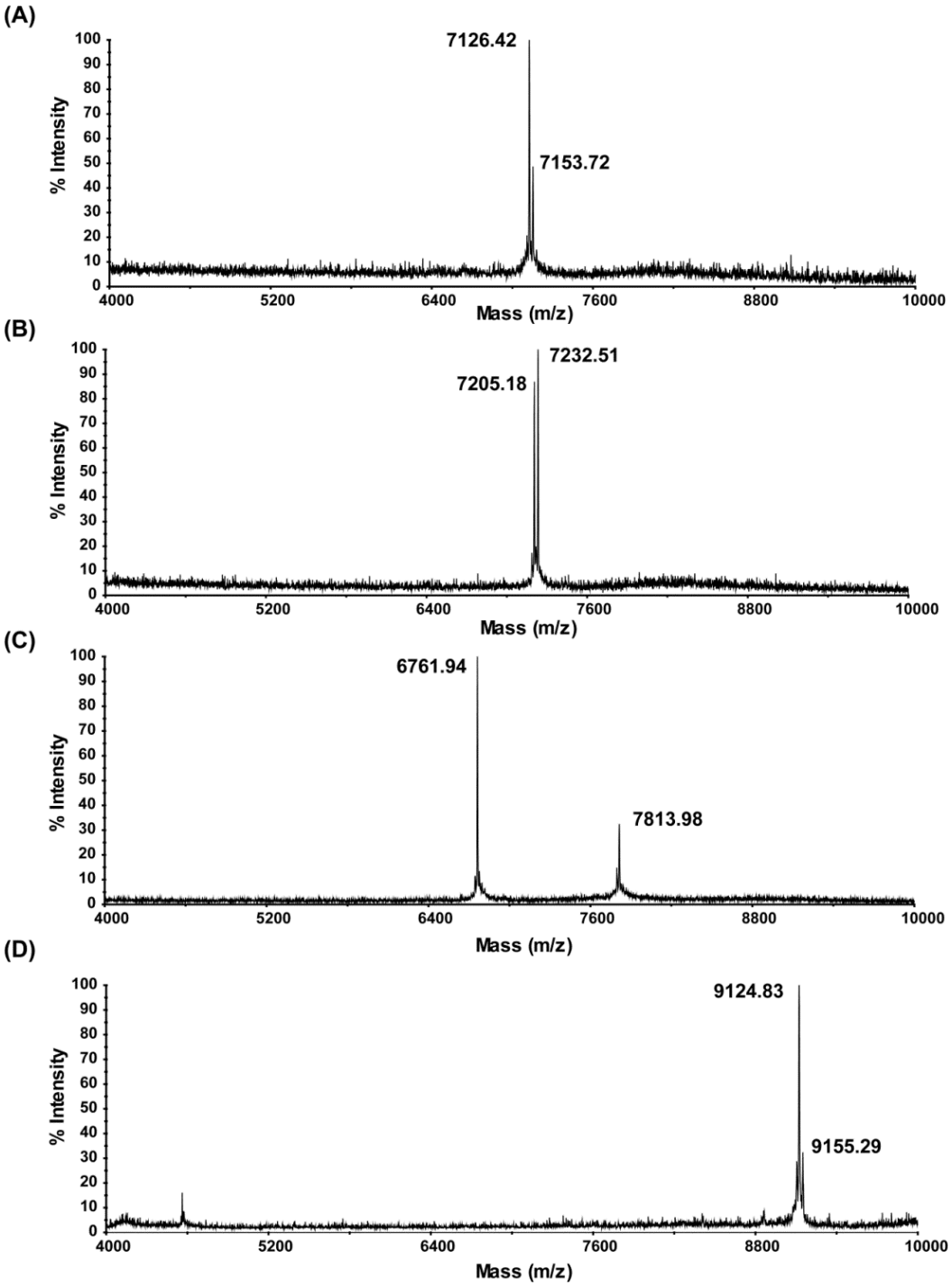

Fig. III-13: MALDI-TOF mass spectra of (A) *C. glutamicum* expressed PorH with mycolic acid (C34:0) modification and CF expressed PorH with different N-terminal sequences: (B) with short AT sequence, (C) with short AT and Thrombin cleavage site and (D) with long AT and PreScission cleavage site. The peak with 7813.98 Da in (C) appeared due to incomplete cleavage by Thrombin. The second peak with a difference of 26 Da appears due to formylation of the initial methionine. CF expressed PorH mass spectra shown correspond to their theoretical MW without mycolic acid modification.

III.9-ii: Circular Dichroism

The secondary structural content of CF expressed and purified PorA and T-PorH were analyzed by CD spectroscopy. The same samples used for NMR HSQC measurements were used for CD measurement in order to compare the overall structural contents using both methods. Protein samples in 20 mM Tris-Cl, pH 6.8 containing LDAO were centrifuged at higher speed (20,000 *g*) and taken in a 0.01 cm path length cuvette for measurements. CD spectra were recorded in a JASCO spectrometer and data were processed in the online software Dichroweb (CONTIN, Provencher and Glockner method, reference database 7) (64, 65). As shown in the figure III-14, PorA has nearly 68 % helical content, whereas PorH has a lower, 31 % helical content and a higher un-ordered fractions. The structural contents were similar whether the P-CF produced proteins were directly resolubilized in LDAO, or first LPPG resolubilized and then exchanged to LDAO upon Ni-NTA chromatography. Further the structural content does not change significantly whether PorA and PorH were expressed either in P-CF or in D-CF mode.

It is interesting to compare the results with the CD spectra obtained in the same conditions, in LDAO micelles, using PorA and PorH purified from *C. glutamicum*, i.e. possessing their post translational mycoloylation. In both cases, a slightly higher helical content was observed with the CF produced proteins, i.e. without the mycoloylation (68 % versus 42 % for PorA, 31 % versus 22 % for PorH), at the expense of the content in unordered structures. It is noteworthy also that in all cases, the amount of β-strand secondary structure is very weak, despite the fact that porins are usually structured as β-barrels.

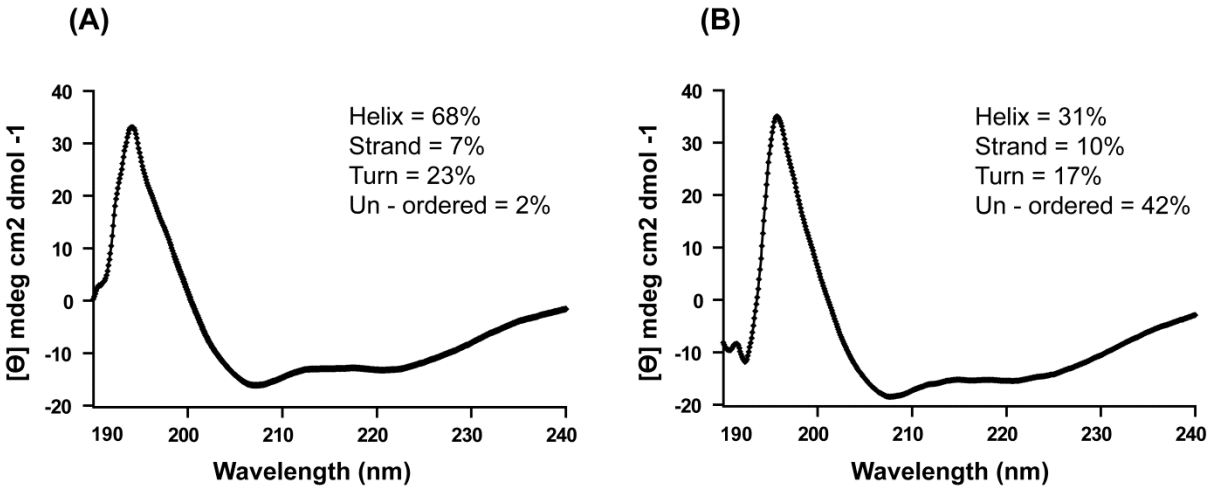

Fig. III-14: CD spectra of CF expressed and purified (A) PorA and (B) T-PorH without mycolic acid modification, solubilized separately in LDAO micelles. CD spectra were recorded in JASCO spectrometer and % secondary structural contents were calculated using Dichroweb.

III.10: Solution state NMR of P-CF and D-CF produced PorA and PorH

Two dimensional [^{15}N,^{1}H]-transverse relaxation optimized spectroscopy (TROSY) spectra (66, 67) of PorA and T-PorH were obtained after preparative scale expression of the proteins in the presence of ^{15}N-labeled amino acids. NMR samples (0.25 mM) were prepared in 20 mM Tris-Cl, pH 6.7 in LDAO (~ 2 %) and the spectra were recorded at 25 ^{0}C. For P-CF expressed proteins, TROSY spectra of good resolution could be obtained for both proteins under identical conditions. The dispersion and signal intensity of P-CF or D-CF produced samples of PorA [Fig. III-15A] or T-PorH did not show significant differences. Further, the spectra of both proteins were identical regardless whether the proteins were directly resolubilized in LDAO, or first LPPG resolubilized and then exchanged to LDAO upon Ni-NTA chromatography [Fig. III-15B]. In addition, other detergents besides LDAO were analyzed for their effects on the quality of NMR spectra. PorA and T-PorH were exchanged into DHPC upon affinity chromatography and recorded NMR spectra were identical to those in LDAO (data not shown). Hence it can be concluded that P-CF or D-CF expressed PorA and T-PorH maintain their structural fold in LDAO and in DHPC. Moreover, the good resolution and spectral diversity gave evidence that the P-CF and D-CF expressed samples are structurally homogenous in LDAO and DHPC, or that the coexisting conformations are in fast exchange at the NMR chemical shift time scale (what random coil conformations would give for instance). These high quality NMR spectra would thus allow structural studies of PorA and T-PorH using NMR spectroscopy provided that the

activities of these CF expressed proteins can be demonstrated (11, 47, 55, 68, 69). Furthermore, the structural fold of both proteins remains unchanged regardless of the presence or absence of mycolic acid modification, as far as a simple HSQC can tell [Fig. III-16]. The extra peaks in CF expressed T-PorH were due to additional residues from the N-terminal expression tag [Fig. III-16B]. Several peaks seem to be shifted between the mycoloylated and non mycoloylated sample, which may be used to localize the post translational modification after complete assignment. This is an interesting outcome of these preliminary results, which is currently being pursued: indeed, although the post translational modification has been localized in the case of PorA (by mutagenesis of the putative Ser sites) (63), the same approach has been unsuccessful in the case of PorH and the site (or sites) of the mycoloylation remains unknown.

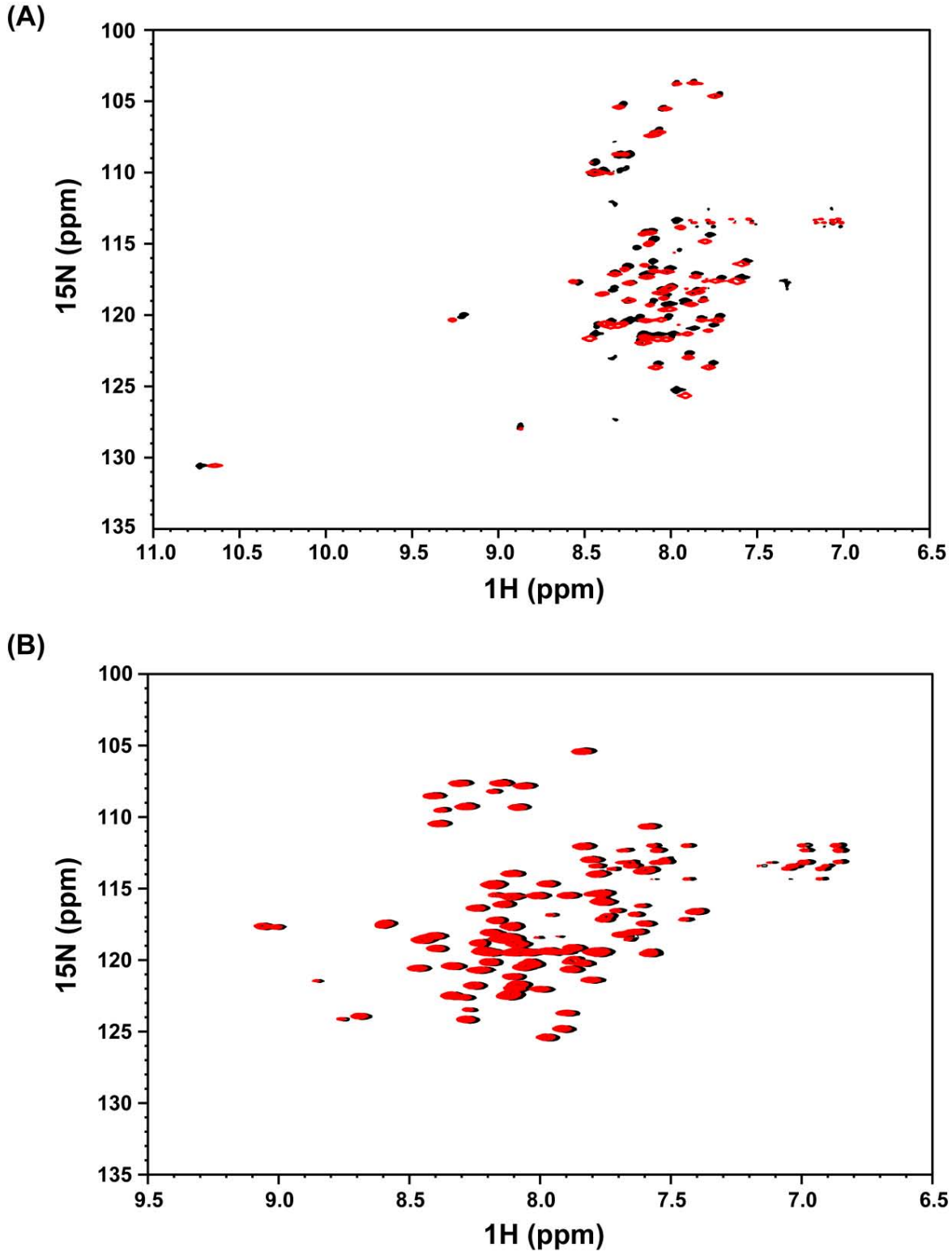

Fig. III-15: Superposition of [^{15}N, ^{1}H]-TROSY spectra of CF expressed U- [^{15}N] labeled (A) PorA in P-CF (in black) and in D-CF (in red) mode expression; (B) P-CF expressed T-PorH directly solubilized in LDAO (in black) or first solubilized in LPPG and then exchanged to LDAO (in red). Spectra were recorded with protein samples in 20 mM Tris-Cl, pH 6.7 containing 2 % LDAO at 25 ^{0}C.

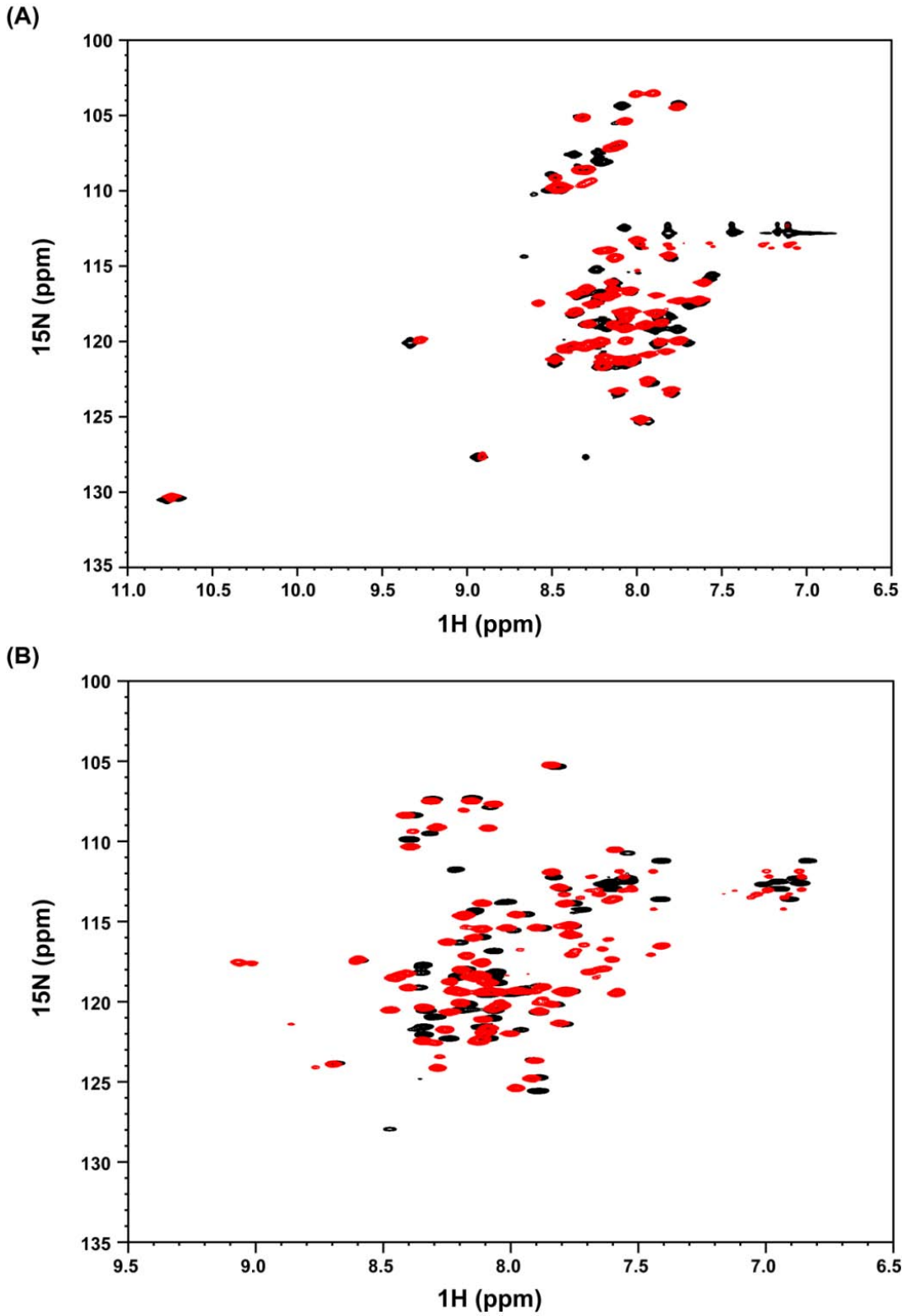

Fig. III-16: Superposition of [^{15}N, ^{1}H]-TROSY spectra of expressed and purified (A) PorA and (B) PorH in *C. glutamicum* (in black) and in CF (in red) expression. The addition peaks in PorH with CF expressed sample were from the extra AT sequences at the N-terminal. The overall structural fold of both proteins looks similar whether modified or unmodified with the mycolic acid modification.

III.11: Ion channel activity of PorA and PorH

As described in the previous chapter, the presence of both PorA and PorH as a complex is required to form a functional ion channel, showing the complete characteristic properties of bacterial porins. To understand the importance of mycolic acid modification on the channel activity, BLM measurements with CF expressed PorA and T-PorH lacking any mycolic acid modification were measured as explained in the experimental procedures. As shown in the fig. III-17, insertion of PorA or T-PorH alone at very high concentrations (500 ng/ml) lead only to noisy profiles and membrane destabilization. When using a 1:1 mixture (w/w) of PorA and T-PorH, progressive insertions were observed with P-CF expressed samples [Fig. III-18A] at high concentrations (500 ng/ml) and with D-CF expressed samples [Fig. III-18B] at lower concentrations (20 ng/ml). However, these insertions persisted only for a short time period (typically less than a min) leading to perturbation and breakage of the membrane and did not result into the voltage dependent characteristics as observed with PorA and PorH mixture with mycolic acid modification (Chapter II, Fig. II-8C).

Furthermore, to understand whether there is an effect on the channel activity by the presence of trehalose dimycolate (TDM, the predominant outer membrane lipid form *C. glutamicum*) in the bilayer or not, BLM measurements were carried out with a bilayer consisting of 10 % TDM in azolectin. Similar results were obtained with multiple insertions but again leading to destabilization of the membrane [Fig. III-18C]. These results indicate that CF expressed proteins, when added to the measurement chamber as a PorA:T-PorH mixture, are able to insert into the membrane, may interact with each other but they create a rapid membrane perturbation instead of a well-defined voltage gated ion channel. This behavior of CF expressed proteins in BLM is similar to pore formation as observed in case of outer membrane-spanning proteins, Oms38 from different *Borrelia* species (70) and also in the pore formation of *Clostridium difficile* toxin B (71).

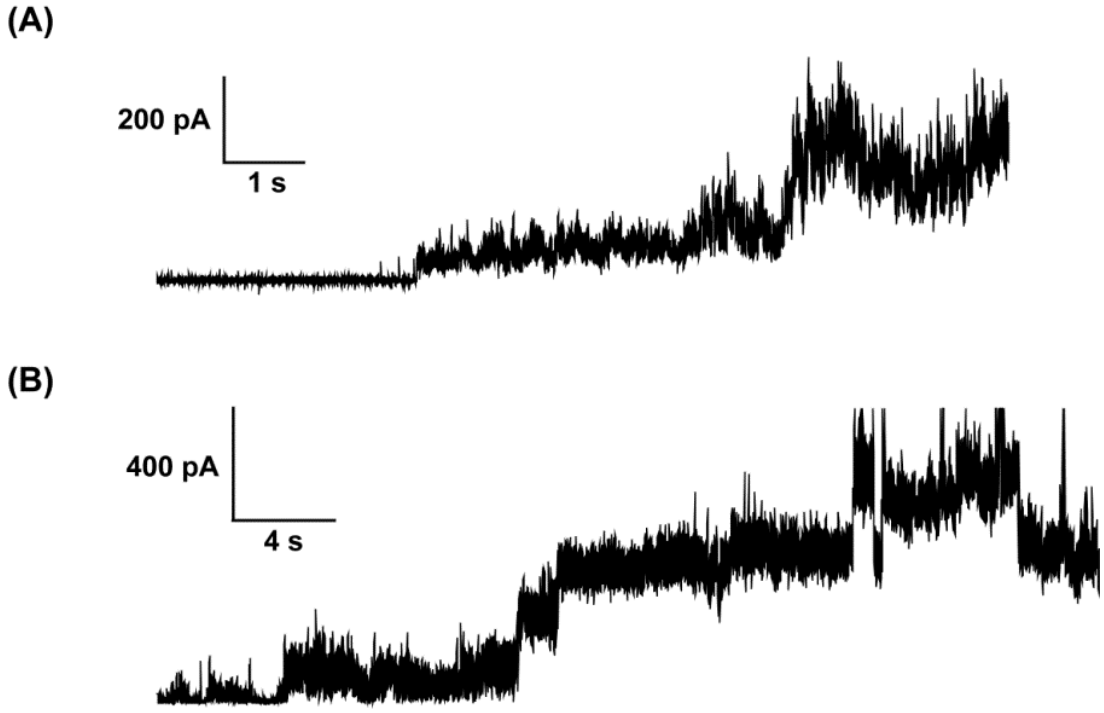

Fig. III-17: Channel activity measurements of CF expressed and purified (A) PorA and (B) T-PorH separately at a protein concentration of 0.5 to 1 µg/ml in the chamber. Noisy perturbation of the bilayer can only be observed without showing characteristic behavior of ion channels.

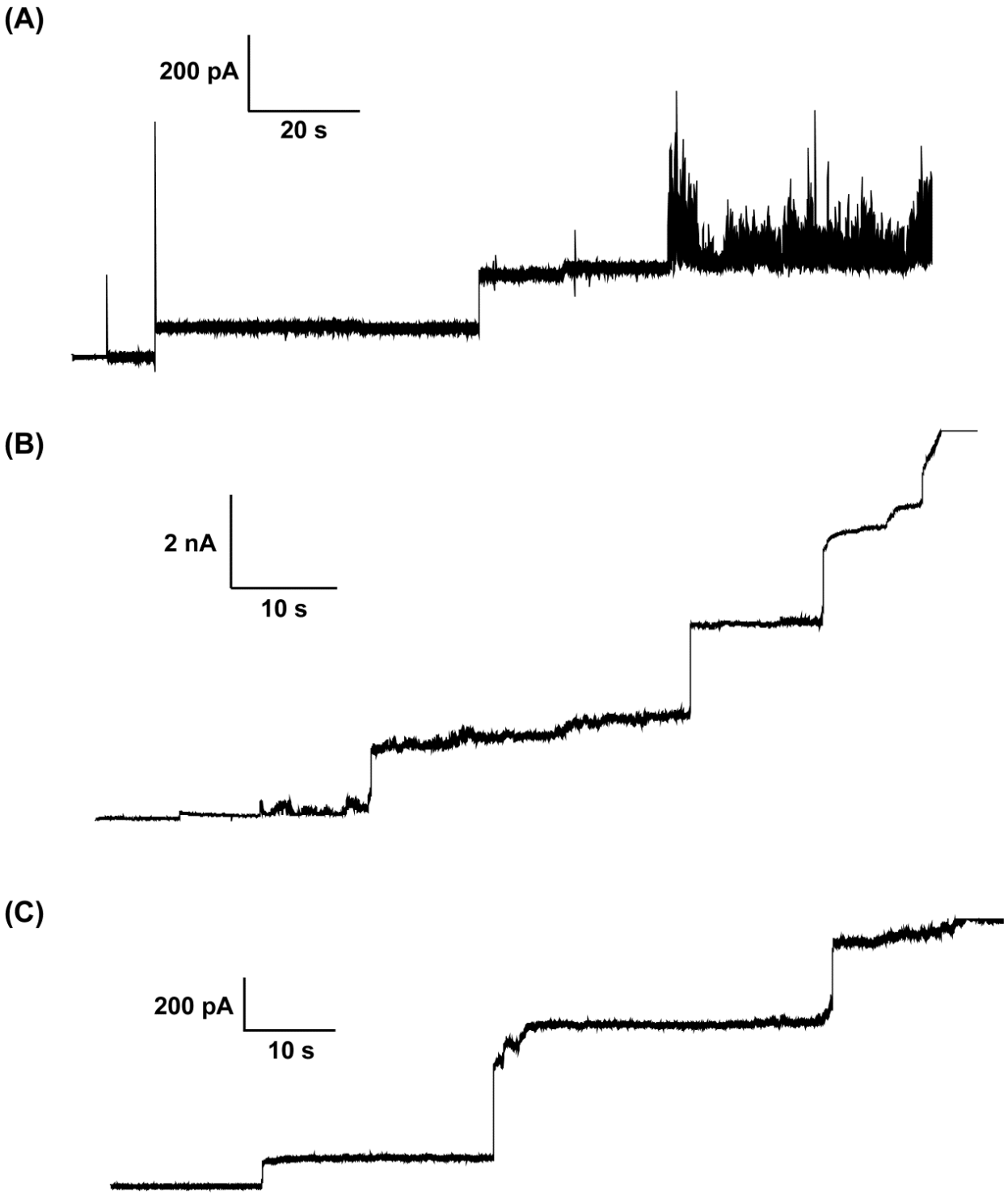

Fig. III-18: BLM measurements with mixture of CF expressed PorA and T-PorH without mycolic acid modification. Sequential insertions were observed with mixture of PorA and T-PorH either from (A) P-CF or (B) D-CF expressed proteins but they lead rapidly to membrane destabilization. The observed conductance did not display any voltage dependence. (C) BLM measurements with a mixture of PorA and S-PorH in presence of a bilayer containing 10 % TDM in azolectin also showed similar patterns.

We thus confirmed that the actual channel consists of both PorA and PorH partners and also the requirement for a covalent attachment of the mycolic acid modification. But it was not clear if both proteins had to be modified to form a functional complex. Therefore we observed the activity of mixed samples, containing one protein purified from *C. glutamicum* (modified) and the other one CF-expressed (un-modified). The PorA-modified : T-PorH-unmodified sample displayed the full characteristics of a voltage dependent ion channel (Fig. III-19A). By contrast, the PorA-unmodified : PorH-modified mixture displayed membrane insertion, but none of the other two typical features, i.e. slow and fast conductance and voltage dependence (Fig. III-19B). Instead of using T-PorH (with 18 extra residues at N-terminus), when S-PorH (with only 4 extra residues) was used, similar results were obtained. Several important conclusions may be drawn from these experiments. First, the CF expressed T-PorH is fully functional when mixed with mycoloylated PorA. It shows that the small AT rich N-terminal expression tag does not prevent the formation of a functional channel and that the CF expressed T-PorH is capable of acquiring rapidly the right fold in the black lipid membranes. Also it is clear that the length of N-terminal expression tags has no effect on the channel activity. It is therefore reasonable to conclude that the mycoloylation on PorH is not a strict requirement for channel activity, but it is the mycoloylation on PorA which is required. This observation is important *per se* for understanding the structure – function relationship of this channel. It is also important for future structural studies because it will allow us to use CF produced stable isotope labeled PorH-in complex with PorA produced from *C. glutamicum* with a different labeling scheme.

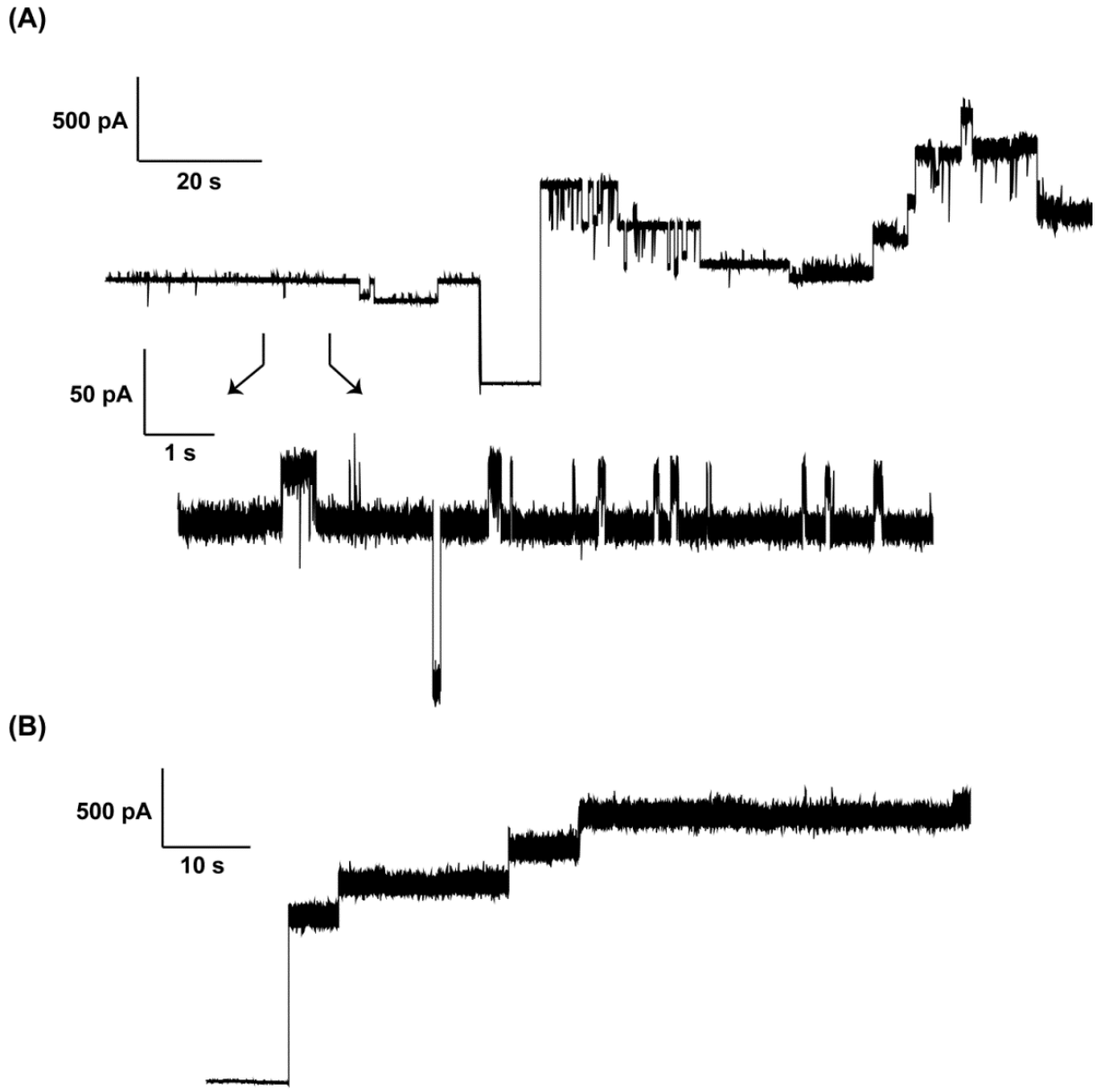

Fig. III-19: BLM measurement with cross-mixture of modified and un-modified proteins expressed and purified from *C. glutamicum* and CF expression respectively. Porin like channels were only observed when (A) a mixture of PorA (modified) and T-PorH (un-modified) was added to the chamber. In contrast (B) a mixture of PorA (un-modified) and PorH (modified) could result in sequential insertions but no slow / fast kinetics or voltage dependence was observed.

REFERENCES

1. Savage, D. F., Anderson, C. L., Robles-Colmenares, Y., Newby, Z. E.&Stroud, R. M. (2007) Cell-free complements in vivo expression of the E. coli membrane proteome *Protein Sci* **16**: 966-76.
2. Sawasaki, T., Ogasawara, T., Morishita, R.&Endo, Y. (2002) A cell-free protein synthesis system for high-throughput proteomics *Proc Natl Acad Sci U S A* **99**: 14652-7.
3. Klammt, C., *et al.* (2006) Cell-free expression as an emerging technique for the large scale production of integral membrane protein *Febs J* **273**: 4141-53.
4. Katzen, F., Chang, G.&Kudlicki, W. (2005) The past, present and future of cell-free protein synthesis *Trends in Biotechnology* **23**: 150-156.
5. Schwarz, D., Dotsch, V.&Bernhard, F. (2008) Production of membrane proteins using cell-free expression systems *Proteomics* **8**: 3933-46.
6. Spirin, A. S. (2004) High-throughput cell-free systems for synthesis of functionally active proteins *Trends in Biotechnology* **22**: 538-545.
7. Grisshammer, R. (2006) Understanding recombinant expression of membrane proteins *Current Opinion in Biotechnology* **17**: 337-340.
8. Wagner, S., Bader, M. L., Drew, D.&de Gier, J. W. (2006) Rationalizing membrane protein overexpression *Trends in Biotechnology* **24**: 364-371.
9. White, S. H. (2004) The progress of membrane protein structure determination *Protein Sci* **13**: 1948-9.
10. Reckel, S., *et al.* (2011) Solution NMR structure of proteorhodopsin *Angew Chem Int Ed Engl* **50**: 11942-6.
11. Maslennikov, I., *et al.* (2010) Membrane domain structures of three classes of histidine kinase receptors by cell-free expression and rapid NMR analysis *Proc Natl Acad Sci U S A* **107**: 10902-7.
12. Berrier, C., *et al.* (2004) Cell-free synthesis of a functional ion channel in the absence of a membrane and in the presence of detergent *Biochemistry* **43**: 12585-91.
13. Kai, L., *et al.* (2010) Preparative scale production of functional mouse aquaporin 4 using different cell-free expression modes *PLoS One* **5**: e12972.
14. Moritani, Y., Nomura, S. M., Morita, I.&Akiyoshi, K. (2010) Direct integration of cell-free-synthesized connexin-43 into liposomes and hemichannel formation *Febs Journal* **277**: 3343-3352.
15. Shimono, K., *et al.* (2009) Production of functional bacteriorhodopsin by an Escherichia coli cell-free protein synthesis system supplemented with steroid detergent and lipid *Protein Science* **18**: 2160-2171.
16. Elbaz, Y., Steiner-Mordoch, S., Danieli, T.&Schuldiner, S. (2004) In vitro synthesis of fully functional EmrE, a multidrug transporter, and study of its oligomeric state *Proc Natl Acad Sci U S A* **101**: 1519-24.
17. Klammt, C., *et al.* (2007) Cell-free production of G protein-coupled receptors for functional and structural studies *Journal of Structural Biology* **158**: 482-493.
18. Kalmbach, R., *et al.* (2007) Functional cell-free synthesis of a seven helix membrane protein: In situ insertion of bacteriorhodopsin into liposomes *Journal of Molecular Biology* **371**: 639-648.

19. Sansuk, K., *et al.* (2008) GPCR proteomics: mass spectrometric and functional analysis of histamine H1 receptor after baculovirus-driven and in vitro cell free expression *J Proteome Res* **7**: 621-9.
20. Kaiser, L., *et al.* (2008) Efficient cell-free production of olfactory receptors: detergent optimization, structure, and ligand binding analyses *Proc Natl Acad Sci U S A* **105**: 15726-31.
21. Barth, E., Barcelo, M. A., Klackta, C.&Benz, R. (2010) Reconstitution experiments and gene deletions reveal the existence of two-component major cell wall channels in the genus Corynebacterium *J Bacteriol* **192**: 786-800.
22. Schwarz, D., *et al.* (2007) Preparative scale expression of membrane proteins in Escherichia coli-based continuous exchange cell-free systems *Nat Protoc* **2**: 2945-57.
23. Wuu, J. J.&Swartz, J. R. (2008) High yield cell-free production of integral membrane proteins without refolding or detergents *Biochim Biophys Acta* **1778**: 1237-50.
24. Kigawa, T.&Yokoyama, S. (1991) A continuous cell-free protein synthesis system for coupled transcription-translation *J Biochem* **110**: 166-8.
25. Craig, D., Howell, M. T., Gibbs, C. L., Hunt, T.&Jackson, R. J. (1992) Plasmid Cdna-Directed Protein-Synthesis in a Coupled Eukaryotic Invitro Transcription-Translation System *Nucleic Acids Research* **20**: 4987-4995.
26. Kigawa, T., *et al.* (2004) Preparation of Escherichia coli cell extract for highly productive cell-free protein expression *J Struct Funct Genomics* **5**: 63-8.
27. Schneider, B., *et al.* (2010) Membrane protein expression in cell-free systems *Methods Mol Biol* **601**: 165-86.
28. Hirose, S., *et al.* (2011) Statistical analysis of features associated with protein expression/solubility in an in vivo Escherichia coli expression system and a wheat germ cell-free expression system *Journal of Biochemistry* **150**: 73-81.
29. Madin, K., Sawasaki, T., Ogasawara, T.&Endo, Y. (2000) A highly efficient and robust cell-free protein synthesis system prepared from wheat embryos: Plants apparently contain a suicide system directed at ribosomes *Proceedings of the National Academy of Sciences of the United States of America* **97**: 559-564.
30. Endo, Y.&Sawasaki, T. (2002) [Highly efficient cell-free protein synthesis system prepared from wheat embryos] *Seikagaku* **74**: 326-30.
31. Katzen, F.&Kudlicki, W. (2006) Efficient generation of insect-based cell-free translation extracts active in glycosylation and signal sequence processing *Journal of Biotechnology* **125**: 194-197.
32. Shimizu, Y., *et al.* (2001) Cell-free translation reconstituted with purified components *Nature Biotechnology* **19**: 751-755.
33. Ohashi, H., Shimizu, Y., Ying, B. W.&Ueda, T. (2007) Efficient protein selection based on ribosome display system with purified components *Biochemical and Biophysical Research Communications* **352**: 270-276.
34. Li, Y., Wang, E.&Wang, Y. (1999) A modified procedure for fast purification of T7 RNA polymerase *Protein Expr Purif* **16**: 355-8.
35. Ishihara, G., *et al.* (2005) Expression of G protein coupled receptors in a cell-free translational system using detergents and thioredoxin-fusion vectors *Protein Expr Purif* **41**: 27-37.

36. Hall, M. N., Gabay, J., Debarbouille, M.&Schwartz, M. (1982) A role for mRNA secondary structure in the control of translation initiation *Nature* **295**: 616-8.
37. Qing, G., Xia, B.&Inouye, M. (2003) Enhancement of translation initiation by A/T-rich sequences downstream of the initiation codon in Escherichia coli *J Mol Microbiol Biotechnol* **6**: 133-44.
38. Freischmidt, A., Liss, M., Wagner, R., Kalbitzer, H. R.&Horn, G. (2012) RNA secondary structure and in vitro translation efficiency *Protein Expression and Purification* **82**: 26-31.
39. Haberstock, S., *et al.* (2012) A systematic approach to increase the efficiency of membrane protein production in cell-free expression systems *Protein Expr Purif* **82**: 308-16.
40. Voges, D., Watzele, M., Nemetz, C., Wizemann, S.&Buchberger, B. (2004) Analyzing and enhancing mRNA translational efficiency in an Escherichia coli in vitro expression system *Biochemical and Biophysical Research Communications* **318**: 601-614.
41. Ahn, J. H., *et al.* (2005) Cell-free synthesis of recombinant proteins from PCR-amplified genes at a comparable productivity to that of plasmid-based reactions *Biochem Biophys Res Commun* **338**: 1346-52.
42. Kralicek, A. V., *et al.* (2011) A PCR-directed cell-free approach to optimize protein expression using diverse fusion tags *Protein Expr Purif* **80**: 117-24.
43. Son, J. M., *et al.* (2006) Enhancing the efficiency of cell-free protein synthesis through the polymerase-chain-reaction-based addition of a translation enhancer sequence and the in situ removal of the extra amino acid residues *Anal Biochem* **351**: 187-92.
44. Yabuki, T., *et al.* (2007) A robust two-step PCR method of template DNA production for high-throughput cell-free protein synthesis *J Struct Funct Genomics* **8**: 173-91.
45. Staunton, D., Schlinkert, R., Zanetti, G., Colebrook, S. A.&Campbell, L. D. (2006) Cell-free expression and selective isotope labelling in protein NMR *Magnetic Resonance in Chemistry* **44**: S2-S9.
46. Klammt, C., *et al.* (2004) High level cell-free expression and specific labeling of integral membrane proteins *Eur J Biochem* **271**: 568-80.
47. Koglin, A., *et al.* (2006) Combination of cell-free expression and NMR spectroscopy as a new approach for structural investigation of membrane proteins *Magn Reson Chem* **44 Spec No**: S17-23.
48. Yokoyama, J., Matsuda, T., Koshiba, S., Tochio, N.&Kigawa, T. (2011) A practical method for cell-free protein synthesis to avoid stable isotope scrambling and dilution *Analytical Biochemistry* **411**: 223-229.
49. Kim, T. W., *et al.* (2007) An economical and highly productive cell-free protein synthesis system utilizing fructose-1,6-bisphosphate as an energy source *Journal of Biotechnology* **130**: 389-393.
50. Kim, T. W., *et al.* (2007) Prolonged cell-free protein synthesis using dual energy sources: Combined use of creatine phosphate and glucose for the efficient supply of ATP and retarded accumulation of phosphate *Biotechnology and Bioengineering* **97**: 1510-1515.
51. Kim, D. M.&Swartz, J. R. (1999) Prolonging cell-free protein synthesis with a novel ATP regeneration system *Biotechnology and Bioengineering* **66**: 180-188.
52. Spirin, A. S., Baranov, V. I., Ryabova, L. A., Ovodov, S. Y.&Alakhov, Y. B. (1988) A Continuous Cell-Free Translation System Capable of Producing Polypeptides in High-Yield *Science* **242**: 1162-1164.

53. Shirokov, V. A., Kommer, A., Kolb, V. A.&Spirin, A. S. (2007) Continuous-exchange protein-synthesizing systems *Methods Mol Biol* **375**: 19-55.
54. Klammt, C., *et al.* (2005) Evaluation of detergents for the soluble expression of alpha-helical and beta-barrel-type integral membrane proteins by a preparative scale individual cell-free expression system *Febs J* **272**: 6024-38.
55. Abdine, A., *et al.* (2010) Structural study of the membrane protein MscL using cell-free expression and solid-state NMR *J Magn Reson* **204**: 155-9.
56. Schagger, H. (2006) Tricine-SDS-PAGE *Nat Protoc* **1**: 16-22.
57. Popot, J. L., *et al.* (2011) Amphipols From A to Z *Annual Review of Biophysics, Vol 40* **40**: 379-408.
58. Lyukmanova, E. N., *et al.* (2012) Lipid-protein nanodiscs for cell-free production of integral membrane proteins in a soluble and folded state: Comparison with detergent micelles, bicelles and liposomes *Biochimica Et Biophysica Acta-Biomembranes* **1818**: 349-358.
59. Roos, C., *et al.* (2012) Co-translational association of cell-free expressed membrane proteins with supplied lipid bilayers *Mol Membr Biol*.
60. Nozawa, A., *et al.* (2011) Production and partial purification of membrane proteins using a liposome-supplemented wheat cell-free translation system *Bmc Biotechnology* **11**.
61. Yang, J. P., Cirico, T., Katzen, F., Peterson, T. C.&Kudlicki, W. (2011) Cell-free synthesis of a functional G protein-coupled receptor complexed with nanometer scale bilayer discs *BMC Biotechnol* **11**: 57.
62. Cappuccio, J. A., *et al.* (2008) Cell-free Co-expression of Functional Membrane Proteins and Apolipoprotein, Forming Soluble Nanolipoprotein Particles *Molecular & Cellular Proteomics* **7**: 2246-2253.
63. Huc, E., *et al.* (2010) O-mycoloylated proteins from Corynebacterium: an unprecedented post-translational modification in bacteria *J Biol Chem* **285**: 21908-12.
64. Greenfield, N. J. (2006) Using circular dichroism spectra to estimate protein secondary structure *Nature Protocols* **1**: 2876-2890.
65. Whitmore, L.&Wallace, B. A. (2004) DICHROWEB, an online server for protein secondary structure analyses from circular dichroism spectroscopic data *Nucleic Acids Res* **32**: W668-73.
66. Pervushin, K., Riek, R., Wider, G.&Wuthrich, K. (1997) Attenuated T-2 relaxation by mutual cancellation of dipole-dipole coupling and chemical shift anisotropy indicates an avenue to NMR structures of very large biological macromolecules in solution *Proceedings of the National Academy of Sciences of the United States of America* **94**: 12366-12371.
67. Renault, M., *et al.* (2009) Solution state NMR structure and dynamics of KpOmpA, a 210 residue transmembrane domain possessing a high potential for immunological applications *J Mol Biol* **385**: 117-30.
68. Shenkarev, Z. O., *et al.* (2010) Lipid-Protein Nanodiscs as Reference Medium in Detergent Screening for High-Resolution NMR Studies of Integral Membrane Proteins *Journal of the American Chemical Society* **132**: 5628-+.
69. Reckel, S., *et al.* (2008) Transmembrane segment enhanced labeling as a tool for the backbone assignment of alpha-helical membrane proteins *Proc Natl Acad Sci U S A* **105**: 8262-7.

70. Thein, M., *et al.* (2008) Oms38 is the first identified pore-forming protein in the outer membrane of relapsing fever spirochetes *J Bacteriol* **190**: 7035-42.
71. Genisyuerek, S., *et al.* (2011) Structural determinants for membrane insertion, pore formation and translocation of Clostridium difficile toxin B *Mol Microbiol* **79**: 1643-54.

THE JOURNAL OF BIOLOGICAL CHEMISTRY VOL. 286, NO. 37, pp. 32525–32532, September 16, 2011
© 2011 by The American Society for Biochemistry and Molecular Biology, Inc. Printed in the U.S.A.

Functional Expression of the PorAH Channel from *Corynebacterium glutamicum* in Cell-free Expression Systems

*IMPLICATIONS FOR THE ROLE OF THE NATURALLY OCCURRING MYCOLIC ACID MODIFICATION**

Received for publication, June 29, 2011, and in revised form, July 22, 2011 Published, JBC Papers in Press, July 28, 2011, DOI 10.1074/jbc.M111.276956

Parthasarathi Rath[‡§], Pascal Demange[‡§1], Olivier Saurel[‡§], Marielle Tropis[‡§], Mamadou Daffé[‡§], Volker Dötsch[¶], Alexandre Ghazi[‖], Frank Bernhard[¶], and Alain Milon[‡§2]

From the [‡]Centre National de la Recherche Scientifique, CNRS UMR 5089, Institut de Pharmacologie et de Biologie Structurale, 205 Route de Narbonne, Toulouse F-31077, Cedex 04, France, the [§]Université de Toulouse-UPS, IPBS, 118 Route de Narbonne, Toulouse 31062, France, the [‖]Université Paris Sud-11, CNRS UMR8619, Institut de Biochimie et Biophysique Moléculaire et Cellulaire, Orsay 91405, France, and the [¶]Center for Biomolecular Magnetic Resonance, Institute of Biophysical Chemistry, Goethe-University of Frankfurt/Main, D-60438 Main, Germany

PorA and PorH are two small membrane proteins from the outer membrane of *Corynebacterium glutamicum*, which have been shown to form heteromeric ion channels and to be post-translationally modified by mycolic acids. Any structural details of the channel could not be analyzed so far due to tremendous difficulties in the production of sufficient amounts of protein samples. Cell-free (CF) expression is a new and remarkably successful strategy for the production of membrane proteins for which toxicity, membrane targeting, and degradation are key issues. In addition, reaction conditions can easily be modified to modulate the quality of synthesized protein samples. We developed an efficient CF expression strategy to produce the channel subunits devoid of post-translational modifications. ^{15}N-labeled PorA and PorH samples were furthermore characterized by NMR and gave well resolved spectra, opening the way for structural studies. The comparison of ion channel activities of CF-expressed proteins with channels isolated from *C. glutamicum* gave clear insights on the influence of the mycolic acid modification of the two subunits on their functional properties.

Corynebacterium glutamicum belongs to the suborder of Corynebacterineae, having an unusual cell wall composition and architecture in comparison with other Gram-negative bacteria. *C. glutamicum* is widely used in fermentation industry for production of L-glutamate and L-lysine. Moreover, *C. glutamicum* genes are orthologues to a number of human pathogens of this group of bacteria, including *Mycobacterium tuberculosis*, *M. leprae*, and *C. diptheriae* (1, 2). The outer membrane of this bacterium contains mycolic acids (long chain α-alkyl and β-hydroxy fatty acids) (3, 4) and four channel forming porins namely, PorA, PorB, PorC, and PorH (5–7). The major porins, PorA (45 amino acids) and PorH (57 amino acids), form cation-selective channels only if present together while PorB and PorC form anion-selective channels (8). The x-ray structure of PorB was solved recently, and it was proposed to exist in the membrane as a putative α-helical porin (9). The porins of some related pathogenic bacteria possessing an outer membrane, *i.e. M. tuberculosis*, *Neisseria meningitides*, *N. gonorrhoeae*, and *Salmonella typhii*, are associated with host-cell recognition and invasiveness during the early stage of infection and thereby contribute to pathogenicity and virulence (10–12). Both PorA and PorH lack signal sequence at their N termini and must be post-translationally modified for trafficking to the cell wall. Recently it was found for the first time in bacteria that these proteins are *O*-acylated by mycolic acids and that this modification plays a critical role in the channel-forming ability of these porins (13). However, many questions on the role and nature of these post-translational modifications still remain unsolved, and structural data are clearly required to fully address these issues. It is also unclear whether the modification is required on both partners or on simply one of them.

In vitro studies on the function and structure of the PorAH channel require large amounts of proteins as well as efficient labeling procedures for the production of samples with incorporated stable isotopes suitable for NMR spectroscopy. However, the recombinant production of membrane proteins (MPs)[3] in heterologous hosts is notoriously difficult as a result of (i) toxic effects due to insertion of MPs into the host cellular membrane, (ii) improper translocation or inefficient transport

* This work was supported by the European Community's Seventh Framework Programme FP7/2007–2013 (Grant 211800) and from the European Drug Initiative on Channels and Transporters (Grant HEALTH-F4–2007-201924) and by the SFB 807 "Transport across membranes."

[1] To whom correspondence may be addressed: Institut de Pharmacologie et de Biologie Structurale, 205 rte. de Narbonne, Toulouse F-31077, Cedex 04, France. E-mail: pascal.demange@ipbs.fr.

[2] To whom correspondence may be addressed: Institut de Pharmacologie et de Biologie Structurale, 205 rte. de Narbonne, Toulouse F-31077, Cedex 04, France. E-mail: alain.milon@ipbs.fr.

[3] The abbreviations used are: MP, membrane protein; CF, cell-free; CECF, continuous exchange CF; RM, reaction mixture; FM, feeding mixture; P-CF, precipitate-forming mode; D-CF, direct soluble expression mode in the presence of detergent; Tricine, *N*-[2-hydroxy-1, 1-bis(hydroxymethyl)ethyl]glycine; BLM, black lipid membrane; TROSY, transverse relaxation optimized spectroscopy; MALDI-TOF, matrix-assisted laser-desorption/ionization time-of-flight; LMPG, 1-myristoyl-2-hydroxy-*sn*-glycero-3-[phosphor-rac-(1-glycerol)]; LMPC, 1-myristoyl-2-hydroxy-*sn*-glycero-3-phosphocholine; LPPG, 1-palmitoyl-2-hydroxy-*sn*-glycero-3-[phosphor-rac-(1-glycerol)]; DHPC, 1,2-dihexanoyl-*sn*-glycero-3-phosphocholine; DPC, dodecylphosphocholine; DDM, *n*-dodecyl-β-D-maltoside; LDAO, lauryldimethylamine oxide; β-OG, *n*-octyl-β-D-glucopyranoside.

Downloaded from www.jbc.org at BIBL SANTE, on September 15, 2011

of overexpressed MPs to the outer membrane destination, (iii) proteolytic cleavage by cytoplasmic protein degradation machines, and (iv) lack of stability during *in vivo* MP extraction from the cell membrane. Indeed, our preliminary attempt to express PorAH channels in *Escherichia coli* failed due to toxic effects upon induction. Cell-free (CF) expression system has emerged as an efficient and multidimensional technique in the rapid production of integral MPs for structural and functional studies as it overcomes most sorts of difficulties (14–19). CF expression reactions can be operated in the batch configuration or in the more efficient continuous exchange CF (CECF) configuration in which the reaction mixture (RM) containing the translation machinery and other high molecular weight compounds is separated from a feeding mixture (FM) containing low molecular weight precursors by a semi-permeable membrane (20). MPs can be CF-produced in different modes. In the precipitate-forming mode (P-CF), no hydrophobic compounds are added into the RM and the synthesized MPs instantly precipitate. Those precipitates often consist of reversible aggregates that can be resolubilized with suitable detergents without preceding refolding procedures. In the direct soluble expression mode in the presence of detergent (D-CF), detergents are provided directly into the RM, and freshly translated MPs can instantly form proteomicelles (21, 22).

To address the challenge of producing sufficient quantities of PorA and PorH and to reveal the impact of the covalent mycolic acid modification on their function, we produced both proteins in an *E. coli*-based CF expression system. After systematic protocol and template optimization, milligram quantities per milliliter of RM as well as of ^{15}N-labeled samples for NMR analysis could be produced within 2 days. CF-synthesized PorA and PorH were completely non-modified in contrast to the proteins purified from their natural host *C. glutamicum*. The proteins were produced in the P-CF and in the D-CF mode, and ion channel activity was analyzed with the single proteins, with PorA-PorH mixture as well as in combinations with the mycoloylated proteins isolated from the natural producer.

EXPERIMENTAL PROCEDURES

DNA Constructs and Cloning Steps—The *C. glutamicum*/*E. coli* shuttle vector pXMJ19 containing multiple cloning sites, and chloramphenicol resistance was used for all DNA manipulations for expression in *C. glutamicum*. pXMJ19-PorA$_{Nhis}$ and pXMJ19-PorH$_{Chis}$ (obtained from Dr. Benz's Laboratory, Jacobs University Bremen, Germany) were used as template to prepare all subsequent constructs for CF expression in T7 promoter-based vectors pET28a and pIVEX2.3d. XbaI-EcoRI fragments from pXMJ19-PorA$_{Nhis}$ and pXMJ19-PorH$_{Chis}$ were ligated into the restricted vector pET28a. Forward primer (5′-GAGAATTTA**CCATGG**AAAACGTTTACGAG-3′) and reverse primer (5′-TTAATTA**CTCGAG**GCTGCCACGCGGCACAAGCAGACCGATGAGGTCAGCAACTGCG-3′) containing NcoI and XhoI restriction sites (shown in bold) were used to amplify PorA from pXMJ19-PorA$_{Nhis}$. The amplified and restricted PCR products were ligated into the vector pIVEX2.3d resulting in the expression of PorA with a C-terminal Poly(His)$_6$ tag and thrombin cleavage site. Moreover, XbaI-XhoI fragments of PorA$_{Nhis}$ and PorH$_{Chis}$ from pET28a were ligated, respectively, into restricted pIVEX2.3d vector resulting in pIVEX2.3d-PorA$_{Nhis}$ and pIVEX2.3d-PorH$_{Chis}$ with Factor Xa cleavage sites. XbaI-EcoRI fragments of pIVEX2.3d-PorA$_{Chis}$ were ligated into restricted pXMJ19 to have pXMJ19-PorA$_{Chis}$. Unless and otherwise mentioned all clones were sequenced and analyzed. DNA templates used for CF expression were isolated from maxi-preparation of resulting constructs in pET28a and pIVEX2.3d using commercial kits (Qiagen).

Expression and Purification—An established CECF expression system based on *E. coli* extracts was used for the *in vitro* expression of PorA and PorH (18, 19). CF S30 (sedimentation, 30,000 × *g*) extract were prepared from *E. coli* strain A19 (23). Analytical scale reactions were performed in Mini-CECF-reactors for optimization and screening steps in which the RM:FM ratio of 1:14 was maintained with a reaction volume of 60 μl (23). Preparative scale expressions with an RM of 2 ml and an RM:FM ratio of 1:17 were carried out in Maxi-CECF-reactors with commercial Slide-A-Lyzer devices (Pierce) as RM container. Unless otherwise mentioned, the RM was separated from the FM by a semi-permeable membrane of cut-off size 10 kDa, and all reactions were carried out at 30 °C for ~20 h with gentle shaking. For MP solubilization either in the P-CF or in the D-CF mode, the following detergents with suitable concentration (indicated under "Results and Discussion") were used: Brij-35, Brij-58, Brij-72, Brij-98, LDAO, and Triton X-100 (Sigma-Aldrich); LMPG, LMPC, LPPG, DHPC, and DPC (Avanti Polar Lipids, Alabaster, AL); β-OG (Glycon Biochemicals, Luckenwalde, Germany); DDM (AppliChem, Darmstadt, Germany); and SDS (Roth, Karlsruhe, Germany).

The P-CF proteins were obtained almost pure after re-solubilization in 20 mM Tris-Cl, pH 7.7, 150 mM NaCl (Buffer A) supplemented with appropriate detergent. The D-CF-expressed proteins were purified in one step by using immobilized metal-chelated affinity chromatography. 2 ml of RM was mixed with 600 μl of Ni^{2+}-loaded NTA resin (Qiagen) for overnight at 4 °C. The resin-bound proteins were washed by gravity flow with 10 ml of buffer B (buffer A plus 0.4% LDAO) followed by sequential washings with 10 ml of 20 mM imidazole in buffer B and finally eluted with 4 ml of 500 mM imidazole. The pure PorA or PorH fractions were concentrated to 2 ml using Vivaspin devices (3-kDa cut-off, Sartorius Biolab, Goettingen, Germany), and imidazole was removed by passing through a 2.5-ml PD-10 column (Sephadex G25, GE Healthcare). Protein samples were analyzed by using 16% Tris-Tricine SDS-PAGE followed by Coomassie Blue staining and/or further detected by immunoblotting using anti-His antibodies (24, 25). Purified proteins were quantified according to their molar extinction coefficient (PorA: 8250 $cm^{-1}\ M^{-1}$; PorH: 1250 $cm^{-1}\ M^{-1}$) by measuring UV absorbance at 280 nm. Furthermore, NMR samples were prepared in 2-ml preparative scale reactions either in the P-CF mode or in the D-CF mode. The unlabeled amino acid mixture in the RM and FM was replaced by a 98% U-^{15}N-labeled amino acid mixture (Cambridge Isotope Laboratories Inc., Andover, MA).

Cleavage of Affinity Tags—The purified PorA and PorH fractions were dialyzed in cleavage buffer containing 50 mM Tris-Cl, pH 8.0, 100 mM NaCl, 5 mM $CaCl_2$, and 0.4% LDAO. Restriction grade thrombin (Novagen) at 1 unit/mg of protein and

Downloaded from www.jbc.org at BIBL SANTE, on September 15, 2011

Factor Xa (Qiagen) at 1 unit/50 μg of protein were used to cleave the C-terminal poly(His) tags from PorA and PorH, respectively. Cleavage was performed at 20 °C for 16 h, and proteases were removed by specific removal resins provided by commercial suppliers. Cleavage with >90% efficiency was observed at protein concentration of 0.8 mg/ml, and furthermore the cleaved protein samples were verified by matrix-assisted laser-desorption/ionization-time-of-flight (MALDI-TOF) mass spectrometry and SDS-PAGE analysis. The N-terminal tag used to promote CF expression of PorH resisted to proteolytic cleavage (PreScission protease) and was used as such, the protein being called T-PorH.

Peptide Sequences after Cleavage of Respective C-terminal Histidine Tags—The sequences used were: PorA (molecular mass = 5146 Da): MENVYEFLGNLDVLSGSGLIGYVFDFLG-ASSKWAGAVADLIGLLG-**LVPR**; PorH (molecular mass = 6617 Da): MDLSLLKETLGNYETFGGNIGTALQSIPTLL-DSILNFFDNFGDLADTTGENLDNFSS**IEGR**; and T-PorH (molecular mass = 9124 Da): **MKYYKYYKYYKLEVLFQGP**-MDLSLLKETLGNYETFGGNIGTALQSIPTLLDSILNFFDN-FGDLADTTGENLDNFSS**IEGR**. (Bold letters represent extra residues after cleavage of tags.)

Mass Spectrometry Analysis—MALDI-TOF spectra of *in vivo*- and *in vitro*-expressed and purified proteins were acquired on a Voyager-DE STR mass spectrometer (PerSeptive Biosystems) fitted with a pulsed nitrogen LASER emitting at 337 nm, and all spectra were analyzed in linear mode using an extraction delay of 100 ns with accelerating voltage of 25 kV. Protein samples were mixed with sinapinic acid as matrix and were loaded onto a metal plate; 2500 shots were accumulated for each sample in a positive ion mode, and all data were acquired with default calibration for the instrument. To reduce problems caused by detergents in measurements, either the ethyl acetate method (26) or the simple-dilution method in water were used to obtain an improved signal-to-noise ratio.

Channel Activity Measurements—Planar lipid bilayers (so-called black lipid membranes (BLMs)) were formed across a 250-μm diameter hole by presenting a bubble of asolectin lipids (Sigma) dissolved in *n*-decane (30 mg/ml). Recordings were performed in symmetric media containing an unbuffered solution of 1 M KCl (as in Ref. 8). Currents were amplified using an Axon 200B patch-clamp amplifier, filtered at 1 kHz through an a-pole Bessel filter, and digitized at 2 kHz. Data were analyzed with pCLAMP software. Unless otherwise mentioned the protein samples were diluted in 1 M KCl to obtain appropriate concentrations for measurements. Control experiments using detergent alone were performed systematically and did not show any characteristic signal.

RESULTS AND DISCUSSION

Optimization of CF Expression Protocols for the Preparative Scale Production of PorA and T-PorH—CECF reaction protocols described before (18–20) were used as the basis to optimize the expression of PorA and PorH. At first the expression of PorA and PorH was evaluated in analytical scale P-CF reactions with the constructs pET28-PorA, pIVEX2.3-PorA, pET28-PorH, and pIVEX2.3-PorH as templates. Good expression levels of PorA from both constructs were observed. The location of the poly(His)$_6$ tag at either the N or C terminus had no detectable effect on expression of PorA. However, no expression of PorH was observed from both templates after analysis by either Coomassie Blue-stained SDS-PAGE or by Western blot analysis with anti-His antibodies. Considering the reduced complexity of protein production in CF systems, complex mRNA secondary structures preventing efficient translation initiation at the translational start codon are primary reasons of insufficient expression yields. The 5′-end of the PorH coding region was therefore modified by fusion with a long AT-rich sequence encoding for 10 additional amino acids. The addition of the small expression tag improved production of PorH to high levels. The expression yields of PorA and T-PorH were further maximized by optimizing Mg^{2+} concentrations in the CF reaction. After Mg^{2+} screening in the range of 8–22 mM, a broad optimum between 10 and 18 mM was identified for PorA, whereas T-PorH showed a rather narrow optimum between 14 and 16 mM (Fig. 1). These identified conditions were used for subsequent preparative scale productions in the P-CF and D-CF modes.

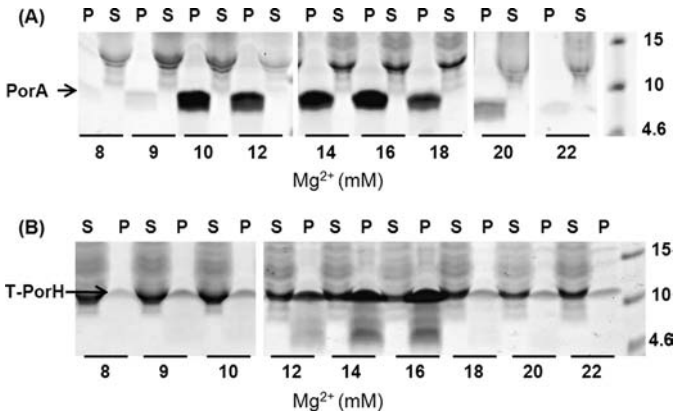

FIGURE 1. **Mg^{2+} screening in analytical scale P-CF reactions of PorA (*A*) and T-PorH (*B*).** 6 μl of precipitate and 3 μl of supernatant was loaded in each well of 16% Tris-Tricine SDS-PAGE followed by Coomassie staining. PorA has a broad optimum from 10 to 18 mM, whereas T-PorH has a narrow optimum from 14 to 16 mM. *P* = precipitate, *S* = supernatant. Molecular mass markers (kilodaltons) are given in the *right lane*.

Production of PorA and T-PorH in Micelles, Using P-CF and D-CF Mode Expressions—In P-CF reactions, PorA and T-PorH instantly precipitate after translation in the RM. However, many P-CF-produced MPs can efficiently be resolubilized in a variety of detergents, whereas the solubilization efficiency of a particular detergent depends on the individual MP (21, 22, 27). We therefore performed a resolubilization screen to identify detergents efficient for the resolubilization of P-CF-generated PorA and T-PorH. The precipitates were centrifuged at 15,000 × *g* for 15 min and washed with Buffer A followed by immediate resolubilization in various detergents without any denaturation/renaturation steps. For resolubilization screening, the following detergents were evaluated: LMPG (1-myristoyl-2-hydroxy-*sn*-glycero-3-[phosphor-rac-(1-glycerol)]) (1%), LMPC (1-myristoyl-2-hydroxy-*sn*-glycero-3-phosphocholine) (1%), LPPG (1-palmitoyl-2-hydroxy-*sn*-glycero-3-[phosphor-rac-(1-glycerol)]) (1%), DHPC (1,2-dihexanoyl-*sn*-glycero-3-phosphocholine) (1%), DPC (dodecylphosphocholine) (1%), DDM (*n*-dodecyl-β-D-maltoside) (1%), LDAO (lauryldimethylamine oxide) (1%), SDS (1%), and β-OG

Downloaded from www.jbc.org at BIBL SANTE, on September 15, 2011

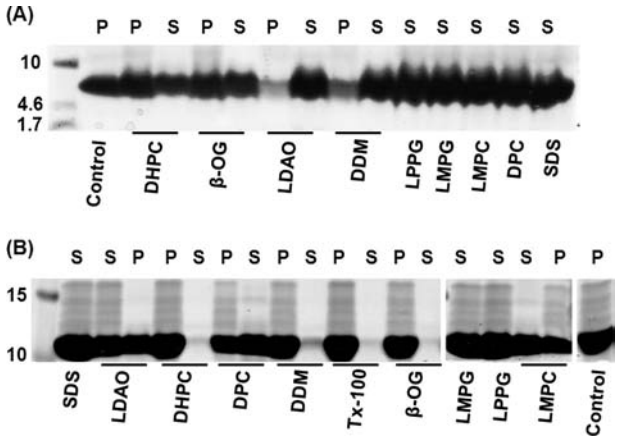

FIGURE 2. **Resolubilization screening of P-CF-expressed PorA (*A*) and T-PorH (*B*).** Precipitates of P-CF reactions were resuspended in equal volumes (60 μl) of buffer (20 mM Tris-Cl, pH 7.7, 150 mM NaCl) containing 1% of one of the detergents: LDAO, LPPG, LMPG, LMPC, DHPC, DPC, DDM, Triton X-100 (*Tx-100*), SDS, or 2% β-OG for 2 h at 30 °C. Non-solubilized proteins was precipitated by centrifugation, and 5 μl of each supernatant and remaining precipitate suspended in the initial volume of buffer was analyzed by 16% Tris-Tricine SDS-PAGE followed by Coomassie Blue staining. Control is the corresponding initial P-CF precipitate. *P* = precipitate, *S* = supernatant. Molecular mass markers (kilodaltons) are indicated in the *left lane*.

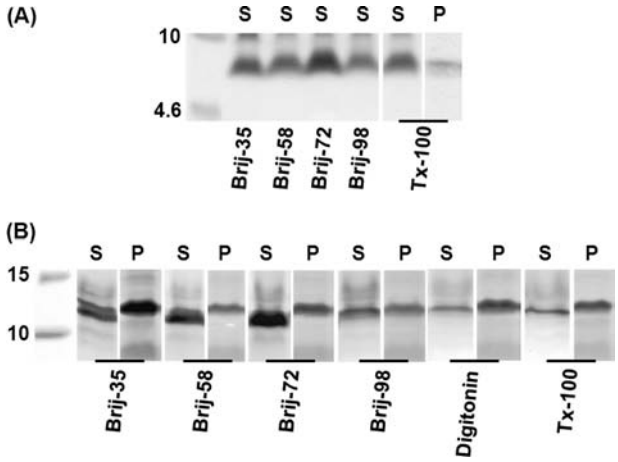

FIGURE 3. **Detergent screening in analytical scale D-CF mode expression of (*A*) PorA and (*B*) T-PorH.** Detergents at final concentrations of Brij-35 (0.5%), Brij-58 (1%), Brij-72 (1%), Brij-98 (1%), Triton X-100 (*Tx-100*) (0.1%), and Digitonin (0.4%) were used. 2 μl each of supernatant and suspended precipitate was analyzed by 16% Tris-Tricine SDS-PAGE and followed by Coomassie Blue staining. *P* = precipitate, *S* = supernatant. Protein markers (kilodaltons) are indicated in the *left lane*.

(n-octyl-β-D-glucopyranoside) (2%). The choice of these detergents was based on a long term experience in solubilizing P-CF-expressed membrane proteins (18). A panel of non-ionic detergents (DDM and β-OG) and zwitterionic (LMPC, DHPC, DPC, and LDAO), and negatively charged (LMPG, LPPG, and SDS) ones was chosen. Many of them display typical phospholipid polar heads (LMPC, LMPG, LPPG, DHPC, and DPC). A specific focus was placed on detergents typically used for solution state NMR spectroscopy and x-ray crystallography of membrane proteins. LDAO was a common detergent throughout this work, because it was efficient in extracting and purifying "*in vivo*" PorAH from *C. glutamicum* membranes, and it gave well resolved NMR spectra on these samples. After incubation for 2 h at 30 °C with gentle shaking, the supernatant and residual precipitates were again separated by centrifugation and analyzed by SDS-PAGE. In comparison with controls, PorA precipitates completely solubilized in LPPG, LMPG, LMPC, DPC, and SDS and to a minor extent but still up to 50% in DHPC, LDAO, DDM, and β-OG. Solubilization of P-CF-produced T-PorH was complete only in LPPG, LMPG, and SDS and up to 50% in DPC, LDAO, and LMPC. Only minor fractions of PorH were solubilized in DHPC, DDM, Triton X-100, and β-OG (Fig. 2).

Alternatively to the resolubilization of P-CF precipitates, PorA and T-PorH were further produced in soluble form in the presence of detergents by using the D-CF expression mode. Suitable detergents that do not inhibit the CF expression system were screened in analytical scale reactions (21). Detergents selected at initial final concentrations were Brij-35 (polyethylene-(23)-laurylether) (0.5%), Brij-58 (polyoxyethylene-(20)-cetylether) (1%), Brij-72 (polyoxyethelene-(2)-stearylether) (1%), Brij-98 (polyoxyethylene-(20)-oleylether) (1%), digitonin (0.4%), and Triton X-100 (0.1%). All Brij derivatives could completely solubilize PorA in the D-CF mode, and no residual PorA precipitate was detectable. The presence of different detergents also modulated the expression efficiency to some extent while highest yields were obtained with Brij-72 (Fig. 3). In contrast, the D-CF solubilization of T-PorH was generally much less effective, and the protein was not fully solubilized in any of the analyzed detergents (Fig. 3). The highest solubilization efficiency was obtained with Brij-72, and complete solubilization was obtained after further increase of the final detergent concentration to 1.2%.

Purification of C. glutamicum and CF-expressed Proteins—In vivo expression and purification of PorA or PorH out of *C. glutamicum* were carried out as described previously to obtain both proteins with mycolic acid modification (8). Because the *in vivo*-expressed samples were analyzed in LDAO (0.4%), we kept the same detergent for sample preparation of CF-expressed PorA and T-PorH. The direct resolubilization of P-CF-expressed PorA and T-PorH in LDAO resulted in relatively pure protein, and hence, those samples were directly used for further characterization. As a second option, the two proteins were expressed in the D-CF mode in the presence of Brij-72, and the detergent was then exchanged to LDAO upon immobilization of the proteins at Ni-NTA affinity columns. The immobilized proteins were washed with 20 mM imidazole and finally eluted in LDAO micelles with 500 mM imidazole. The purity and homogeneity of both *in vivo* and CF-expressed proteins were analyzed by SDS-PAGE followed by Coomassie Blue staining (Fig. 4). After cleavage of the C-terminal poly(His)$_6$ tags the samples were further characterized by mass spectrometry and with respect to their pore-forming activities. The final expression yield of 200 μM/liter of culture for *in vivo* expression and 200 μM/ml of RM for *in vitro* expression were obtained.

Biochemical Characterization of PorA and PorH by Mass Spectrometry—The presence or absence of mycolic acid modification on *in vivo*- and *in vitro*-expressed PorA and PorH were characterized by MALDI-TOF mass spectrometry. The theoretical masses of native PorA and PorH without modification are, for ($M + H^+$), 4681 Da and 6162 Da, respectively (13). In the case of the recombinant PorA and PorH constructs, after cleavage of the affinity tags used for purification of PorA and

Downloaded from www.jbc.org at BIBL SANTE, on September 15, 2011

PorH, the predicted ($M + H^+$) masses without mycoloylation are 5147 Da for PorA, 6618 Da for PorH, and 9125 Da for T-PorH modified with the N-terminal expression tag. As shown in Fig. 5 (*A* and *C*), MALDI-TOF spectra of purified PorA expressed in *C. glutamicum* and CF synthesis confirmed the presence of mycolic acid modification with a difference of 506 Da corresponding to C34:0 naturally occurring corynomycolic residues, as was described previously (13). Similarly, we observed the absence of mycolic acid modification on CF-expressed T-PorH according to the theoretical molecular weight. The increase in molecular mass of CF-expressed PorH resulted from the N-terminal modification with the AT-rich expression tag. The mycolic acid post-translational modification has been described as an esterification reaction; hence, it is susceptible to alkaline treatment. This was further confirmed by treatment of *in vivo*-expressed PorA and PorH with 0.1 M NaOH, and the subsequent MALDI-TOF spectra analysis confirmed the loss of 506 Da.

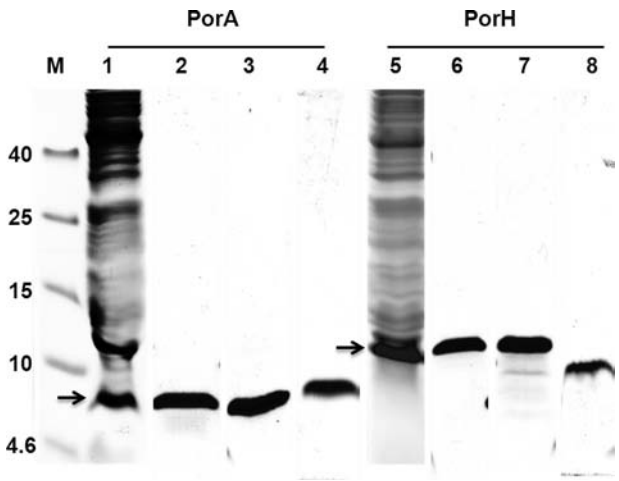

FIGURE 4. **Purification of PorA and PorH (T-PorH for CF).** Samples were analyzed by 16% Tris-Tricine SDS-PAGE and Coomassie Blue staining. *Lanes 1* and *5*: CF reaction mixture after D-CF expression; *lanes 2* and *6*: Ni-NTA-purified sample from D-CF expression; *lanes 3* and *7*: P-CF-expressed and -resolubilized samples; *lanes 4* and *8*: *C. glutamicum*-expressed and -purified samples. *M*, protein marker in kilodaltons.

NMR Spectroscopy—Two-dimensional, $^{15}N,^{1}H$ transverse relaxation optimized spectroscopy (TROSY) spectra (28, 29) of PorA and T-PorH were obtained after preparative scale expression of the proteins in the presence of labeled amino acids. NMR samples (0.25 mM) were prepared in 20 mM Tris-Cl, pH 6.7, in LDAO (~2%), and the spectra were recorded at 25 °C. For P-CF-expressed proteins, TROSY spectra of good resolution could be obtained for both proteins (Fig. 6). The spectra of both proteins were identical regardless whether the proteins were directly resolubilized in LDAO, or first LPPG-resolubilized and then exchanged to LDAO upon Ni-NTA chromatography (data not shown). Furthermore, ^{15}N-labeled D-CF-produced samples of PorA and T-PorH were generated and measured under identical conditions. The dispersion and signal intensity of P-CF- or D-CF-produced samples of PorA and T-PorH did not show significant differences (Fig. 6). In addition, other detergents besides LDAO were analyzed for their effects on the quality of NMR spectra. PorA and T-PorH were exchanged into DHPC upon affinity chromatography, and recorded NMR spectra were identical to those in LDAO (data not shown). Hence, it can be concluded that P-CF- or D-CF-expressed PorA and T-PorH maintain their structural fold in LDAO and in DHPC. Moreover, the good resolution and spectral diversity gave evidence that the P-CF- and D-CF-expressed samples are structurally homogenous in LDAO or DHPC. This result opens the way for structural studies of PorA and T-PorH using NMR spectroscopy provided that the activities of these CF-expressed proteins can be demonstrated (30–33).

Ion Channel Activity of in Vivo- and in Vitro-expressed PorA and PorH—In recent years the functionality of PorA and PorH has been studied with protein extract from the cell wall of *C.*

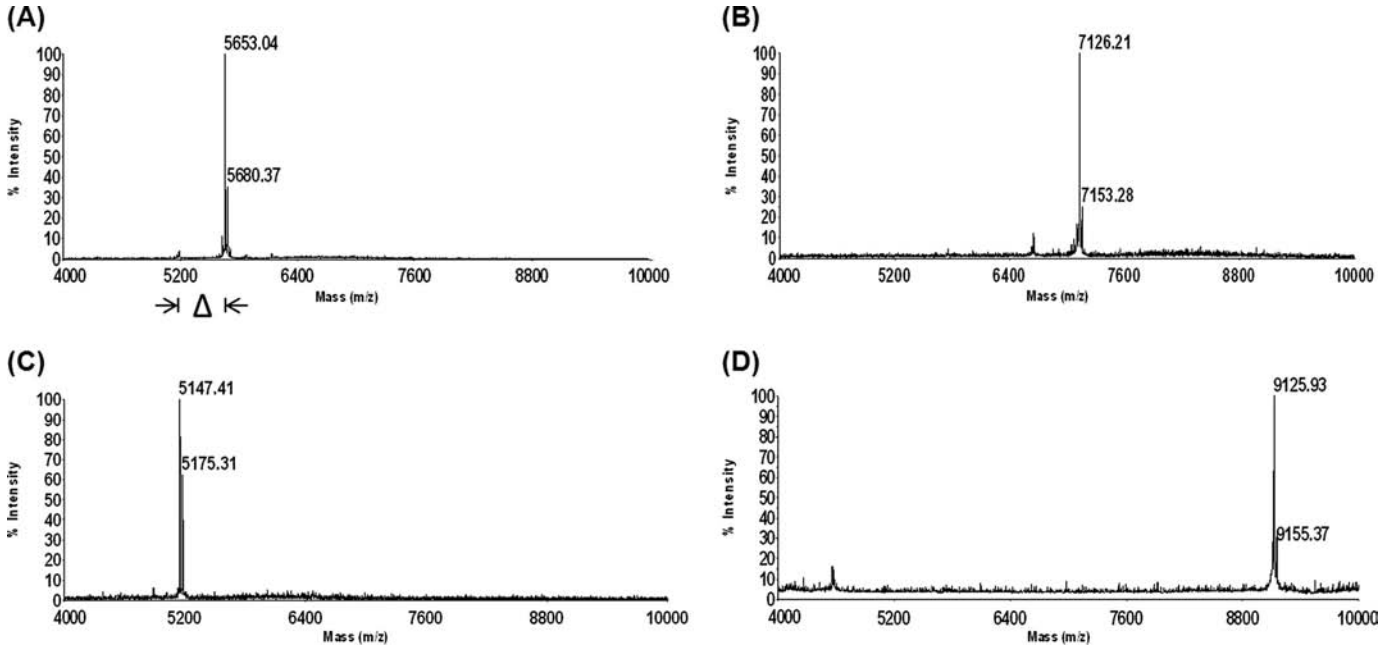

FIGURE 5. **MALDI-TOF mass spectra of *in vivo*-expressed PorA (*A*) and PorH (*B*) with mycolic acid Δ (C34:0) modification; CF-expressed PorA (*C*) and T-PorH (*D*) corresponding to their theoretical molecular mass without mycolic acid modification.**

Downloaded from www.jbc.org at BIBL SANTE, on September 15, 2011

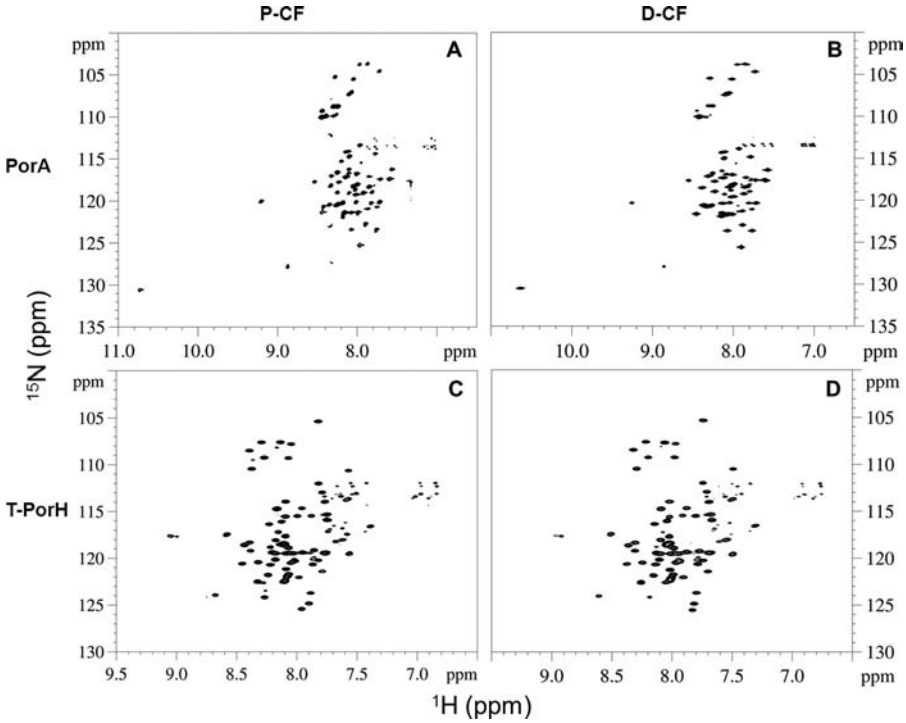

FIGURE 6. **^{15}N,^{1}H TROSY spectra of CF-expressed U-^{15}N-labeled PorA and T-PorH in 20 mM Tris-Cl, pH 6.7, containing 2% LDAO at 25 °C.** *A*, PorA from P-CF; *B*, PorA from D-CF; *C*, T-PorH from P-CF; *D*, T-PorH from D-CF.

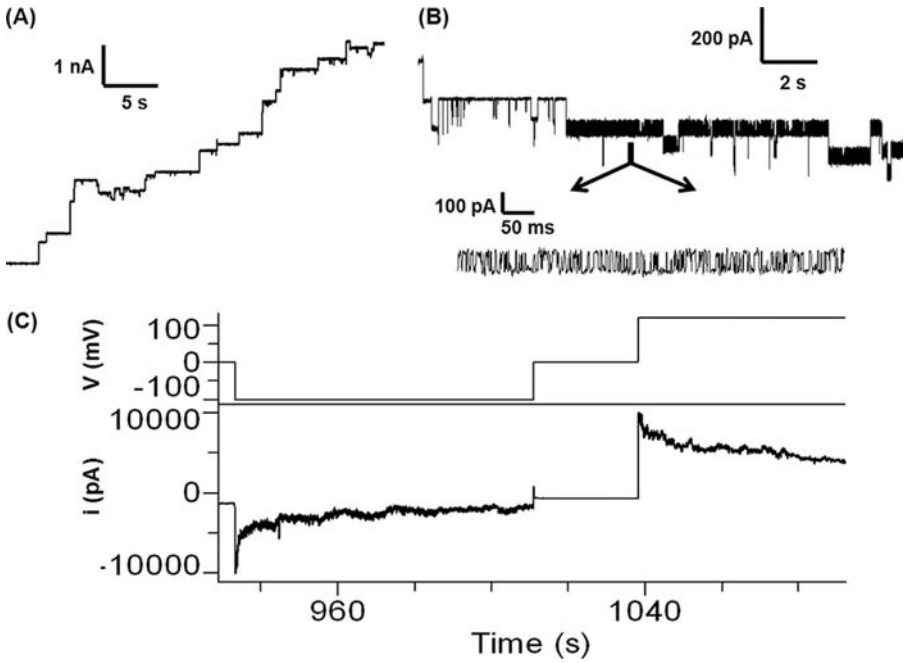

FIGURE 7. **Porin channel activity of a mixture of *in vivo*-expressed PorA and PorH.** The aqueous phase contained 1 M KCL. *A*, multiple insertions in the membrane upon addition of the mixture in the bilayer chamber. *B*, slow and fast kinetics of closure of the channels upon application of +40 mV. *C*, application of −100 mV to a bilayer containing a large number of channels resulted in the closure of channels that could be re-opened upon return to 0 mV. The channels closed, but with a different time course, upon application of +100 mV.

glutamicum, and results indicate the formation of a functional complex out of both proteins (8), in addition to the requirement of mycolic acid modifications (on position Ser-15 in the case of PorA) for pore-forming activity (13).

In the present study, we investigated ion channel activity, using expressed and purified protein samples with (proteins expressed from *C. glutamicum*) and without mycolic acid modification using the advantage of *E. coli*-based CF expression. In the latter case, we are in a position to use purified proteins, without any chemical treatment and after mass spectrometric characterization. When a mixture of *in vivo* PorA and PorH was added to the chamber, porin-like channel activity could be observed for a concentration as low as 1 ng/ml. Fig. 7*A* shows the profile characteristic of multiple channel insertion in the

Downloaded from www.jbc.org at BIBL SANTE, on September 15, 2011

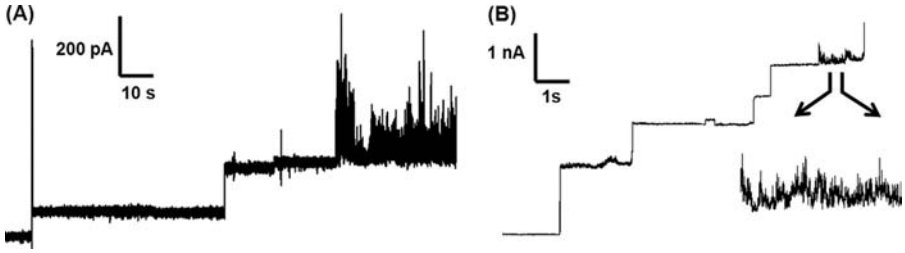

FIGURE 8. **BLM measurements with CF-expressed PorA and T-PorH without mycolic acid modification.** Sequential insertions were observed with mixture of PorA and T-PorH either from (*A*) P-CF- or (*B*) D-CF-expressed proteins, but they lead rapidly to membrane destabilization. The observed conductance did not display any voltage dependence (data not shown).

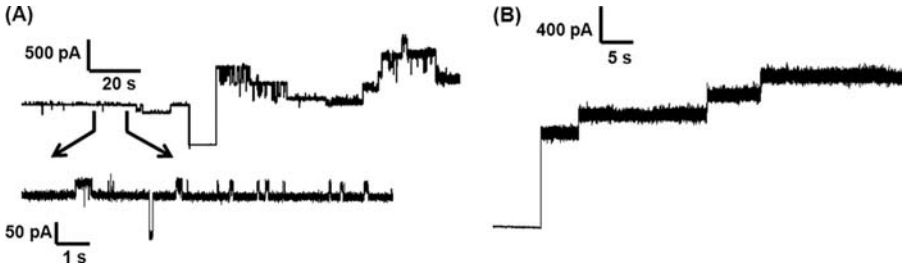

FIGURE 9. **BLM measurement with a cross-mixture of *in vivo*- and *in vitro*-expressed proteins.** Porin-like channels were only observed when (*A*) a mixture of PorA (*in vivo*) and T-PorH (*in vitro*) was added to the chamber. These channels displayed the characteristic voltage dependence shown in Fig. 7*C* (data not shown). In contrast (*B*) a mixture of PorA (*in vitro*) and PorH (*in vivo*) could result in sequential insertions, but no voltage dependence was observed.

bilayer with time. The channels that were opened around 0 mV closed upon application of a membrane potential, positive or negative. Fig. 7*B* shows that opening and closing of the channels occurred with two distinct kinetics, one with a millisecond time scale, the other with an approximate time scale of seconds. Different conducting states could be clearly observed. As shown in Fig. 7*C* the tendency to close at high membrane potentials was greater at one polarity. When *in vivo*-expressed PorA and PorH were added to the chambers separately, no such channel activity could be recorded. At very high concentrations (0.5–1 μg/ml) noisy perturbations of the membrane could be detected, indicating that some proteins could insert in the bilayer. Our results confirm the requirement of both PorA and PorH to form a proper ion channel (8). They show in addition that the PorA-PorH channel shares the characteristic fingerprints of channels such as bacterial porin (34) and also mitochondrial porin (35): closure at positive and negative potential with fast and slow kinetics, asymmetric voltage dependence, and multiple conductance states. Similar porin channels can be found in related families of bacteria, *C. diphtheria*, *C. efficiens*, and *N. farcinia* (8, 36, 37).

To understand further the importance of mycolic acid modification on channel activity, we repeated the BLM measurement with CF-expressed PorA and T-PorH lacking any mycolic acid modification. Insertion of PorA or T-PorH alone lead to noisy profiles and membrane destabilization. When using a 1:1 mixture (w/w) of PorA and T-PorH, progressive insertions were observed with P-CF-expressed samples (Fig. 8*A*) at high concentrations (500 ng/ml) and with D-CF-expressed samples (Fig. 8*B*) already at 25-fold lower concentrations (20 ng/ml). However, these insertions persisted only for a short time period (typically less than a minute) leading to perturbation and breakage of the membrane and did not result into the voltage-dependent characteristics as observed with a PorA and PorH mixture with mycolic acid modification. This indicates that CF-expressed proteins, when added to the measurement chamber as a PorA:T-PorH mixture, are able to insert into the membrane, but they create a rapid membrane perturbation instead of a well defined voltage-gated membrane channel. This behavior of CF-expressed proteins in BLM is similar to pore formation as observed in the case of outer membrane-spanning proteins, Oms38 from different *Borrelia* species (38) and also in the pore formation of *Clostridium difficile* toxin B (39). The same experiment has been performed using "*in vivo*"-produced and -purified proteins, chemically treated to remove the mycolic acid modification, using the protocol described before (13). In this case, the 1:1 mixture of PorA and PorH gave no signal at all and no sign of insertion. This may indicate that the chemical treatment makes more than just the expected deacylation in terms of the proteins primary or tertiary structure.

Because naturally occurring PorA and PorH are modified by mycolic acids, and because it was not clear whether both modifications on PorA and on PorH are required for the formation of a functional channel, we decided to observe the activity of mixed samples, containing one protein purified from *C. glutamicum* ("*in vivo*") and the other one CF-expressed ("*in vitro*") (Fig. 9). The PorA *in vivo*-T-PorH *in vitro* sample displays the complete set of characteristic of a voltage-dependent ion channel (Fig. 9*A*). By contrast, the PorA *in vitro*-PorH *in vivo* mixture displayed membrane insertion, but none of the other two typical features, *i.e.* slow and fast conductance and voltage dependence (Fig. 9*B*). Several important conclusions may be drawn from these experiments. First, the CF-expressed T-PorH is fully functional when mixed with mycoloylated PorA. It shows that the small AT-rich N-terminal expression tag does not prevent the formation of a functional channel and that the CF-expressed T-PorH is capable of acquiring rapidly the right fold in the black lipid membranes. Although T-PorH differs from PorH by an N-terminal extension, it is hardly possible that this hydrophilic tail compensates for the absence of mycoloyla-

Downloaded from www.jbc.org at BIBL SANTE, on September 15, 2011

tion, and it is therefore reasonable to conclude that the mycoloylation on PorH is not a strict requirement for activity. The *vice versa* mixture PorA *in vitro*-PorH *in vivo* gave also channels in BLM experiments, but these did not possess the entire expected functional characteristic. The behavior of PorA *in vitro* in complex with PorH *in vivo* is therefore clearly different from that of PorA *in vitro* alone or from the complex of PorA *in vitro*-T-PorH *in vitro*. The membrane stays stable, and the detected channel activity most likely reflects some stabilization of PorA *in vitro* by interaction with the cotranslocated PorH *in vivo*.

In summary, the results indicate for the first time that the post-translational modification by mycolic acids is not an absolute requirement for the function of PorH as part of a voltage-dependent ion channel, whereas it is so in the case of PorA. Furthermore, CF expression has been shown to be a valuable tool for the study of these ion channels as (i) large amounts of pure and functionally active protein can be synthesized in less than 3 days, (ii) it allows the straightforward analysis of the role of post-translational modifications by the production of non-modified protein derivatives, and (iii) labeled and structurally folded proteins can be produced for studies by NMR spectroscopy. Approaches by NMR spectroscopy will further be supported by the fast production of combinatorially labeled samples or by the preparation of PorA-PorH complexes in which only one protein will be labeled. The comparison of activities between PorA/PorH alone or in complex clearly shows that one should determine the structure of a functional PorA-PorH complex, mycoloylated at least on PorA, whereas the structures of individual proteins may give insights on folding and complex formation mechanisms.

Acknowledgments—Roland Benz is acknowledged for providing DNA plasmids, Frank Löhr for management of the Frankfurt NMR facility and access to the spectrometers, and Emilie Huc for her help with mass spectrometry.

REFERENCES

1. Zuber, B., Chami, M., Houssin, C., Dubochet, J., Griffiths, G., and Daffé, M. (2008) *J. Bacteriol.* **190,** 5672–5680
2. Hoffmann, C., Leis, A., Niederweis, M., Plitzko, J. M., and Engelhardt, H. (2008) *Proc. Natl. Acad. Sci. U.S.A.* **105,** 3963–3967
3. Daffe, M. (2005) in *Handbook of Corynebacterium glutamicum* (Lothar Eggling, M. B., ed) pp. 121–148, Tayler and Francis group A, CRC Press Book, Boca Raton, FL
4. Brennan, P. J., and Nikaido, H. (1995) *Annu. Rev. Biochem.* **64,** 29–63
5. Hünten, P., Costa-Riu, N., Palm, D., Lottspeich, F., and Benz, R. (2005) *Biochim. Biophys. Acta* **1715,** 25–36
6. Lichtinger, T., Burkovski, A., Niederweis, M., Krämer, R., and Benz, R. (1998) *Biochemistry* **37,** 15024–15032
7. Costa-Riu, N., Maier, E., Burkovski, A., Krämer, R., Lottspeich, F., and Benz, R. (2003) *Mol. Microbiol.* **50,** 1295–1308
8. Barth, E., Barceló, M. A., Kläckta, C., and Benz, R. (2010) *J. Bacteriol.* **192,** 786–800
9. Ziegler, K., Benz, R., and Schulz, G. E. (2008) *J. Mol. Biol.* **379,** 482–491
10. Nikaido, H. (2003) *Microbiol. Mol. Biol. Rev.* **67,** 593–656
11. Massari, P., Ram, S., Macleod, H., and Wetzler, L. M. (2003) *Trends Microbiol.* **11,** 87–93
12. Svetlíková, Z., Skovierová, H., Niederweis, M., Gaillard, JL., McDonnell, G., and Jackson, M. (2009) *Antimicrob. Agents Chemother* **53,** 4015–4018
13. Huc, E., Meniche, X., Benz, R., Bayan, N., Ghazi, A., Tropis, M., and Daffé, M. (2010) *J. Biol. Chem.* **285,** 21908–21912
14. Savage, D. F., Anderson, C. L., Robles-Colmenares, Y., Newby, Z. E., and Stroud, R. M. (2007) *Protein Sci.* **16,** 966–976
15. Klammt, C., Löhr, F., Schäfer, B., Haase, W., Dötsch, V., Ruterjans, H., Glaubitz, C., and Bernhard, F. (2004) *Eur. J. Biochem.* **271,** 568–580
16. Berrier, C., Park, K. H., Abes, S., Bibonne, A., Betton, J. M., and Ghazi, A. (2004) *Biochemistry* **43,** 12585–12591
17. Klammt, C., Schwarz, D., Löhr, F., Schneider, B., Dötsch, V., and Bernhard, F. (2006) *Febs. J.* **273,** 4141–4153
18. Reckel, S., Sobhanifar, S., Durst, F., Löhr, F., Shirokov, V. A., Dötsch, V., and Bernhard, F. (2010) *Methods Mol. Biol.* **607,** 187–212
19. Schwarz, D., Junge, F., Durst, F., Frölich, N., Schneider, B., Reckel, S., Sobhanifar, S., Dötsch, V., and Bernhard, F. (2007) *Nat. Protoc.* **2,** 2945–2957
20. Shirokov, V. A., Kommer, A., Kolb, V. A., and Spirin, A. S. (2007) *Methods Mol. Biol.* **375,** 19–55
21. Kai, L., Kaldenhoff, R., Lian, J., Zhu, X., Dötsch, V., Bernhard, F., Cen, P., and Xu, Z. (2010) *PLoS One* **5,** e12972
22. Klammt, C., Schwarz, D., Fendler, K., Haase, W., Dötsch, V., and Bernhard, F. (2005) *Febs. J.* **272,** 6024–6038
23. Schneider, B., Junge, F., Shirokov, VA., Durst, F., Schwarz, D., Dötsch, V., and Bernhard, F. (2010) *Methods Mol. Biol.* **601,** 165–186
24. Schägger, H. (2006) *Nat. Protoc.* **1,** 16–22
25. Sambrook, J., and Russell, D. W. (2000) *Molecular Cloning: A Laboratory Manual*, 3rd Ed., Cold Spring Harbor Laboratory Press, Cold Spring Harbor, NY
26. Yeung, Y. G., Nieves, E., Angeletti, R. H., and Stanley, E. R. (2008) *Anal. Biochem.* **382,** 135–137
27. Wuu, J. J., and Swartz, J. R. (2008) *Biochim. Biophys. Acta* **1778,** 1237–1250
28. Pervushin, K. V., Wider, G., and Wüthrich, K. (1998) *J. Biomol. NMR* **12,** 345–348
29. Renault, M., Saurel, O., Czaplicki, J., Demange, P., Gervais, V., Löhr, F., Réat, V., Piotto, M., and Milon, A. (2009) *J. Mol. Biol.* **385,** 117–130
30. Abdine, A., Verhoeven, M. A., Park, K. H., Ghazi, A., Guittet, E., Berrier, C., Van Heijenoort, C., and Warschawski, D. E. (2010) *J. Magn. Reson.* **204,** 155–159
31. Maslennikov, I., Klammt, C., Hwang, E., Kefala, G., Okamura, M., Esquivies, L., Mörs, K., Glaubitz, C., Kwiatkowski, W., Jeon, Y. H., and Choe, S. (2010) *Proc. Natl. Acad. Sci. U.S.A.* **107,** 10902–10907
32. Koglin, A., Klammt, C., Trbovic, N., Schwarz, D., Schneider, B., Schafer, B., Lohr, F., Bernhard, F., and Dotsch, V. (2006) *Magn. Reson. Chem.* **44** Spec No, S17–23
33. Reckel, S., Sobhanifar, S., Schneider, B., Junge, F., Schwarz, D., Durst, F., Löhr, F., Güntert, P., Bernhard, F., and Dötsch, V. (2008) *Proc. Natl. Acad. Sci. U.S.A.* **105,** 8262–8267
34. Berrier, C., Besnard, M., and Ghazi, A. (1997) *J. Membr. Biol.* **156,** 105–115
35. Benz, R. (1994) *Biochim. Biophys. Acta* **1197,** 167–196
36. Schiffler, B., Barth, E., Daffé, M., and Benz, R. (2007) *J. Bacteriol.* **189,** 7709–7719
37. Klächta, C., Knörzer, P., Riess, F., and Benz, R. (2011) *Biochim. Biophys. Acta* **1808,** 1601–1610
38. Thein, M., Bunikis, I., Denker, K., Larsson, C., Cutler, S., Drancourt, M., Schwan, T. G., Mentele, R., Lottspeich, F., Bergström, S., and Benz, R. (2008) *J. Bacteriol.* **190,** 7035–7042
39. Genisyuerek, S., Papatheodorou, P., Guttenberg, G., Schubert, R., Benz, R., and Aktories, K. (2011) *Mol. Microbiol.* **79,** 1643–1654

Downloaded from www.jbc.org at BIBL SANTE, on September 15, 2011

Chapter IV

Biophysical studies of Trehalose 6,6’- dimycolate from

Corynebacterium glutamicum

Summary

The outer membrane lipids from *C. glutamicum* have been purified by using adsorption and anion exchange chromatography. The purity and homogeneity of the lipids were verified by thin layer chromatography and MALDI TOF mass spectrometry. The membrane forming properties of the major outer membrane lipid, trehalose dimycolate (TDM) was studied by preparing the vesicles either alone by dialysis protocol or with cardiolipin by spontaneous hydration method. The size distributions of the vesicles were analyzed by Dynamic Light Scattering and Electron microscopy. With the protonated and perdeuterated lipid mixture, the gel to liquid crystalline phase transition was studied by ^{2}H-NMR spectroscopy. Furthermore, over-expressed and purified PorA and PorH from *C. glutamicum* were reconstituted in TDM liposomes and their functionality was verified by ion channel conductance measurements.

This work is in preparation for submission to *J. Lipid Research* as:

Parthasarathi Rath, Olivier Saurel, Marielle Tropis, Mamadou Daffé, Alexandre Ghazi, Pascal Demange and Alain Milon,

Membrane forming properties of cord factor (trehalose 6,6'-dimycolate) from

Corynebacterium glutamicum

IV.1: Introduction

As observed in chapter II and III by channel activity measurements using PorA and PorH with and without the covalent mycolic acid modification; besides the obligatory presence of both proteins, the covalent attachment is also required to form a proper voltage dependent ion channel. To understand the importance of this covalent interaction further, we therefore thought to provide a similar environment with trehalose dimycolate (TDM) (mycolic acid containing lipid) to the CF expressed unmodified proteins and in this case, the mycolic acid will be present surrounding the proteins but without any covalent attachment with the proteins. To verify further the importance of non-covalent interaction for channel activity, channel activity measurements were planned in presence of an artificial TDM bilayer. Hence TDM has to be produced in purified form and also in large quantity to perform the above experiments. Furthermore, though the biological importance of this predominant glycolipid is only studied and surprisingly in presences of detergents, its membrane forming properties are poorly understood so far. The experiments were described in the annex section and a summary of the results obtained are discussed below briefly.

IV.2: Results and discussion

The outer membrane lipids from the *C. glutamicum* culture were extracted using organic solvents and further purified using adsorption and ion exchange chromatography on Quaternary Methyl Ammonium (QMA) column (Fig 1, page 129). 27 mg of pure TDM could be extracted from a liter of culture. The purity and composition of chain lengths are characterized by MALDI TOF mass spectrometry and it was found that TDM is composed of both odd and even number of mycolic acids, predominantly containing 32 to 36 carbon atoms with and/or without insaturations (Fig 2, page 130 and fig S1, page 134). Out of several methods, only dialysis method was successful to make vesicles of TDM alone. However, TDM vesicles could be prepared spontaneously with water buffers only in a mixture with ~80 % of cardiolipin (CL). The size distributions of the vesicles were characterized by dynamic light scattering and negatively stained transmission electron microscopy. In fact, the vesicles prepared by dialysis protocol were smaller (~ 200 nm), whereas spontaneously made TDM/CL vesicles were relatively larger (in µm range) in diameter (Fig 3, page 131).

Furthermore, with the perdeuterated lipids produced in a similar way helped to characterize the dynamics and phase behavior of TDM by ^{2}H-NMR spectroscopy. Vesicles prepared by dialysis protocol could only result isotropic signal due to rapid orientation of the small vesicles and also of the lipids within the vesicles. However, spontaneously made TDM vesicles in presence of CL resulted typical ^{31}P powder spectrum and ^{2}H NMR spectrum with a quadrupolar splitting of 23.6 KHz of the most ordered methylene along the side chains (Fig S4, page 136 and fig 4, page 132). By recording the ^{2}H NMR spectra at various temperatures, a gel to liquid crystalline phase transition in between 285 and 292 K were observed (Fig 4, page 132). These results indicated that a homogenous TDM/CL mixture could be prepared without phase separation which could explain the behavior the natural lipid membrane at the growth temperature of 303 K.

To understand the importance of covalent interaction of mycolic acid on the channel activity of PorA and PorH, both proteins, either produced with their natural mycolic acid modification in *C. glutamicum* or without modification using *E. coli* based Cell-Free expression were reconstituted successfully into TDM liposomes. In fact, channel activity measurements confirmed the necessity of covalent attachment to form a proper PorAH voltage dependent ion channel (Fig 5, page 133). The preparation of an artificial bilayer made up of only TDM remain unsuccessful with lower capacity to perform channel activity. The results obtained in this chapter are described in detail as manuscript format and planned to be submitted to a journal.

Title: Membrane forming properties of cord factor (trehalose 6,6'-dimycolate) from *Corynebacterium glutamicum*

Authors: Parthasarathi Rath[1,2], Olivier Saurel[1,2], Marielle Tropis[1,2], Mamadou Daffé[1,2], Alexandre Ghazi[3], Pascal Demange[1,2*] and Alain Milon[1,2*]

[1] Institute of Pharmacology and Structural Biology, Université de Toulouse, UPS, 205 route de Narbonne, 31077 Toulouse, France

[2] IPBS, UMR 5089, CNRS, 205 route de Narbonne, BP 64182, 31077 Toulouse, France[3]

[3] Université Paris Sud-11, CNRS UMR8619, Institut de Biochimie et Biophysique Moléculaire et Cellulaire, 91405 Orsay, France

* To whom correspondence should be addressed:

Alain Milon : +33561175423 ; Email : alain.milon@ipbs.fr

Pascal Demange: +33561175419; Email: pascal.demange@ipbs.fr

Abstract

Trehalose 6,6'-dimycolate (TDM) is the major lipid in the outer membrane of *Corynebacteria* and *Mycobacteria*. Although its role is well recognized in the immune response phenomena and the bacterial – host responses, its membrane biophysical properties remains largely unknown and it has often been studied in presence of detergents. We purified the main components of the outer membrane from *Corynebacterium glutamicum*, and analyzed their membrane forming properties. In mixture with endogenous cardiolipin, but not alone, TDM spontaneous hydration gives rise to liposomes. As a pure component, TDM was shown to form vesicles only by the detergent dialysis method. These vesicles were characterized in terms of size distribution by light scattering and electron microscopy. Using perdeuterated natural lipids and deuterium NMR, the cardiolipin-TDM lipid mixtures were shown to exhibit a gel to liquid crystalline phase transition over a 273-295 K temperature range, for cell grown at 303 K and thus to be in a liquid crystalline state at physiological temperature. Finally it was shown that a functional ion channel from the *Corynebacterial* envelope (the PorA-PorH channel) could be reconstituted in TDM liposomes and display the typical voltage dependent ion channel activities of porin like channels.

Supplementary keywords: cardiolipin, lipid vesicle, ^{2}H NMR, mass spectrometry, ion channel, phase transition

Abbreviations:

CL : Cardiolipin

^{2}H NMR : Deuterium Nuclear Magnetic Resonance

MALDI TOF : matrix-assisted laser-desorption/ionization-time-of-flight

OG : n-octyl-β-D-glucopyranoside

PG : Phosphatidylglycerol

PI : Phosphatidylinositol

PIMs : Phosphatidylinositol-mannosides

TDM : Trehalose 6,6’ – dimycolate

TMM : Trehalose – monomycolate

PorA-PorH: major outer membrane protein complex from *Corynebacterium glutamicum*

INTRODUCTION

The cell envelope organization of the group of bacteria in the suborder *Corynebacterineae* may explain why specific long chain fatty acids are indispensable for their survival. These bacteria present a unique cell envelope that contains an outer membrane, also called mycomembrane, involved in a permeability barrier resembling that of in Gram-negative bacteria. The mycomembrane consistings of a bilayer composed of an inner leaflet of mycolic acids covalently linked to the cell wall arabinogalactan, which in turn is attached to peptidoglycan, and an outer leaflet of various non-covalently linked lipids that also include mycolic acid-containing glycoconjugates such as trehalose mono- and di-mycolate (1, 2).

Trehalose 6,6'-dimycolate (TDM) is a surface glycolipid present abundantly in the mycomembranes of this group of bacteria providing a potent biological barrier. TDM is also called "cord factor" as it helps these bacteria to form cords and make them impermeable and resistant to (i) many antibiotics, (ii) killing by acidic and alkaline compounds, (iii) osmotic lysis and (iv) lethal oxidations and survival inside macrophages (3-6). It plays a major role in the immunological response and the *Mycobacteria* – host interactions (7, 8). It is composed of a molecule of trehalose esterified by two alpha-alkyl, beta-hydroxy fatty acids (mycolic acids) of variable chain lengths: 70-90 carbon atoms in *Mycobacteria*, 46-90 carbon atoms in *Nocardia*, and shorter 22-38 carbon atoms in *Corynebacteria* (9, 10). Other lipids are proposed to be associated with this outer membrane such as phospholipids and in mycobacteria, species-specific lipids (11-14).

Recently the exact lipid composition of the outer membrane of *Corynebacterium glutamicum* has been reassessed by two groups independently, who tried to prevent contamination by inner membrane lipids. First Bansal-Mutalik and Nikaido (15), using a reverse surfactant micelles extraction protocol, proposed that the outer membrane contains cardiolipin tightly associated with the peptidoglycan-arabinogalactan complex in the inner leaflet, and predominantly TDM in the outer leaflet. Then, Marchand et al. isolated the mycomembrane by flotation density gradient, and analyzed its lipid and protein composition extensively (16). Based on their separation protocol, they found that the predominant lipid was TDM. Both studies point to the major role played by TDM in the physical organization of the outer membrane, either alone or in mixture with cardiolipin.

Although a huge amount of biophysical data have been accumulated over the last decades about the spontaneous self-assembly of many membrane lipids and the corresponding membrane physical properties (see for instance (17) and references herein), including cardiolipin (18) , surprisingly, very little is known about the self-organization of TDM and/or TDM/cardiolipin lipid mixtures. The term “TDM micelle”, which seems contradictory with being the major component of an impermeable outer membrane, is often found in the literature, however it usually refers to TDM solubilisation in Freund’s incomplete adjuvant, or in other detergent mixtures (5, 8). Its interaction with preformed lipid bilayers has been studied, and it was shown to inhibits Ca^{2+}-induced fusion between phospholipid vesicles (19, 20), and to affect bilayer water permeability and bilayer electrical capacitance of phosphatidylcholine bilayers (21) . Finally, the influence of mycolic acid chain length on the phase properties of *Corynebacterineae* cell walls has been assessed, and it was shown by differential scanning calorimetry that a phase transition occurs around 60-70 °C for the longer chains of mycobacteria while *Corynebacteria* displayed a transition around 30 °C, indicating a clear correlation between mycolic acid structure and the fluidity and permeability of mycobacterial cell walls (22).

This prompted us to extract and purify TDM from *C. glutamicum* cell wall and to analyze its membrane forming properties. After characterization of its mycolic chain distribution by MALDI-TOF mass spectrometry, we established protocols to form vesicles with pure TDM as well as with TDM/cardiolipin mixtures. It was found that although pure TDM cannot be rehydrated spontaneously in water buffer like phospholipids, this is possible in mixture with cardiolipin. TDM can be dispersed in water and form lipid vesicles by the detergent dialysis method, and these vesicles were characterized by transmission electron microscopy (TEM) and dynamic light scattering (DLS). After growing *C. glutamicum* in D_2O and purifying perdeuterated TDM and cardiolipin, we could use deuterium NMR to assess the lipid order parameters and to observe a gel to liquid crystalline phase transition in cardiolipin – TDM mixture just below the cell growth temperature. We finally demonstrated that pure TDM liposomes can be used for the functional reconstitution of an ion channel from the outer membrane of *C. glutamicum*, the PorA-PorH complex. These observations clearly establish for the first time that TDM, both alone and in mixture with cardiolipin, may self-organize into a stable, non-permeable environment for a functional outer membrane.

EXPERIMENTAL PROCEDURES

Extraction and purification of TDM from *C. glutamicum*

C. glutamicum stain ATCC 13032 was used for extraction and purification of Trehalose dimycolate. The total cell lipid extract were obtained as described previously (23, 24). Briefly, from a primary culture, *C. glutamicum* cells were grown to late exponential phase (16 h) in brain heart infusion (BHI) media at 30 ^{0}C with continuous shaking at 200 rpm. Cells were harvested by centrifugation at 4000 g for 20 min. The cell wall was extracted three times successively in $CHCl_3$: CH_3OH (1:2, 1:1 and 2:1 [vol/vol]) proportions (12 ml per gram of cell mass) for 12 hs at room temperature with continuous stirring. The organic solvent extracts were separated after each extraction step by centrifugation at 4000 g at room temperature. The insoluble material was eliminated by filtration through a Whatman paper. All organic solvents were removed by vacuum rotary evaporator. The organic extract was dissolved in $CHCl_3$. To eliminate the polysaccharides, an equal volume of water was mixed followed by gentle shaking and allowed to separate the organic phase from the aqueous phase. The lower organic phase containing lipids was collected, evaporated to dryness, quantified and solubilized in 2-3 ml of $CHCl_3$. To analyze the total cell lipids, a diluted fraction was applied on a TLC plate and developed in $CHCl_3$: CH_3OH: H_2O (65:25:4 [vol/vol/vol]). Glycolipids were identified after spraying the TLC plates with 0.2 % (wt/vol) anthrone in H_2SO_4 followed by heating, whereas the phospholipids were revealed by the Dittmer reagent (25).

TDM from the total lipid extract containing glycolipids (TDM, TMM) and phospholipids (PI, PIMs, PG/CL) was purified using Quaternary Methyl Ammonium (QMA spherosil M, Pall BioSepra, Cergy, France) chromatography (24, 26). Before application of the total lipids, the QMA matrix was activated with three times (3x) column volume (CV) of 0.2 M ammonium acetate in $CHCl_3$: CH_3OH (1:2) followed by washing first with 5x CV of $CHCl_3$:CH_3OH (1:2, [vol/vol]) and then with 3x CV of $CHCl_3$. The total lipid mixture in $CHCl_3$ was applied on the activated QMA column up to 100 mg/ml, and a maximum of 200 mg of lipid per 25 g of matrix. The glycolipids were separated by increasing proportions of CH_3OH in $CHCl_3$ such as 10:0, 9:1, 8:2, 7:3, 6:4, 1:1 and 1:2 [vol/vol]. Then the phospholipids were eluted by application of a gradient of ammonium acetate (from 50 to 200 mM) in $CHCl_3$: CH_3OH (1:2, [vol/vol]). Fractions of 10 ml volume were collected and analyzed by TLC. Before quantification, ammonium acetate was removed from the purified phospholipid fractions by re-dissolving the lipid fractions in $CHCl_3$ followed by filtration. For solid state NMR

measurements, perdeuterated lipids were obtained from cells grown in D_2O BHI medium. Perdeuterated lipids were extracted and purified similarly as described above. The purity and chemical composition of ^2H labeled or unlabeled TDM and other lipids were analyzed by TLC and MALDI TOF mass spectrometry.

Mass spectrometry

MALDI-TOF spectra of purified TDM were acquired on a Voyager-DE STR mass spectrometer (PerSeptive Biosystems). Ionization was achieved by irradiation with a pulsed nitrogen LASER emitting at 337 nm. The spectra were recorded in reflectron mode using an extraction delay of 100 ns and an accelerating voltage of 25 kV. The 2,5-dihydroxybenzoic acid (DHB) matrix (10 mg/ml) was dissolved in $CHCl_3$:CH_3OH (1:1, [vol/vol]). In a typical experiment, 2 µl of TDM $CHCl_3$:CH_3OH 1:1 (1 mg/ml) and 2 µl matrix were mixed and 0.5 µl was disposed onto a metal plate. A total of 2,500 shots were accumulated for each sample in a positive ion mode and all data were acquired with default calibration for the instrument.

Liposome preparation

Three different methods were tried to prepare TDM vesicles: (i) Standard liposome preparation protocol: gentle and direct hydration of a dried lipid film made up of 5 mg of TDM and CL at the following ratio (TDM/CL: 1/0, 4/1, 3/2, 1/1, 2/3 1/4 and 0/1) (ii) Reverse-phase evaporation protocol as described in (27) (iii) Detergent dialysis protocol: 5 mg of TDM was solubilized in 2 ml of 10 % Octylglucoside (OG) until the solution turned to be transparent. This TDM-OG solution was dialyzed three times against 2 L of water in a 3 kD cut-off membrane at room temperature with gentle stirring. To avoid any organic solvent contamination, all the lipids were dried overnight in a vacuum pump before any liposome preparation.

Dynamic Light Scattering (DLS)

The diameter and size distribution of TDM vesicles prepared either by dialysis or by hydration in presence of cardiolipin were estimated from dynamic light scattering recorded on a DynaPro instrument equipped with laser source of wavelength 663 nm (Wyatt Technologies). Samples were diluted in filtered water to 50 – 200 times before measurement. The mean light scattering from each solution was calculated from 20 independent measurements, each recorded at 25 °C with a 10 s acquisition time. The data were analyzed using DYNAMICS software 7.1 (Wyatt technologies).

Electron microscopy

The shape and size distribution of TDM vesicles prepared as described above were analyzed by transmission electron microscopy (TEM). The samples were prepared using the conventional negative staining procedure. Drop of liposomes suspension (10 - 20 µl) were adsorbed onto a glow-discharged carbon-coated copper grid. The grids were blotted on a filter paper and then negatively stained with uranyl acetate (1 %). Grids were examined with a transmission electron microscope (JEOL JEM 1400) at 80 kV and 120 kV. The images were acquired using a digital camera (GATAN ORIUS SC 1000B model 832) from 20,000 to 50,000 X magnifications. The liposome's diameter was evaluated using the software.

^{2}H and ^{31}P solid state NMR sample preparation and measurements

For NMR sample preparation, we used either perdeuterated-TDM (d-TDM) or perdeurated-cardiolin (d-CL). Vesicles composed of a mixture of d-TDM/CL or TDM/d-CL in 2:8 molar ratio were prepared by hydrating the lipid film with 2 ml of deuterium-depleted water (Sigma-Aldrich) at 37 °C for 1 h with gentle shaking. The vesicles were concentrated to 200 µl at 50,000 g for 30 min before NMR measurement. Perdeuterated CL (d-CL) alone sample was prepared similarly. ^{2}H NMR measurements were recorded with a DMX-500 Bruker spectrometer at a Larmor frequency of 76.77 MHz with a spectral width of 1 MHz using a quadrupolar echo sequence with an echo delay of 40 µs (28). For each condition a total of 25,600 scans of 4 K time domain were accumulated with a repetition delay of 1 s. Prior to Fourier transform the first points before the top of the echo were removed. Then a squared cosine function was applied to the FID. ^{2}H-NMR spectra were recorded at various temperatures between 278 K and 313 K. First moment of the spectra were computed over a 100 kHz spectral width by the equation (28) :

$$M_1 = \frac{\sum_{\omega=0}^{\omega=10^{+5}} |\omega| \times I(\omega)}{\sum_{\omega=0}^{\omega=10^{+5}} I(\omega)}$$

Where ω is the shift in frequency from the central Larmor frequency in Hertz, I(ω) is the spectrum intensity at frequency ω.

^{31}P NMR spectra were recorded on a DMX-500 Bruker spectrometer at a Larmor frequency of 202.45 MHz using a standard spin echo pulse sequence, using a 90° pulse of 8.0 µs and an interpulse delay of 20 µs, and a spectral width of 500 kHz.

TDM / PorA-PorH Proteoliposome preparation

PorA and PorH are major membrane proteins present in the outer membrane of *C. glutamicum*. They were expressed and purified from *C. glutamicum* cultures as described in (29). Equimolar quantities of both proteins were precipitated in cold ethanol (20x volume) and 12 % of 5 M NaCl during 24 h at -20 °C. The precipitate was recovered by centrifugation at 10,000*g* for 30 min, 4 °C. The precipitate was kept at room temperature for two hours to remove traces of ethanol. The pellet was gently solubilized by adding TDM/OG mixed micelles solution. OG was removed slowly by dialysis in a 3 kDa cut-off membrane against 10 mM Tris-Cl, pH 8.0 (5 hs, > 6 times). Proteoliposomes were prepared at two protein/lipid molar ratio: 1:30 and 1:50. The quality of the reconstitution was analyzed by DLS and EM, whereas the ion channel activity was carried out using black lipid membrane ion channel activity measurements.

Channel activity measurements

Channel activity of reconstituted proteoliposomes was recorded using planar bilayer measurements. The planar bilayers were formed across a 250 μm diameter hole by presenting a bubble of either azolectin (Sigma) or a mixture of azolectin containing 10 mol % of TDM dissolved in n-decane (30 mg/ml). Recordings were performed at room temperature with a membrane potential of 40 mV in a 10 mM HEPES, pH 7.4 and 400 mM KCl buffer solution. Currents were amplified using an Axon 200B patch-clamp amplifier, filtered at 1 kHz through a-pole Bessel filter and digitized at 2 kHz. Data were analyzed with pCLAMP software.

RESULTS AND DISCUSSION

Extraction and purification of TDM and other polar lipids from *C. glutamicum*

An optimized and efficient protocol has been used to extract the total cell lipids from *C. glutamicum* cell wall, following (23, 24) with further optimizations. After successive extraction steps using different proportions of $CHCl_3$:CH_3OH, nearly 2 g of crude cell extract were obtained from 2 liters of culture. Lipid extraction steps gave 500 ± 20 mg of total cell lipids composed mostly of glycolipids (TDM, TMM) and phospholipids (CL, PG, PI and PIMs) (Fig. 1, lane 1).

As compared with other strategies previously described (including silica gel chromatography), QMA ion exchange chromatography proved to be the most efficient and hence allowed complete separation of the individual lipid species in one step (Fig. 1). Most of the lipids were identified by TLC with respect to known standards, except PG and CL which displayed the same TLC profiles and were identified by reflectron mode MALDI TOF mass spectrometry. PG came first followed by CL in our chromatographic conditions.

After lipid separation and weight determination the approximate proportion of each lipid in the crude lipid mixture was (per 200 mg of lipid mixture): TDM 27 mg, TMM 5 mg, CL/PG 55 mg, PI + PIM 28 mg and the remaining are polar lipid extracts. This approach provided a rapid and efficient way of preparing large amount of individual lipids, in protonated and deuterated form, for subsequent biophysical analyses.

Biochemical characterization of TDM by mass spectrometry

The molecular characterization of purified TDM from *C. glutamicum* was analyzed by MALDI TOF mass spectrometry. Reflectron mode data were collected to get high resolution mass spectra of TDM as pseudo-molecular species (M + Na^+ ions). As shown in Fig. 2A, the mass spectrum of TDM consists of complex distribution of with m/z between 1236 and 1471. Each ensemble of peaks consists of different molecular species of TDM with a combination of mycolic acids of varying carbon and number of insaturations. Our data agree with previous work showing that the predominant forms of corynomycolic acids in TDM are C32:0, C34:1 and C36:2 (30) and that mycolic acids with odd carbon atoms number do exist in *Corynebacterineae* (31, 32).

In the mass spectra of TDM, each group of peaks differs from its neighboring ones with a mass of 14 amu corresponding one $–CH_2-$ group. In fact the most predominant corynomycolates with odd number of carbon atoms are C35:0 and C37:1 which is also verified by the mass spectra analysis of trehalose monomycolate (Fig. S1A). While mass spectra of purified CL showed predominantly three different molecules of m/z 1428, 1450 and 1472 which were the possible combination of C16:0, C18:0 and C18:1 fatty acid chain lengths (Fig 2B). Similar mass spectrometric characterizations of TDM, TMM have been carried out previously and exposed the divergence of carbon chain lengths in various species of *Corynebacterineae* (33, 34).

The mass spectra of purified perdeuterated TDM (Fig. S1B) and CL showed corresponding increase in molecular mass profiles and allowed to estimate the deuteration extent in our growth condition as in (35). Using peaks corresponding to the same molecular species allowed calculating the average deuteration extent of our lipids. For instance, for the C66:1 TDM molecules (140 H atoms), one measures a m/z of 1347 for the protonated molecules and a pattern centered on 1481 for the perdeuterated molecules (i.e. with identical intensities for the two consecutive 1480 and 1481 peaks), corresponding to an average deuteration extent of 96%. This is the average D/H ratio in the growth medium indicating that in our growth conditions, complete H/D exchange occurred between the water and the carbon source during the lipid biosynthesis.

TDM and CL/TDM liposome preparation

Several methods were tried to prepare homogenous dispersions of pure TDM in water buffers and to characterize them. We first tested the standard protocol of liposome formation which consists of slowly hydrating thin lipid films formed by evaporation of chloroform solutions. None of the hydrations conditions, including at temperatures up to 60 °C and low power bath sonication, allowed rehydrating the sample. High power probe sonication (typically used to form small unilamellar vesicles in the case of phospholipids) gave an inhomogeneous opaque suspension with visible large aggregates. The reverse phase evaporation method (27) also failed to produce homogenous TDM suspensions. By contrast, *C. glutamicum* cardiolipin mixtures, which is the other major lipid been described in the literature (17) to be part of the cell wall could be rehydrated easily and form liposome preparations by standard methods, as expected for this class of phospholipids (18). Several CL to TDM ratio were tested and we found that at least 80 % CL is required for the spontaneous and rapid rehydration of a lipid film. Therefore TDM, unless it is mixed with high amount of cardiolipin (or detergents, as typically

done for immunological applications) cannot be easily dispersed in buffer solution like standard phospholipids.

Finally, we tested another typical preparation method for the formation of lipid vesicles as well as proteoliposomes, the detergent dialysis method (36) . In the presence of octyl glucoside, TDM could be fully solubilized and dispersed, and after detergent removal by dialysis, the preparation remained homogenous and displaying little turbidity. This method worked well both with pure TDM and with CL/TDM mixtures in any proportion.

TDM and CL/TDM liposome characterization

A large number of methods are available to characterize the phases formed by lipid dispersions in water, among which X-ray and neutron scattering, ^{31}P and ^{2}H NMR, differential scanning calorimetry, fluorescence, EPR, IR and raman spectroscopies, electron microscopy and atomic force microscopy, light scattering (for an exhaustive description see for instance (17) and references herein). In order to demonstrate that TDM may behave as a membrane forming lipid (and not a micelle forming lipid), we focused on light scattering and electron microscopy to determine the size distribution of TDM vesicles demonstrated the existence of a well-defined internal space, and ^{2}H NMR to determine the chain order parameters and the lipid dynamics, as well as characterize phase transition temperature ranges. Finally, we used a major membrane protein complex from *C. glutamicum* outer membrane to show that TDM may be used to form proteoliposomes and is compatible with the functional reconstitution of a membrane protein.

The size distribution of TDM vesicles were analyzed DLS and EM (37). As shown in fig 3A TDM vesicles formed by dialysis were largely monodisperse in size with nearly 90 % of the vesicles having an average diameter of 260 nm. TDM/CL 2/8 liposomes prepared by the film hydration method presented an average size of 1677 nm, with a broader distribution in size as expected for crude liposome preparations (Fig. 3B). The size distribution of these vesicles as obtained by light scattering is in agreement with the size distributions obtained by analyses of TEM images of negatively stained vesicles (Fig. 3C and D).

^{31}P and ^{2}H NMR of TDM vesicles

The dynamics and phase behavior of TDM membranes were analyzed by ^{2}H-NMR spectroscopy. As expected from the size determined by DLS, vesicles made of ^{2}H-TDM with the detergent dialysis method gave isotropic ^{2}H NMR spectra due to the rapid reorientation of the vesicles and of the lipids within the vesicles. In contrast, the liposomes composed of TDM and CL (2:8) prepared by simple hydration of a dried lipid film were large enough to be analyzed by ^{2}H and ^{31}P NMR. The ^{31}P spectrum (Fig. S4) displayed the typical ^{31}P powder spectrum of cardiopilin in a lipid bilayer phase (38). We analyzed by ^{2}H NMR, three samples: two consisted of TDM/CL vesicles with either perdeuterated-TDM (d-TDM) or perdeuterated-cardiolipin (d-CL), and a control sample with d-CL alone (fig 4). The ^{2}H spectra recorded at 313K of d-CL with TDM showed a standard powder spectrum characteristic of a phospholipid bilayer in the fluid phase. One can distinguish three characteristic regions in the spectrum: a) the so-called "plateau region" with a quadrupolar splitting of 23.6 KHz which corresponds to the most ordered methylene along the side chains, roughly from C3 to C10 position from the carboxylate group; b) the splitting of 2.34 KHz which corresponds to the fatty acid terminal methyls; and c) an intermediate region in the spectrum which corresponds to the second half of the acyl chain as well as to the glycerol methylenes which exhibit a quadrupolar splitting about 13 KHz (39). The comparison between vesicles composed of d-CL alone and d-CL/TDM vesicles show that the presence of 20 mol % TDM does not affect much the CL order parameters. The ^{2}H spectrum of perdeuterated TDM from *C. glutamicum* has a distinct lineshape from standard phospholipids since there is a strong contribution from the trehalose deuterons as was observed in glycosphingolipids (40). The TDM methyl group's resonances have a quadrupolar splitting of 1.75 KHz, indicating higher methyl mobility in TDM than in cardiolipin.

^{2}H NMR spectra were recorded at various temperatures between 278 K and 303 K while the cell growth temperature was 303 K. Upon decreasing the temperature the spectral width increased and the spectral components typical of gel phases appeared in the spectra of d-CL/TDM (Fig. 4A, also visible in the d-TDM ^{2}H NMR spectra, Fig S5). The first moment (M1) of the ^{2}H spectra provides a quantitative measure of the spectrum broadening as a function of temperature. The plots on Fig 4C clearly show a gel to liquid crystalline phase transition occurring between 285 K and 292 K for the pure CL sample. When 20 % TDM is incorporated into CL vesicles, the transition temperature range is enlarged and starts at slightly lower temperature, i.e. around 280 K., indicative of a loss of cooperativity conjugated with slightly higher membrane fluidity due to the introduction of TDM. Importantly, the observed temperature

range of transition is the same whether one measures ^{2}H spectra on CL or on TDM in the CL/TDM 8/2 mixtures, indicating that the two lipids form a homogenous mixture and not separated phases. It is striking that the phase transition temperature occurs just below the cell growth conditions: it shows that the CL side chain composition, in terms of chain length and degree of unsaturation, is chosen by *C. glutamicum* to provide a fluid environment for the outer membranes. This tuning of the lipid composition and phase behavior with growth temperature has already been described for *E. coli* cytoplasmic and outer membrane (41, 42) . Interestingly also the range of phase transition that we have observed with TDM and CL lipid mixtures correlates well with early differential scanning calorimetry measurements on *Corynebacterial* cell walls .

TDM membranes as a suitable environment for functional reconstitution of membrane proteins

Recently the lipid composition of the inner and outer membrane of *C. glutamicum* has been established (15, 16). While Bansal-Mutalik et al. found mostly CL and TDM, Marchand et al. described the outer membrane as being composed majorly of TDM, together with trehalose monomycolate (TMM) and free mycolic acids. In such a case, pure TDM membranes should be capable of functionally solubilizing membrane proteins from the outer membrane of *C. glutamicum.* One of the major proteins found in this outer membrane is the PorA-PorH complex acting as a voltage dependent ion channel (29, 30, 43). We thus tried to form proteolipomes with the PorA-PorH complex and to characterize them structurally and functionally.

The detergent dialysis protocol was tried with several TDM to protein molar ratio. At lipid to protein ratio of 50 and above, homogenous vesicle preparation could be obtained, while at lower ratio visible protein aggregates started to be observed as seen by by DLS and EM (Suppl fig S2 and S3).

The proteoliposomes functionality was then assessed in terms of PorA-PorH ion channel activity by black lipid membrane (BLM) measurements. Before applying the proteoliposomes directly for channel recording, we tried to make stable BLM, suitable for electrical measurement, made up of various TDM/azolectin ratio. We observed that up to 10 mol % of TDM can be mixed with azolectin and form a stable bilayer with a stability and capacitance compatible with electrical recordings, while higher amount gave membrane with a lower capacitance. This is in agreement with previous observation with trehalose dicorynomycolate from *Corynebacterium diphtheriae* (21). We first used proteoliposomes made of TDM and

covalently mycoloylated PorA-PorH produced in *C. glutamicum* and applied them in the cis-side of the chamber: they fused to the bilayer and showed sequential multiple insertions, slow and fast opening and closing of ions channels (Fig 5). These channels displayed voltage dependence on both positive and negative side of the potential as expected for a fully functional protein complex (29). In contrast, when the TDM-PorA-PorH proteoliposomes were made with unmodified proteins produced by cell-free expression, they fused to the bilayer but did not display the characteristic porin channel activity. Hence the covalent attachement of mycolic acid to the protein, and not only their presence as a lipid in the protein surrounding seems to be a requirement for the channel activity. It was shown before that lipids can play a role in stabilizing the oligomeric state, folding and also voltage dependent gating of potassium channels (44, 45). Moreover, lipid composition has distinct effects on the mechanosensitivity of MscL and MscS ion channels (46, 47) and also in case of connexins (48). Here however, mycolic acid containing lipids such as TDM could not restore the function of PorA-PorH channels devoid of their naturel post-translational modification.

Conclusion

In the present work, we could perform a detailed biophysical characterization of TDM, so called cord factor from *C. glutamicum*, from the point of view of its capacity to form stable and functional membranes. TDM was shown to be able to form stable membranes, both alone and in mixture with cardiolipin. The TDM/CL mixtures could be dispersed easily in buffer solution by simple rehydration protocol, while detergent dialysis was required in the case of pure TDM. This new protocol for the formation of TDM dispersions in water may represent a useful alternative to the commonly employed detergent mixtures. ^{2}H NMR studies showed that CL/TDM mixtures do form lipid bilayers in a liquid crystalline state at physiological temperatures and have a phase transition temperature towards a gel phase just below. TDM moderately influences the CL membrane fluidity and is homogenously mixed with CL up to 20 mol %. Finally, taking the major ion channel from *C. glutamicum* as a model membrane protein, the PorA-PorH voltage dependent ion channel, we could observe that pure TDM may provide a suitable environment for the functional reconstitution of proteins form the outer membrane. This should prove very useful for future biophysical and structural studies of these membrane proteins.

ACKNOWLEDGEMENTS

We acknowledge M.A. Angladon and I. Iordanov for his help in lipid purification and mass spectrometry. S. Balor and C. Plisson (TRI genotoul platform) is acknowledged for electron microscopy and F. Bernhard for continuous advice of cell-free expression systems. P. Rath was financed by the European Community's Seventh Framework Programme [FP7/2007-2013] under grant agreement n° [211800] and by the “Fondation pour la Recherche Médicale” (FRM) - Paris.

REFERENCES

1. Minnikin, D. (1982) *The Biology of Mycobacteria* Academic, London.
2. Daffe, M. (2005) in *Handbook of Corynebacterium glutamicum*, ed. Bott, L. E. a. M. (CRC Press, Inc., Boca Raton, FL., pp. 121-148.
3. Daffe, M.&Draper, P. (1998) The envelope layers of mycobacteria with reference to their pathogenicity *Adv Microb Physiol* **39**: 131-203.
4. Chami, M., *et al.* (2002) Priming and activation of mouse macrophages by trehalose 6,6'-dicorynomycolate vesicles from Corynebacterium glutamicum *FEMS Immunol Med Microbiol* **32**: 141-7.
5. Fujita, Y., *et al.* (2007) Molecular and supra-molecular structure related differences in toxicity and granulomatogenic activity of mycobacterial cord factor in mice *Microb Pathog* **43**: 10-21.
6. Vergne, I.&Daffe, M. (1998) Interaction of mycobacterial glycolipids with host cells *Front Biosci* **3**: d865-76.
7. Hunter, R. L., Armitige, L., Jagannath, C.&Actor, J. K. (2009) TB Research at UT-Houston - A review of cord factor: new approaches to drugs, vaccines and the pathogenesis of tuberculosis *Tuberculosis* **89**: S18-S25.
8. Davidsen, J., *et al.* (2005) Characterization of cationic liposomes based on dimethyldioctadecylammonium and synthetic cord factor from M. tuberculosis (trehalose 6,6 '-dibehenate) - A novel adjuvant inducing both strong CMI and antibody responses *Biochimica Et Biophysica Acta-Biomembranes* **1718**: 22-31.
9. Minnikin, D. E., Patel, P.&Goodfellow, M. (1974) Mycolic acids of representative strains of Nocardia and the 'rhodochrous' complex *FEBS Lett* **39**: 322-4.
10. Collins, M. D., Goodfellow, M.&Minnikin, D. E. (1982) A Survey of the Structures of Mycolic Acids in Corynebacterium and Related Taxa *Journal of General Microbiology* **128**: 129-149.
11. Minnikin, D. E., Patel, P. V., Alshamaony, L.&Goodfellow, M. (1977) Polar Lipid-Composition in Classification of Nocardia and Related Bacteria *International Journal of Systematic Bacteriology* **27**: 104-117.

12. Ortalo-Magne, A., *et al.* (1996) Identification of the surface-exposed lipids on the cell envelopes of Mycobacterium tuberculosis and other mycobacterial species *J Bacteriol* **178**: 456-61.
13. Ortalo-Magne, A., Andersen, A. B.&Daffe, M. (1996) The outermost capsular arabinomannans and other mannoconjugates of virulent and avirulent tubercle bacilli *Microbiology* **142 (Pt 4)**: 927-35.
14. Brennan, P. J. (1988) *In Microbial Lipids, ed* (London: Academic.
15. Bansal-Mutalik, R.&Nikaido, H. (2011) Quantitative lipid composition of cell envelopes of Corynebacterium glutamicum elucidated through reverse micelle extraction *Proc Natl Acad Sci U S A* **108**: 15360-5.
16. Marchand, C. H., *et al.* (2012) Biochemical disclosure of the mycolate outer membrane of Corynebacterium glutamicum *J Bacteriol* **194**: 587-97.
17. Dopico, A. M. (2007) in *Methods in Molecular Biology* (Humana press, Vol. 400.
18. Lewis, R. N. A. H.&McElhaney, R. N. (2009) The physicochemical properties of cardiolipin bilayers and cardiolipin-containing lipid membranes *Biochimica Et Biophysica Acta-Biomembranes* **1788**: 2069-2079.
19. Crowe, L. M., Spargo, B. J., Ioneda, T., Beaman, B. L.&Crowe, J. H. (1994) Interaction of Cord Factor (Alpha,Alpha'-Trehalose-6,6'-Dimycolate) with Phospholipids *Biochimica Et Biophysica Acta-Biomembranes* **1194**: 53-60.
20. Spargo, B. J., Crowe, L. M., Ioneda, T., Beaman, B. L.&Crowe, J. H. (1991) Cord Factor (Alpha,Alpha-Trehalose 6,6'-Dimycolate) Inhibits Fusion between Phospholipid-Vesicles *Proceedings of the National Academy of Sciences of the United States of America* **88**: 737-740.
21. Imasato, H., Procopio, J., Tabak, M.&Ioneda, T. (1990) Effect of Low Mole Fraction of Trehalose Dicorynomycolate from Corynebacterium-Diphtheriae on Water Permeability and Electrical Capacitance of Lipid Bilayer-Membranes *Chemistry and Physics of Lipids* **52**: 259-262.
22. Liu, J., Barry, C. E., 3rd, Besra, G. S.&Nikaido, H. (1996) Mycolic acid structure determines the fluidity of the mycobacterial cell wall *J Biol Chem* **271**: 29545-51.
23. Puech, V., *et al.* (2001) Structure of the cell envelope of corynebacteria: importance of the non-covalently bound lipids in the formation of the cell wall permeability barrier and fracture plane *Microbiology* **147**: 1365-82.
24. Tropis, M., *et al.* (2005) The crucial role of trehalose and structurally related oligosaccharides in the biosynthesis and transfer of mycolic acids in Corynebacterineae *J Biol Chem* **280**: 26573-85.
25. Dittmer, J. C.&Lester, R. L. (1964) A Simple, Specific Spray for the Detection of Phospholipids on Thin-Layer Chromatograms *J Lipid Res* **15**: 126-7.
26. Layre, E., *et al.* (2011) Deciphering sulfoglycolipids of Mycobacterium tuberculosis *J Lipid Res* **52**: 1098-110.
27. Szoka, F.&Papahadjopoulos, D. (1978) Procedure for Preparation of Liposomes with Large Internal Aqueous Space and High Capture by Reverse-Phase Evaporation *Proceedings of the National Academy of Sciences of the United States of America* **75**: 4194-4198.
28. Davis, J. H. (1979) Deuterium magnetic resonance study of the gel and liquid crystalline phases of dipalmitoyl phosphatidylcholine *Biophys J* **27**: 339-58.

29. Rath, P., *et al.* (2011) Functional expression of the PorAH channel from Corynebacterium glutamicum in cell-free expression systems: implications for the role of the naturally occurring mycolic acid modification *J Biol Chem* **286**: 32525-32.
30. Huc, E., *et al.* (2010) O-mycoloylated proteins from Corynebacterium: an unprecedented post-translational modification in bacteria *J Biol Chem* **285**: 21908-12.
31. Welby-Gieusse, M., Laneelle, M. A.&Asselineau, J. (1970) Structure of the corynomycolic acids of Corynebacterium hofmanii and their biogenetic implication *Eur J Biochem* **13**: 164-7.
32. Nikaido, H., Kim, S. H.&Rosenberg, E. Y. (1993) Physical organization of lipids in the cell wall of Mycobacterium chelonae *Mol Microbiol* **8**: 1025-30.
33. Fujita, Y., Naka, T., McNeil, M. R.&Yano, I. (2005) Intact molecular characterization of cord factor (trehalose 6,6'-dimycolate) from nine species of mycobacteria by MALDI-TOF mass spectrometry *Microbiology* **151**: 3403-16.
34. Fujita, Y., Naka, T., Doi, T.&Yano, I. (2005) Direct molecular mass determination of trehalose monomycolate from 11 species of mycobacteria by MALDI-TOF mass spectrometry *Microbiology* **151**: 1443-52.
35. Tropis, M., Bardou, F., Bersch, B., Daffe, M.&Milon, A. (1996) Composition and phase behaviour of polar lipids isolated from Spirulina maxima cells grown in a perdeuterated medium *Biochimica Et Biophysica Acta-Biomembranes* **1284**: 196-202.
36. Rigaud, J. L., *et al.* (1997) Bio-beads: An efficient strategy for two-dimensional crystallization of membrane proteins *Journal of Structural Biology* **118**: 226-235.
37. Hallett, F. R., Watton, J.&Krygsman, P. (1991) Vesicle sizing: Number distributions by dynamic light scattering *Biophys J* **59**: 357-62.
38. Powell, G. L.&Marsh, D. (1985) Polymorphic Phase-Behavior of Cardiolipin Derivatives Studied by P-31 Nmr and X-Ray-Diffraction *Biochemistry* **24**: 2902-2908.
39. Spooner, P. J. R., Duralski, A. A., Rankin, S. E., Pinheiro, T. J. T.&Watts, A. (1993) Dynamics in a Protein-Lipid Complex - Nuclear-Magnetic-Resonance Measurements on the Headgroup of Cardiolipin When Bound to Cytochrome-C *Biophysical Journal* **65**: 106-112.
40. Jones, D. H., Hodges, R. S., Barber, K. R.&Grant, C. W. M. (1997) Pilin C-terminal peptide binds Asialo-GM(1) in liposomes: A H-2-NMR study *Protein Science* **6**: 2459-2461.
41. Nakayama, H., Mitsui, T., Nishihara, M.&Kito, M. (1980) Relation between Growth Temperature of Escherichia-Coli and Phase-Transition Temperatures of Its Cytoplasmic and Outer Membranes *Biochimica Et Biophysica Acta* **601**: 1-10.
42. Morein, S., Andersson, A. S., Rilfors, L.&Lindblom, G. (1996) Wild-type Escherichia coli cells regulate the membrane lipid composition in a "window" between gel and non-lamellar structures *Journal of Biological Chemistry* **271**: 6801-6809.
43. Barth, E., Barcelo, M. A., Klackta, C.&Benz, R. (2010) Reconstitution experiments and gene deletions reveal the existence of two-component major cell wall channels in the genus Corynebacterium *J Bacteriol* **192**: 786-800.
44. Raja, M., Spelbrink, R. E., de Kruijff, B.&Killian, J. A. (2007) Phosphatidic acid plays a special role in stabilizing and folding of the tetrameric potassium channel KcsA *FEBS Lett* **581**: 5715-22.
45. Zheng, H., Liu, W., Anderson, L. Y.&Jiang, Q. X. (2011) Lipid-dependent gating of a voltage-gated potassium channel *Nat Commun* **2**: 250.

46. Berrier, C., *et al.* (2004) Cell-free synthesis of a functional ion channel in the absence of a membrane and in the presence of detergent *Biochemistry* **43**: 12585-91.
47. Nomura, T., *et al.* (2012) Differential effects of lipids and lyso-lipids on the mechanosensitivity of the mechanosensitive channels MscL and MscS *Proc Natl Acad Sci U S A* **109**: 8770-5.
48. Cascio, M. (2005) Connexins and their environment: effects of lipids composition on ion channels *Biochim Biophys Acta* **1711**: 142-53.

Figure and legends:

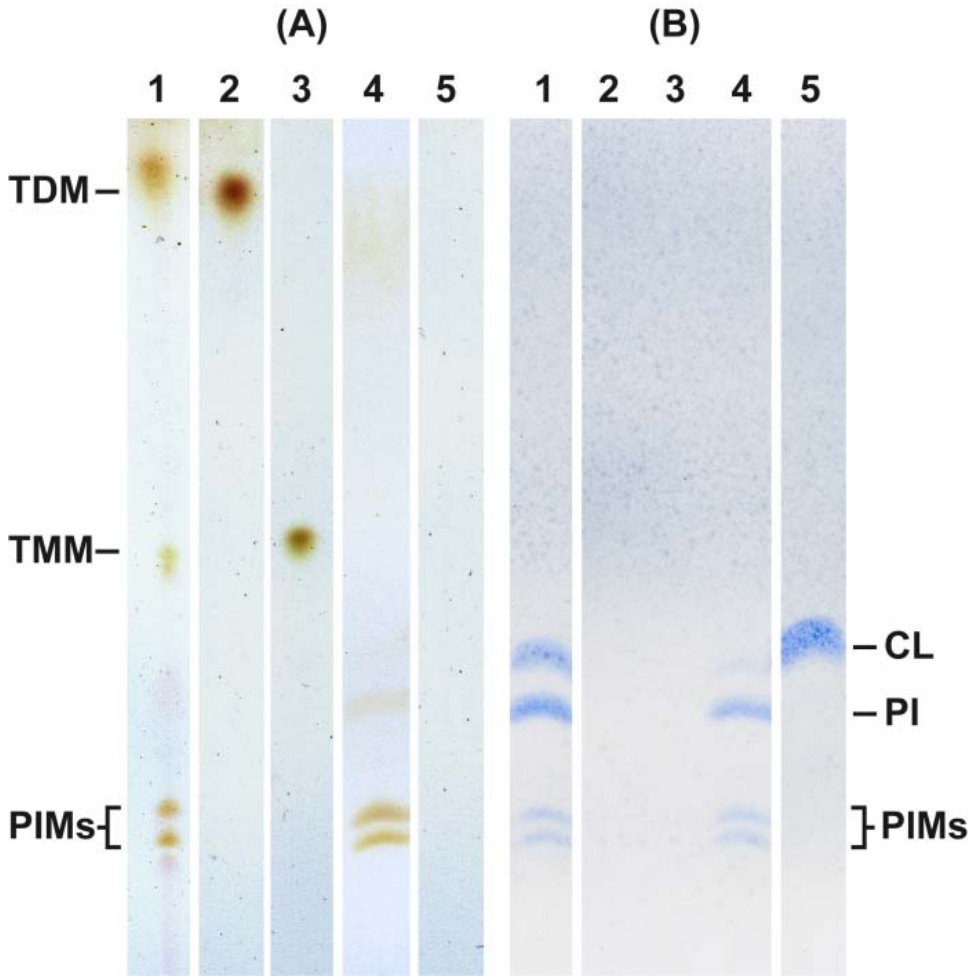

Fig. 1: TLC analysis of *C. glutamicum* cell wall lipids after purification on Quaternary Methyl Ammonium Spherosil M (QMA) column. Lane 1: total lipid extracts before purification, lane 2: TDM (elution with $CHCl_3$:CH_3OH 9:1), lane 3: TMM (elution with $CHCl_3$:CH_3OH 7:3), lane 4: PI and PIMs (elution with 100-125 mM ammonium acetate in $CHCl_3$:CH_3OH 1:2), lane 5: CL (elution with 150-200 mM ammonium acetate in $CHCl_3$:CH_3OH 1:2). The TLC were developed with $CHCl_3$:CH_3OH:H_2O (65:25:4 [vol/vol/vol]) followed by staining with (A) anthrone and (B) Dittmer reagents for detection of glycolipids and phospholipids respectively.

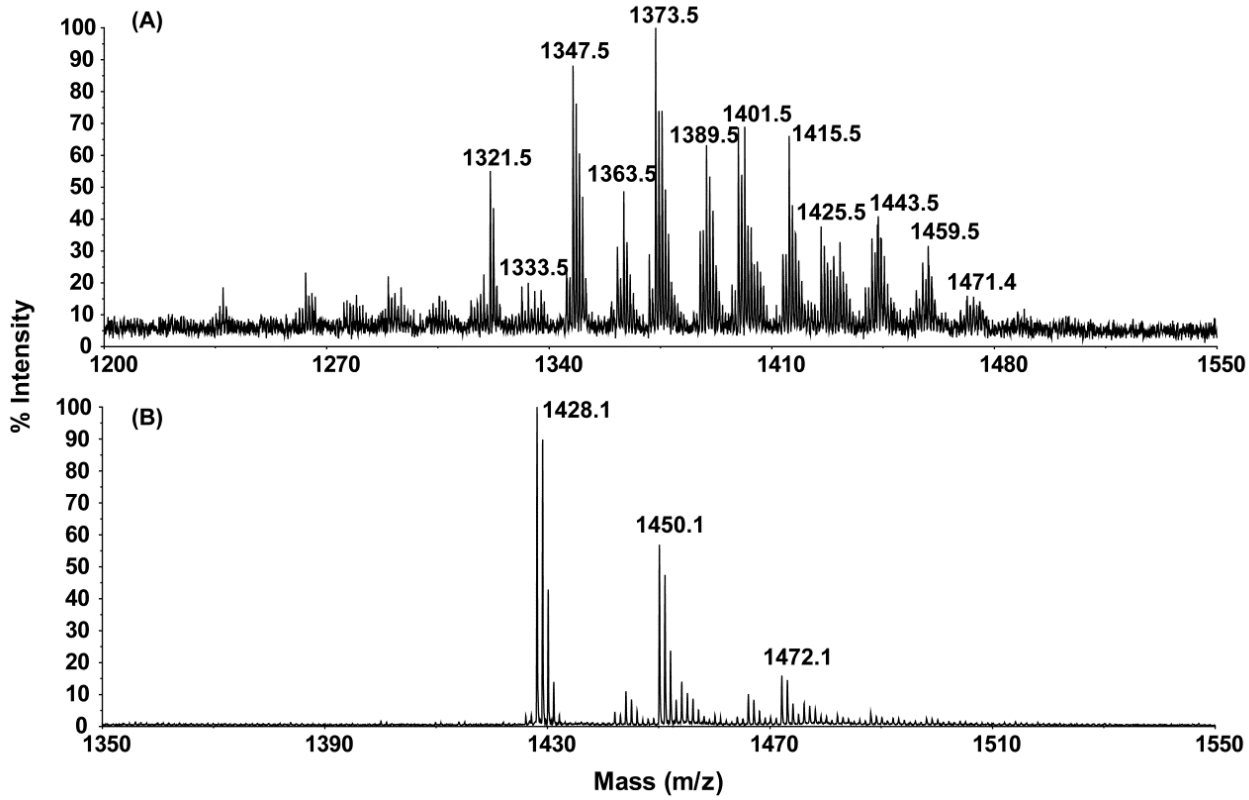

Fig. 2: MALDI TOF mass spectra of purified (A) Trehalose dimycolate (TDM) and (B) Cardiolipin (CL) from *C. glutamicum* cell wall. TDM molecular species showed a combination of both even and odd number of carbon atoms in the hydrophobic part of the lipid predominantly with C32:0, C34:1 and C36:2, while CL shows a combination of C16:0, C18:0 or C18:1 molecular species.

Fig 2A peak assignment (the number given are the sum of two chains, with multiple possible combinations): m/z 1321 (C64:0, i.e. for instance C32:0 + C32:0), m/z 1333 (C65:1) m/z 1347 (C66:1), m/z 1363 (C67:0), m/z 1373 (C68:2), m/z 1389 (C69:1), m/z 1401 (C70:2), m/z 1415 (C71:2), m/z 1425 (C72:4), m/z 1443 (C73:2), m/z 1459 (C74:1) and m/z 1471 (C75:2). Fig 2B peak assignment: m/z 1428 (2*C16:0+2*C18:0), m/z 1450 (C16:0+C18:1+2*C18:2), m/z 1472 (2*C18:1+2*C18:2).

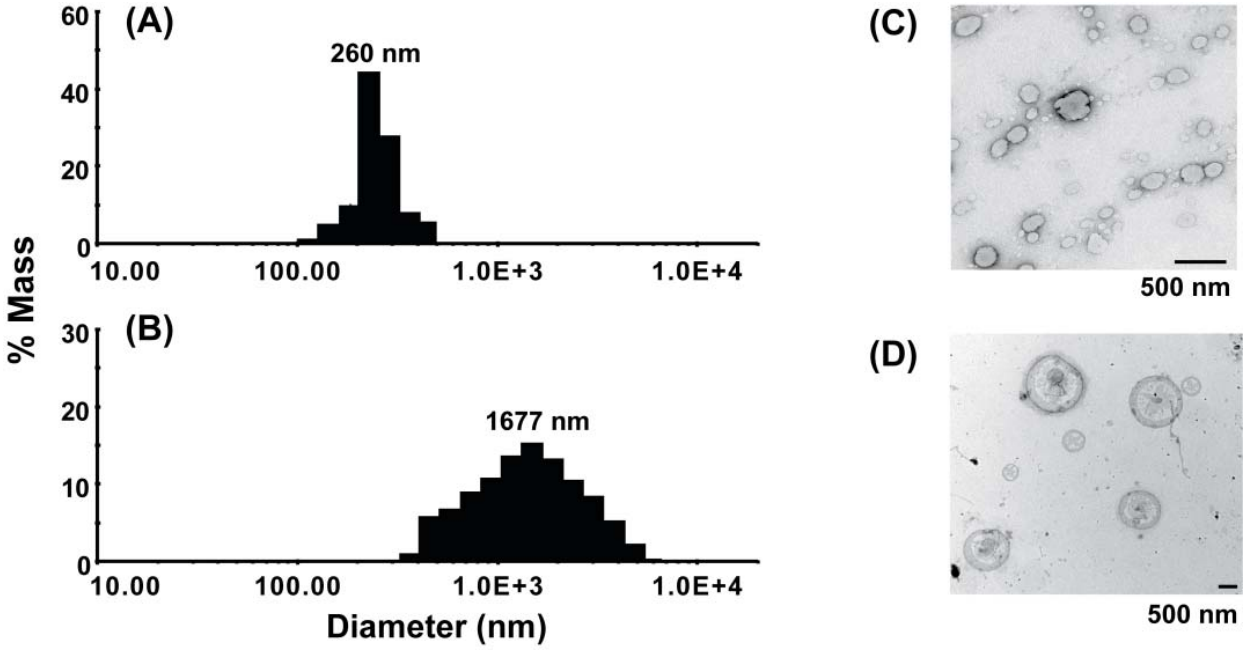

Fig. 3: Dynamic light scattering of vesicles made up of (A) TDM, prepared by dialysis and (B) TDM / CL (2:8 molar ratio) prepared by spontaneous hydration of lipid film; the average diameters are 260 and 1677 nm respectively. Negative staining Transmission electron microscopy of uranyl acetate stained vesicles composed of (C) TDM and prepared by dialysis and (D) composed of TDM / CL (2:8) and prepared by hydration of lipid film. Scale bar corresponds to 500 nm.

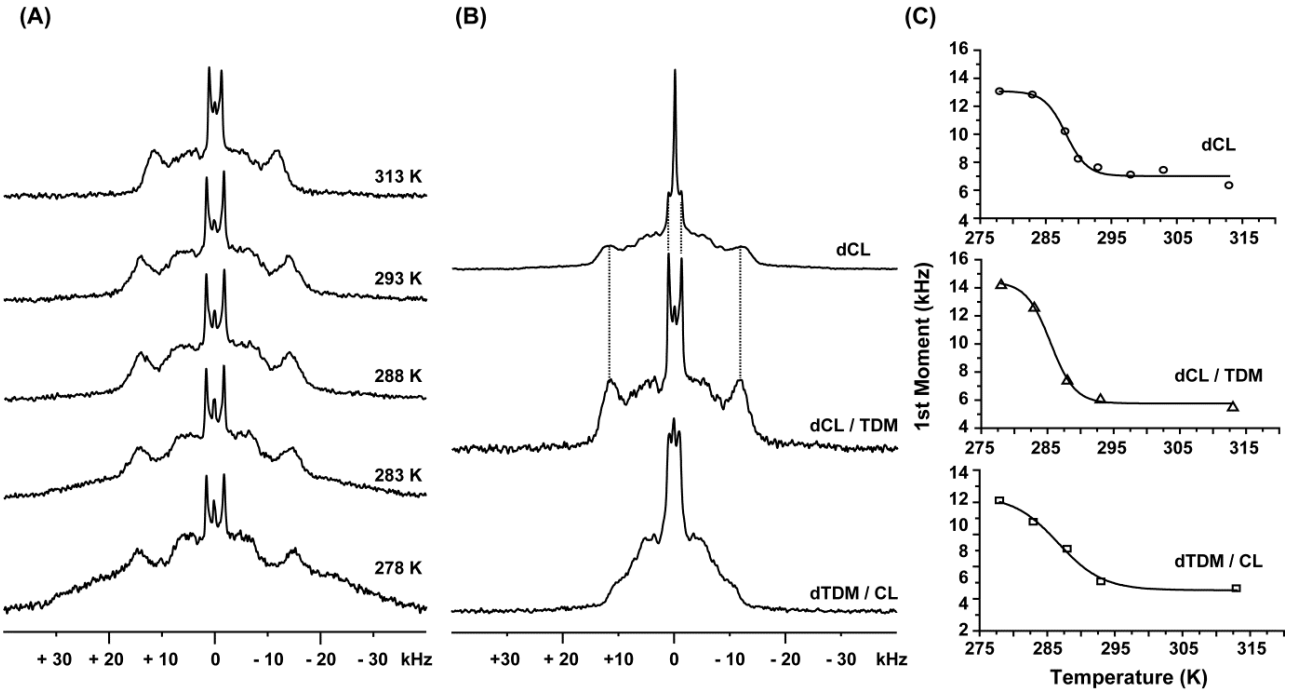

Fig. 4: ^{2}H NMR spectra of liposomes containing perdeuterated CL (d-CL), perdeuterated TDM in non-deuterated CL (d-TDM/CL : 2/8) and perdeuterated CL in non-deuterated TDM (d-CL/TDM : 8/2). (A) ^{2}H NMR of d-CL/TDM vesicles at various temperatures around the phase transition. (B) ^{2}H NMR of different lipid mixtures at 313 K and (C) First moments of these lipid mixtures as a function of temperature: in squares (d-TDM/CL), in triangles (d-CL/TDM) and in circles (d-CL).

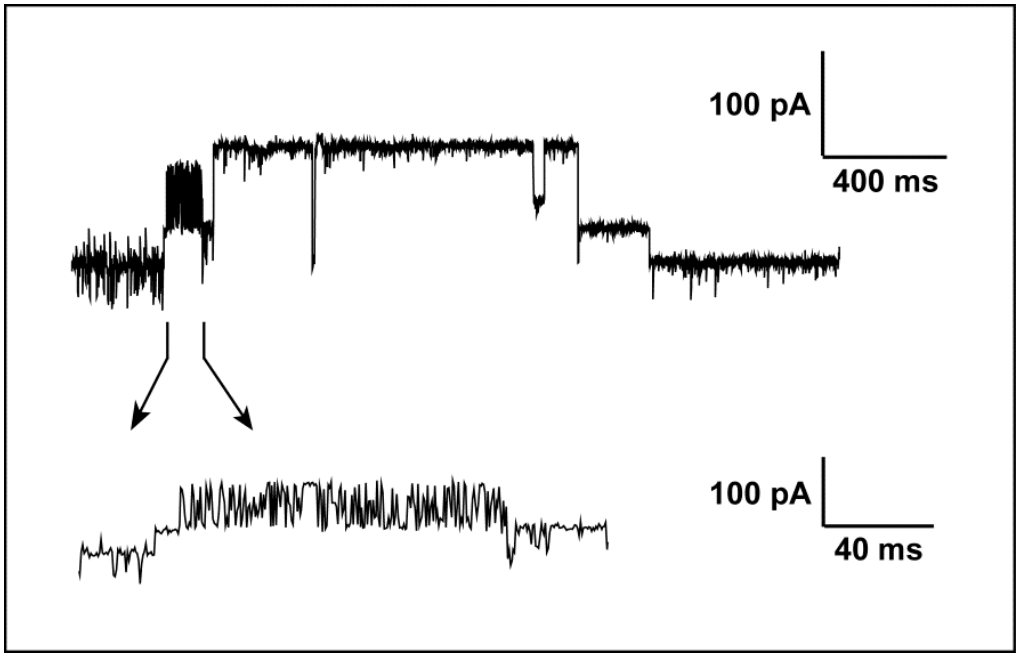

Fig. 5: Porin channel activity of reconstituted PorA: $PorH_{Chis}$ with covalent mycolic acid modification in trehalose dimycolate (TDM) liposomes. Characteristic sequential insertions, slow and fast kinetics with opening and closing of channels and voltage dependence were observed at +40 mV.

Supplementary figures and legends:

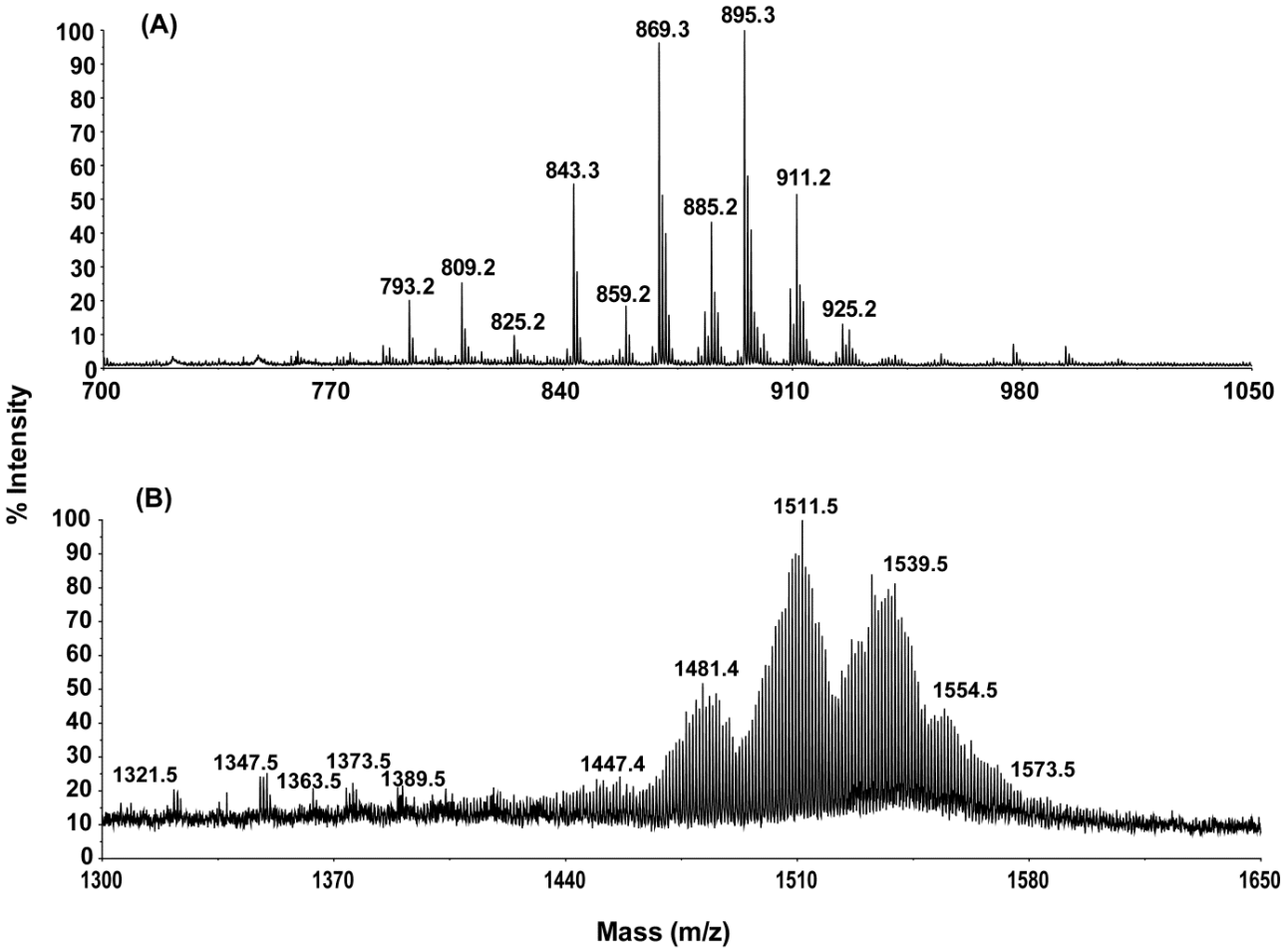

Fig S1: (A) MALDI TOF mass spectrum of purified trehalose monomycolate (TMM) from *C. glutamicum* cell wall. The molecular mass of each molecule notified with respective mass are the possible even and/or odd combination of mycolic acids as follows : m/z 793.2 (C29:3), m/z 809.2 (C30:3), m/z 825.2 (C31:2), m/z 843.3 (C32:0), m/z 859.2 (C33:0), m/z 869.3 (C34:1), m/z 885.2 (C35:0), m/z 895.3 (C36:2), m/z 911.2 (C37:1), m/z 925.2 (C38:1). To reduce the complexity with peaks composed of other molecular species, only peaks with higher intensity are marked in the figure. (B) MALDI TOF mass spectrum of perdeuterated TDM. The pattern observed is due to both ^{12}C-^{13}C isotopomers and to ^{1}H-^{2}H isotopomers and, by comparison with the protonated TDM spectrum in the same condition, it allowed to calculate an average deuteration extent of 96 %.

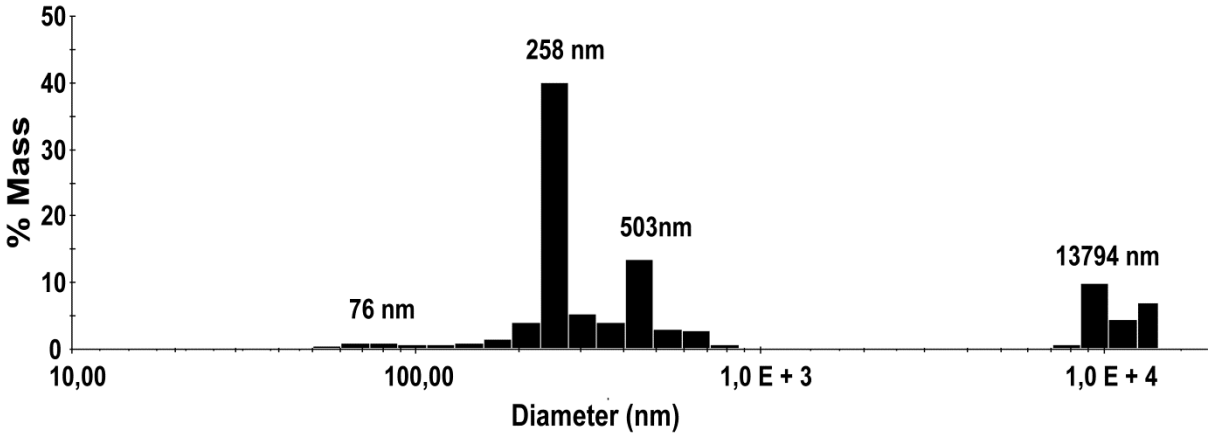

Fig S2: Dynamic light scattering of reconstituted PorA and PorH into TDM liposomes. Figure shows better quality of reconstitution with less mass percentage of aggregation with higher lipid to protein molar ratio of 50:1.

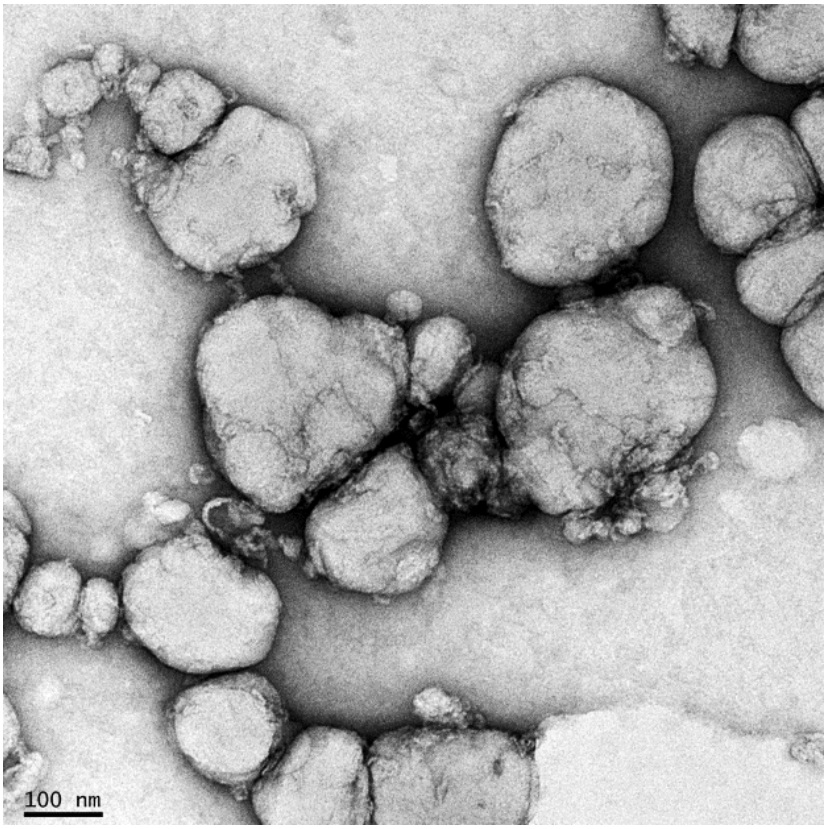

Fig S3: Negative staining Transmission electron microscopy of proteoliposomes made up of PorA and PorH expressed and purified from *C. glutamicum* in TDM liposomes. Scale bar corresponds to 100 nm.

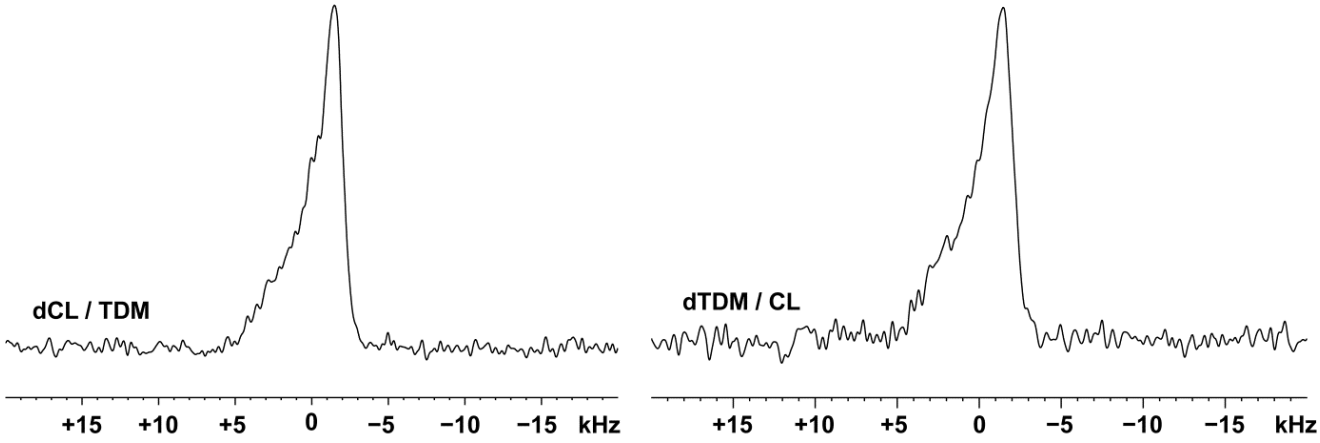

Fig S4: ^{31}P NMR of vesicles made up of perdeuterated CL in non-deuterated TDM (dCL/TDM : 8/2) and perdeuterated TDM in non-deuterated CL (dTDM/CL : 2/8) recorded at 313 K. ^{31}P line shapes are typical of a lipid bilayer organization.

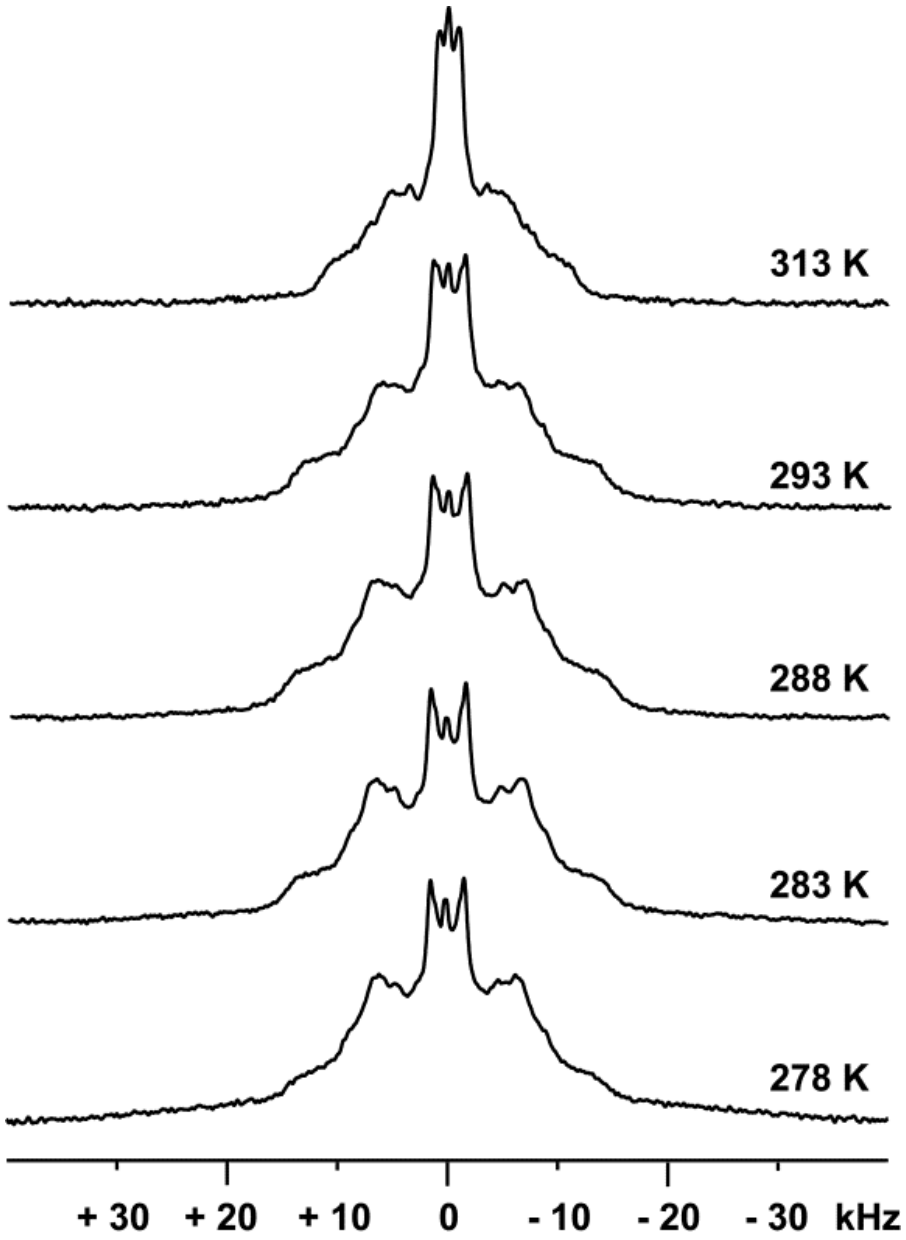

Fig S5: ^{2}H NMR of vesicles composed of perdeuterated TDM in non-deuterated CL (dTDM / CL : 8/2) vesicles at various temperatures around the phase transition.

Chapter V

In vitro reconstitution and characterization of PorAH complex in micelles and in Trehalose dimycolate (TDM) vesicles

Summary

This chapter summarizes briefly the premature results obtained in the later part of the thesis period. To move forward towards the actual structure of PorAH ion channel, we need to make the complex *in vitro*. However, our initial experiments in LDAO micelles did not show any complex formation, which was verified by affinity chromatography and titration experiment on 2D HSQC measurement. By contrast, the organic solvent extract of the co-expressed PorH-$PorA_{Chis}$ operon indicated the presence of a stable complex between both proteins. Electron microscopic images further show porin like configuration. Western blot analysis of the reconstituted proteoliposomes also specified a complex between PorA and PorH. However, more experimental evidences are required to obtain a complete characterization of the complex *in vitro*, which will direct towards the structure determination of this new class of outer membrane porins.

V.1: Introduction

As described and observed in chapter II and III by channel activity measurements, we need the obligatory presence of both PorA and PorH to form a functional voltage dependent hetero-oligomeric channel which can actually mimic the natural porin present in the outer membrane of *C. glutamicum* (1, 2). In fact, PorA and PorH, taken separately, have partially folded structures, and are unable to display porin-like activity, although they are able to insert into the artificial planar bilayer. Hence we can presume three possible explanations of the complex formation in the bilayer measurement. First, one channel forming unit i.e. a complete PorAH channel is formed in the buffered solution (in the presence of micelles) and then insert into the bilayer. Second, the complex is happening on the interface between the bilayer and solvent, and then shows channel activity and third, both proteins insert to the bilayer independently, find each other inside the bilayer and form a functional channel. Hence, in this chapter, we tried different experiments to reconstitute the complex *in vitro*.

V.2: Experimental evidences of the complex formation in micelles

The first experiment to show the complex formation is a simple pull-down experiment through a Ni-NTA affinity column. As mentioned in chapter II and III, both proteins were produced and reconstituted in LDAO micelle with His-tag at their C-terminus either in their natural host or in CF expression. Also, as the presence of His-tag on both proteins affected the channel activity (chapter II, Fig II-9), the His-tag was removed from PorH by using factor Xa cleavage. Mycolic acid modified $PorA_{Chis}$ and PorH without any tag in BufferA (50 mM Tris-Cl, pH 8.0, 100 mM NaCl and 0.4 % LDAO) were allowed to interact overnight at room temperature and then mixed with Ni-NTA matrix for ~ 5 h. The unbound proteins were washed out completely with buffer A and the bound proteins were eluted in buffer A containing 0.5 M imidazole. In principle, if there is a complex happening in this condition, one should observe both proteins in the SDS-PAGE, since $PorA_{Chis}$ will be retained on the column, together with PorH. The absence of PorH in the eluted fraction revealed the absence of complex formation within LDAO micelles. Moreover, a similar experiment with co-resolubilization of the precipitate mode CF expressed $PorA_{Chis}$ and T-$PorH_{Cstrep}$ did not show the complex formation (data not shown). Furthermore, a titration experiment with both proteins with different proportions (2:1, 1:1, 1:2 and 1:3) did not show any change in secondary structural content, neither by CD (data not shown) nor by 2D HSQC measurement (Fig. V-1), in which ^{15}N-

$PorH_{Chis}$ was mixed with unlabeled PorA. Hence, all these experiments ruled out the first explanation of formation of a complete channel in LDAO micelles.

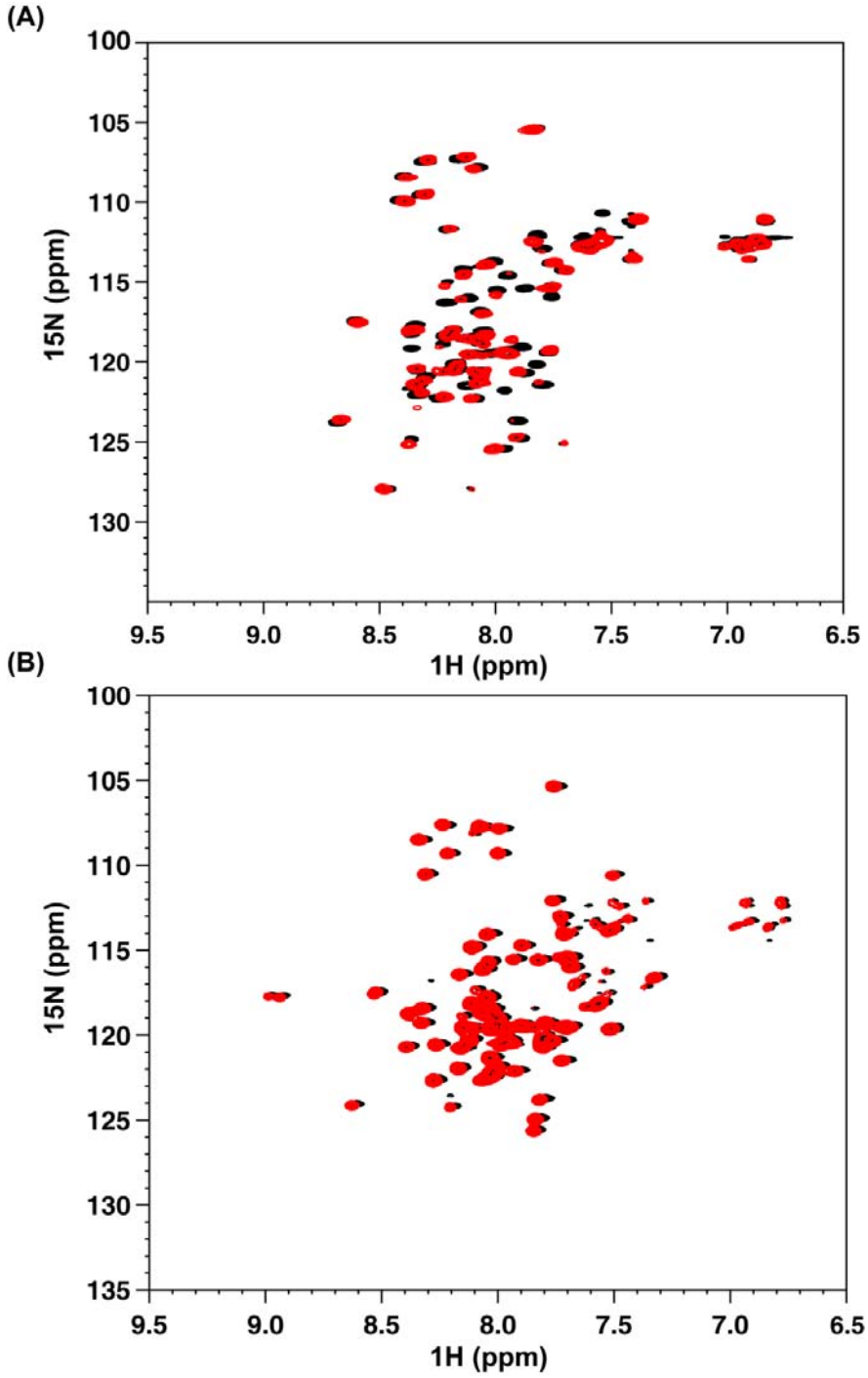

Fig. V-1: Superposition of the HSQC spectra of ^{15}N-PorH (in black) and ^{15}N-PorH in mixture with unlabeled PorA (in red) at a proportion of 1:3. The HSQC spectra of ^{15}N-PorH did not make any difference in the titration experiment with various concentrations of PorA (1:1, 1:2 and 1:3), whether the proteins were taken with (A) or without (B) mycolic acid modification. However, due to reduced concentration, several peaks had a reduced intensity and are not visible on this plot.

V.3: Cloning and expression of PorHA$_{Chis}$ operon in *C. glutamicum*

As the *in vitro* complex formation was not successful in detergent environment, we thought to make it in an alternative approach. *Barth et al.,* have shown that such two component PorA and PorH porins are found in the same transcript in the genome of *Corynebacteria* and are supposed to be co-transcribed (detail in chapter I) (1). Hence, we took the complete operon and cloned it into pXMJ19 vector (*C. glutamicum* and *E. coli* shuttle vector) for *in vivo* expression and to pIVEX2.3d for *in vitro* expression. In these constructions, only PorA has a C-terminus His-tag for affinity purification. The intermediate 73 bps sequence is present naturally in the *C. glutamicum* genome (Fig V-2A). The over-expression in the host *C. glutamicum* and in *E. coli* was carried out similarly as described in chapter I.

V.4: Extraction, purification and characterization of the PorA$_{Chis}$-PorH complex

The over-expression in *E. coli* (BL21, DE3) was unsuccessful because of toxicity upon induction. Hence *E. coli* based cell-free co-expression should be planned for the operon expression (work in process). On the other hand, for extraction of the over-expressed operon from the *C. glutamicum* cell membrane, extraction procedure with LDAO (0.6 %) was applied as described previously in chapter I for PorA and PorH extraction. In principle, if the LDAO extracted cell membrane is applied on Ni-NTA column, we should see both proteins in the elution profile unless the complex is destabilized during the extraction procedure. Since we observed only PorA$_{Chis}$ in the elution profile, we concluded that the complex is inhibited or destabilized in the presence of LDAO.

To confirm this, the *C. glutamicum* cell membrane over-expressing the operon was extracted using the organic solvent approach (Fig V-2B). The $CHCl_3$: CH_3OH extracted cell wall was precipitated in diethyl ether. The precipitate was then solubilized in two different buffers; in 10 mM Tris-Cl, pH 8.0 (Buffer A) or in buffer A containing twice the CMC of various detergents (LDAO, OG, DDM). After binding and successive washing steps, the bound proteins were eluted in buffer A containing 0.5 M imidazole. As shown in fig V-2C, in the eluted fractions, besides PorA$_{Chis}$ other bands containing PorH and possibly oligomeric forms are clearly observed in the Coomassie blue stained SDS-PAGE of the sample which was resolubilized in the absence of any detergent. By contrast, whenever a detergent was used for resolubilizing the $CHCl_3$: CH_3OH extract, only PorA$_{Chis}$ was retained on the column. Hence, none of the detergents we tried could stabilize the complex between PorA$_{Chis}$ and PorH.

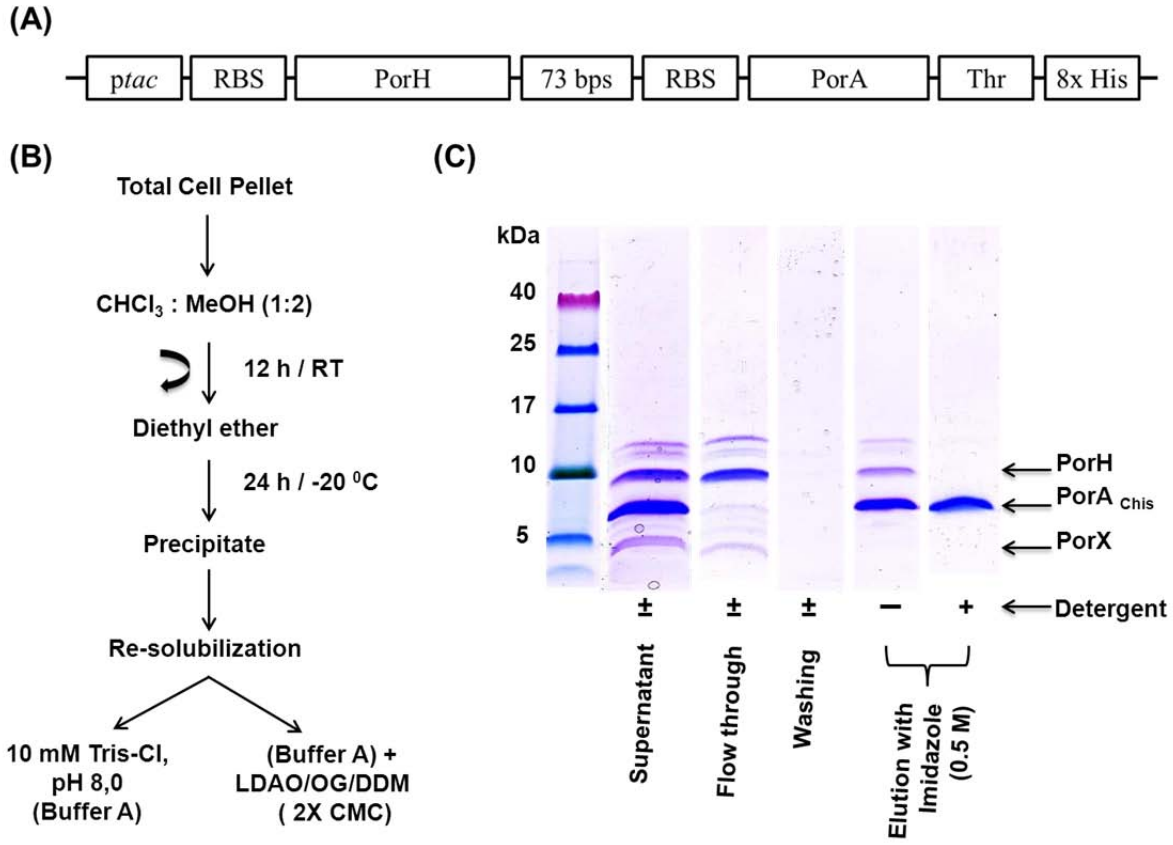

Fig V-2: (A) Construction of $PorHA_{Chis}$ operon in pXMJ19 (for *in vivo* expression) and in pIVEX (for *in vitro* expression). A sequence of 73 bps is present naturally between PorH (172 bps) and PorA (135 bps) in the *C. glutamicum* genome; RBS: ribosome binding site, Thr: Thrombin protease site, 8x His: 8 histidines affinity tag. (B) Protocol for extraction of the cell wall by organic solvent ($CHCl_3$: CH_3OH), followed by precipitation of the proteins by diethyl ether (remove the major part, but not all of the lipids). The precipitate was solubilized either in buffer A (10 mM Tris-Cl, pH 8.0) without any detergent (marked as -) or in buffer A plus twice the CMC of each detergent (marked as +); LDAO, OG and DDM. The supernatant after the re-solubilization step was applied to a Ni-NTA affinity column. (C) Coomassie blue stained 16 % Tris-Tricin SDS-PAGE of protein samples from various steps of Ni-NTA column. The supernatant, flow through and washing fractions does not show a difference without (-) or with (+) each detergent. The flow through shows as expected that $PorA_{Chis}$ is retained on the column. The eluted fractions clearly show the absence of PorH and other higher band proteins in the samples containing detergents, while they are present in the absence of detergent.

.

When we see the elution profile of the precipitate which came from the organic solvent extraction procedure and re-solubilized only in a buffer devoid of any detergent, it points some questions and some key points about the complex. First, how is this complex so stable in absence of any detergent? We assumed that during the diethyl ether precipitation some natural lipids also precipitated along with the protein and we confirmed it by thin layer chromatography (TLC). Also, after the Ni-NTA binding and much washing of the matrix, we observed a complex association between both proteins. This indicates a model (Fig V-3A), which shows that when the precipitated proteins and the lipids are resolubilized in buffer A, it forms some vesicles containing randomly distributed proteins inside. As the His-tag is accessible to the Ni-NTA, it binds and hence the complete vesicle is coming out in the elution fraction containing $PorA_{Chis}$, PorH. One could thus argue that PorH is not retained because it forms a complex with PorA, but simply because it is present in a common vesicle with $PorA_{Chis}$. Interestingly, we observed that PorX (~ 4 kDa), which is the recently discovered peptide from *C. glutamicum* outer membrane (3) is absent in the eluted fraction, although it is visible in the supernatant and flow through fractions.

The eluted fraction were characterized by DLS and showed an average diameter of 7 nm (Fig V-3B), while are typically greater than 100 nm, as we confirmed in the case of TDM vesicles, and even if larger in case of vesicle formed by other phospholipids (CL, PI/PIMs) from *C. glutamicum* (as described in chapter IV). Moreover, the TLC of the eluted fraction showed traces of trehalose dimycolate (TDM) and a phospholipid (probably cardiolipin, according to its migration) when developed with Anthrone and Dittmer respectively (Fig V-3C) (4). Hence, these experimental evidences eliminate the hypothetical situation as shown in fig V-3A, rather imposing another situation as depicted in fig. V-3D, which explain a complex association between PorA and PorH in a bicelle like environment containing TDM and CL.

Channel conductance measurements were also carried out with these eluted fractions. Multiple insertions similar to detergent extracted PorA and PorH, were observed, but the voltage dependence was not so coherent and symmetric (data not shown). Thus the organic solvent extraction protocol might affect the complex structure. We started to visualize the complex using transmission electron microscopy. The Uranyl acetate negative staining images confirmed the presence of small particles with an approximate diameter of 8 to 10 nm (Fig V-4). These images are planned to be improved using cryoelectron microscopy. Electron microscopy has been shown to be efficient for the study of reconstituted MspA from *M. smegmatis* (5), before the X-ray structure of MspA was resolved (6).

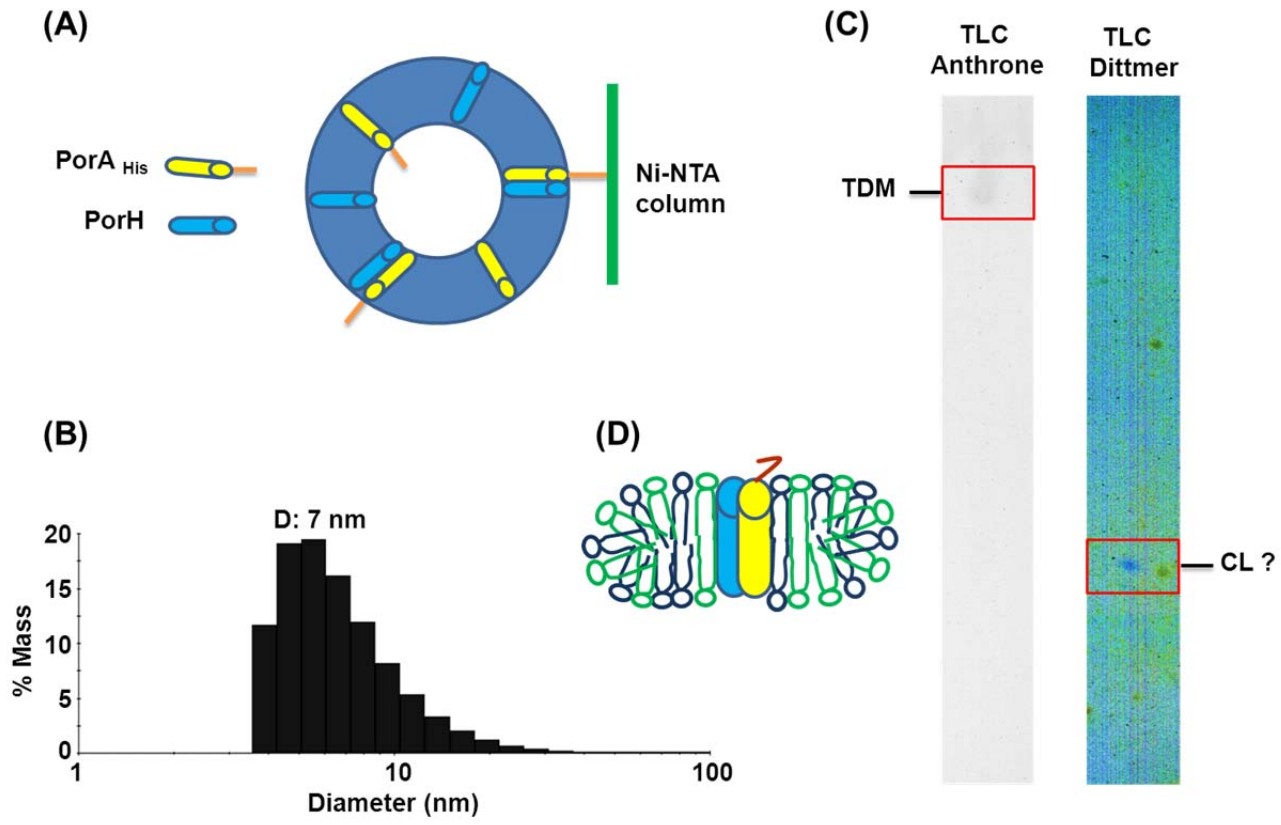

Fig V-3: (A) Illustrated a hypothetical model of the elution profile of the fractions without detergent as shown in figure V-3C, pointing a question; whether a vesicle containing homo- or hetero-oligomeric mixture of PorH-PorA$_{Chis}$ binds to the Ni-NTA column and further eluted in together? (B) Shows the DLS of the eluted fraction indicating the size of the objects with an average diameter of 7 nm. (C) Shows the Thin Layer Chromatography (TLC) of the same eluted fraction indicating the presence of trace amount of TDM and CL in the sample. Hence, the most possible way of organization of the proteins and lipids are depicted in (D), which eliminates the probability of the situation shown in (A).

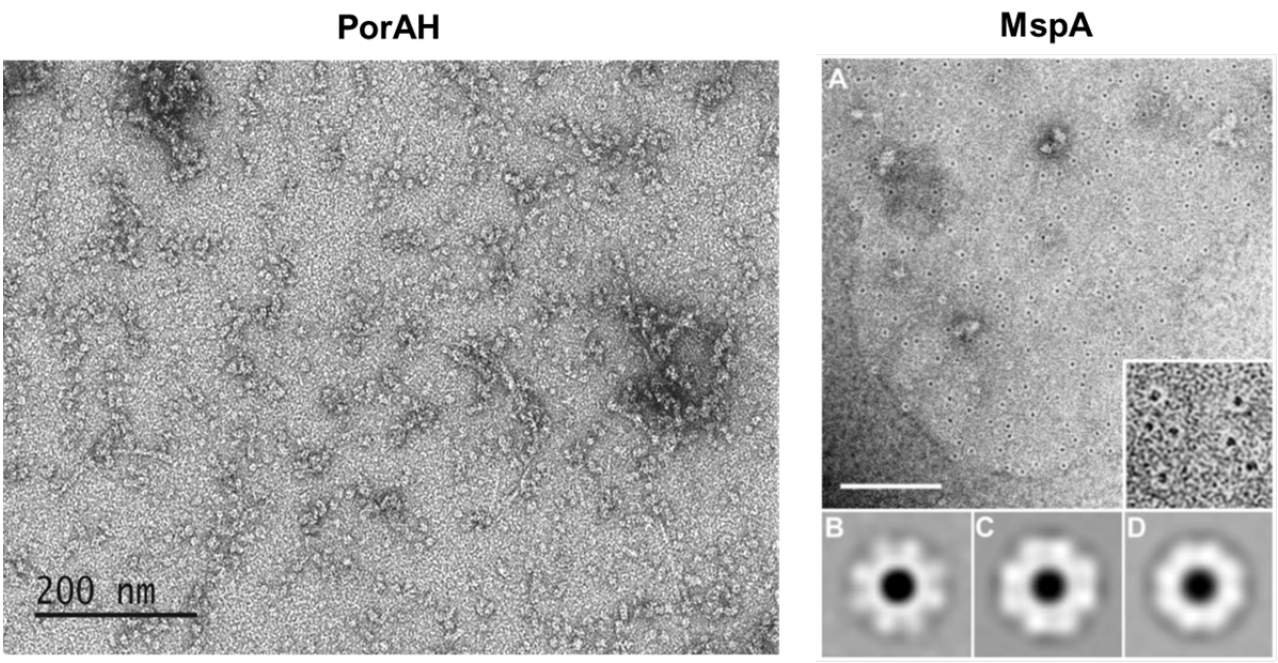

Fig V-4: Electron microscopy of organic solvent extracted and purified PorAH fraction. The eluted fraction was dialyzed against 10 mM Tris-Cl, pH 8.0 to remove imidazole completely. A protein concentration of ~0.2 mg/ml was applied to carbon-coated copper grids and then negatively stained with 99 % uranyl acetate for about 20 s and inspected through Jeol transmission electron microscope. The MspA figure was taken from the article of *Engelhardt et al.,* (JBC, 2002)(5), where the authors showed a similar negative stained MspA fractions from *M. smegmatis*. White scale bar in MspA figure represents 100 nm. Oligomeric MspA pores are stain-filled and appears as black dots (diameter of 2.5 nm) surrounded by a bright ring (diameter of 10 nm) mimicking the natural porin from the bacterial outer membrane. Cryoelectron microscopy has been planned with the PorAH sample in order to get a better resolution.

V.5: Reconstitution of PorA and PorH as proteoliposomes and their characterization

The reconstitution of mycolic acid modified or unmodified PorA and PorH into TDM vesicles was described in the annexe section (page 187). Also, the characterization of the proteoliposomes was described in chapter IV. It showed that reconstituted proteoliposomes with a protein to lipid molar ratio of 1:50 are active in BLM measurement. To characterize further, the proteoliposomes were treated with Laemmili buffer containing 1 % SDS and deposited on a 16 % Tris-Tricin SDS-PAGE (8) and then followed by a western blotting protocol as described in the biochemical method (Annexe, page 179). As shown in the figure V-5, the presence of a band at ~ 15 kDa in the samples containing both PorA and $PorH_{Chis}$ whether reconstituted with or without their natural mycolic acid modification. This band is absent when $PorA_{Chis}$ or $PorH_{Chis}$ were reconstituted separately in TDM vesicles or in LDAO micelles. Hence this band reveals the presence of a complex between PorA and $PorH_{Chis}$ in TDM vesicles. Interstingly, the difference between PorH, with and without N-terminal extension (as used for CF expression) can also be observed in the figure (marked in fig V-5).

Further characterization of the complex is required to determine the exact oligomeric state and hence the actual molecular weight of the hetero-oligomeric channel. However these preliminary results are extremely promising, and show that the reconstitution of a functional hetero-oligomer *in vitro* will be possible.

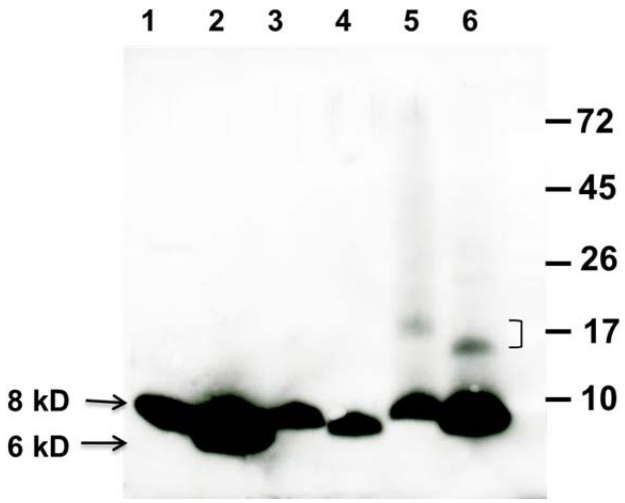

Fig V-5: Western blot analysis of $PorA_{Chis}$ (6 kDa) and $PorH_{Chis}$ (8 kDa) separately or in mixture, reconstituted in LDAO as proteo-micelles and in TDM as proteo-liposomes. Anti-his antibodies were used to develop the transferred proteins from the PVDF membrane. Lane 1 and 2: mycolic acid modified $PorA_{Chis}$ and $PorH_{Chis}$ in LDAO micelle respectively. Lane 3 and 4: mycolic acid modified $PorA_{Chis}$ and $PorH_{Chis}$ in TDM liposomes. The proteo-liposomes were prepared by dialysis protocol as described in Chapter-IV. Lane 5: Cell-free expressed unmodified S-$PorH_{Chis}$ and PorA mixture (1:1) in TDM liposomes, and lane 6: mycolic acid modified $PorH_{Chis}$ and PorA mixture (1:1) in TDM liposomes. The band of higher molecular weight corresponds to a PorA-PorH dimer, indicating the formation of a hetero-oligomeric complex. Further, these higher bands were absent when each protein is reconstituted alone as proteo-micelles or even if as proteo-liposomes.

REFERENCES

1. Barth, E., Barcelo, M. A., Klackta, C.&Benz, R. (2010) Reconstitution experiments and gene deletions reveal the existence of two-component major cell wall channels in the genus Corynebacterium *J Bacteriol* **192**: 786-800.

2. Rath, P., *et al.* (2011) Functional expression of the PorAH channel from Corynebacterium glutamicum in cell-free expression systems: implications for the role of the naturally occurring mycolic acid modification *J Biol Chem* **286**: 32525-32.

3. Huc, E., *et al.* (2010) O-mycoloylated proteins from Corynebacterium: an unprecedented post-translational modification in bacteria *J Biol Chem* **285**: 21908-12.

4. Dittmer, J. C.&Lester, R. L. (1964) A Simple, Specific Spray for the Detection of Phospholipids on Thin-Layer Chromatograms *J Lipid Res* **15**: 126-7.

5. Engelhardt, H., Heinz, C.&Niederweis, M. (2002) A tetrameric porin limits the cell wall permeability of Mycobacterium smegmatis *Journal of Biological Chemistry* **277**: 37567-37572.

6. Faller, M., Niederweis, M.&Schulz, G. E. (2004) The structure of a mycobacterial outer-membrane channel *Science* **303**: 1189-92.

7. Lichtinger, T., Burkovski, A., Niederweis, M., Kramer, R.&Benz, R. (1998) Biochemical and biophysical characterization of the cell wall porin of Corynebacterium glutamicum: the channel is formed by a low molecular mass polypeptide *Biochemistry* **37**: 15024-32.

8. Schagger, H. (2006) Tricine-SDS-PAGE *Nat Protoc* **1**: 16-22.

Conclusion and Perspectives

Considering the previously obtained results about the existence of unique PorA and PorH ion channels in the cell wall of *C. glutamicum*, the PhD project was started in 2009 with the ultimate objective to solve the structure of PorA and/or PorH ion channels. We first addressed the classical (but nevertheless difficult) problem of producing recombinant and stable isotope labeled proteins, both by homologous expression in *C. glutamicum* and by Cell-Free expression (in collaboration with the group of F. Bernhard, University of Frankfurt). They were first studied in detergent solutions: a screen of various classical detergent showed that LDAO and DHPC give rise to high quality HSQC NMR spectra. The first striking observation has been found (by CD and NMR spectroscopy) that, a fairly high α-helical structural content of each individual protein in detergent solution, which was not expected for a bacterial outer membrane porins, typically expected to be in a β-barrel conformation. Further, the functionality of this channel became clearer when *Barth et al.* in 2010 showed that the actual channel consists of a hetero-oligomeric complex between the two polypeptides PorA and PorH (1). Later in the same year 2010, *Huc et al.* showed for the first time that these proteins are post-translationally modified by mycolic acids and that this modification plays a role in their channel forming properties (2). The structural problem thus became extremely challenging, since we know now that one should deal with a hetero-oligomer, of unknown molecular weight and number of subunits, and with proper post translational modifications. With all these exciting facts we looked forward to understand the structural and functional mechanism of the complex ion channel and the following conclusions were obtained over the period of thesis work.

Up to date routine production of sufficient quantity of functional membrane proteins is still a major obstacle for structure determination by NMR spectroscopy or by diffraction techniques such as X-ray or Electron microscopy. In fact in the present work, both PorA and PorH were produced in the host *C. glutamicum* to obtain the proteins with their natural mycolic acid modification. Further fermentation was used to maximize the yield of expression. The presence of mycolic acid on both proteins was verified by MALDI TOF mass spectrometry analysis. CD and NMR spectra of uniformly labeled proteins indicated a certain degree of structuration of the individual proteins in detergent micelles. However, functionality of both proteins in BLM measurements showing the characteristics of bacterial porins confirmed the necessity of both partners to form a voltage dependent ion channel.

Although mutational experiments and tandem mass spectrometry approach succeeded to localize the position of mycolic acid modification on PorA (at Ser 15 position), they failed to localize the modification on PorH (2). Hence we thought to apply NMR based sequential assignments and NOE measurements to localize the position of modification. However, so far, with the limited sample concentration (190 µM in LDAO micelles) and sequential assignment, only 40 % backbone of PorH could be assigned. Also as major targets of modifications, 3 Ser and one Thr out of 7 Ser and 6 Thr could not be assigned so far. Besides the low signal to noise ratio due to limited double labeled (^{13}C- / ^{15}N-PorH) sample quantity, line broadening, conformational and chemical heterogeneity are the major reasons for the partial sequence assignment. Therefore, we decided to apply a different strategy: by solubilizing the protein in DMSO rather than in micelles, we hope to have less conformational heterogeneity and sensitivity to chemical modifications. Indeed, we could obtain high quality spectra with ~1mM ^{15}N-PorH sample, and the sequential assignment is in progress.

During the central period of the thesis, *E. coli* based Cell-Free (CF) expression system was used to produce the proteins without the mycolic acid modification. Also the CF system helped to overcome the toxicity problem during standard *E. coli* expression. Hence PorA and PorH were produced in high quantities as precipitates which were resolubilized in various detergents and also directly as soluble forms in presence of mild detergents. Further, the absence of mycolic acid modification on both proteins was confirmed by MALDI TOF mass spectrometry. The quality of CF expressed samples was again verified by CD and NMR spectroscopy. In fact similar structural properties with helical to random coil contents were observed with individual proteins in both modified and un-modified form. Finally, we could demonstrate with our recombinant proteins that the modification on PorH is not an absolute requirement to form a voltage dependent ion channel, while PorA absolutely requires its modification (3).

Recently the lipid composition of *C. glutamicum* cell membrane was characterized more precisely based on new protocols for mycomembrane purification (4, 5). *Marchand et al.* found that the outer membrane of these bacteria is mostly composed of trehalose dimycolate (TDM) and traces of phosphatidylinositol mannosides (PIM), whereas phospholipids like cardiolipin (CL), phosphatidylglycerol (PG), phosphatidylinositol (PI) and PIM constitutes the inner membrane (5). Using a different protocol, *Bansal-Mutalik et al.* found Cardiolipin as a second major component of the outer membrane (4). Interestingly both articles mentioned the presence of PorA in their outer membrane preparations. Although the role of TDM was well

known in the bacterial pathogenicity and host-immune response, its membrane forming properties had never been properly characterized. Further the covalent or non-covalent interaction of the natural TDM environment on the functional properties of PorAH ion channel was not so clearly understood.

Therefore to address the above questions, TDM, TMM and other phospholipids were purified from *C. glutamicum* cell wall using adsorption and ion-exchange chromatography on Quaternary Methyl Ammonium (QMA) column. The membrane forming properties of TDM was studied alone and in mixture with CL. Vesicles of TDM could only be prepared by the dialysis method, whereas nearly 80 % of CL was required to form TDM vesicles by the spontaneous hydration method. Electron microscopy and DLS showed that the vesicles formed by dialysis are relatively small (~ 200 nm diameter), whereas spontaneously formed TDM vesicles with CL mixture are larger in diameter (~ µm range) as expected for liposomes. Moreover, using perdeuterated purified natural lipids and deuterium NMR, the CL-TDM lipid mixtures were shown to exhibit a gel to liquid crystalline phase transition over a 273-295 K temperature range, for cell grown at 303 K and thus to be in a liquid crystalline state at physiological temperature. Furthermore, PorA and PorH were reconstituted in TDM as proteoliposomes and their characteristic ion channel properties were observed in bilayer measurements. On the other hand, CF expressed proteins reconstituted in TDM vesicles or in TDM/LDAO mixed-micelle did not show the characteristic voltage dependence, again confirming the requirement for covalently attached mycolic acid on PorA.

Over the thesis period the major objective of producing both membrane proteins separately with and without post-translational modification in high quality and quantity (unlabeled) for structural and functional studies has been achieved. CD and NMR spectra of individual proteins indicate helical content in their secondary structure which is unusual compared to other bacterial outer membrane β-barrel porins. However the functional data confirmed that a hetero-oligomeric complex is required for a proper voltage dependent ion channel. So far our experimental data revealed the existence of PorAH complex only in *C. glutamicum* lipids, and not in detergent micelles, suggesting a hypothetical model for the insertion and complex formation of both PorA and PorH in the bacterium (Fig 1). Accordingly, the true hetero oligomeric complex happens after individual insertion of both proteins into the cell membrane (2^{nd} pathway in fig 1) rather a preforming complex in the cytoplasm insert together into the cell membrane destination (1^{st} pathway in fig 1). However, the transport of

these proteins to the outer membrane (whether by Sec / Tat pathways or by other chaperons) is not known so far.

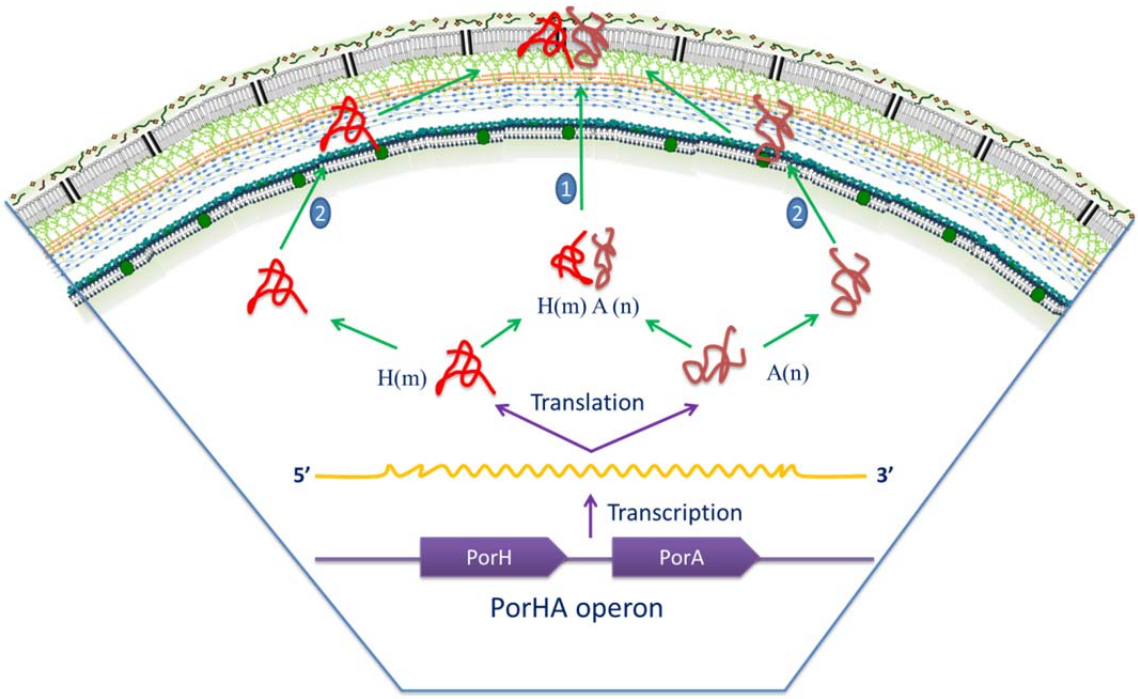

Fig 1: Hypothetical model of PorAH operon expression and insertion pathways to the cell membrane destination. Two possible pathways may exist for the real hetero-oligomeric complex formation between PorA and PorH. First, both proteins form the complex in the cytoplasm and then inserts to the membrane and second, both proteins independently inserts to the membrane and then form a stable complex with the help of the natural lipid environment. Our experimental data so far agrees with the second pathway for the complex formation.

With the above obtained results, the future perspectives are proposed to understand further the structure and function of PorAH ion channel:

➢ In a traditional way, various detergents alone or in mixture with TDM as mixed micelles have to be screened to obtain the complex *in vitro*. This would also help to obtain the actual size and stoichiometry of the complex with the knowledge of their individual oligomeric states. This a prerequisite, before obtaining the actual structure of the complex ion channel by using solution state NMR spectroscopy (if in micelles), solid state NMR (if in bilayers) or by X-ray or Electron crystallography.

- Considering the recent advance of cell-free expression in real native like environment using nanodiscs (6, 7), the purified outer membrane lipids (TDM / TMM) can be used to prepare nanodiscs and further supplied in the CF reaction mixture. In this step, both PorA and PorH DNA constructs can be provided separately or together as an operon in the reaction mixture. In addition this approach will help to understand the complex formation by NMR spectroscopy as was described (8). Further PorAH complex in reconstituted nanodiscs can be characterized biochemically to obtain the oligomeric states and stoichiometry of the actual ion channel.
- In another approach the most advanced method to study membrane protein in their natural environment i.e. directly in the bacterial cell envelope can be studied by in-cell NMR spectroscopy (9). In fact, we already have the construct consisting PorA and PorH as an operon system in the *C. glutamicum* strain deficient of both genes. But the expression condition has to be optimized to get sufficient sample for structural investigation. Otherwise, DNP-NMR can be applied to get the NMR constraints with µmolar protein concentrations (10, 11).

REFERENCES

1. Barth, E., Barcelo, M. A., Klackta, C.&Benz, R. (2010) Reconstitution experiments and gene deletions reveal the existence of two-component major cell wall channels in the genus Corynebacterium *J Bacteriol* **192**: 786-800.
2. Huc, E., *et al.* (2010) O-mycoloylated proteins from Corynebacterium: an unprecedented post-translational modification in bacteria *J Biol Chem* **285**: 21908-12.
3. Rath, P., *et al.* (2011) Functional expression of the PorAH channel from Corynebacterium glutamicum in cell-free expression systems: implications for the role of the naturally occurring mycolic acid modification *J Biol Chem* **286**: 32525-32.
4. Bansal-Mutalik, R.&Nikaido, H. (2011) Quantitative lipid composition of cell envelopes of Corynebacterium glutamicum elucidated through reverse micelle extraction *Proc Natl Acad Sci U S A* **108**: 15360-5.
5. Marchand, C. H., *et al.* (2012) Biochemical disclosure of the mycolate outer membrane of Corynebacterium glutamicum *J Bacteriol* **194**: 587-97.
6. Lyukmanova, E. N., *et al.* (2012) Lipid-protein nanodiscs for cell-free production of integral membrane proteins in a soluble and folded state: Comparison with detergent micelles, bicelles and liposomes *Biochimica Et Biophysica Acta-Biomembranes* **1818**: 349-358.
7. Roos, C., *et al.* (2012) Co-translational association of cell-free expressed membrane proteins with supplied lipid bilayers *Mol Membr Biol*.
8. Shenkarev, Z. O., *et al.* (2010) Lipid-Protein Nanodiscs as Reference Medium in Detergent Screening for High-Resolution NMR Studies of Integral Membrane Proteins *Journal of the American Chemical Society* **132**: 5628-+.
9. Renault, M., *et al.* (2012) Cellular solid-state nuclear magnetic resonance spectroscopy *Proc Natl Acad Sci U S A* **109**: 4863-8.
10. Renault, M., *et al.* (2012) Solid-state NMR spectroscopy on cellular preparations enhanced by dynamic nuclear polarization *Angew Chem Int Ed Engl* **51**: 2998-3001.
11. Jacso, T., *et al.* (2012) Characterization of membrane proteins in isolated native cellular membranes by dynamic nuclear polarization solid-state NMR spectroscopy without purification and reconstitution *Angew Chem Int Ed Engl* **51**: 432-5.

ANNEXES

I: Molecular biology

I-1: DNA and Protein sequences of $PorA_{Chis}$, $PorH_{Chis}$ and PorHA operon

pXMJ19 constructs for *C. glutamicum* expression

PorA : PorA-Thrombine-6x His (62 amino acids)

MENVYEFLGNLDVLSGSGLIGYVFDFLGASSKWAGAVADLIGLLG*LVPRGS*PGGGSH

HHHHH

PorH : PorH - *Factor Xa*-8x His (74 amino acids)

MDLSLLKETLGNYETFGGNIGTALQSIPTLLDSILNFFDNFGDLADTTGENLDNFSS*IE*
*GR*ASRGSHHHHHHHH

$PorHA_{Chis}$ operon :


```
 M  D  L  S  L   L  K  E  T   L  G  N   Y  E  T   F  G  G  N   I  G  T   A  L  Q   S  I  P  T   L  L  D   S  I  L
ATGGATCTTTCCCTT CTCAAGGAAA CCCTCGGCAA CTACGAGACC TTCGGTGGCA ACATCGGTAC CGCTCTTCAG AGCATCCCAA CCCTGCTCGA TTCCATCCTT
TACCTAGAAAGGGAA GAGTTCCTTT GGGAGCCGTT GATGCTCTGG AAGCCACCGT TGTAGCCATG GCGAGAAGTC TCGTAGGGTT GGGACGAGCT AAGGTAGGAA

 N  F  F  D   N  F  G   D  L  A   D  T  T  G   E  N  L   D  N  F   S  S
AACTTCTTCG ACAACTTCGG AGATCTCGCT GACACCACCG GCGAGAATCT GGATAACTTC TCTTCCTAAG AGAAATCCGA TTTGGCTGAT TGGCTAAAAT
TTGAAGAAGC TGTTGAAGCC TCTAGAGCGA CTGTGGTGGC CGCTCTTAGA CCTATTGAAG AGAAGGATTC TCTTTAGGCT AAACCGACTA ACCGATTTTA

                                                          M  E  N   V  Y  E   F  L  G  N   L  D  V   L  S  G
CCACAGCCTT CCCCCTTCCC CCTCATCTCA ACTCTTAATA GGAGAATTTA AAATGGAAAA CGTTTACGAG TTCCTTGGAA ACCTTGATGT CCTTTCCGGC
GGTGTCGGAA GGGGGAAGGG GGAGTAGAGT TGAGAATTAT CCTCTTAAAT TTTACCTTTT GCAAATGCTC AAGGAACCTT TGGAACTACA GGAAAGGCCG

 S  G  L  I   G  Y  V   F  D  F   L  G  A  S   S  K  W   A  G  A   V  A  D  L   I  G  L   L  G  L  V  P  R  G
TCCGGCCTCA TCGGCTACGT CTTCGACTTC CTCGGCGCTT CCAGCAAGTG GGCTGGCGCA GTTGCTGACC TCATCGGTCT GCTTGGCCTG GTGCCGCGTG
AGGCCGGAGT AGCCGATGCA GAAGCTGAAG GAGCCGCGAA GGTCGTTCAC CCGACCGCGT CAACGACTGG AGTAGCCAGA CGAACCGGAC CACGGCGCAC

 ·  S  L  E   R  A  P   G  G  G  S   H  H  H   H  H  H
GATCCCTCGA GCGAGCTCCC GGGGGGGGTT CTCATCATCA TCATCATCAT
CTAGGGAGCT CGCTCGAGGG CCCCCCCCAA GAGTAGTAGT AGTAGTAGTA
```

pIVEX2.3d constructs for cell-free expression

PorA : PorA-*Thrombine*-6x His (62 amino acids)

MENVYEFLGNLDVLSGSGLIGYVFDFLGASSKWAGAVADLIGLLG*LVPRGS*PGGGSH

HHHHH

S-PorH : sAT- PorH - *Factor Xa*-8x His (78 amino acids)

MKYYMDLSLLKETLGNYETFGGNIGTALQSIPTLLDSILNFFDNFGDLADTTGENLD
NFSS*IEGR*ASRGSHHHHHHHH

LAT- PorH : lAT-*PreScission* - PorH - *Factor Xa*-8x His (93 amino acids)

MKYYKYYKYYK*LEVLFQGP*MDLSLLKETLGNYETFGGNIGTALQSIPTLLDSILNFFD
NFGDLADTTGENLDNFSS*IEGR*ASRGSHHHHHHHH

I-2: Vectors used

- The *C. glutamicum* (Cg) / *E. coli* shuttle vector pXMJ19 (*tac* - promotor) containing multiple cloning sites and chloramphenicol resistance was used for all DNA manipulations for expression in *C. glutamicum* (1).
- pXMJ19-$PorA_{Nhis}$ and pXMJ19-$PorH_{Chis}$ (2) (obtained from Dr. Benz's Lab, Jacobs University Bremen, Germany) were used as template to prepare all subsequent constructs for CF expression in T7 promotor based vectors pET28a (kanamycin resistant) and pIVEX2.3d (ampicillin resistant).

I-3: Polymerase Chain Reaction (PCR) reactions

- For 200 µl of PCR reaction, 4 µl of 10 µM each forward primer and reverse primer, 4 µl of 10 µM dNTPs, 2 µl of fusion polymerase, 2 µl of template DNA (0.1 µg/ µl), 40 µl of 5X polymerase buffer and 144 µl of milliQ water were used to amplify the DNA of interest using the PCR condition as shown in the figure.
- The amplified DNA was purified using Quiagen PCR purification column and provided protocol

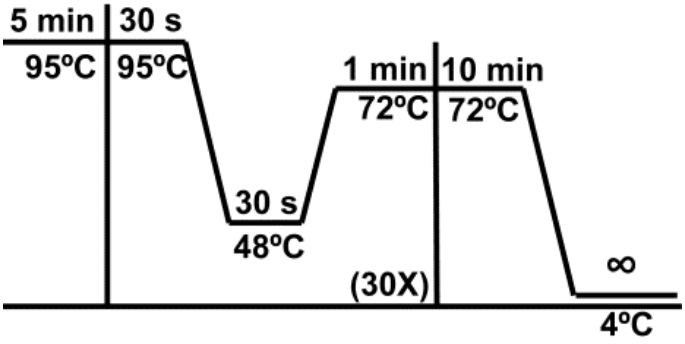

I-4: Restriction cleavage and ligation

- Digestion with restriction enzymes (products from New England Biolab (NEB), Fermentas) were carried out at 37 ^{0}C using the suitable digestion buffer according to specific enzymes. Ligation reaction was carried out using T4 DNA ligase (NEB) at room temperature for ~ 16 h.
- Ligated DNA were transformed into *E. coli* (Top10, DH5α and BL21 λDE3) and *C. glutamicum* (ΔPorA ΔPorH) competent cells using either electroporation or heat treatment at 42 ^{o}C for 90 s followed by plating in agar plates containing specific antibiotics for specific vectors.
- Screening of clones was carried out using specific restriction digestion or by colony PCR method.

I-5: Preparation of electrocompetent cells of *E. coli* and *C. glutamicum* strains

- *C. glutamicum* (ΔPorA ΔPorH) strains were used to prepare electrocompetent cells for transformation of the resulting DNA constructs after cloning process
- 10 µl glycerol stock was streaked on BHI plates containing 1.5 % agar without antibiotic and grown overnight (O/N) at 34 ^{o}C. A single colony was inoculated O/N in 3 ml media. A 100 ml culture was started from the pre-culture with a OD of 0.2
- The culture was stopped at OD of 4 -5 (mid-exponential phase) and put it on ice for 20 mins.
- Cells were centrifuged at 3000 *g* for 15 mins at 4 ^{o}C followed by washing twice with 25 ml of cold sterile water.
- Cells were washed again twice with 20 ml of 10 % glycerol. After final washing step, cells were mixed properly with 1 ml (1/100 of start culture) of 10 % glycerol, aliquoted 100 µl each, frozen immediately in liquid N2 and stored at -80 ^{o}C for future transformation purpose.

  [For *E. coli* DH5α or Top10 competent cell preparation, LB media were used instead of BHI and the culture was stopped at OD of 0.4-0.6 before washing steps]
- Electroporation condition
  - Voltage: 2.5 V
  - Capacitance : 25 µF
  - Resistance : 200 Ohm

I-6: Cloning into pET28a, pIVEX2.3d and pXMJ19 expression vectors

- *XbaI – EcoRI* fragments from pXMJ19-PorA$_{Nhis}$ and pXMJ19-PorH$_{Chis}$ were ligated into the restricted vector pET28a resulting pET28a-PorA$_{NHis}$ and pET28a-PorH$_{CHis}$.
- Forward primer, 5'-GAGAATTTA**CCATGG**AAAACGTTTACGAG-3' and reverse primer, 5'-TTAATTA**CTCGAG**GCTGCCACGCGGCACAAGCAGACCGATGAGGTCAGC AACTGCG-3' containing *NcoI* and *XhoI* restriction sites (shown in bold) were used to amplify PorA from pXMJ19-PorA$_{Nhis.}$
- The amplified and restricted PCR products were ligated into the vector pIVEX2.3d resulting in the expression of PorA with c-terminal Poly(His)$_6$-tag and Thrombin cleavage site.

- *XbaI – XhoI* fragments of $PorA_{Nhis}$ and $PorH_{Chis}$ from pET28a constructs were ligated respectively into restricted pIVEX2.3d vector resulting pIVEX2.3d-$PorA_{Nhis}$ and pIVEX2.3d-$PorH_{Chis}$ with Factor Xa cleavage sites.
- *XbaI - EcoRI* fragments of pIVEX2.3d-$PorA_{Chis}$ were ligated into restricted pXMJ19 to have pXMJ19-$PorA_{Chis}$ with Thrombin cleavage sites.
- Unless and otherwise mentioned all clones were sequenced and analyzed. DNA templates used in this study were isolated from maxi-preparation of the resulting constructs in pET28a, pIVEX2.3d and pXMJ19 using Qiagen commercial kits.
- For expression for PorA and PorH, the resulting constructs were transformed into either electrocompetent and chemocompetent cells of *E. coli* strains and *C. glutamicum* (ΔPorA-ΔporH) as described previously.

I-7: PCR reactions and cloning strategies for N-terminal tag variation of PorH for cell-free expression

- The general strategy is demonstrated in the figure below
- The first PCR reaction was set taking P3 and P4 primers and using pIVEX-$PorH_{Chis}$ as template following the same PCR condition as shown in the above
- The amplified DNA was verified on 1 % agarose gel and purified using Qiagen PCR purification kit
- The second PCR was set taking P1forward primer, P2 reverse primer containing various expression tags and the 1^{st} PCR product as DNA template. The molar ratio of P2 and P3P4 template should be 1:1.
- For the complete expression system, the second PCR may contain P4 reverse primer containing the T7 terminator site or a 3^{rd} PCR may be used taking P1, P4 primers and the product of the 2^{nd} PCR as template.
- The final PCR product was purified and used directly for analytical mode expression.
- Once the expression yield is analyzed, PorH with lAT or sAT modification was cloned into pIVEX2.3d vector for further expression in preparative scale.

I-8: List of primers for N-terminal tag variation of PorH for Cell-Free expression

Primer name		Primer sequence (5’ – 3’)
P3 forward (Psc-PorH)		**CTG GAA GTG CTG TTT CAG GGC CCG** ATG GA T CTT TCC CTT CTC AAG GAA ACC CTC
P2 reverse	Psc-5His-NdeI-Vector	**CGGGCCCTGAAACAGCACTTCCAG**TGATGATGATGATGATGA***CATATG***TATATCTCCTTCTTA
	Psc-GC-NdeI-Vector	**CGGGCCCTGAAACAGCACTTCCAG**GCGCCGGCGCCGGCGCCG***CATATG***TATATCTCCTTCTTA
	Psc-AGC-NdeI-Vector	**CGGGCCCTGAAACAGCACTTCCAG**GCGCCGGCGCCGGCGTTT***CATATG***TATATCTCC TTCTTA
	Psc-AT-NdeI-Vector	**CGGGCCCTGAAACAGCACTTCCAG**ATAATATTTATAATATTT***CATATG***TATATCTCCTTCTTA
	Psc-sAT-NdeI-Vector	**CGGGCCCTGAAACAGCACTTCCAG**ATAATATTT***CATATG***TATATCTCCTTCTTA
	Psc-lAT-NdeI-Vector	**CAGCACTTCCAG**TTTATAATATTTATAATATTTATAATATTT***CATATG***TATATCTCCTTCTTA
P1 forward		GAT CGA GAT CTC GAT CCC GCG
P4 reverse		GCTG AAA GGA GGA ACT ATA TCC
P3 forward (NdeI-sAT-Thr-PorH)		GAATTC***CATATG***AAATATTAT**CTGGTGCCGCGTGGATCC**ATGGATCTTTCCCTTCTCAAGGAAACCCTC
P3 forward (NdeI-sAT-PorH)		GAATTC***CATATG***AAATATTATATGGATCTTTCCCTTCTCAAGGAAACCCTC

Psc : PreScission protease site (in bold letters)

Thr : Thrombin protease site (in bold letters)

NdeI restriction site : in bold italic letters

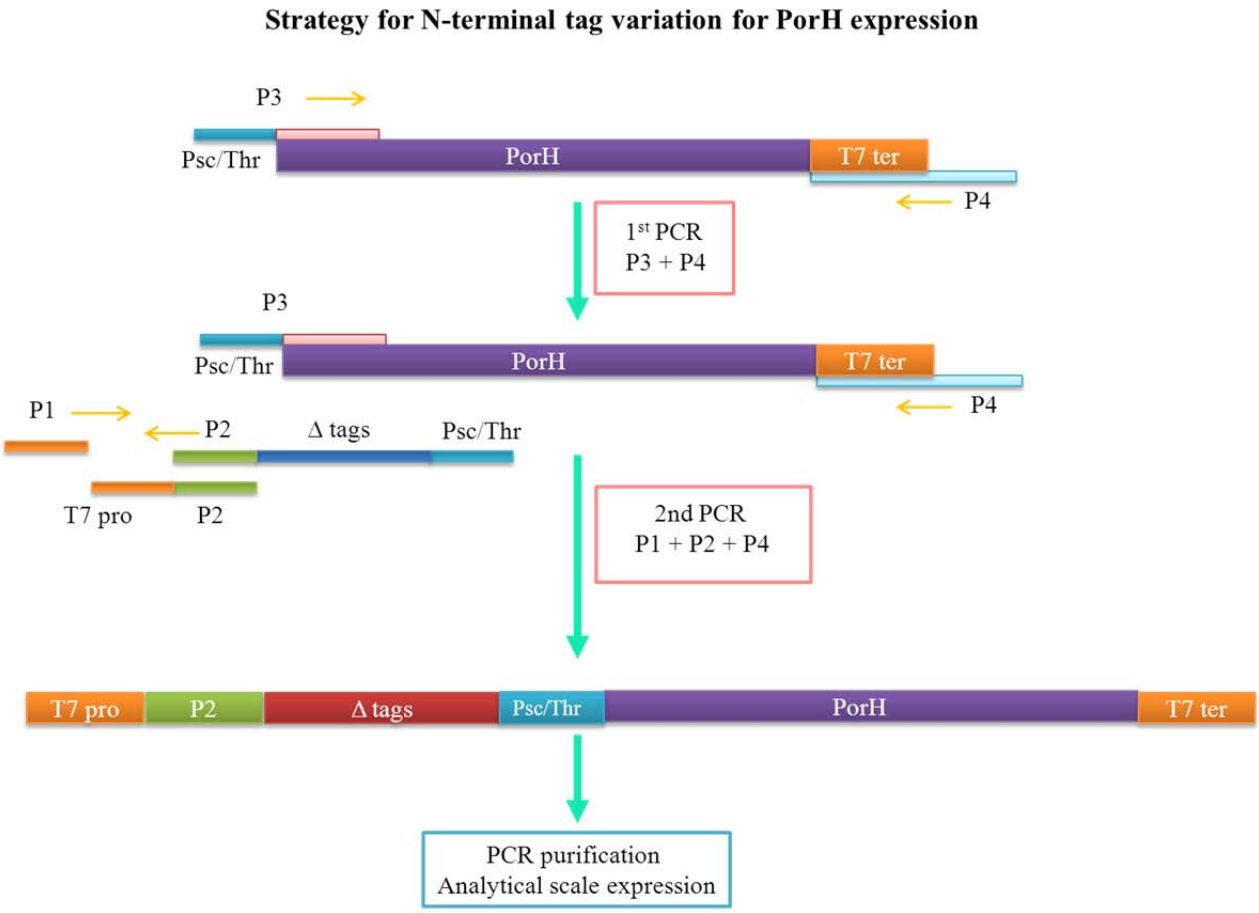

Fig: The first PCR reaction was set taking P3 and P4 primers and using pIVEX-PorH$_{Chis}$ as template. The second PCR was set taking P1 as forward primer, P2 as reverse primer containing various expression tags and the 1st PCR product as DNA template. The molar ratio of P2 and P3P4 template should be 1:1. For the complete expression system, the second PCR may contain P4 reverse primer containing the T7 terminator site.

II - Expression and purification in *C. glutamicum*

II-1 :Bacterial Stains used in this work

C. glutamicum ATCC 13032: The complete genome of *C. glutamicum* was sequenced in 2003 (3). The size of the genome is nearly 3.2 Mbps consisting of around 3138 genes coding for 2489 putative functional proteins which was obtained by sequence homology with known protein sequences. The bacteria are very much used in the industry for production of amino acids such as L-lysine and L-glutamate.

II-2 : Media, buffer compositions and culture condition

- Rich Brain Heart Infusion media (BD, France)
  Mix 37 g per liter of water at warm temperature and autoclaved before use.
- Minimal medium for *C. glutamicum* (modified) with the composition described below.
- 50 ml culture in 250 ml Erlenmeyer flask grown at 30 ^{0}C in 220 rpm.
- 500 ml culture in 3 L Erlenmeyer flask for batch expression and a maximum of 3 L culture in 5 L fermentor.

Solution I (1X)

NH_4Cl : 2 g/L

Na_2HPO_4, $2H_2O$: 2.43 g/L

KH_2PO_4 : 6 g/L

Glucose : 2 %

pH : 7.3

Solution II (1000X)

$FeSO_4$, $7H_2O$: 10 g/L

$ZnSO_4$, $7H_2O$: 1 g/L

$MnSO_4$, H_2O : 10 g/L

$CuSO_4$: 0.2 g/L

$NiCl_2$, $6H_2O$: 0.02 g/L

Solution III (1000X)

$MgSO_4$, $7H_2O$: 1 M

$CaCl_2$: 0.1 M

Protocatechuic acid: 30 mg/L

Biotin : 200 mg/L

II-3 : Expression in rich BHI and minimal medium

1) Form a frozen aliquot of *C. glutamicum* (Δ PorA ΔPorH) cells transformed with pXMJ19 plasmid containing PorA or PorH, a 5 ml primary culture in BHI media (50 µg/ml Chloramphenicol, Cm) was grown overnight (O/N) at 30 ^{0}C.
2) The secondary culture of 200 ml BHI media supplemented with 10 µg/ml of Cm was inoculated with the primary culture at a minimum OD of 0.2 and grown at 30 ^{0}C with vigorous shaking at 200 rpm.
3) Optical density (OD) at 600 nm was measured at regular intervals.
4) The culture was induced with 1 mM IPTG at OD between 2 to 3 and allowed to grow O/N.
5) Cells were harvested by centrifugation at 4000 rpm for 15 min at 4 ^{0}C and used for extraction and purification steps.
    - For expression in minimal medium, 1 L of media (10 µg/ml of Cm) were inoculated with the primary culture grown in 50 ml BHI media (50 µg/ml of Cm). Cells were induced at OD between 6 and 7 followed by continuous shaking in the same condition for another 16 hs. Different NH_4Cl and Glucose concentrations were optimized to maximize the OD of culture for better protein expression.
    - As the pH of the culture change during expression in Batch mode, Fermentation was used for protein expression in the minimal medium under the following conditions of pH 7.3, pO_2 25-30 and RPM 300. The pH was adjusted with 3 M NaOH and 20 % of H_3PO_4. Excessive foaming can be prohibited by adding minimum volume (< 1 ml) of antifoam reagent (Sigma).

II-4 : Extraction of PorA and PorH from *C. glutamicum* cultures

- The harvested cells were washed with 500 ml of buffer A. [The washed pellet can be kept at -80 ^{0}C up to 1 month before extraction of cell wall proteins]. The washed total cell pellet were weighted and thoroughly mixed with buffer A containing 0.46 % LDAO (5 times volume per gram of cell pellet) followed by continuous shaking at room temperature for a minimum of 3 h.
- pH of the extraction solutions were checked at regular interval of 1h and adjusted to 8.0.
- The extracted cells were centrifuged twice. 1st at 4000 *g* / 15min / 4 ^{0}C and 2nd at 18000 *g* / 30 min / 4 ^{0}C. The supernatant were collected and followed by affinity purification steps.

- For detergent screening, 2x CMC of each $C_{12}E_8$, Triton-X100, Triton-X114, Brij 35, OG and LDAO were used to extract 0.4 g of total cell pellet. Different extracts were analyzed using SDS-PAGE and western blotting.

II-5 : Affinity Purification by Ni-NTA column

- The supernatant containing total cell wall proteins from the extraction steps were passed at flow rate of 1 ml/min through 3 ml of Ni-NTA affinity column (Qiagen) prewashed with Buffer B. All the purification steps were monitored in an AKTA Prime (Amersham biosc) connected to the Ni-NTA column.
- After complete loading, the resin bound column was washed with buffer B containing 10 mM imidazole. A gradient (2 to 100 %) of total volume 30 ml was applied to elute the proteins in buffer B containing 500 mM imidazole. The elution was monitored in the AKTA prime by protein absorbance.
- All fractions containing proteins were analyzed on SDS-PAGE.
- The fractions containing PorA or PorH were pulled, concentrated to 2-3 ml using 3 kD cut-off viva spin and dialyzed against cleavage buffer for Factor Xa or Thrombin protease.

Buffer A : 50 mM Tris-Cl, pH 8.0 and 200 mM NaCl.

Buffer B : BufferA + 0.46 % LDAO

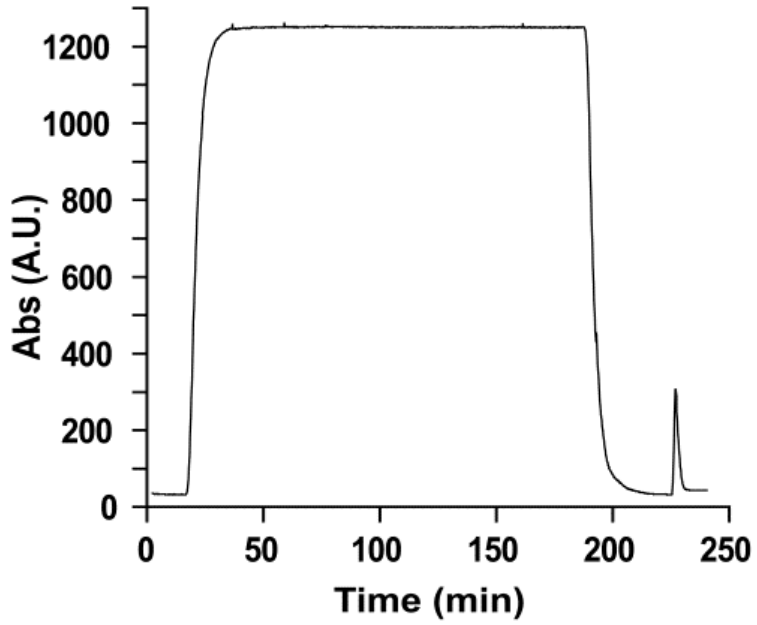

II-6 : Cleavage of affinity tags by proteolytic cleavage

1) The purified PorA and PorH fractions were dialyzed in cleavage buffer containing 50 mM Tris-Cl, pH 8.0, 100 mM NaCl, 5 mM $CaCl_2$ and 0.4 % LDAO.
2) Restriction grade Thrombin (Novagen, 1 unit / mg of protein) and Factor Xa (Qiagen, 1 unit / 50 µg protein) at 20 ^{o}C for 16 hrs were used respectively to cleave C-ter Histidine tags from PorA and PorH.
3) After cleavage the remaining Factor Xa were removed by supplied Xa removal resins (Qiagen, 50 µl per 4 unit of Xa).
4) For cleavage with Prescission protease, protein samples were dialyzed in 50 mM Tris-Cl, 7.0, 100 mM NaCl, 1 mM DTT, 1 mM EDTA and 0.4 % LDAO. The cleavage reactions were continued at 4 ^{0}C for 16 hs.
5) The cleavage was verified by MALDI-TOF mass spectrometry and SDS-PAGE.

II-7 : Purification through Superdex 200 size exclusion column

- Proteins after Ni-NTA affinity column or after proteolytic cleavage were passed through the Superdex 200 column pre-equilibrated with 50 mM Na_2HPO_4, pH 7.6 plus 0.4 % LDAO. The purification process was monitored by observing the protein absorbance in the connected AKTA Prime.

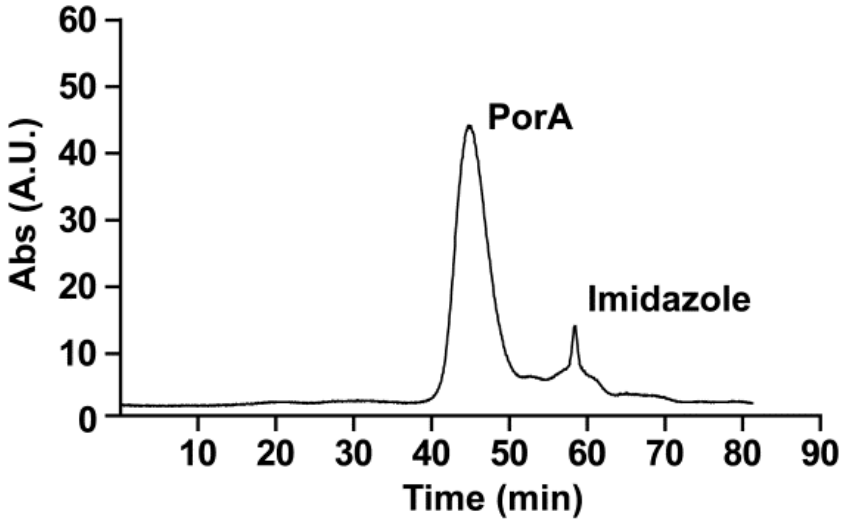

- Purified proteins were quantified according to their molar extinction coefficient (PorA : 8250 cm^{-1} M^{-1}; PorH : 1250 cm^{-1} M^{-1}) by measuring UV absorbance at 280 nm or by BCA procedure as explained in biochemical methods.

II-8 : Expression and purification of ^{15}N- or ^{15}N / ^{13}C - PorA and PorH

- Labeled protein samples were prepared using $^{15}NH_4Cl$ (2 g/L) and ^{13}C-Glucose (0.75 % / L) as source of Nitrogen and Carbon respectively. Only ^{15}N / ^{13}C PorH sample was prepared using 6 g of $^{15}NH_4Cl$ and 22.5 g of ^{13}C-Glucose for 3 L of culture.
- For each expression, a preculture was grown O/N in 100 ml BHI media. Cells were washed in milliQ water and inoculated to the fermenter containing labeled minimal media.
- For the production of mycolic acid modified PorA and PorH, cells were grown in unlabeled BHI medium up to OD of 8 – 10 and after washing of the cells in water, cells were transferred to fermentor containing labeled minimal medium with a starting OD of 2 – 3. Cells were allowed to grow one more growth doubling period to OD of 5 - 6 and then induced with 1 mM IPTG for O/N.
- After induction and over-expression, extraction and purification steps were done similar to un-labeled proteins as explained above.

III: Expression and purification in Cell - Free expression system

III-1: Preparation of reaction components

Substance	MW	Company	Weight (mg)	Volume (ml)	Stock[x]	Unit	Comments	Storage (^{0}C)
tRNA E.coli	500mg stock	Roche	40	1	40	mg/ml		-20
AcP	184.1	Aldrich	368.2	2	1000	mM	≥ pH 7+ 20 µl of 10M KOH	-20
PEP	206.1	Aldrich	412.2	2	1000	mM	≥ pH 7+ 470 µl of 10 M KOH	4
Pyruvate Kinase		Roche			10	mg/ml	In solution already	4
ATP	605.2	Sigma	435.7	2	360	mM	≥pH 7+ 233 µl of 5 M NaOH	4

GTP	567.1		272.2	2	240	mM	≥ pH 7+ 72 µl of 5 M NaOH	-20
CTP	527.1		253	2	240	mM	≥ pH 7+ 144 µl of 5 M NaOH	-20
UTP	550.1		264	2	240	mM	≥ pH 7+ 66 µl of 5 M NaOH	-20
NTP mix					75		Same volume of each stock solution	
Folinic Acid	511.5	Fluka	10	1	10		=19.6 mM	RT
DTT	154.2		154	2	500	mM		4
HEPES-KOH	238.3		28596	48	2500	mM	≥ pH 8.0 + 6480 µl 0f 10 M KOH	RT
EDTA	292.3		146.125	1	500	mM		RT
HEPES-EDTA					24	X	24vol HEPES [2.5 M]+ 1vol EDTA [0.5 M]	RT
$Mg(oAc)_2$	214.4		4288	10	2000	mM		RT
KoAc	98.13		19626	50	4000	mM	Sterile filter	RT
PEG 8000		Fluka	20000	50	40	%	Shake at 30 ^{0}C O/N	RT
NaN_3	65.01	Roth	100	1	10	%		RT
Complete		Roche	1 tablet	1	50	x		4

III-2: Stock Solutions for Cell-Free Expression

Amino acids	MW	Weight (mg)	Volume (ml)	Comments	Stock[x]	Unit	Storage (^{0}C)
Arginine (R)	210.7	316.1	15		100	mM	-20
Asparagine (N)	132.1	198.2		Sonicate			
Alanine(A)	89.09	133.6					
Aspartate* (D)	133.1	199.7		+100 µl 10 M KOH			
Glutamate* (E)	147.1	220.7		+30 µl 10 M KOH			
Glutamine (Q)	146.1	219.2					
Glycine (G)	75.07	112.6					
Histidine (H)	209.6	314.4					
Isoleucine (I)	131.2	196.8					
Leucine (L)	131.2	196.8					
Phenylalanine (F)	165.2	247.8					
Proline (P)	115.1	172.7					
Lysine (L)	146.2	219.3					
Serine (S)	105.1	157.7					
Tryptophan* (W)	204.2	306.3		100 mM HEPES pH 8			
Threonine (T)	119.1	178.7					
Valine (V)	117.1	175.7					
Cysteine (C)	175.6	263.4					
Methionine (M)	149.2	223.8					

Tyrosine* (Y)	181.2	181.2	50		20		
aa Stock			50	2 ml each aa + 10 ml Tyrosin	4		
RCWMDE			24		16.7		

- All critical solutions can be heated up to 50 ^{0}C and sonicated to solubilize
- After solubilization all solutions are stored at -20 ^{0}C

- All amino acids are from Sigma

III-3: *E. coli* S30 extracts preparation (for 10 Liter of YTPG broth in a Fermentor)

Day 1:

1. Prepare 100 ml of fresh overnight culture (A19 strain) in LB
2. Prepare 10 L of YPTG medium and sterilize inside fermenter
3. Prepare 50X stock solution of S30 buffer A, B and C and sterilize by filtering
4. Prepare 12 L of distilled water and kept at 4 ^{0}C

Day 2:

5. Fill buffer, medium and glucose in the fermenter and set the temperature at 37 ^{0}C
6. Inoculate the fermenter with (1:100) preculture and incubate at 37 ^{0}C with vigorous shaking to ensure better aeration (excessive foam formation can be prevented by adding 1 ml of antifoam reagent)
7. Take OD600 at regular interval upto 2.3 to 3.0 (should not be more than 4.0 i.e. should be harvested in the logarithmic phase)
8. Cool down the cells rapidly by putting / circulating ice-cold water to less than 12 ^{0}C
9. Harvest the cells by centrifugation at 5000 *g* for 15 min at 4 ^{0}C
10. Re-suspend the cell pellet in total volume of 300 ml ice cold S30 buffer A and pellet again at 8000 *g* for 10 mins at 4 ^{0}C. Repeat this step twice with final centrifugation for 30mins.
11. Weight the pellet and resuspend in 110 % (vol/wt) of ice cold S30 buffer B. (55ml for 50 g of pellet)

12. Broke the cells at 20,000 psi using French press
13. Centrifuge at 30,000 *g* for 30 mins at 4 ^{0}C. Centrifuge again the non-turbid 2/3rd of the supernatant.
14. To the supernatant, add 400 mM final concentration of NaCl and incubate the extract in a water bath at 42 ^{0}C for 45 mins. The extract will become cloudy.
15. Dialyze the turbid extract against 5 L of cold S30 buffer C for 2-3 hrs at 4 ^{0}C. Exchange the buffers and dialyze again overnight at 4 ^{0}C.

Day 3:

16. Centrifuge the dialyzed extract at 30,000 *g* at 4 ^{0}C. Aliquot the upper, non-turbid 2/3rd of supernatant in appropriate volumes and freeze shock them immediately in liquid nitrogen. The frozen extract can be stored at -80 ^{0}C for several months. Aliquots should not be re-used once upon thawing and Mg concentration should be determined for each new batch of S30 extract preparation.

<u>5L 2xYTPG</u>:

2YT: 160 g Tryptone, 100 g Hefeextract, 50 g NaCl to 5 L (gets autoclaved in fermentor)

2 L Phosphate: 29.9 g KH_2PO_4, 91.3 g K_2HPO_4 to 2 L (autoclave seperately)

1 M Glucose: 198 g to 1 L (filter seperately)

<u>S30 buffers (50x)</u>

A/B (50x): 60.6 g Tris, 150.1 g $Mg(OAc)_2$, 224 g KCl to 1 L (adjust pH to 8.2 with acetic acid)

C (50x): 60.6 g Tris, 150.1g $Mg(OAc)_2$, 294 g KOAc to 1 L (adjust pH to 8.2 with acetic acid)

<u>2 M DTT :</u> 1.54 g in 5 ml H_2O

<u>100 mM PMSF</u> : 34.8 mg in 2 ml EtOH

III-4: Protocol for *E. coli* T7RNA Polymerase (T7RNAP) preparation

1. An overnight primary culture is prepared from a freshly streaked LB plate containing BL21 star x pAR1219.
2. Inoculate 4 L of LB from the primary culture (1:100) and allow it to grow at 37 ^{0}C with vigorous shaking until the OD reaches 0.6 – 0.8. The cells are induced with 1 mM IPTG for minimum 5 hrs under the same conditions.
3. Cells were harvested at 5000 *g* for 15 mins at 4 ^{0}C. (Cells can be stored at -80 ^{0}C up to 4 weeks)
4. The cell pellet was re-suspended with 120 ml of T7 buffer (30 mM Tris-Cl, pH 8.0, 10 mM EDTA, 50 mM NaCl, 5 % glycerol and 10 mM of β- mercaptoethanol)
   (* always ensure reducing condition during preparation steps)
5. Cells were disrupted using French press device at 20,000 psi pressure followed by centrifugation at 20,000 *g* for 30 mins at 4 ^{0}C.
6. To the supernatant, a final concentration of 2 % streptomycin sulphate was dropwise added with gentle stirring from a 10 % stock to suppress the presence of nucleic acids.
7. The precipitated nucleic acids were removed upon centrifugation at 30,000 *g* for 30 mins at 4 ^{0}C.
8. The supernatant was loaded to a Q-sepharose anion exchange column (vol 10 ml) at a flow rate of 1 ml/min. The loaded column was washed excessively with T7 buffer and eluted further with a gradient of 50 to 500 mM NaCl with 15 column volume at a flow rate of 3 ml/min.
9. Fractions were analyzed on 10 % SDS-PAGE, and the fractioned containing T7RNAP were pooled and dialyzed (membrane cut of 30 kD) extensively against 10 mM Tris-Cl, pH 8.0, 1 mM EDTA, 1mM DTT and 10 mM NaCl. (Precipitation of the protein can be prevented by adding 10 % of glycerol in the dialyzed buffer)
10. Dialyzed protein is concentrated up to 4 mg/ml (should not be concentrated more otherwise the protein will be precipitated) by amicon ultrafiltration. (The maximum purity of 50 % can be achieved in the final sample)
11. The activity of prepared T7RNAP can be tested by in vitro transcription assay and has to be compared with commercial available (Roche Diagnostics) protein as control. A plasmid encoding a target gene (PorH) under the control of T7 promoter can be chosen for in vitro transcription assay. The plasmid is linearized by cutting with a unique restriction enzyme at the 3'-end of the transcription end and purified by either

ethanol precipitation or commercial PCR purification kits (Quiagen). The reaction mixture consists of 50 ng of linearized plasmid, 10 X reaction buffer (40 mM Tris-Cl, pH 8.0, 12 mM MgCl2, 5 mM DTT, 1mM spermidine) and produced T7RNAP as various concentrations. The reaction is incubated at 37 ^{0}C for ~2 hrs and terminated with 1 µl of 50 mM EDTA solution. Transcribed mRNA product is analyzed and quantified (using softwares) on agaroge gels stained with ethidium bromide.

12. The prepared T7RNAP can be stored for months at -80 ^{0}C in suitable aliquots in 10 mM Tris-Cl, 8.0, 1 mM EDTA, 10 mM NaCl, 1 mM DTT and 50 % glycerol.

III-5: Excel sheet for calculation of reaction mixture (RM) and feeding mixtures (FM)

Unit	Stock conc	RM components	RM [µl]	End conc	Mg^{2+} [mM]	K^+ [mM]
µg/ml	10	*E.coli* lipids	**0.0**	0.00		
x	1	S30-Extrakt	**136.5**	0.35	**4.9**	**0.21**
mg/ml	0.97	Plasmid	**6.0**	0.015		
U/µl	40	RiboLock	**2.93**	0.30		
U/µl	350	T7-RNA Pol.	**16.71**	15.0		
mg/ml	40	tRNA *E.coli*	**6.83**	0.70		
mg/ml	10	Pyruvat Kinase	**3.12**	0.08		
%	10	Brij 98	*0.0*	0.00		
mM	16.67	RCWMDE	*23.4*	1.00		
mM	4.0	AA-Mix	*48.8*	**0.50**		
mM	1000	AcP	*7.8*	20.00		**22**
mM	1000	PEP	*7.8*	20.00		**67**
x	75	NTP	*5.2*	1.0		
mM	500	DTT	*1.6*	2.0		
mg/ml	10	Folinic acid	*3.9*	0.10		
x	50	Complete	*7.8*	1		
x	24	Puffer (H-E)	*14.3*	1.0		**50**
mM	1000	$Mg(OAc)_2$	*4.7*	12.1	**9.1**	
mM	4000	KOAc	*14.7*	150.8		**150.8**
%	40	PEG8000	*19.5*	2		
%	10	NaN_3	*2.0*	0.05		
		H_2O	**56.5**			
			333.5			
		MIX I Vol.	***390.0***			
		Volume RM	***390***	TOTAL	**14.0**	**290.0**
		RM/FM	**161.4**		mM Mg^{2+}	mM K^+

End conc	FM components	RM/FM [µl]	FM [µl]
	S30-Puffer		1890
			84
			41
			231
			95
			43
	Brij 98	**0.0**	*0*
	RCWMDE	**347.4**	
0.55	AA-Mix	**723.8**	**743**
	AcP	**115.8**	
	PEP	**115.8**	
	NTP	**77.2**	
	DTT	**23.2**	
	Folinic acid	**57.9**	
	Complete	**115.8**	
	Buffer (H-E)	**212.3**	
	$Mg(OAc)_2$	**70.1**	
	KOAc	**218.3**	
	PEG8000	**289.5**	
	NaN_3	**29.0**	
	H_2O	*838.8*	**533**
		4951	*4867*
		2396	4867
	RM+FM	**5790**	**5400**
		2396	**Volume**
	for RM	***-161.4***	**FM**
	for FM	**2234.5**	

- Mg^{2+} concentration set to 17 mM and Potassium set to 290 mM
- The reaction components are calculated for 6 reactions with two repeats each taking FM of 850 µl and RM of 55 µl.
- For Mg^{2+} and K^{+} screening, Mg^{2+} concentrations to be calculated from a stock of 100 mM or higher $Mg(oAc)_2$ solution and adjusted with the volume of water to the final volume of RM.

III-6: Purification steps for CF expressed PorA and PorH

- The P-CF proteins were obtained almost pure after re-solubilization in Buffer A supplemented with appropriate detergent.
- The D-CF expressed proteins were purified in one step by immobilized metal-chelated affinity chromatography. 2 ml of RM was mixed with 600 µl of Ni^{2+} loaded NTA resin (Qiagen, Germany) for overnight at 4 ^{o}C. The resin bound proteins were washed by gravity flow with 10 ml buffer B (buffer A plus 0.4 % LDAO) followed by sequential washings with 10 ml of 20 mM imidazole in buffer B and finally eluted with 4 ml of 500 mM imidazole.
- The pure PorA or PorH fractions were concentrated to 2 ml using Vivaspin devices (3 kDa cut-off, Sartorius Biolab, Germany) and imidazole was removed by passing through 2.5 ml PD-10 column (Sephadex G25, GE Healthcare).

- Protein samples were analyzed by 16 % Tris-Tricin SDS-PAGE followed by Coomassie Blue staining and/or further detected by immunoblotting using anti-His antibodies.
- Purified proteins were quantified according to their molar extinction coefficient (PorA : 8250 cm^{-1} M^{-1}; PorH : 1250 cm^{-1} M^{-1}) by measuring UV absorbance at 280 nm.
- Furthermore, NMR samples were prepared in 2 ml preparative scale reactions either in the P-CF mode or in the D-CF mode. The unlabeled amino acid mixture in the RM and FM was replaced by a 98 % U-^{15}N labeled amino acid mixture (Cambridge Isotope Laboratories Inc., MA, USA).

Buffer A : 20 mM Tris-Cl, pH 7.7, 150 mM NaCl

Buffer B : Buffer A plus 0.4 % LDAO

III-7: List of detergents used in P-CF and D-CF mode of expression

	Detergents	Concentration (%)
PCF mode	LMPG	1
	LMPC	1
	LPPG	1
	DHPC	1
	DPC	1
	DDM	1
	LDAO	1
	SDS	1
	Triton X100	1
	β-OG	2

	Detergents	Concentration (%)
DCF mode	Brij 35	0.5
	Brij 58	1
	Brij 72	1
	Brij 98	1
	Triton X100	0.1
	Digitonin	0.4

IV- Biochemical methods

IV-1: Tricin-SDS-PAGE (4)

Reagents	Running (16 %)		Stacking (4 %)	
A/B : :19:1	2 ml	2.67 ml	0.25 ml	0.5 ml
Gel buffer	2 ml	2.67 ml	0.75 ml	1.5 ml
Glycerol (50 %)	1.2 ml	1.6 ml	----	-----
water	0.660 ml	0.9 ml	1.9 ml	3.9 ml
SDS (10 %)	60 µl	90 µl	30 µl	60 µl
APS (10 %)	60 µl	90 µl	30 µl	60 µl
TEMED	6.5 µl	7.0 µl	3 µl	6 µl
Total (ml)	**6 ml**	**8 ml**	**3 ml**	**6 ml**

Stock Reagents

- Reducing sample buffer (3X): SDS 12 % (w/v), Mercaptoethanol 6 % (v/v)
- Glycerol 30 % (w/v), Coomassie blue (0.05 %), Tris-HCl 150 mM, pH 7.0
- Gel buffer (3X): 3 M Tris-HCl, pH 8.45
- Anode buffer (10X): 1 M Tris-HCl, pH 8.9 [working 1X]
- Cathode buffer (10X): 1 M Tris, 1M Tricine, 1 % SDS, pH 8.25 (don't need to adjust pH) [working 1X]
- Fixing solution: (for Coomassie or Silver staining only)
- 50 % methanol, 10 % acetic acid

- Prevent boiling samples for membrane proteins

Electrophoresis conditions:

- voltage for stacking gel: 50 V
- voltage for separating gel: 180 V

Protein visualization:

- Incubate the gel in fixing solution for 15min
- Stain the gel with 0.025 % Coomassie die in 10 % acetic acid and 40 % CH_3OH (15min)
- Destain the gel with 10 % acetic acid and 40 % CH_3OH (15-60 min)

IV-2: Western Blotting

Transfer buffer:

- 25 mM Tris
- 192 mM Glycine
- 20 % Methanol
- 0.1 % SDS

Composition for 1 L of transfer buffer:

- 3.0285 g Tris
- 14.41 g Glycine
- Add 700 ml milli-Q
- 200 ml Methanol
- Make up the volume to 1 L
- Add 10 ml of 10 % SDS

Procedure: Electro-transfer

- Run the SDS-PAGE completely with pre-stained marker
- Cut proper size of filter paper and PVDF membrane according to the size of gel
- Wash the membrane 1st in methanol (2-5 mins) and then in transfer buffer
- Put the gel, filter paper and membrane inside transfer buffer (5-10 mins)
- Put in order:
    - Cathode plate
    - Pre-wet filter paper
    - Equilibrated gel
    - Pre-wet membrane
    - Pre wet filter paper
    - Bottom platinum anode plate

- Remove air bubbles between layers by rolling over the top
- Put cathode and safety cover
- Condition of electro-blotting
    - Mini-gel 10 V for 30 min or 15 V for 15 min
    - Large gel 25 V for 30 min or 15 V for 60 min

(Do not exceed 25 V and 3 mA/cm^2 current for large gels or 5.5 mA/ cm^2 for mini gels)

(After transfer the pre-stained marker should be visible on the membrane)

- Incubate the gel for O/N at 4 ^{0}C or 2 h at room temp with PBS-T (1X) + 5 % milk
- Wash 2 times for 10 mins with PBS-T (1X)
- Wash once for 10 mins with PBS (1X)

- Incubate with primary (1^0) antibody (8 µl in 20 ml PBS-T….store at 4 ^{0}C) for 1 hour
- Wash 2 times for 10 mins with PBS-T (1X)
- Wash once for 10 mins with PBS (1X)
- Incubate with secondary (2^0) antibody (Peroxidase, 1 µl in 10 ml PBS-T (1X)) for 1 hour
- Wash 2 times for 10 mins with PBS-T (1X)
- Wash once for 10 mins with PBS (1X)

Development of the blot

Requirements:

- Forceps to handle membrane
- Luminol and oxidizing reagent (Western lightening, Perkin Elmer)
- 1ml Pipette and tips, tissue paper, transparent sheets
- Kodak film

- Discard all PBS and keep the membrane intact
- Add 1-2 ml each Luminol and oxidizing reagent on the membrane, mix properly and incubate in dark for at least 2 min
- (After the reaction green light can be visualized in dark)
- Put the bottom of the membrane over tissue paper to remove the lightening reagents
- Put the membrane in between the transparent sheets
- In dark* illuminate the Kodak film by putting it over the transparent sheet containing membrane
- Put the illuminated Kodak film inside the illuminator and wait for the result
- Color the membrane in Amido Black, incubate for few minutes and after coloration wash the membrane with water
  (* open the Kodak film only in dark)

IV-3: Silver Staining

Reagents

Solution A: 50 ml of 40 % ethanol + 25 µl of 37 % formaldehyde

Solution B (5X): 0.5 g $Na_2S_2O_3$ in 500 ml water

Solution C: 0.05-0.08 g $AgNO_3$ in 50 ml water

Solution D (5X): 75 g Na_2CO_3 in 500 ml water

Protocol

1. Fixation with solution A for 10 min.
2. Washing with water for 5 min (2 times).
3. 50 ml of 1X solution B for 1 min.
4. Washing with water for 20 seconds (2 times).
5. Solution C for 10 min.
6. Washing with 50 ml of 1X solution D for 3 min.
7. 50 ml of 1X solution D + 100 µl $Na_2S_2O_3$ (10 mg/ml) + 25 µl of 37 % formaldehyde (untill complete coloration)
8. Stop coloration with 2.5 ml of 2.3 M citric acid.
9. Store the gel in water.

IV-4: Protein Estimation by Bicinchoninic acid (BCA) method

- Prepare BSA standards from 20 µg/ml to 2 mg/ml and 5 µg/ml to 250 µg/ml in water or buffer from a stock of 2 mg/ml
- Dilute the unknown protein sample in proper dilution factor.
- Mix the assay reagent A and B in the ratio 50:1

Procedure

1. Pipette out each standard, controls and diluted protein samples into micro plate wells in duplicate.
2. Add 100 µl of BCA assay reagent mix (A:B :: 50:1) to each well and mix it properly (careful about cross contamination).
3. Incubate at 37 ^{0}C for 30 min.
4. Measure the absorbance at 562 nm.
5. Plot the standard curve and calculate the unknown protein concentration from the graph.

IV-5: Physico-chemical parameters of PorA and PorH

Protein construct	Length (aa)	Mol Wt (gram/mole) (+ myc acid)	Extinction Coeff (cm^{-1} M^{-1})	Isoelectric Point (PI)
PorA	45	4680 (4680+478=5158)	8250	6.2
PorH	57	6161 (6161+478=6639)	1280	5.4
PorA-Chis	62	6468 (6468+478=6946)	8250	
PorA (Thr)	49	5146 (5146+478=5624)	8250	
PorH-Chis	76	8415 (8415+478=8893)	1280	
PorH (Thr)	61	6617 (6617+478=7095)	1250	
LAT-PorH-Chis	93	10680	8960	
LAT-PorH (FXa)	80	9124	8960	
PorH-Chis (Psc)	76	8327	1280	
PorH (FXa-Psc)	63	6771	1280	
sAT-PorH-Cstrep	79	8830	9530	
sAT-PorH (FXa)	65	7203	3840	
PorH (Thr - FXa)	63	6761	1280	

- Thr : after Thrombin cleavage
- FXa : after Factor Xa cleavage
- PSc : after PreScission proteage cleavage
- FXa-Psc : after Factor Xa and PreScission proteage cleavage
- Thr-FXa : after Thrombin and Factor Xa cleavage

V: Mass Spectrometry

V-1: Basic theory: In principle, a mass spectrometer consists of an ion source, a mass analyzer that measures the mass / charge (m/z) ratio of the ionized molecules and a detector to detect the number of ions at each m/z value. In fact the mass analyzer is the most important part of the technique which determines the sensitivity, resolution and accuracy of the MS spectra profile. In general, matrix-assisted laser desorption / ionization (MALDI) and electrospray ionization (ESI) are the two methods commonly used for MS analysis of proteins. In MALDI the samples are ionized out of a dry, crystalline matrix via laser pulses, whereas in ESI samples are directly analyzed out of a solution and therefore linked to liquid based separation. Out of different analyzers, MALDI is commonly linked to time-of-flight (TOF) analyzer where the ions are accelerated to high kinetic energy, separated along the flight tube as a result of different velocities. These ions are turned around in a reflector and then collide to a detector that counts the number of arriving ions (5-7).

V-2: MALDI TOF mass spectrometry in linear mode (used for protein analysis)

MALDI-TOF (matrix-assisted laser-desorption/ionization-time-of-flight) mass spectra in linear positive ion mode were acquired on a Voyager-DE STR mass spectrometer (PerSeptive Biosystems) fitted with a pulsed nitrogen LASER emitting at 337 nm. All spectra were analyzed in linear mode using an extraction delay of 100 ns with accelerating voltage of 25 kV. Samples were mixed with sinnapinic acid as matrix and were loaded onto a metal plate, co-crystallized at room temperature. A total of 2,500 shots were accumulated in a positive ion mode and all data were acquired with default calibration for the instrument. For protein samples containing detergents, washing with ethyl acetate or simple dilution steps were used to improve the signal-to-noise ratio.

Preparation of sinnapinic acid matrix (5 mg/ml): 2.5 mg of sinnapinic acid were solubilized in 250 µl solution containing 0.1 % TFA/H_2O. To this mixture, 250 µl of 0.1 % TFA / Acetonitrile solution was added and well mixed and sonicated for 1 min.

V-3: MALDI TOF mass spectrometry in reflectron mode (used for Lipid analysis)

MALDI-TOF mass spectra in reflectron positive ion mode were acquired on a Voyager-DE STR mass spectrometer fitted with a pulsed nitrogen LASER emitting at 355 nm with a frequency of 200 Hz. All spectra were analyzed in reflectron mode using an extraction delay of 100 ns with accelerating voltage of 20 kV. Lipid samples (1 mg/ml) were mixed with 2,5-dihydroxybenzoic acid (DHB) as matrix dissolved in $CHCl_3$:CH_3OH (1:1 by vol) and were loaded onto a metal plate, co-crystallized at room temperature. A total of 2,500 shots were accumulated in a positive ion mode and all data were acquired with default calibration for the instrument.

VI: Circular Dichroism spectroscopy

Basic theory: Basically CD is detected as the unequal absorption of left-handed and right-handed circularly polarized light. When light is polarized by passing through suitable prism or filters, the electric field (E) component associated with the light oscillates in a sinusoidal manner in a single plane. This sinusoidal wave can be visualized as the resultant of two vectors of equal lengths; one which rotates clockwise (E_R) and the other which rotates counterclockwise (E_L) and both give rise to a circle. Both waves are 90^0 out of phase and can be separated by using various electronic devices or prisms. When an optically active (chiral / asymmetric) molecule interact with light, they absorbs the left- or right- handed polarized light to different extents and leading to different refractive indices for each waves. Hence it is called as circular dichroism and therefore the plane of the light is rotated with the resultant of E_L and E_R vectors leading to an ellipse and the light is now elliptically polarized. Therefore the unit of CD is reported as ΔE (the difference in absorbance of E_R and E_L) or in $[\theta]^0$ ellipticity which is the angle whose tangent is the ratio of major to minor axis of the ellipse. Also as molar ellipticity in deg cm^2 $dmol^{-1}$ this is equal to 3.298 times ΔE. More details about the theory are illustrated in the following articles (8-10).

Sample Preparation and analysis: PorA and PorH samples were centrifuged at 15,000 *g* for 20 min at 4 ^{0}C and diluted to appropriate concentration before use. 10 mM Na_2HPO_4, pH 6.8 was filtered before used for CD measurements. Measurements were done using either Jobin Yvon or Jasco spectrometer.

VII-Extraction and purification of lipids

VII-1: Extraction of total cell wall lipids from *C. glutamicum*

1) From 10 ml of primary culture, *C. glutamicum* cells were grown to late exponential phase (16 h) in 2 L of brain heart infusion (BHI) media at 30 ^{0}C with continuous shaking at 200 rpm.
2) Cells were harvested by centrifugation at 4000 *g* for 20 mins.
3) The cell wall was extracted three times successively in $CHCl_3$: CH_3OH (1:2, 1:1 and 2:1) proportions (12 ml per gram of cell mass) for 12 h at room temperature with continuous stirring.
4) The organic solvent extracts were separated after each extraction step by centrifugation and then by filtration through a filter paper.
5) All organic solvents were removed by vacuum rotor vapor and the extract was redisolved only in $CHCl_3$.
6) To eliminate the polysaccharides, equal volume of water was mixed followed by gentle shaking and allowed to separate the organic phase from the aqueous phase. The lower organic phase containing lipids were collected, evaporated to dryness, quantified, resolubilized in 2-3 ml of $CHCl_3$ and analyzed by TLC.

VII-2: Thin layer chromatography

1) Diluted lipid fractions in $CHCl_3$ or $CHCl_3$: CH_3OH (1:2) were deposited on TLC plate (Alugram Xtra SILG, GM, 20x20 cm) and developed with $CHCl_3$: CH_3OH: H_2O (65:25:4 by volume) for 1-2 h.
2) The presence of glycolipids was identified by spraying the TLC plate with 0.2 % anthrone in H_2SO_4 followed by heating, whereas the phospholipids were revealed by spaying with Dittmer reagent.
3) The stained TLC plates were immediately scanned for keeping the images.

VII-3: QMA anion exchange chromatography

Materials:

20 cc pre-packed QMA column (Sep Pack-Waters) or QMA matrix (PALL Biospera, France)

$CHCl_3$, CH_3OH, NH_4Ac (Prepare 1 M stock in $CHCl_3$: CH_3OH=1:2)

Procedures:

1. Activate the column/matrix with 3 Column Volume (3x CV) of 0.2 M ammonium acetate in $CHCl_3$: CH_3OH (1:2)
2. Wash the matrix first with 5x CV of $CHCl_3$: CH_3OH (1:2) and then with 3x CV of $CHCl_3$.
3. Apply the total lipid mixture in CHCl3 on the activated column up to 100 mg/ml with a maximum of 200 mg of lipid can be applied per 25 g of matrix.
4. Apply 3xCV of CH_3OH in $CHCl_3$ with increasing proportions such as 10:0, 9:1, 8:2, 7:3, 6:4, 1:1 and 1:2. [For elution of glycolipids]
5. Apply 3xCV of $CHCl_3$: CH_3OH (1:2) containing a gradient of ammonium acetate (from 50 to 200 mM). [For elution of phospholipids]
6. 10ml fractions were collected and verified by a TLC column, developed and revealed as explained above.
7. For quantification of phospholipids, ammonium acetate was removed from the purified phospholipid fractions by redisolving the dried lipid fractions only in $CHCl_3$ and then eliminate the salts by filtration.

VIII: TDM / PorAH Proteoliposome preparation

1) Equimolar quantities of PorA and PorH were precipitated in cold ethanol (20x volume) and 12 % of 5 M NaCl for minimum of 24 h. The precipitate was recovered by centrifugation at 10,000 *g* for 30 mins. The precipitate was kept at room temp for nearly 2 h to eliminate ethanol completely.
2) The protein precipitates were mixed with TDM in OG (10 %) mixed micelles in different protein / lipid molar ratio of 1:30 and 1:50.
3) The ternary mixture were transferred to a dialysis tube of appropriate cut off (3 kD, SpectraPor) and dialyzed twice against 2 L of detergent free buffer (10 mM Tris-Cl, pH 8.0, 100 mM NaCl) at room temperature for 3-5 hs with gentle stirring.
4) The next 2-3 dialysis steps were continued at 37 ^{0}C (to stay in higher gel-liquid phase transition temperature) without stirring until an opaque proteoliposomes formed in the dialysis tube.
5) The proteoliposomes were stored at 4 ^{0}C and further characterized.

IX : Dynamic Light Scattering (DLS)

The diameter and size distribution of TDM vesicles prepared either by dialysis or by hydration in presence of Cardiolipin were analyzed by DLS. Samples were diluted in filtered water to 50 – 200 times before measurement. The experiments were performed with a DynaPro-DLS instrument (Wyatt technology) equipped with laser source of wavelength 663 nm. For each measurement, 20 acquisitions were acquired with 10 s acquisition time. All data were processed with DYNAMICS software provided with the instrument.

X : Electron microscopy

The shape and size distribution of TDM vesicles prepared as described above were analyzed by transmission electron microscopy (TEM). The samples were prepared using the conventional negative staining procedure. Drop of liposomes suspension (10 - 20 µl) were adsorbed onto a glow-discharged carbon-coated copper grid. The grids were blotted on a filter paper and then negatively stained with uranyl acetate (1 %). Grids were examined with a transmission electron microscope (JEOL JEM 1400) at 80 kV and 120 kV. The images were acquired using a digital camera (GATAN ORIUS SC 1000B model 832) from 20,000 to 50,000 X magnifications. The liposome's diameter was evaluated using the software.

XI : Channel activity measurements

- Channel activity of PorA and PorH separately, in mixture with molar proportion of 1:3, 1:1 and 3:1, and as reconstituted proteoliposomes were recorded using planar bilayer measurements. [Also called as Black Lipid Membrane (BLM) measurements]
- The planar bilayers were formed across a 250 μm diameter hole by presenting a bubble of either azolectin lipids (Sigma) or mixture of azolectin containing 10 % trehalose dimycolate (TDM) dissolved in n-decane (30 mg/ml).
- Recordings were performed at room temperature with a membrane potential of 40 mV in a buffered solution containing 1M KCL in 10 mM Tris-Cl, pH 8.0 or in 10 mM HEPES, pH 7.4 containing 400 mM KCl solution.
- Currents were amplified using an Axon 200B patch-clamp amplifier, filtered at 1 kHz through a-pole Bessel filter and digitized at 2 kHz. Data were analyzed with pCLAMP software.
- Protein samples were diluted from pg/ml to μg/ml in 1M KCl for measurements.
- Control experiments using detergent (up to 1 % LDAO) alone were performed systematically and did not show any characteristic signal

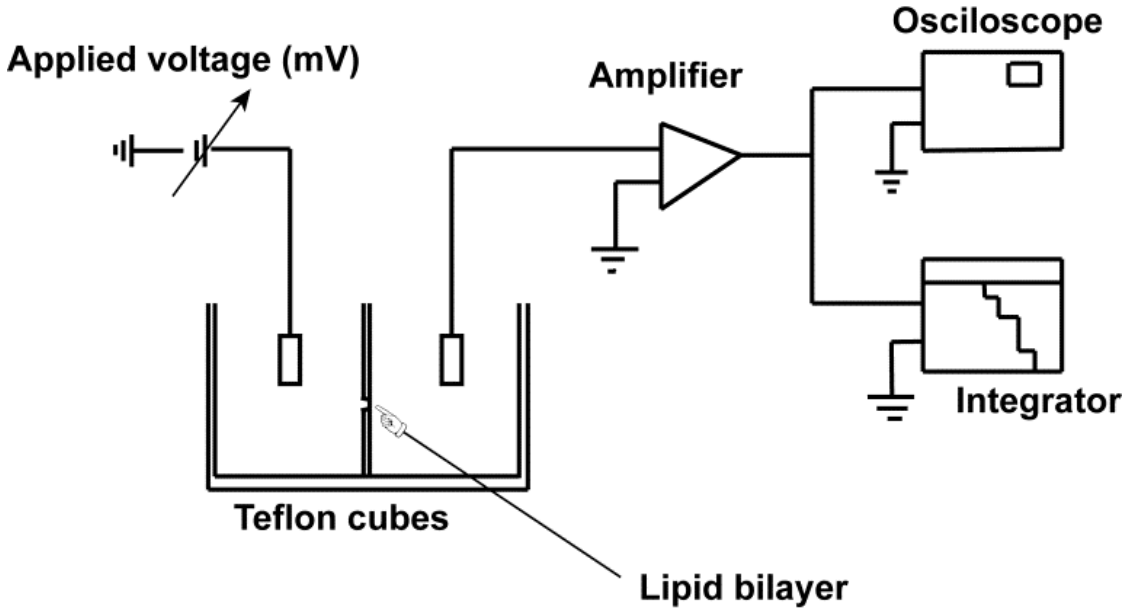

XII : NMR experiments, spectrometers and observations

Basic theory: In this spectroscopic method, the environment of atomic nuclei is studied by looking at their intrinsic quantum property called ‘ spin ’ which is determined by the spin quantum number. These spin precess around the magnetic field vector and the frequency of this precession can be measured. As the atomic nuclei have different position in a molecule, they have different electronic environment. Because of this electronic cloud they shield the nucleus from the magnetic field and hence reduce the effective field and thus reduce the precession frequency of the nuclear spin. Such effect is named as chemical shift and can be used to distinguish between the ^{1}H, ^{15}N or ^{13}C in different amino acids. The second important effect on the spin is called NOE which is a cross-relaxation between spins caused by the dipolar coupling. The dipolar coupling only depends on the distance between the spins and independent of the number of bonds between them. The basic theories of NMR are beyond the scope of the thesis and hence literatures can be referred to build better concepts on NMR (11, 12). Furthermore, as relaxation times in NMR are widely used to extract dynamics informations, that is essential complements to the structural information. As both HSQC and TROSY based experiments were measured in the thesis work, the two dominant mechanisms influencing the experiments are briefly explained here.

Chemical Shift Anisotropy (CSA): Chemical shift of a nucleus is a function of orientation of the molecule in a magnetic field and this chemical shift keep changing constantly when the molecule tumbles in solution and hence leading to relaxation. The rate of relaxation is proportional to square of the gyromagnetic ratio of the nucleus (γ), magnetic field strength (B_o) and also to chemical shift anisotropy (Δσ). The transverse relaxation rate (R_{CSA}) is given by the following equation:

$$R_{CSA} = \frac{2}{15}\,\gamma^2\,Bo^2\,(\Delta\sigma)^2\,\tau_c$$

Where as τ_c is the correlation time of molecular motion which is proportional to viscosity of the solution and inversely to temperature. For a rigid spherical object of radius r, τ_c can be written as

$$\tau_c = \frac{4\pi\eta r^3}{3kT}$$

Hence it should be kept in mind when studying membrane proteins in detergent micelles that the detergent concentration should be kept low. Otherwise this will increase τ_c and thereby contribute directly to relaxation.

Dipole-Dipole interactions: The DD coupling interactions depends on primarily the distance between the nuclei and the angular relationship between the magnetic field and the internuclear vectors. When the molecule tumbles in solution the DD coupling constantly changes as the vector relationship change and hence the magnetic field at each nucleus also changes. This fluctuation in magnetic fields leads to nuclear relaxation. The strongest nucleus causing DD relaxation is ^{1}H and this can either be homonuclear (^{1}H – ^{1}H) or heteronuclear (^{1}H – ^{15}N and ^{1}H – ^{13}C). The transverse DD relaxation rate (R_{DD}) by two different nuclei x and y is given by the equation:

$$R_{DD} = \gamma_x^2 \gamma_y^2 (\frac{h}{2\pi})^2 \tau_c \frac{1}{r_{xy}{}^6}$$

Where as τ_c is the correlation time of molecular motion

γ_x , γ_y are the gyromagnetic ratios

r_{xy} is the distance between x and y nucleus being relaxed

Sequential assignment

In general triple resonance experiments were commonly used for sequential assignments of membrane proteins as well as soluble proteins. As membrane protein – detergent size is quite large, TROSY based experiments such as HNCA, HNCO, HN(CO)CA, HNCACB and CBCA(CO)NH are used with a ^{15}N and ^{13}C labeled protein sample (11-14). The spectra were recorded at minimum ^{1}H larmor frequency of 600 MHz in order to achieve enough spectral dispersion and resolution. The dipolar interactions during transverse ^{13}C relaxation can be reduced by perdeuteration and hence the spectral resolution and sensitivity can further be improved for assignment. Using these methods complete or nearly complete backbone assignments have been achieved for the following membrane proteins as cited (15-18).

Experiments	Spectrometer	Observations
1D ^{2}H	500	^{2}H NMR of liposomes
1D ^{31}P	500	^{31}P NMR of liposomes
2D ^{15}N HSQC	600 - 700	Optimization - titration
2D ^{15}N HSQC	600	Sequential assignment
2D ^{13}C HSQC	600	Sequential assignment
3D ^{15}N HSQCNOESY	600	Sequential assignment
3D HNCA	600 - 950	Sequential assignment
3D HNCACB	600 - 950	Sequential assignment
3D CBCACONH	600 - 950	Sequential assignment

All spectra were acquired using Bruker spectrometers, processed with Topspin and analyzed in CARA for sequential assignment.

REFERENCES

1. Jakoby, M., Ngouoto-Nkili, C. E.&Burkovski, A. (1999) Construction and application of new Corynebacterium glutamicum vectors *Biotechnology Techniques* **13**: 437-441.
2. Barth, E., Barcelo, M. A., Klackta, C.&Benz, R. (2010) Reconstitution experiments and gene deletions reveal the existence of two-component major cell wall channels in the genus Corynebacterium *J Bacteriol* **192**: 786-800.
3. Kalinowski, J., *et al.* (2003) The complete Corynebacterium glutamicum ATCC 13032 genome sequence and its impact on the production of L-aspartate-derived amino acids and vitamins *Journal of Biotechnology* **104**: 5-25.
4. Schagger, H. (2006) Tricine-SDS-PAGE *Nat Protoc* **1**: 16-22.
5. Karas, M.&Hillenkamp, F. (1988) Laser Desorption Ionization of Proteins with Molecular Masses Exceeding 10000 Daltons *Analytical Chemistry* **60**: 2299-2301.
6. Fenn, J. B., Mann, M., Meng, C. K., Wong, S. F.&Whitehouse, C. M. (1990) Electrospray Ionization-Principles and Practice *Mass Spectrometry Reviews* **9**: 37-70.
7. Fenn, J. B., Mann, M., Meng, C. K., Wong, S. F.&Whitehouse, C. M. (1989) Electrospray Ionization for Mass-Spectrometry of Large Biomolecules *Science* **246**: 64-71.
8. Greenfield, N. J. (2006) Using circular dichroism spectra to estimate protein secondary structure *Nature Protocols* **1**: 2876-2890.
9. Beychok, S. (1966) Circular dichroism of biological macromolecules *Science* **154**: 1288-99.
10. Chen, Y. H., Yang, J. T.&Chau, K. H. (1974) Determination of the helix and beta form of proteins in aqueous solution by circular dichroism *Biochemistry* **13**: 3350-9.
11. Malcolm H, L. (2002) *Spin Dynamics (Basics of Nuclear magnetic Resonance)* (WILEY, New York, NY 10158-0012, USA).
12. Wuthrich, K. (1986) *NMR of Proteins and Nucleic Acids* (Wiley, New York.
13. Salzmann, M., Wider, G., Pervushin, K., Senn, H.&Wuthrich, K. (1999) TROSY-type triple-resonance experiments for sequential NMR assignments of large proteins *Journal of the American Chemical Society* **121**: 844-848.
14. Yang, D. W., Venters, R. A., Mueller, G. A., Choy, W. Y.&Kay, L. E. (1999) TROSY-based HNCO pulse sequences for the measurement of (HN)-H-1-N-15, N-15-(CO)-C-13, (HN)-H-1-(CO)-C-13, (CO)-C-13-C-13(alpha) and (HN)-H-1-C-13(alpha) dipolar couplings in N-15, C-13, H-2-labeled proteins *Journal of Biomolecular Nmr* **14**: 333-343.
15. Yang, D. W.&Kay, L. E. (1999) TROSY triple-resonance four-dimensional NMR spectroscopy of a 46 ns tumbling protein *Journal of the American Chemical Society* **121**: 2571-2575.
16. Wider, G. (1998) Technical aspects of NMR spectroscopy with biological macromolecules and studies of hydration in solution *Progress in Nuclear Magnetic Resonance Spectroscopy* **32**: 193-275.
17. Arora, A., Abildgaard, F., Bushweller, J. H.&Tamm, L. K. (2001) Structure of outer membrane protein A transmembrane domain by NMR spectroscopy *Nature Structural Biology* **8**: 334-338.

18. Renault, M., *et al.* (2009) Solution state NMR structure and dynamics of KpOmpA, a 210 residue transmembrane domain possessing a high potential for immunological applications *J Mol Biol* **385**: 117-30.
19. Fernandez, C., Adeishvili, K.&Wuthrich, K. (2001) Transverse relaxation-optimized NMR spectroscopy with the outer membrane protein OmpX in dihexanoyl phosphatidylcholine micelles *Proceedings of the National Academy of Sciences of the United States of America* **98**: 2358-2363.
20. Chill, J. H., Louis, J. M., Miller, C.&Bax, A. (2006) NMR study of the tetrameric KcsA potassium channel in detergent micelles *Protein Science* **15**: 684-698.

• • • • •

Author: Parthasarathi Rath

Title: Structural and functional characterization of PorA and PorH; the two major porins from *Corynebacterium glutamicum*

Supervisor: Alain Milon

Location and date of defense: Amphitheatre Fernard Gallais (LCC, 205 rte de Narbonne, 31077-Toulouse, France), 14th December 2012

Abstract

PorA (5 kDa) and PorH (7 kDa) are two major membrane proteins from the outer membrane of *Corynebacterium glutamicum* which belongs to the suprageneric group of Gram-positive bacteria containing number of human pathogens such as *Mycobacterium tuberculosis*, *M. leprae* and *C. diphtheriae*. Both PorA and PorH have been shown to form heteromeric ion channels and to be post-translationally modified by mycolic acids (α-alkyl, β-hydroxy fatty acids).

Both proteins were produced in their natural host with mycolic acid modification, as well as in *E. coli* based continuous exchange cell-free expression system and thus devoid of mycolic acid modification. The presence or absence of mycolic acid modification on *in vivo* and *in vitro* expressed proteins was confirmed by MALDI-TOF mass spectrometry. CD and NMR spectra of $^{15}N/^{13}C$ uniformly labeled PorA and PorH solubilized in LDAO micelles indicated mono-dispersed and partially folded proteins, compatible with structure determination by NMR. However, functional assays (via black lipid membrane ion-channel conductance measurements) confirmed that a complex associating both proteins is required for function and that the mycolic acid modification on PorA (but not PorH), is an absolute requirement for the formation of a voltage dependent ion-channel.

To understand further the importance of covalent or non-covalent interaction of their natural lipid environment on the complex formation, the major *C. glutamicum* outer membrane lipids [Trehalose dimycolate (TDM), Trehalose monomycolate (TMM) and Cardiolipin (CL)] were purified using adsorption and ion exchange chromatography, both in protonated and perdeuterated form. Prior to proteoliposome reconstitution, the membrane forming properties of TDM alone or in mixture with CL were studied by ^{2}H-NMR, Dynamic Light Scattering and Electron Microscopy. Furthermore, after *in vitro* reconstitution of PorA and PorH in TDM vesicles (and not in LDAO micelles or DMPC vesicles), evidence for the formation of the hetero oligomeric complex was observed. The 3D structure determination, by liquid and/or solid state NMR, of a functional PorA-PorH complex in its natural lipid environment is now feasible.

Key words: Ion channels, Porins, Protein expression and purification, cell-free expression, mycolic acids, solution and solid state NMR, mass spectrometry, black lipid membrane measurements, electron microscopy

Laboratory address: IPBS-CNRS, UMR 5089, 205 rte de Narbonne, 31077-Toulouse Cedex France